

‘Spatial Epidemiology of Lung Cancer Mortality: Geographical Heterogeneity and Risk-Factors Assessment’

Supervisors:

Dr. Richard J.Q. McNally

Prof. Stephen P. Rushton

Dr. Mark S. Pearce

PhD student name: **Basilio Gómez-Pozo**

Student number: **069 118 278**

Institute of Health and Society

Sir James Spence Institute (Level 4)

Royal Victoria Infirmary

Queen Victoria Road, Newcastle NE1 4LP

Email: basilio.gomez-pozo@ncl.ac.uk

basilio.gomez.sspa@juntadeandalucia.es

bgomezp@gmail.com

Date of first registration: 13/12/2006

Date of report submission: 12/12/2011



Abstract

Cancer is the leading cause of mortality in Andalucía (southern Spain) for both men and women, and lung cancer is the main cause of cancer mortality for men. Radon-gas exposure is the second most important cause of lung-cancer after tobacco-smoking, which also causes larynx cancer, and Chronic Obstructive Pulmonary Disease (COPD). Radon-gas is a radioactive decay element which originates from radium. Consequently, presence in the soil varies according to lithology (rock composition) which is a surrogate measure for potential radon-gas exposure. Lithology can explain some lung-cancer deaths, but not deaths due to either larynx cancer or COPD.

A small-area analysis was implemented for the period 1986-1995. Fully-Bayesian regression analysis was used to assess the association between lithology and the spatial distribution of lung-cancer deaths (25,006 cases). Area-level deprivation, a surrogate measure for tobacco-smoking, was accounted for. The number of deaths due to larynx cancer (3,653 cases) and COPD (5,143 cases) were also modelled for comparison purposes. Computation was accomplished via Markov Chain Monte Carlo methods, using WinBUGS software.

The spatial distribution of lung-cancer deaths (but neither larynx cancer, nor COPD) was positively associated with lithology, which is consistent with current epidemiological knowledge. These results remained after adjusting for area-level deprivation. The model used allows for separate estimation of risk due to both lithology (RR = 1.02; 95% Credible Interval (CI) = 1.015 – 1.031) and deprivation (RR = 1.04; 95% CI = 1.033 – 1.048). This lithology score overcomes the difficulties in obtaining actual radon-gas measurements, and can be further improved. The results go some way to explaining the regional variability in lung cancer mortality in Southern Spain.

Dedication

In memory of José María Baena Arjona, my father in law.

Acknowledgmentsⁱ

Doing a research thesis is not only a professional endeavour and a personal challenge, but also a great human experience. I am deeply indebted to the many people that have made contributions, directly or indirectly, to ease the way for this piece of research to be accomplished.

Dr Richard J.Q. McNally guided me through the whole process from the very beginning (when I was still in Spain, and this research thesis was only a project) until the writing up and submission stages. Our weekly meetings helped me build progressively the scaffolding leading to this study. He also gave me the opportunity to work for the Institute of Health and Society (IHS), where I had the privilege of working together with, and learning from, many colleagues.

Prof Stephen P. Rushton kept visiting us at the Sir James Spence Institute on a weekly basis, for about two years. During that period, he provoked on me a serious conversion: since then, I cannot help thinking of the letter R. Later on, it was two of us that used to pay him back weekly visits; I think it was then, when he became overtly Bayesian.

Dr Mark S. Pearce was always willing to read any progress report (even on trains, or planes) and tried his best to keep me on track. His epidemiological perspective and critical appraisal were always very useful to me. I wish I could have managed my time more efficiently, so that I had had the opportunity to read all the books he was willing to lend me.

I am also grateful to my assessors, Prof Tanja Pless-Mulloli and Dr Roy Sanderson. They always read my progress reports with interest and made useful suggestions, which motivated me to keep working.

Dr Jane Salotti and Dr Peter W. James carefully proofread various drafts of this thesis. I hope I have been able to put into practice most of their advice, as I really appreciate their time and effort.

To all of them, and many others who cannot be individually acknowledged in such a short space, my most sincere gratitude.

ⁱ This PhD thesis has been partially funded through a fellowship granted by the Spanish body Instituto de Salud Carlos III (ref BAE06/90003).
The mortality data were kindly provided by the Andalusian Health Office, department of Information and Evaluation (Dr J. García León), through the Andalusian Mortality Registry (Dr M. Ruiz Ramos).

Table of contents

Abbreviations and glossary	viii
List of tables	xvii
List of figures	xix
Chapter 1. Introduction	1
1.1 Background.....	1
1.2 Rationale.....	5
1.3 Main Hypotheses.....	10
1.4 Secondary hypotheses	10
1.5 General Aim.....	10
1.6 Specific objectives	10
1.7 Introduction summary	11
Chapter 2. Literature review.....	12
2.1 Aims and strategy.....	12
2.2 Overview	12
2.3 Spatial heterogeneity of mortality in Andalucía	13
2.4 Main causes of mortality	19
2.4.1 Aetiology and epidemiology of lung cancer	26
2.4.2 Aetiology and epidemiology of Chronic Obstructive Pulmonary Disease (COPD).....	32
2.4.3 Aetiology and epidemiology of larynx cancer	37
2.5 Socio-economic status and mortality due to cancer	40

2.6 Radon-gas exposure	45
2.6.1 Joint effect of radon-gas exposure and tobacco smoking	51
2.6.2 Literature review summary	53
Chapter 3. Data collection and handling	55
3.1 Overview	55
3.2 Administrative Boundaries and lithological data.....	55
3.3 Mortality data.....	58
3.4 Population and socio-economic data.....	61
Chapter 4. Methods.....	65
4.1 Overview	65
4.2 Health outcomes estimates	66
4.2.1 Estimates of the expected number of cases.....	66
4.2.2 Modelling of Standardised Mortality Ratios.....	70
4.3 Software description and analysis implementation.....	75
4.4 Ecological analysis	78
4.4.1 Socio-economic Status.....	78
4.4.2 Potential radon-gas exposure	78
4.5 Disease Mapping.....	79
Chapter 5. Results.....	82
5.1 Overview	82
5.2 Structural Equation Modelling.....	83

5.2.1 Measurement model	83
5.2.2 Structural model	87
5.2.3 Summary of the Structural Equation Model	92
5.3 Lung-cancer mortality modelling.....	92
5.3.1 Besag-York-Mollié model: males	92
5.3.2 Besag-York-Mollié model: females	107
5.3.3 Mapping of lung-cancer mortality modelling: males	114
5.3.4 Mapping of lung-cancer mortality modelling: females	132
5.4 Summary of lung-cancer mortality modelling.....	136
Chapter 6. Discussion	137
6.1 Findings	137
6.2 Strengths and limitations	143
6.2.1 Bayesian analysis and modelling	143
Chapter 7. Conclusions	151
7.1 Summary.....	151
7.2 Contribution.....	152
7.3 Future research.....	153
Chapter 8. References	155

Abbreviations and glossary

Adjacency matrix: Or, broadly speaking, neighbourhood weight matrix. It is used in Conditional Autoregressive (CAR) models for neighbourhood definition.

Neighbourhood weight matrices can be defined using adjacency-based or distance-based criteria, as well as key variable information. The way the adjacency matrix is built determines the degree of smoothing of the estimates.

AIC: Akaike Information Criterion (or penalised log-likelihood). It provides a means for model selection by adjusting the deviance according to the number of parameters present in the model: $AIC = \text{deviance} + 2 * (\text{No. of explanatory variables} + 1)$. The preferred model is the one with the lowest AIC. If the difference between magnitudes of AIC is less than 2, models are considered to be of the same value.

ArcGIS: Proprietary GIS software by Environmental Systems Research Institute (ESRI)

Bayesian analysis: Bayesian statistical analysis deals with uncertainty of estimates through Bayes' rule of conditional probabilities. It allows modifying prior assumptions in parameter estimates, according to the evidence provided by the data. The combination of the prior probability and the data (the likelihood) produces the posterior probability.

Burn-in period: Number of values sampled from the posterior (also known as the target) distribution, which are discarded from the whole MCMC computation. A burn-in period is needed given that sampled values obtained by MCMC algorithms are highly correlated to each other, at the beginning of the process. Therefore, starting values do not adequately represent the target distribution.

BGR: Brooks-Gelman-Rubin statistic (\hat{R}). It helps deciding when convergence of different MCMC chains has been achieved. It is computed as the square root of the variance of pooled chains (between-chain variance) divided by the average within-chain variance. As a rule of thumb, \hat{R} should be ≤ 1.1 for all parameter estimates.

BMI: Body Mass Index. It is computed as the ratio of the person's body weight by the square of the person's body height; it is measured in Kg/m^2 , or lb/in^2 .

BYM: Besag-York-Mollié model. It is a hierarchical Bayesian model which incorporates random effects due to both spatially-correlated (or clustering) and non-

spatial heterogeneity. The inclusion of these effects are responsible for the local and global smoothing effects, respectively, of RRs estimates.

CAR model: Conditional Autoregressive model. It is used in spatial epidemiology for local smoothing of RRs estimates, by means of adjacency matrices, or broadly speaking, neighbourhood weight matrices.

Carstairs-Morris index: Area-level socio-economic index, which is indicative of material deprivation. The census variables used to build this index are: overcrowding, male unemployment, low social class, and lack of car ownership.

CH: Spatially-correlated heterogeneity, or general clustering. It is one of the two components of the residual variance within the BYM model.

CI: Credible Interval. The CI summarises the range of values of the posterior distribution that encompasses a specified area (e.g. 95% CI); that is to say, the parameter of interest is itself a variable. Conversely, a confidence interval (its frequentist counterpart) is the range of values containing the true parameter (in this case an unknown constant) with certain probability, if a sample was repeatedly drawn.

CO: Carbon Monoxide. It is a colourless, odourless, and tasteless gas which is a toxic ambient-air pollutant produced by incomplete combustion of compounds that contain carbon, such as biomass fuel, or vehicles exhaust. Tobacco smoking is also a CO source.

CO₂: Carbon dioxide. CO₂ is a byproduct of normal human metabolism which is expelled with the air exhaled through the lungs. CO₂ is also produced by burning fossil fuel, as well as from decomposing vegetation, or chemical reactions in the soil.

Compositional variables: Individual-level characteristics.

Contextual variables: Area-level (geographical) characteristics.

COPD: Chronic Obstructive Pulmonary Disease. COPD is a health condition that causes permanent damage of the air flow and eventually leads to disability and death. COPD is known to be mainly due to tobacco smoking.

CR: Confirmation rate. CR, or Positive Predictive Value (PPV), is the conditional probability of cases being classified as cancer by the gold standard (clinical records and/or pathology), given that they were classified as cancer by death certificates.

CRF: Chronic Respiratory Failure. CRF is characterised by high levels of CO₂ in the blood (hypercapnia), low levels of oxygen (hypoxemia), or both. COPD is frequently associated with CRF.

CVD: Cardiovascular Diseases. The most important causes of CVD mortality are: Ischaemic Heart Disease (or heart attack) , Cerebrovascular Disease (or stroke), and Hypertensive Heart Disease (or high blood pressure).

DIC: Deviance Information Criterion. DIC is the the Bayesian counterpart of the AIC when applied to multilevel models. The DIC is computed from the mean posterior deviance and the effective number of parameters (pD). $DIC = \text{mean deviance} * pD$.

DNA: deoxyribonucleic acid. DNA is responsible for the transmission of the genetic information and, hence, the hereditary characteristics of individuals.

DNA-adducts: Linking of DNA with chemical substances (e.g. TSNs). Although DNA-adducts are supposed to be initiated by the human body as a detoxifying mechanism, this process actually triggers carcinogenesis.

DR: Detection rate. DR (or sensitivity) is the conditional probability of cases being classified as cancer by death certificates, given that they were classified as cancer by the gold standard (clinical records and/or pathology).

EB: Empirical Bayes. EB estimation is a type of Bayesian analysis where the prior probabilities are obtained from the data under scrutiny. Conversely, in Fully Bayesian analysis (as in the present research study), the prior probabilities are obtained from information other than the data under analysis (in this case, data from a previous time period).

Ecological fallacy: Systematic bias that happens when group-level characteristics are attributed to the individuals. This is why findings from ecological studies need confirmation at the individual level.

Ecological study: Epidemiological study-design that gathers information at the group-level (instead of the individual-level), for both the exposure and event of interest.

EPA: US Environmental Protection Agency.

Epi Map: Free software for statistical analysis and mapping, by the US Centers for Disease Control and prevention (CDC).

EPIC: European Prospective Investigation into Cancer and nutrition.

ETS: Environmental Tobacco Smoke. Also known as secondhand, passive, or involuntary tobacco smoking.

FB: Fully Bayesian analysis (see EB).

FEV1: Forced Expiratory Volume in 1 second. FEV1 is obtained by spirometry (test of respiratory function) and is correlated to the magnitude of airway obstruction and quality of life, in patients with COPD.

GeoBUGS: WinBUGS add-on software for mapping.

GeoDa: Free GIS software by Luc Anselin.

GIS: Geographic Information Systems.

GRASS: Geographic Resources Analysis Support System. Free, open source, GIS software.

GSTMG1: enzyme glutathione S-transferase mu gene. Although DNA-adducts are responsible for triggering carcinogenesis, lack of DNA adducts formation due to the inherited absence of GSTMG1 can also promote tumorigenesis.

Hyperparameters: Parameters of prior distributions. Contrary to the frequentist approach (where parameters are considered to be unknown constants), in Bayesian statistics parameters (and hyperparameters) are considered to be variables with their own probability distribution.

Hierarchical regression model: Also known as random-effects model, multilevel model, or mixed model. Hierarchical regression allows for the computation of estimates with lower MSE than non-hierarchical modelling; this is achieved as parameter estimates come from data grouped within hierarchies (e.g. deaths within municipalities). Parameter estimates are pooled down in relation to their variance (see Smoothing). The BYM model is a Bayesian hierarchical model.

HRQoL: Health-Related Quality of Life.

IARC: International Agency for Research on Cancer.

ICD: International Classification of Diseases.

Iteration: Every value sampled from the posterior distribution by means of MCMC algorithms, such as Metropolis-Hastings and Gibbs sampling.

INE: Spanish National Statistics Institute

IQR: Interquartile range. The IQR is a measure of statistical dispersion, which is computed as the difference between the 3rd and the 1st quartiles.

Kriging: Method of interpolation of unknown values, based on sample points.

LET: Linear Energy Transmission.

Lithology: Rock composition. According to lithology, the main types of rocks are: sedimentary, plutonic, volcanic and metamorphic.

MAGNA: Spanish National Geological Map.

MAPE: Mean Absolute Predictive Error. As DIC, MAPE can be used as a measure of goodness of fit of the model. Together with MSPE, MAPE is a loss function which compares observed and predicted values and it is computed according to the formula: $MAPE_j = \sum_i |Y_i - Y_{ij}^{pred}| / m$, where Y_i and Y_{ij}^{pred} denotes the i th observed and predicted data, respectively, under each model (j subscript), while m represents the number of observations. An alternative measure is MSPE (Mean Square Predictive Error); $MSPE_j = \sum_i (Y_i - Y_{ij}^{pred})^2 / m$. Models with lowest values of MAPE and MSPE are preferred.

MC error: Monte Carlo error. MC error measures the variability of the estimates obtained by MCMC simulation. The MC error should be kept lower than 5% of the posterior standard deviation of the corresponding parameter estimate. In this case, convergence is considered to have been reached. The more values are simulated, the lower the MC error will be.

MCMC: Markov Chain Monte Carlo methods. MCMC are a set of algorithms devised for sampling of random values from a target distribution. Simulation, that is, generation of pseudo-random numbers, is the basis for Monte Carlo methods. When many different values are simulated, a chain is said to be obtained. If any future value does not depend on previous estimates, a Markov process is being used. Both Metropolis-Hastings and Gibbs sampling algorithms are MCMC methods.

Meta-analysis: Quantitative statistical method for synthesising results of research studies.

MLE: Maximum Likelihood Estimate. The one with highest probability under the probability distribution assumed for the sampled data.

MSE: Mean Square Error. A frequentist criterion for reliability of estimates, that accounts for both bias and variance simultaneously. Bayesian computation can produce estimates with lower MSE than their frequentists counterparts; this is due to higher precision of the estimates obtained by MCMC methods.

MSPE: Mean Square Predictive Error (see MAPE).

NCO: Spanish National Classification of Occupations.

NHL: non-Hodgkin's lymphoma. NHL is a large group of malignant lymphomas originated from either B or T lymphocytes.

NHST: Null Hypothesis Significance Testing. Frequentist statistical method used to measure the evidence against (null hypothesis) the research (alternative) hypothesis. NHST make use of p values and confidence intervals. Decisions made by means of

NHST are subject to the so called type I (where the null hypothesis is wrongly rejected) and type II (if the null hypothesis is erroneously not rejected) errors.

NO₂: Nitrogen Dioxide. NO₂ is a toxic gas from sources such as automobile engines and tobacco smoking.

NPV: Negative Predictive Value. NPV is the conditional probability of a person being healthy given that the diagnostic test was negative.

Overdispersion: It is present when the variance of a random variable is larger than the mean. Under these circumstances the Poisson assumption can no longer be upheld. Overdispersion can be due to spatial autocorrelation, excess of zero values, and/or random heterogeneity.

PAH: Polycyclic Aromatic Hydrocarbons. PAH are ambient-air pollutants. Common sources of PAH are combustion of fossil fuels and tobacco. Some PAH are responsible for triggering carcinogenesis.

PAR: Population Attributable-Risk. PAR, or aetiologic fraction, is computed as the relative difference between the risk of disease in the total population (R_t) and the risk in the non-exposed population (R_{ne}). $PAR = (R_t - R_{ne}) / R_t * 100$. In spatial analysis PAR can also be computed as $P_E(RR_E - 1) / P_E(RR_E - 1) + 1 * 100$, where P_E denotes the proportion of the population that is exposed (that is, residing in some specific geographical area) and RR_E is the relative risk of the same population.

PC-axis: Free software developed by Statistics Sweden. It is used by many statistical offices around the world.

PCFA: Principal Component Factor Analysis. PCFA is a statistical technique based on finding a small number of linear combinations of the original variables in a dataset, so that this smaller dataset can represent most of the variation found in the original one.

PHCD: Primary Health Care Districts. PHCD are the administrative health-areas in Andalucía.

PM: Particulate Matter. Indoors and outdoors ambient-air pollutant consisting of particles of solid matter. Mortality from CVD and COPD is directly associated with presence of PM in the ambient air.

PPL: Posterior Predictive Loss. PPL functions are used to measure model adequacy (see MAPE and MSPE).

Posterior probability: In Bayesian analysis, the posterior probability $-p(\theta/D)-$ is computed as the prior probability $-p(\theta)-$ times the likelihood $-p(D/\theta)$, where θ

represents the values of the parameter which is to be estimated, and D represents the observed data. Therefore, $p(\theta/D) = p(\theta) * p(D/\theta)$.

Prior probability: Prior assumptions (or weights) used in Bayesian analysis that in conjunction with the likelihood (expressed by the data) produce the posterior probability (see Posterior probability).

PPV: Positive Predictive Value (see CR).

QGIS: Quantum GIS. Open source software.

R: Free software environment for statistical computing and graphics.

Radon: Radioactive, colourless, odourless and tasteless gas that is originated from radium. Radon-222 gas is found in certain types of rocks such as granite, which belongs in the plutonic lithological class and shales, which belongs in the sedimentary group. Radon-gas desintegration produces even more radioactive components (radon daughters) which are responsible for producing lung cancer.

RAM: Random Access Memory. Computer memory used for computation.

REDIAM: Andalusian Environmental Information Network

ROC: Receiver Operating Characteristics curve. The ROC curve is obtained by plotting the false positive rate (on the x axis) against the true positive rate (on the y axis). The higher the area under the ROC curve the better the discriminative power of the classification criteria that were used.

RR: Relative Risk, or Risk Ratio. RR is the ratio of the risk of becoming ill (or dying) in the exposed population as compared to the non-exposed population. High RRs support cause-and-effect associations.

Radon daughters: See radon.

SCLC: Small Cell Lung Cancer. SCLC is one of the main histological types of lung cancer. Other types include: squamous cell carcinoma, adenocarcinoma (more frequently diagnosed in women) and large cell carcinoma.

SEM: Structural Equation Model. SEM are characterised by presence of both observable variables (as in usual regression analysis) and non-observable (or latent) variables (as in PCFA). Content of radon-gas in the soil can be treated as a latent quantity, which can be measured via a surrogate variable (lithology).

SES: Socio-economic status.

Shapefile format: ESRI digital file format for using in GIS. They can store vector-data (points, lines and polygons) as well as its related feature attributes (ID codes, names, area, or population size).

SMR: Standardised (usually, age standardised) Mortality/Morbidity Ratio. SMRs allow for comparing rates between groups of differing age (or any other potentially confounding factor) structures. $SMR = \sum O_i / \sum E_i$, where O_i is the observed number of cases, for each i th age-group in the exposed population, and E_i is the expected number of cases if the age (or any other confounder) specific rates were the same as those of a non-exposed population. Therefore, $E_i = \sum n_{exp_i} * Y_{non_exp_i} / n_{non_exp_i}$, where n_{exp_i} is the number of exposed people for each i th age-category, $Y_{non_exp_i}$ is the observed number of cases, in each age stratum, of a non-exposed population, and $n_{non_exp_i}$ is the non-exposed population size for each i th age-category.

Smoothing: Shrinking, or partial-pooling analysis (see CAR). In hierarchical models, parameters are estimated as a weighted average of the mean of the observations in a specific area and the mean over all geographical areas (most EB methods), or over the subset of neighbouring areas (as in Fully Bayesian methods, such as BYM modelling). The general form of the weighting scheme is given by $(n_i / \sigma^2_{within} * \tilde{Y}_i) + (1 / \sigma^2_{between} * \tilde{Y}_{neighbours}) / (n_i / \sigma^2_{within}) + (1 / \sigma^2_{between})$, where n_i is the number of observations within a specific area, σ^2_{within} is the within-area variance and \tilde{Y}_i is the mean of the observed values within the i th area. $\sigma^2_{between}$ is the variance amongst neighbouring areas, and $\tilde{Y}_{neighbours}$ is the mean of the observed values for all neighbouring areas. Hence, the higher the variance within a specific area the smaller the weight will be for \tilde{Y}_i ; conversely, in these circumstances, the weight will be higher for the pooled, more precise, estimate $\tilde{Y}_{neighbours}$.

Statistical interaction: It is said to exist when the effect of a certain exposure is modified by the level of other exposure (e.g. the effect of radon-gas depends on the smoking habit; that is to say, tobacco smoking modifies the effect of radon-gas exposure, which is analytically checked by testing for interaction).

Thinning interval: As consecutive values sampled from the target distribution, during MCMC computation, may be very similar to one another (high autocorrelation) a n^{th} thinning interval can be used; this means that only 1 value every n^{th} iterations will be used for parameter estimation. Another advantage of thinning is that some computer resources are saved, as WinBUGS (and OpenBUGS) stores all sampled values in the computer RAM. As a drawback, computation will take longer.

THS: Third-Hand Smoke. Pollutants from tobacco smoke, such as nicotine, are known to persist in the environment (e.g. surfaces in smoker's cars, or homes) for months. These pollutants can further react with other chemicals (e.g. nitrous acid) to produce carcinogenic substances (for instance, TSNs)

Townsend index: Index of material deprivation based on four variables taken from censuses, as the percentage of: unemployment amongst people economically active who are ≥ 16 years old; non-car ownership; non-home ownership, and household overcrowding. These four variables are combined to give an index score. The higher the score, the more deprivation is thought to exist.

TSNs: Tobacco-Specific Nitrosamines. TSNs (together with PAH) are potent carcinogenic substances produced during tobacco combustion. Their carcinogenic effect is mediated through DNA damage, which leads to uncontrolled cell proliferation.

UH: Uncorrelated (or non spatially-correlated) Heterogeneity. One of the two components (together with CH) which the residual variance is partitioned into, when the BYM model is used. CH expresses within area variability (see CH).

VPC: Variance Partition Coefficient. The VPC is computed similarly to an Intraclass Correlation coefficient to convey what the proportion of the residual variance is due to CH, which in turn is thought to be due to contextual variables. Therefore, $VPC = (CH / CH + UH) * 100$

Vague prior: A situation where there is not strong prior assumptions; a low-weight prior probability does not modify the likelihood to much extent.

WHO: World Health Organisation

WinBUGS: Free software for Bayesian analysis Using Gibbs Sampling (see MCMC).

ZIP model: Zero Inflated Poisson model. ZIP models are used when overdispersion exists that is due to excess of zero values, such as in the rare-disease context, or for small geographical areas.

List of tables

Table 5.1. Measurement model. Lithology-indicator loadings: posterior estimates. ...	83
Table 5.2. Structural Model: lithology-score regression coefficients estimates for Chronic Obstructive Pulmonary Disease (COPD), larynx cancer, and lung-cancer mortality, in men.....	87
Table 5.3 The structural part of the model: estimates for the deprivation-score regression coefficients. Chronic Obstructive Pulmonary Disease (COPD), larynx cancer, and lung-cancer mortality, in men.	89
Table 5.4 Besag-York-Mollié model: relative goodness of fit of observed data, for all different models. Lung-cancer in men.	93
Table 5.5 Besag-York-Mollié model. Relative goodness of predictive ability (MSPE) for all different models. Lung cancer in men.	95
Table 5.6 Besag-York-Mollié model. Relative goodness of predictive ability (MAPE) for all different models. Lung cancer in men.	96
Table 5.7 Besag-York-Mollié model. Regression-coefficients estimates (log scale). Lung-cancer in men.	97
Table 5.8 Besag-York-Mollié model: regression-coefficients estimates (ratio scale). Lung-cancer in men.	97
Table 5.9 Average values of the SMR and RR, for lung-cancer mortality in men.	98
Table 5.10. Besag-York-Mollié model: Variance Partition Coefficient (VPC) estimates. Lung-cancer in men.	107
Table 5.11. Besag-York-Mollié model: Relative goodness of fit of observed data, for all different models. Lung cancer in women.	108
Table 5.12. Besag-York-Mollié model: relative goodness of predictive ability (MSPE) for all different models. Lung-cancer in women.	109

Table 5.13. Besag-York-Mollié model: Relative goodness of predictive ability (MAPE) for the different models. Lung cancer in women.	109
Table 5.14. Besag-York-Mollié model: regression coefficients estimates on the log scale (two upper rows) and ratio scale (two lower rows). Lung-cancer in women. ...	112
Table 5.15. Variance Partition Coefficient: posterior estimates. Lung-cancer in women.	113

List of figures

Figure 1.1. The Spanish autonomous region of Andalucía (red area).	1
Figure 1.2. Administrative boundaries of Andalucía.....	2
Figure 2.1. Main causes of mortality in men.....	20
Figure 2.2. Main causes of mortality in women.....	21
Figure 2.3. Cancer mortality in men.....	24
Figure 2.4. Cancer mortality in women.....	25
Figure 3.1. The Andalusian towns overlaying the lithological map.....	57
Figure 5.1. The measurement part of the model: posterior probability-density distributions of the lithology-indicator loadings.	84
Figure 5.2. The measurement part of the model: autocorrelation plots and Brooks-Gelman-Rubin graphs for the lithology-indicator loadings.	85
Figure 5.3. The measurement model. Lithology-indicator loadings: history plots.	86
Figure 5.4. The structural part of the model: posterior probability-densities for the Relative Risk (RR) of mortality explained by the lithology score, in the modelling of Chronic Obstructive Pulmonary Disease (COPD), larynx cancer and lung cancer, in men.....	88
Figure 5.5. The structural part of the model: posterior probability-densities for the relative risk (RR) explained by the deprivation-score.	90
Figure 5.6. The structural part of the model: convergence of the deprivation-score estimates.....	91
Figure 5.7. Ranking of posterior estimates of Relative Risk boxplots, for all 101 municipalities in the province of Almería. Lung-cancer in men.....	99

Figure 5.8. Ranking of posterior estimates of Relative Risk boxplots, for all 42 municipalities in the province of Cádiz. Lung-cancer in men.....	100
Figure 5.9. Ranking of posterior estimates of Relative Risk boxplots, for all 75 municipalities in the province of Córdoba. Lung-cancer in men.	101
Figure 5.10. Ranking of posterior estimates of Relative Risk boxplots, for all 166 municipalities in the province of Granada. Lung-cancer in men.....	102
Figure 5.11. Ranking of posterior estimates of Relative Risk boxplots, for all 79 municipalities in the province of Huelva. Lung-cancer in men.	103
Figure 5.12. Ranking of posterior estimates of Relative Risk boxplots, for all 96 municipalities in the province of Jaén. Lung-cancer in men.....	104
Figure 5.13. Ranking of posterior estimates of Relative Risk boxplots, for all 99 municipalities in the province of Málaga. Lung-cancer in men.	105
Figure 5.14. Ranking of posterior estimates of Relative Risk boxplots, for all 102 municipalities in the province of Sevilla. Lung-cancer in men.....	106
Figure 5.16. Besag-York-Mollié model: posterior probability-densities for lithology and deprivation. Lung-cancer in women.....	111
Figure 5.17. Standardised Mortality Ratio estimates for lung-cancer mortality in men.	114
Figure 5.18. Posterior Relative Risks of lung-cancer mortality in men.....	115
Figure 5.19. Exceedance-probabilities map (<i>Probability [Relative Risk > 1]</i>). Lung-cancer mortality in men.....	116
Figure 5.20. Exceedance-probabilities map (<i>Probability [Relative Risk < 1]</i>). Lung-cancer mortality in men.....	117
Figure 5.21. Relative Risks explained by lithology scores. Lung-cancer mortality in men.....	118

Figure 5.22. Exceedance-probabilities map for lithology scores (<i>Probability [Relative Risk > 1]</i>). Lung-cancer mortality in men.	119
Figure 5.23. Exceedance-probabilities map for lithology scores (<i>Probability [Relative Risk < 1]</i>). Lung-cancer mortality in men.....	120
Figure 5.24. Relative Risks explained by deprivation scores. Lung-cancer mortality in men.....	121
Figure 5.25. Exceedance-probabilities map for deprivation scores (<i>Probability [Relative Risk > 1]</i>). Lung-cancer mortality in men.	122
Figure 5.26. Exceedance-probabilities map for deprivation scores (<i>Probability [Relative Risk < 1]</i>). Lung-cancer mortality in men.	123
Figure 5.27. Residual Relative Risks. Lung-cancer mortality in men.	124
Figure 5.28. Exceedance-probabilities map for residual Relative Risks (<i>Probability [Relative Risk > 1]</i>). Lung-cancer mortality in men.	125
Figure 5.29. Exceedance-probabilities map for the residual Relative Risks (<i>Probability [Relative Risk < 1]</i>). Lung-cancer mortality in men.	126
Figure 5.30. Relative Risks explained by spatially Correlated Heterogeneity. Lung-cancer mortality in men.....	127
Figure 5.31. Exceedance-probabilities map for Relative Risks explained by spatially Correlated Heterogeneity (<i>Probability [Relative Risk > 1]</i>). Lung-cancer mortality in men.....	128
Figure 5.32. Exceedance-probabilities map for Relative Risks explained by spatially Correlated Heterogeneity (<i>Probability [Relative Risk < 1]</i>). Lung-cancer mortality in men.....	129
Figure 5.33. Relative Risks explained by Uncorrelated Heterogeneity. Lung-cancer mortality in men.....	130

Figure 5.34 Exceedance-probabilities map for Relative Risks explained by Uncorrelated Heterogeneity (<i>Probability [Relative Risk > 1]</i>). Lung-cancer mortality in men.....	131
Figure 5.35. Exceedance-probabilities map for Relative Risks explained by Uncorrelated Heterogeneity (<i>Probability [Relative Risk < 1]</i>). Lung-cancer mortality in men.....	131
Figure 5.36. Standardised Mortality Ratios. Lung-cancer mortality in women.....	132
Figure 5.37. Posterior Relative Risks of lung-cancer mortality in women.....	133
Figure 5.38. Exceedance-probabilities map (<i>Probability [Relative Risk > 1]</i>). Lung- cancer mortality in women.....	134
Figure 5.39. Exceedance-probabilities map (<i>Probability [Relative Risk < 1]</i>). Lung- cancer mortality in women.....	135
Figure 5.40. Relative Risks explained by spatially Correlated Heterogeneity. Lung- cancer mortality in women.....	136
Figure 6.1. Pathways in the association of deprivation with lung cancer and radon-gas.	140

Chapter 1. Introduction

1.1 Background

Understanding the causes of spatial patterning in the incidence of disease and mortality is important for both understanding the aetiology of disease, and also in mitigating their effects [1]. Cumulative evidence from research accomplished in Spain has shown that there is a pattern of higher mortality rates in the south-west of the country, due to all-cause as well as certain specific causes. Numerous investigations dealing with the spatial distribution of mortality have been implemented in Spain over the last 26 years [2-16]. One conspicuous result of this research is the spatial patterning in mortality showing higher age-adjusted rates (for both men and women) in the southern autonomous region of Andalucía. This is the most populated region in the country (more than 8 million inhabitants, or 18% of the whole Spanish population [17]) and the second-largest one geographically (87,597 km², which represents 18% of the area of the country [18]). Figure 1.1 shows the geographical location of Andalucía (own elaboration using QGIS software [19]; the digital Andalusian borders were obtained from the Andalusian Health Office; countries borders and raster layer were downloaded from *Natural Earth* [20]).

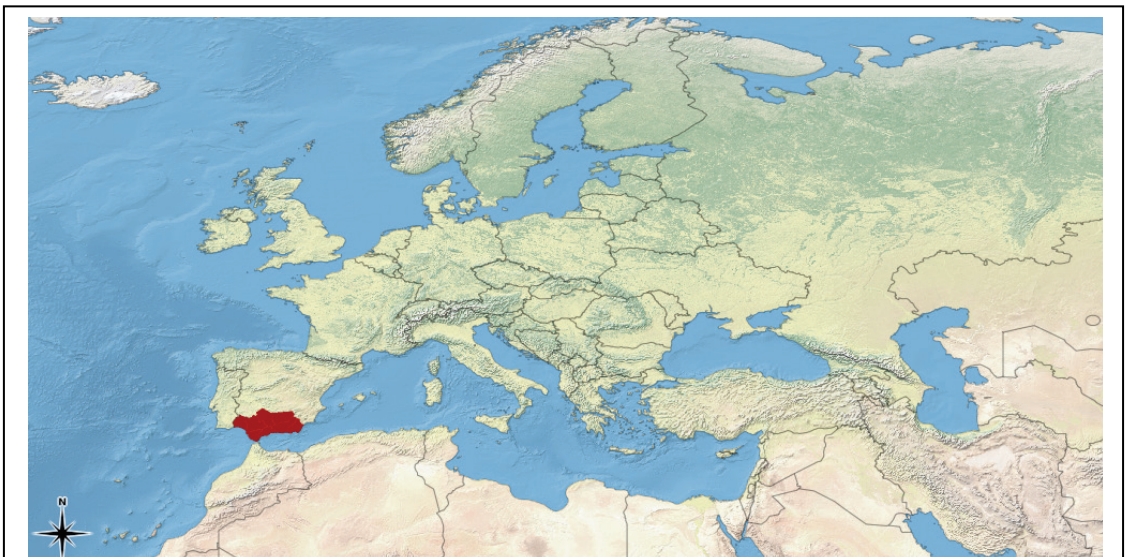
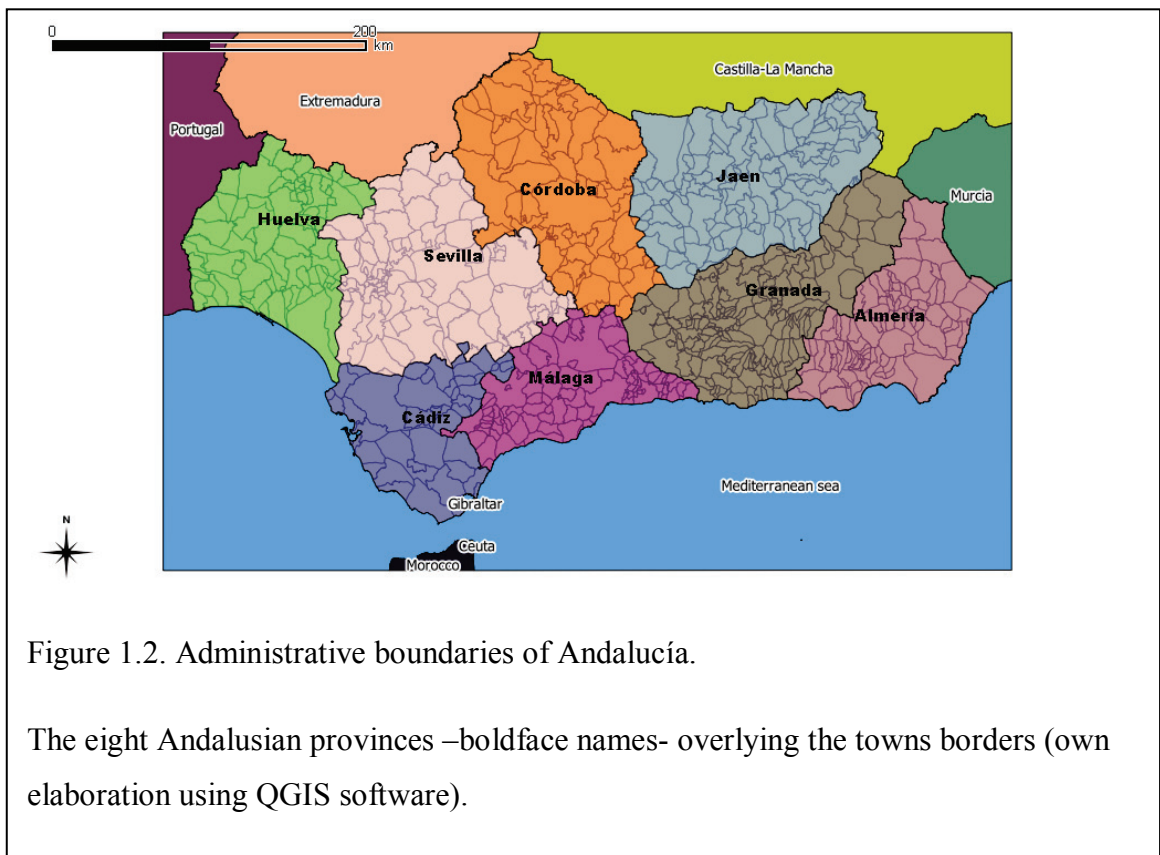


Figure 1.1. The Spanish autonomous region of Andalucía (red area).

Spain is divided administratively into 17 autonomous communities, which are further subdivided into provinces (eight in Andalucía -Figure 1.2) and municipalities [21, 22]. The 1978-1992 Spanish Atlas of Mortality from Cancer [9, p. 19, 214-9, 244] showed that four of the eight Andalusian provinces (Cádiz, Málaga, Huelva and Sevilla) had the highest age-adjusted mortality rates among all the Spanish provinces, when considering neoplasms associated with tobacco smoking and alcohol drinking: cancers of the lung, larynx, oesophagus and bladder. The male-female ratio was greater than



6:1 for all these causes together. For larynx cancer, the male-female ratio was 38:1. Furthermore, the province of Cádiz had the highest all-cause age-adjusted mortality rates: 1,166.65 per 10⁵ inhabitants versus an average value of 951.55 for Spain (or 23% more than average) and 682.8 versus 579.52 in Spain (or 18% more than average) for men and women, respectively. These differences were even higher when lung cancer was analysed (91.44 in Cádiz versus 60.16 for Spain, or 52% higher). It is interesting to note that this pattern of mortality was no longer seen when ill-defined causes, a measure of data quality regarding mortality analysis, was considered. For

these causes, rates for both men and women were slightly lower than the average value for Spain.

However, around one third of deaths caused by cancer in men within Andalucía were due to lung cancer. It is also important to note that lung cancer was responsible for nearly 30% of Years of Potential Life Lost (YPLL), or premature death due to cancer, as the mean age at death was 66 years. An atlas from Andalucía for the period 1975-1997 [23] identified lung cancer as the leading cause of cancer-related mortality for men with 44,027 deaths for the whole period or 31% of all deaths; in women, it was the fourth cause of mortality with 4,532 deaths or 6%, in that 22-year period.

Another Spanish small-area mortality analysis, for the period 1987-1995 [10, 11, 13], also showed the earlier-mentioned pattern of higher mortality rates in the south-west of the country. The Andalusian provinces of Huelva, Sevilla, Cádiz and Málaga (Figure 1.2) were revealed as those which accounted for the greatest number of areas with the highest risk of mortality due to all causes, as well as specific causes including lung cancer. At a smaller area-level, the Spanish municipal atlas of cancer mortality for the period 1989-1998 [16], not only confirmed the previous findings on lung cancer, but also highlighted that the situation had extended to the region of Extremadura which is situated to the north-west of Andalucía. Furthermore, mortality due to lung cancer was again shown to be much higher in men residing in the south-western part of Spain; conversely, the geographical pattern of mortality for women showed the highest rates in the north-west of the country.

The authors of this Spanish atlas of mortality [16] suggested that the heterogeneity in the spatial distribution of lung-cancer mortality (by sex) might be related to the influence of distinct carcinogenic exposures: tobacco smoking for men and radon-gas for women; although a possible interaction between tobacco smoking and radon-gas may play a role. The study period targeted by this analysis included mainly cohorts of women born before the 1940s; that is to say, those who would not yet have massively acquired the habit of tobacco smoking. The hypothesis of distinct risk factors for men and women for developing lung cancer was also consistent with a recognised differential-prevalence in the histological type of tumours [16]: Small Cell Lung Cancer (SCLC) as well as non-SCLC (squamous-cell carcinoma type) for men; while non-SCLC (adenocarcinoma type) is more prevalent amongst women.

Low socio-economic status (SES) is known to be associated with lower life expectancy, as well as higher risk for cancer development and poorer survival rates after diagnosis [24]. The excess of cancer risk in populations with lower socio-economic status has been consistently shown in many (but not all) countries, for cancers of the lung and larynx. SES, in turn, is known to vary by small geographical areas. Therefore, the study of the spatial distribution of SES at area level is relevant in understanding heterogeneity in the mortality distribution of these cancer sites. Thus, the 1989-1998 Spanish municipal atlas of cancer mortality [16] showed that all variables related to SES (including income, illiteracy and unemployment) exhibited a north-south pattern. This drew attention to Andalucía again, as one of the more deprived regions of the country. Furthermore, a high variation of SES has been shown to exist within cities [25-28]. Another ecological study for the period 1987-1995 [29] found the same north-south geographical pattern for both mortality and deprivation. In this study, both of two different indices of deprivation were associated with the geographical distribution of mortality. The so called *index I* (a summary compound of social class, unemployment and illiteracy) was associated with mortality in the oldest group (aged 65 years or more). *Index II* (comprising overcrowding, unemployment and illiteracy), was more closely associated with mortality (showing a steeper gradient) in the youngest group (0-65 year-olds).

Later research on the relationship between deprivation and mortality, for the period 1987-1995 [30] reported a further analysis on the association of the above mentioned deprivation indices (I and II) with mortality due to different causes. Index I was associated (amongst others) with Chronic Obstructive Pulmonary Disease (COPD) for both men and women. Index II was shown to be strongly and positively associated with mortality due (but not exclusively) to lung cancer and COPD, in men. More recent research [27] has investigated the relationship between SES and mortality in Andalucía, at a smaller area-level (census tracts) within the capital cities. A summary deprivation index (comprising social class, unemployment and illiteracy) showed to be positively associated with mortality in seven of the eight Andalusian capital cities; this association was found for both men and women. Within cities, mortality was found to be higher in more deprived census tracts.

As was mentioned earlier, lower SES has been consistently found to be associated with higher mortality. Moreover, it has been also associated with higher incidence due

to all-malignant tumours and some specific sites (such as lung and larynx cancer), across different populations and countries [24, 31]. All this has been partially explained by the association between lower SES with some well-known intermediate health risks: particularly tobacco smoking, but also lack of physical exercise, alcohol drinking, as well as occupational and environmental exposures. Tobacco smoking has been causally associated with a number of cancer sites, such as lung and larynx, but also with some non-cancer conditions such as COPD. Although lower SES (deprivation) is usually associated with tobacco smoking, SES also operates through some other intermediate factors which are not completely understood. For instance, incidence of lung cancer is higher amongst men with lower SES, even if they are not smokers [31, 32].

Lower SES has been also associated with poorer survival after diagnosis. This is relevant not only from a public health perspective, but also from an analytical point of view; it makes analysis of incidence-data preferred over mortality-data in instances of low fatality rate [33, p. 65]. Furthermore, SES has been reported to vary across geography. Hence, concerning the spatial heterogeneity of disease distribution, geography is thought to serve as a compound surrogate of different factors, such as lifestyle, environmental exposures, socio-economic characteristics, as well as genetic traits [1, 14, 34-42]. So, the spatial heterogeneity of distribution of the key determinants of health could be responsible for distinct geographical patterns of morbidity and mortality, not only at the international, national, or regional level, but also at much smaller geographical level like municipalities, and census tracts within cities.

1.2 Rationale

Understanding why the incidence of disease varies is critical to managing it. Where spatial patterns occur it is not often easy to explain why. A formal analytical approach at the individual level is not always feasible. In a spatial context, the information may not be available, or it may be unlikely to obtain ethical approval. Nowadays, ecological studies can be used to analyse risk factors for disease, regarding not only large-scale, but also small-area level populations. Some recent advances have promoted development of Spatial Epidemiology, e.g. the availability of modern Geographic Information Systems (GIS) and development of new statistical tools [43-

54]; also, computational availability and increased accessibility to routinely collected data on health-related factors [55, 56]. Some field-related disciplines are especially relevant to this research area: namely, GIS and Applied Spatial Data Analysis. An increasing availability of commercial (e.g. ArcGIS) and free software (e.g. GRASS, GeoDa, R) has provided a means to implement small-area-analysis research. Also, complex statistical modelling can nowadays be applied to better understand the heterogeneity of health-status distributions.

In some cases, ready-to-use information includes data regarding socio-economic characteristics as well as health-related behaviour concerning the study populations, such as smoking, alcohol drinking and physical activity [57]. In other instances there is availability of attributes related to the surrounding environment that are thought to be hazardous and therefore monitored, including chemical products and biological agents present in drinking water, soil and ambient air [1, 14, 46, 57-59]. For example, a digitised map exists on lithology that gives detailed information on the rocks composition, for the Andalusian soils [60]. This allows lithology to be used as a surrogate measure for potential radon-gas exposure at the small area-level [61]. Other data sources, such as mortality registries as well as censuses, provide necessary information with respect to socio-demographic factors. Municipal registries, in Spain, also provide demographic information on a yearly basis. Therefore, statistical modelling and disease mapping can provide better identification and interpretation of health differences among populations [62, 63].

Ecological studies can contribute to the knowledge of the epidemiological features of the health status of populations, by describing the distribution of their essential attributes ('person', 'place', and 'time'). However, area-level analyses on the significance of risk factors are hindered by potential biases, as well as confounding. These potential issues can arise from unmeasured variables (frequently SES [1, 34, 64, 65]). The ecological fallacy is especially relevant, where there is a systematic bias which attributes group-level-characteristics to the individuals. Nevertheless, using information at small geographical level helps to lessen this bias by making exposure measurement closer to the individual level [1]. Moreover, current analytical techniques in statistical modelling allow for different important issues, such as spatial autocorrelation [63, p. 10], to be addressed. As a result, analysis at the small-area level has expanded in order to both describe spatial heterogeneity, and determine the main

sources of variability. Even though findings at group-level analysis need to be confirmed at the individual-level, spatial analyses can be hypothesis-generating.

Another important point is whether to use incidence-data or mortality-data. The former is more appropriate to measure the risk of disease and therefore to establish cause-effect associations. This is especially the case, when the outcome of interest has a low fatality rate [33, p. 65]; this hinders mortality from being a good surrogate measure for incidence, as it may also reflect other influences, some of which may be related to survival status [66]: thus, accuracy of death-certificate records, health-care accessibility, prompt diagnosis, treatment availability, or variability in clinical practice. Notwithstanding all these advantages of incidence-data over mortality-data, practicality often calls for death-records to be used instead, as they are readily available. Additionally, that mortality analysis has a long history of major contributions to the knowledge of cancer epidemiology [33, p. 65-6], although incidence is preferred whenever is available.

It is also important to bear in mind that mortality data have been widely structured according to international recommendations by the World Health Organisation (WHO) [67]. This helps to lessen misclassification problems. In this respect, statistics derived from death certificates have been reported to underestimate death due to cancer in just 4% of the cases; misclassification is considered to be greater for more difficult diagnoses such as brain and liver cancer. Therefore, mortality (instead of morbidity) was considered, given easy accessibility to the Andalusian Mortality Registry. Reliability of death certificates in Spain is thought to be similar to other countries [68] for some health events, such as lung cancer. Also, given the high fatality rate of some conditions (especially lung cancer), mortality would not be much affected by differentials in survival rates throughout different geographical areas.

In Spain, data from mortality registries is considered to be the only comprehensive source of information on cancer for the whole country, or at the regional level. Pérez-Gómez et al. published a review of studies about the quality of data dealing with mortality due to cancer of different sites, for the period 1980-2002 [69]. The detection (DR) and confirmation (CR) rates were estimated for different types of cancer. Clinical and/or pathology data was considered to be the gold standard which death-certificates information was compared with. DR (or sensitivity) was computed as the

conditional probability of cases being classified as cancer by death certificates, given that they were classified as cancer by the gold standard; that is to say, the probability of a case being classified as cancer, given that it truly is a cancer case. CR (or positive predictive value) was calculated as the conditional probability of cases being classified as cancer by the gold standard, given that they were classified as cancer by death certificates; that is to say, the probability of a case classified as cancer being a true cancer case. Accuracy of death certification was considered to be good if both DR and CR were $\geq 80\%$. Over-certification was considered to occur with DR $\geq 80\%$ and CR $\leq 80\%$. Conversely, under-certification was thought to exist if DR $\leq 80\%$ and CR $\geq 80\%$. Cases where both DR and CR were $\leq 80\%$ were considered to be ill-certified (low proportion of ill-certification being considered characteristic of a high-quality standard of information).

Published reports from different cancer registries in Spain, including the one in the province of Granada (Andalucía), showed that lung cancer mortality had been well certified during the study period, while larynx cancer had been over-certified [69]. Interestingly, during the 1980s mortality registries at the regional level became responsible for dealing with these data. During these years, the trend of both ill-certified tumours and ill-certified non-cancer conditions decreased, while they rose in 1999 (by 31%, for tumours) and then stabilised. The increment in ill-certified cases in 1999 coincided with the introduction of the 10th revision of the International Classification of Diseases (ICD-10) in Spain. Ill-certification was proportionally higher (lower quality of data) in women than in men, along all the study period, even when age-adjusted rates were used.

Some variables, especially age and sex, are well known to account for heterogeneity in the distribution of overall and cause-specific mortality, among different populations. To adjust for these potential confounding variables, the Standardised Mortality Ratio (SMR) has been widely used as a comparison measure. SMR is considered to be a Maximum Likelihood Estimate of Relative Risk (RR) and is calculated as the ratio of observed to expected number of cases (O/E) [63, p. 4-5]. Different methods have been devised to estimate E [51, 70-75] assuming a multiplicative model. The downside of the SMRs are that in the case of absence of observed cases (which is frequently the case at the small-area-level), E cannot be computed (so, the ratio is null). Moreover, estimates can be statistically unstable (small changes in E can produce large variation

in SMRs). Given that mortality analysis is concerned with count events, a Poisson distribution is usually assumed to fit this kind of data [62, p. 314, 76, p. 86, 183-96, 77, p. 250, 528-39]. Therefore, the observed number of cases is modelled instead to give SMR estimates.

The Poisson assumption is supported by the data in some scenarios. Nevertheless, over-dispersion is a drawback to always bear in mind [44, 77, p. 540-6, 78, p. 21, 114-6, 320]. In these cases, the data show extra-variability which causes the sampling distribution not to fit to a theoretical Poisson distribution. This is just one of the reasons for fitting different models to count-data: e.g. a Negative Binomial or its Bayesian counterpart, the hierarchical Poisson-Gamma model.

Bayesian modelling offers some advantages over frequentist analysis [79, 80]: Thus, Bayes' theorem is, always, the only basic principle used in every analytical situation. This theorem allows for prior knowledge to be incorporated into the analysis of current data (also known as the likelihood) to produce direct posterior probability estimates; these estimates concern the actual dataset being analysed. Conversely, the frequentist approach resorts to the Null Hypothesis Significance Testing (NHST) paradigm [81]. In this case, confidence intervals are not related to the actual data gathered by the researcher. Instead, they are referred to all potential datasets fitting a theoretical sampling distribution: nothing is assumed about the specific dataset under analysis [79]. Furthermore, Bayesian analysis usually produces more precise estimates than those obtained by frequentist methods [82]; this is especially the case when dealing with small sample sizes. In these situations, Bayesian estimates surpass frequentist estimates even if the former ones are biased. This is due to larger precision of the Bayesian estimates, which produce smaller Mean Square Errors (MSE); the MSE is a frequentist criterion for reliability of estimates, that accounts for both bias and variance simultaneously [76, p. 164, 82].

Bayesian modelling can be broadly categorised into Empirical Bayes (EB) and Fully Bayesian (FB) methods. EB methods estimate prior parameters from the data; conversely, FB methods make use of external information, or assume a range of plausible values. This is the reason why EB methods do not take into consideration uncertainty of prior parameters information. FB methods accounts for this potential source of variability [82]. A whole range of EB models are in use [50, 62, p. 316-21].

Some of them (Poisson-Gamma model, Log-Normal, Marshall) shrink SMRs to a global mean calculated from the data, and some are computationally unstable. To overcome these problems, Fully Bayesian (FB) methods have been proposed that make the SMRs to be locally smoothed by taking into account the estimates of neighbouring areas. Furthermore, some of these hierarchical models (Besag-York-Mollié [BYM]) allow for covariates to be incorporated [63, ch. 8, 83].

1.3 Main Hypotheses

There is spatial variation in mortality due to lung cancer, COPD and larynx cancer, in Andalucía. Spatial variation in lung-cancer mortality is dependent on presence of radon-gas, and area-level deprivation which is a surrogate for smoking. These two factors may interact; they are also dependent on the lithology which determines the source of radon and also the deprivation of those residents in the landscape (Figure 6.1).

In contrast, spatial variation in larynx cancer and COPD are dependent on deprivation (as a surrogate for smoking) but not on radon and the lithology that determines it.

1.4 Secondary hypotheses

Lithology, as a surrogate measure for potential radon-gas exposure, can help to explain heterogeneity in the spatial distribution of lung cancer mortality.

Lithology cannot help to explain heterogeneity in the spatial distribution of either larynx cancer or COPD.

1.5 General Aim

To analyse the potential value of lithology in explaining the spatial distribution of lung cancer mortality in Andalucía, for the period 1986-1995

1.6 Specific objectives

To develop a lithology score, as a surrogate measure for potential radon-gas exposure, by municipalities in Andalucía

To model the spatial distribution of lung-cancer mortality in Andalucía, using lithology as a potential explanatory variable, while adjusting for area-level socio-economic status (SES)

To model the spatial distribution of mortality due to larynx cancer and COPD, using lithology as a potential explanatory variable, while adjusting for area-level SES

To map the distribution of lung cancer mortality in Andalucía as explained by the whole model, as well as the individual components

1.7 Introduction summary

Several mortality analyses published in Spain have shown that all-causes mortality, as well as mortality due to some specific diseases such as lung cancer, is higher in the southern autonomous region of Andalucía. Although this geographical pattern of mortality has been known for a long time, reasons remain incompletely understood. Both tobacco smoking and ambient-air pollution by radon-gas have been shown to be the most important causes of lung cancer mortality. As individual-level information on these two was unavailable, an ecological study was mandatory. Furthermore, lung cancer mortality, as well as some risk factors (such as radon-gas exposure), is known to vary by small geographical areas. The same variation has been reported for SES at the area-level, which is known to be a surrogate measure for tobacco smoking, while lithology can be used as a surrogate measure for radon-gas exposure. Spatial epidemiology at the small-area level is thought to counteract the ecological fallacy; this is done by producing aggregated measurements that are closer to the individual-level characteristics than the ones provided by large-scale studies. Geo-referenced data (at the small-area level) dealing with mortality, population size, SES, and lithology was available in digital format. Nowadays, GIS software eases the use of spatial data and current statistical tools (such as the BYM model) can handle some of the downsides of spatial analysis at the small-area level (instability of rates, spatial autocorrelation, and excess of zero values).

Chapter 2. Literature review

2.1 Aims and strategy

This literature review was intended for retrieving the most relevant scientific literature concerning the spatial patterning of mortality in Andalucía. The four main areas of interest were: firstly, current knowledge about main causes of mortality in Andalucía and their distribution according to place, person and time characteristics; secondly, the state of the art in small-area analysis in relation to the statistical modelling, computation and spatial representation of mortality distribution; thirdly, the epidemiology of lung cancer. Interest was focused on influence and area-level measurement of tobacco smoking, radon-gas exposure, and SES. In addition, the epidemiology of larynx cancer and COPD was also reviewed.

Different databases were searched (Medline, Scopus, and Web of Knowledge) and bibliographic alerts were set up for additional papers to be identified whenever they cited key articles. Key words for the literature search were identified by means of Medical Subject Headings (MeSH) thesaurus, which is available through PubMed online [84]. Some MeSH terms used were ‘small-area analysis’, ‘exp Mortality’, ‘social class’, and ‘socio-economic factors’; also, ‘exp Radon/ae [Adverse Effects]’, ‘Air pollution, Indoor/ae [Adverse Effects]’, and ‘Geographic Information Systems/is, ut [Instrumentation, Utilization]’. When needed, the literature search was narrowed by means of MeSH terms which are indicative of quality of study design (i.e. ‘Cohort Studies’, ‘Case-Control Studies’, or ‘Cross-sectional Studies’). To retrieve relevant information on the spatial distribution of mortality in Andalucía, various reports were also accessed online through the Andalusian Health Office website [23, 85, 86]. Some grey literature was also identified which was significant to the purpose of this review [51]. Although the bibliographic search was meant to find the most up-to-date information, some old but highly influential papers were also reviewed [87, 88]. EndNote software [89] was used to store citations together with their respective articles in PDF format, so that an annotated bibliography could be built and eventually cited and referenced.

2.2 Overview

The main causes of mortality in Andalucía are reviewed, emphasising the heterogeneity of its geographical distribution, across the region. Lung cancer mortality

is subsequently appraised and the two most important aetiological factors associated with it (i.e., tobacco smoking and radon exposure) are addressed. Surrogate measures of potential radon-gas exposure are taken into consideration. Socio-economic status (SES) is dealt with in some detail, given the relevance of this variable to predict many different health outcomes. Several indices of area-level deprivation are discussed. Methodological approaches to the spatial analysis of disease distribution are also evaluated: the analytical process stresses the need of a hierarchical model and the advantages and limitations for a Bayesian perspective. Finally, mapping alternatives are put into the context of current availability of tools for both computation and representation of spatial data.

2.3 Spatial heterogeneity of mortality in Andalucía

The particular patterning in mortality rates, which shows higher rates in the southern autonomous region of Andalucía, has been extensively investigated. This pattern is due to all-cause mortality, as well as specific causes, in both men and women. One major publication was a comprehensive study authored by López-Abente et al. [9], who analysed mortality due to cancer and other causes for a 15-year period (1978-1992). This mortality atlas described patterns of mortality by geographical areas at the provincial level (52 such areas, plus two autonomous cities, in Spain) and studied mortality time-trends over three five-year periods, while accounting for a total of fifteen million deaths which occurred in the whole country. The 1975 and 1986 municipal population registries, as well as the 1981 and 1991 census databases were used to obtain population data by age and sex. Information on deaths, provided by the National Statistics Institute of Spain, was classified using the 9th revision of the International Classification of Diseases (ICD-9). Mortality rates were adjusted by the direct method using the standard European population, given similarities with the age-structure of the Spanish population. Poisson regression analysis was used to model the observed number of cases while accounting for age, geographical area, and time-period. Interestingly, mortality rates due to some cancer sites associated with tobacco smoking and alcohol drinking (lung, bladder, larynx and oesophagus) were highest in the west of Andalucía; especially in the province of Cádiz, but also in those of Málaga, Huelva, and Sevilla. The male-female ratio was 6:1 for lung cancer and 38:1 for larynx cancer. This indicates distinct lifestyles between Spanish men and women, at that time, concerning exposure to the main risk factors. The authors also found that

mortality rates due to diabetes and cardiovascular diseases were highest, as well, in western Andalucía. This geographical study was not a small-area analysis and did not take into account potential overdispersion due to spatial autocorrelation, or excess of zero values; if overdispersion had been present, too narrow confidence intervals (or credible intervals, if a Bayesian analysis had been used) would have been obtained, which would have led to false alarms [90]. However, this study by López-Abente et al. [9] produced a very comprehensive mortality atlas that uncovered many different mortality patterns, on numerous diseases. Moreover, in a further study [16] at a much smaller area level (see pg. 25) this author confirmed the same results by means of a Bayesian model that took overdispersion into consideration.

Ischaemic heart disease (heart attack) was also studied at the provincial level to analyse mortality during two four-year periods (1988-1991 and 1994-1997) in Spain. Boix-Martínez et al. [12] analysed mortality data provided by the National Statistical Institute of Spain, while population data were computed by the authors using interpolation methods on census data. Log-linear Poisson regression was used to estimate time-trends while adjusting for age. Smoothing techniques were not applied, nor was socio-economic status accounted for. A decreasing time-trend in mortality due to ischaemic heart disease was found in Spain between the two study periods. Overall mortality rates in Spain were second lowest (after France) when compared with mortality rates of all European countries. Nevertheless, high spatial variation was observed within the country. Andalucía was amongst the regions with higher mortality rates, especially in the provinces of Sevilla and Cádiz.

A subsequent study by Ramis-Prieto et al. [91] undertook a spatial analysis at a smaller geographical unit of analysis: 8077 municipalities were analysed to study the geographical distribution of haematological neoplasms. These malignancies included leukaemia, non-Hodgkin's lymphoma (NHL) and multiple myeloma. Data on cases for the period 1989-1998 were provided by the National Statistics Institute of Spain, and population data by age and sex were obtained from the 1991 census and 1996 municipal registries. Standardised Mortality Ratios (SMRs) were computed by the indirect method, using the whole Spanish population as the source of rates (internal standardisation) by age-group and sex. Three different Bayesian hierarchical models were compared: The BYM model (section 5.3) [92], the Zero Inflated Poisson [44, 90, 93] (ZIP) (see pg. 67) model and Lawson's mixtures model [94]. All three gave

similar results, the BYM model being the more conservative one as it caused fewer false alarms; that is to say, Relative Risks (RRs) estimates were less frequently higher than 1 that is raw SMRs were not indicative of an excess in risk. Highest RRs were estimated in municipalities within Barcelona province (northern Spain) as well as the Canary Islands. With regard to Andalucía, the western cities of San Juan de Aznalfarache, Huelva, and Sevilla showed the highest risks. In eastern Andalucía, it was the city of Granada which emerged as a high risk area for haematological malignancies. The authors concluded that this concentration of risk in highly urbanised areas could be explained by environmental factors in relation to industrialisation, as this is the case for western Andalusian provinces. According to the authors, an alternative aetiological hypothesis that associates childhood leukaemia with common infections and population mixing [36] would be plausible in Barcelona. Nevertheless, the observed geographical pattern was only due to mortality in older age-groups.

Another small-area analysis at the municipal level was carried out by Aragonés-Sanz et al. [95] to investigate the geographical distribution of mortality due to cancer of the oesophagus in Spain during the period 1989-1999. The 1991 census and 1996 municipal registries were used to obtain population data by age and sex. The SMRs were computed using the indirect method; the overall Spanish population (internal standardisation) provided the rates to compute the expected number of cases. The authors used Bayesian analysis by means of the BYM model to smooth the RRs estimates. An excess risk was found amongst men residing in, but not only, municipalities in the provinces of Cádiz and Sevilla, in western Andalucía.

Conversely, an excess of risk was found for women in the south-east of Andalucía (Málaga and Granada). The authors attributed this spatial heterogeneity in risk by sexes to differences in the distribution of some risk factors such as tobacco smoking, alcohol drinking, obesity, and diet. They recommended that future studies should account for socio-economic status, as a surrogate measure for exposure to various risk factors: low socio-economic level has been associated with higher rates of oesophageal cancer, as well as other cancer sites [95]. With regard to cancer of the oesophagus, this association was thought to be due to higher levels of tobacco smoking and alcohol consumption in people of lower socio-economic status. In addition, people in lower socio-economic strata tend to live in more polluted areas, follow less healthy diets, and have more difficulties in accessing health services.

Another Spanish atlas of mortality, at a smaller geographical level than the previous one [2], was produced by Benach et al. [11]. They studied mortality due to 14 different causes of death in 2218 small-areas in Spain, during the period 1987-1995. The units of analysis were constructed by GIS software using municipalities (8077 according to the 1991 census) as the building structure; these new small-areas had a minimum of 3500 inhabitants to preserve confidentiality, in agreement with the National Statistical Institute of Spain. For this same reason, deaths were aggregated over a nine-year period. Socio-demographic data were also obtained from the census. The expected numbers of cases were computed by means of Indirect, internal standardisation. Empirical Bayes analysis was used to compute RR estimates. The authors considered that data from mortality registries were the most important source of information for small-area analysis in Spain. This was not only due to ready availability of information, but also because the quality of death certificates in Spain was considered to be of a similar standard compared with other European countries. In this paper, the authors published results concerning lung cancer as well as breast cancer. Andalucía was one of the four Spanish autonomous regions (out of 17) with highest mortality rates due to lung cancer. An excess of risk was detected in areas within the provinces of Huelva, Sevilla, Cádiz and Málaga (western Andalucía). This excess of risk was found for both age-groups studied, people less than 65 years old, and age 65 years and older. Most high risk areas for breast cancer were concentrated in Cataluña (northern Spain). However, areas within some western provinces of Andalucía (Cádiz and Sevilla) also showed excess mortality risk. The authors considered the inclusion of socio-economic and environmental indicators to be of major importance in future research to help explain this spatial variation in risk of death. This small-area analysis published by Benach et al. [11] used EB analysis, instead of FB methods as was the case in the study by López-Abente et al. [16]; interestingly, both studies (which analysed overlapping periods of time, 1987-1995 and 1989-1998, respectively) found the same spatial patterning of higher mortality in western Andalucía. However, none of them either formally tested any hypothesis about exposure to potential risk factors, or adjusted for any confounders other than age. Later research on small-area analysis [96] confirmed these results (although confined to people aged 65 years and older) during the whole period 1981-2006.

More recently, Ocaña-Riola et al. [15, 27] addressed an ecological study to analyse the association between deprivation and all-cause mortality for the period 1992-2002. These researchers used the smallest geographical units of analysis readily available: census-tracks (between 500 and 2000 inhabitants). The capital cities of Andalucía (southern Spain) and Cataluña (northern Spain) were studied so that regions with different levels of deprivation could be compared; at that time, per capita income in Cataluña was 54% higher than in Andalucía. Information on deaths was supplied by the Regional Ministry of Health in each of the two autonomous regions. The 1991 census was used to obtain population data. Principal Component Factor Analysis (PCFA) was used to derive an area-deprivation index comprised of the percentage of manual workers, unemployment and illiteracy. A BYM was fitted to the observed number of cases, via Markov Chain Monte Carlo methods (MCMC). Results for men showed higher mortality rates in more deprived areas of both Andalucía and Cataluña. However, this pattern was not so obvious for mortality in women in either region. These consistent results through very different socio-cultural contexts suggest that this deprivation index is appropriate to measure socio-economic differences at the area-level in Spain, at least in men. The results were also in agreement with previous research using this same deprivation index at the provincial or municipality level. After adjusting for deprivation, residual (not explained by the model) variation was mainly due to the spatially-structured component in the model. This finding was attributed by the authors to contextual effects. These were considered to be area-level (neighbourhood) characteristics that might be related to deprivation, especially in women, which would explain differences between sexes. Another interesting characteristic of this study is the use of the smallest spatial units of analysis (census-tracks). The association found in this study [15, 27] between the index of deprivation and mortality, and the fact that this index worked well in distinct socio-economic settings, provided a useful measure of deprivation for using in the analysis of spatial epidemiology in Spain.

There has also been considerable research on the relationship of health events (particularly different types of cancers) with putative environmental risk factors. One of these studies, by López-Abente et al. [97], carried out a spatial point-source analysis in relation to mortality due to cancer. The aim was to analyse Spanish towns close to nuclear power plants and nuclear fuel facilities, for the period 1975-1993. Log-linear

models were used and socio-demographic variables at the area-level (such as income, unemployment and illiteracy) were accounted for. "Near versus far" comparisons were used to analyse differences between exposed and unexposed towns, while adjusting for population size and deprivation at the area-level. An excess of risk was detected for mortality due to lung and renal cancers in towns nearby nuclear fuel facilities. The authors recommended monitoring of incidence and mortality in areas close to health-hazard facilities. In this study [97] the number of deaths was modelled while allowing for important covariates (deprivation and population size); overdispersion was also accounted for. An interesting result was the association between residence nearby nuclear fuel facilities, and lung-cancer mortality. Although relevant, this finding cannot explain the characteristic patterning of higher mortality in western Andalucía; there is just one such facility in the region, which is located in the province of Córdoba (Figure 1.2). In addition, the exposure area that was considered to be biologically plausible was only 30 km around the plant.

Another ecological study at the municipal level (López-Abente et al. [98]) assessed the link between environmental factors associated with farm-related activities, such as pesticides, and mortality due to brain cancer in northern Spain. This study highlighted the suitability of small-area analysis using Bayesian hierarchical models to allow for true mortality patterns to emerge. Furthermore, Bayesian hierarchical models, such as BYM that include a spatial auto-correlated term, help in accounting for residual variation in risk. This residual variance is considered to be due to unmeasured risk factors which are linked to geography (contextual effects).

Putative environmental factors responsible for cardiovascular diseases have been also investigated. In this way, Ferrándiz et al. [14, 99] analysed influence of water hardness (due to presence of calcium and magnesium) in relation to mortality risk from cardiovascular diseases, for the period 1991-1998. Both cerebrovascular disease (stroke) and ischaemic heart disease (heart attack) were studied. This was a small-area analysis at the municipal level in the autonomous region of Valencia (eastern Spain). Indirect, internal standardisation was used to compute expected number of cases, using the overall population of interest as the source for the rates. An Empirical Bayes (EB) hierarchical Poisson-gamma model was used to fit the data (see pg. 144). The authors took into account deprivation at the area-level, by means of an index comprised of the percentage of illiterate and unemployed people, as well as the number of vehicles per

person. They found a weak U-shaped protective effect of magnesium concentration in drinking water, from mortality due to cardiovascular diseases. That is to say, magnesium seems to be protective at medium concentrations, which the authors found to be in agreement with previous research in France. This study highlights suitability of ecological studies to address research concerning small environmental risks which, in addition, show slight spatial variations.

2.4 Main causes of mortality

Cardiovascular diseases and cancer of different sites were the most important causes of mortality for both men and women residing in Andalucía, during the 22-year period spanning from 1975 to 1997. Amongst all cancer sites, lung cancer was the leading cause of mortality, with a total of 48,559 deaths (or 25.8% of all deaths due to cancer [23]). Figure 2.1, Figure 2.2, Figure 2.3, and Figure 2.4 (own elaboration with data from the Andalusian Health Office) show information obtained from a study accomplished for the period 1975-1997 [23]. The geographical units of analysis used in this study were Primary Health Care Districts (PHCD), whose population ranged in size from 11,000 to 300,000 inhabitants in the year 1988. Information on deaths included in this study was provided by the National Statistical Institute of Spain for the period 1975-1991 and by the Andalusian Statistical Institute for the period 1992-1997.

Data on sex, age, and year of death were analysed according to the 8th revision of the International classification of diseases (ICD) for the first period, while the ICD-9th revision was used to classify deaths for the second period. Crude rates, as well as age-adjusted ones were computed; for the latter ones, the European population was used as a reference source to obtain the expected number of cases. SMRs were also obtained using indirect, internal standardisation; in this case, the overall Andalusian population was used as source for the rates to derive the expected numbers of cases. Years of Potential Life Lost and percentage of change (year-to-year, and first-to last-five year periods) were calculated for cancer, cardiovascular diseases (CVD), diabetes, traffic accidents and other causes. Deprivation was, nevertheless, not accounted for.

Figure 2.1 and Figure 2.2 show that the four most important causes of mortality were the same for both men and women: CVD, cancer, respiratory and digestive diseases. Respiratory diseases were responsible for 73,869 male deaths (or 11.7% of all-cause mortality in men) and 48,497 female deaths (or 8.5% of all-cause mortality in women). Amongst all respiratory diseases, Chronic Obstructive Pulmonary Disease (COPD) was the major cause of mortality amongst both men (37,718 deaths) and women

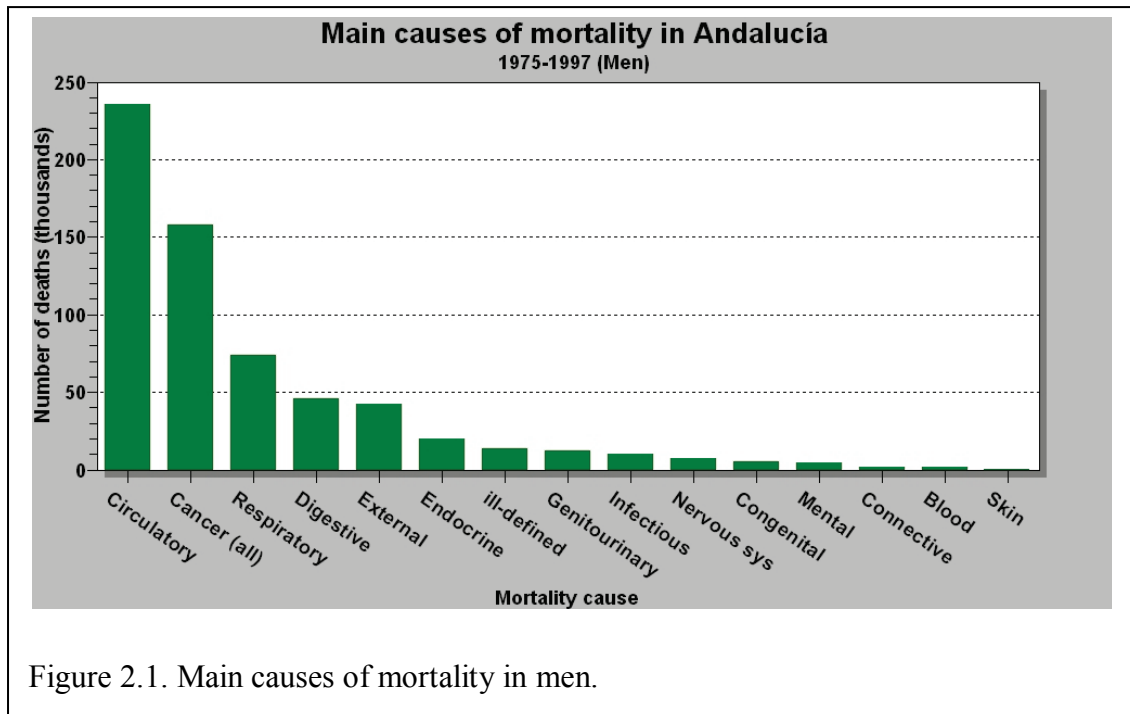


Figure 2.1. Main causes of mortality in men.

(14,598 deaths). These differences between sexes can be explained by gender heterogeneity in the exposure to the main risk factor for COPD (tobacco smoking [100]); the male-female mortality rate ratio was 2.8:1 in 1975 and 5.8:1 in 1997. Concerning the spatial distribution of mortality, a previous report on these data [85] found the characteristic pattern of higher risk in western Andalucía, when all-cause mortality was mapped at this small geographical level. Thus, PHCD in the provinces of Cádiz, Sevilla, and Huelva, had the highest risk of mortality. When causes of death were analysed by groups, the same spatial pattern remained: this was the case for CVD and cancer (all sites) as well as lung cancer. Interestingly, mortality due to ill-defined causes did not show any geographical pattern. This group of causes of mortality not clearly identified is commonly used as a quality indicator of death certification. Therefore, lack of heterogeneity in the spatial distribution of ill-defined causes showed that geographical disparities in quality of certification were not responsible for the

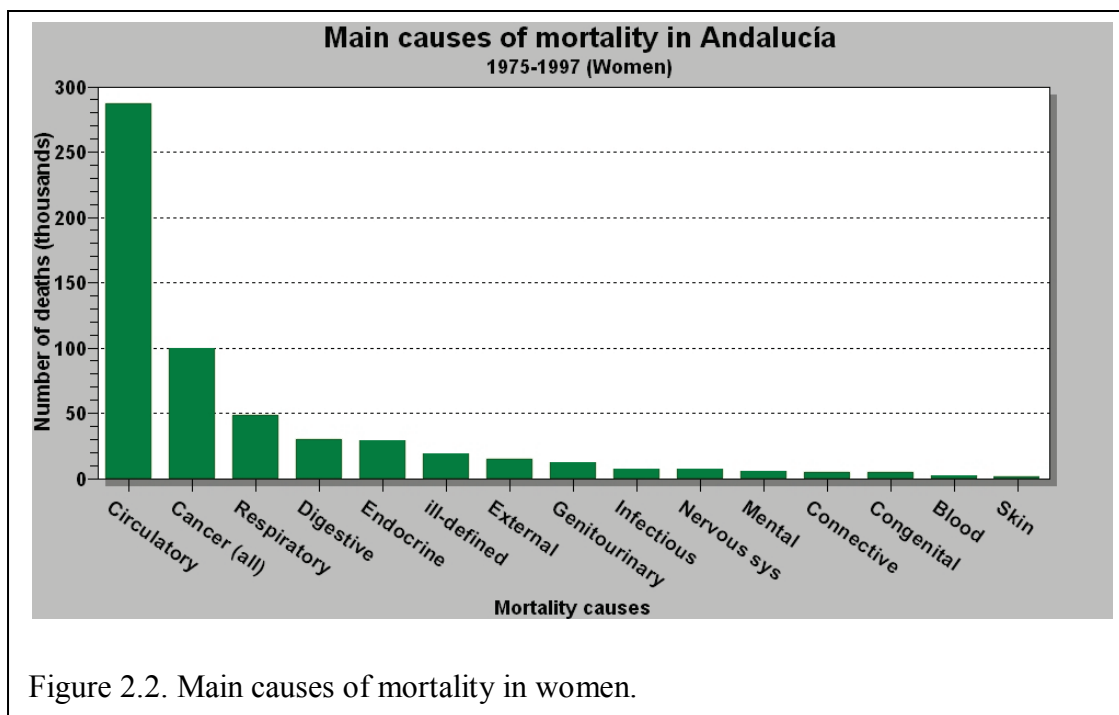


Figure 2.2. Main causes of mortality in women.

geographical pattern in mortality. Only a small proportion of deaths were recorded under this category for both men and women: 2.2% and 3.3%, respectively.

Many risk factors (including tobacco smoking, obesity, arterial hypertension, low rates of physical activity, poor diet, heterogeneity in access to health-care services and quality of health care) have been studied with an aim of explaining geographical disparities in mortality. Also SES, at the individual or area level, has been considered because of its predictive value as a surrogate measure for risk factors exposure.

Nevertheless, known risk factors and socio-economic determinants, as studied to date, are only considered to account for a small fraction of the known variability. Although not completely understood, environmental, social and occupational factors have been also suggested that should be related to this mortality pattern. Thus, an editorial published by Benach [10], highlighted the pattern of higher mortality in western Andalucía, during the period 1987-1995: only 8% of the Spanish population lived in the provinces of Cádiz, Huelva and Sevilla. In contrast, one third of all deaths in Spanish high-risk mortality areas occurred in towns within these three provinces. Occupational, environmental and socio-economic factors were considered worthy of further investigation, as up-to-date knowledge had not provided a complete answer to this public health issue.

In addition, some components of SES seem to play an important role in this striking pattern of geographical disparity: namely illiteracy, unemployment and overcrowding.

Moreover, some already known risk factors, such as tobacco smoking, are strongly related to SES [24, 31]. This strong dependency between SES and tobacco smoking led Escolar-Pujolar [101] to think that the relevance of factors responsible for this geographical pattern of higher mortality in south-western Spain has varied with time. Based on the Atlas of Mortality in the Province of Cádiz for the period 1975-1979, the author concluded that this mortality pattern already existed before current industries started operating in the province. Neither petrochemical plants nor manufacturing industries such as cellulose, gas, steel, or thermal power stations operated before 1967. The author hypothesised that no single factor was responsible for this mortality pattern and causes are probably changing across time. Therefore, higher mortality observed in the area of '*Campo de Gibraltar*' (towns of Jimena de la frontera, Castellar de la frontera, San Roque, La Línea, Los Barrios, Algeciras and Tarifa) was thought to be mediated by poverty and tobacco exposure. Poverty, acting as a surrogate measure for exposure to various risk factors, could explain the excess of mortality due to cancer of different sites. Low SES has been associated with worse living conditions and less healthy life-style (including higher rates of tobacco smoking). According to the author, this was the case in *Campo de Gibraltar* for many decades before the study period (1975-1979) while new environmental hazards may contribute to the excess mortality which occurred afterwards. That deprivation may play a substantial role in the spatial distribution of mortality in Andalucía is in accord with an earlier small-area analysis by Benach et al. [7]; the spatial distribution of a deprivation index (that comprised unemployment, illiteracy, and overcrowding) was shown to mimic that of higher mortality rates in western Andalusian municipalities.

Tomatis [31] showed, in a review paper, how lower SES is related to higher incidence and mortality due to differing cancer. Thus, lung and larynx cancer are amongst the tumours for which this differential has been found to be greatest. SES is considered to be an intermediate factor between different kinds of exposures and disease incidence and mortality. Many different variables are in use to measure SES. For instance, lower education is associated with worse living and working conditions, material deprivation, and less healthy life-styles. Furthermore, education seems to be a better predictor (of incidence and mortality due to cancer) than occupation. Exposure differences between people of high and low SES are related to well-known aetiological risk factors, such as tobacco smoking and alcohol drinking, which are

more frequent amongst people of lower SES. Nevertheless, these risk factors cannot completely explain differences in mortality. Hence, the residual higher risk remaining in lower SES groups when analysing lung cancer, even after adjusting for tobacco smoking habit. This review [31] highlights the need of accounting for deprivation in small-area studies, as this covariate is not only a surrogate measure (and a potential confounder) for tobacco smoking [102], but also for many other exposures [103].

Kogevinas et al. [24, 66] also reviewed the association between SES and cancer. An excessive incidence of and mortality from respiratory cancers (lung, larynx, and nose) has been reported in men of lower SES; there is also an excess of risk, in people of lower SES, for tumours of the mouth, pharynx, oesophagus, stomach, and cancer as a whole, in different populations from various countries. Conversely, higher SES has been associated with some other cancer sites (colon, brain and skin). Tobacco smoking has been aetiologically associated with cancer of different sites, especially lung, larynx, mouth, pharynx and bladder. In most industrialised countries (including Spain) rates of tobacco smoking are higher in people of lower social class and these differences are greatest amongst men. Occupation is another important intermediate factor frequently measured as a component variable of SES, as manual workers tend to be more frequently exposed to hazardous substances with carcinogenic effect. An excess of risk for cancer development and mortality has also been associated with unemployment. Interestingly, this risk remains after tobacco smoking, social class and alcohol drinking are accounted for. Exposure to environmental factors is also mediated by SES; some evidence suggests that people of lower SES are more frequently exposed to certain air pollutants, which in turn is a risk factor for lung cancer [103, 104]. Notwithstanding this link between deprivation and exposure to environmental pollutants, recent research has shown that this association can be either positive or negative, depending on the environmental factor under consideration. As an opposite example to tobacco smoking, a negative association has been shown to exist between deprivation and radon-gas exposure; that is to say, people residing in less deprived areas have been found to be more exposed to radon-gas [103].

Amongst various mortality causes due to different cancer sites, lung cancer was identified as the leading cause of cancer-related mortality for men, in the report published by the Andalusian Health Office for the period 1975-1997 [23]. With age-standardised rates of 81 deaths per 100,000 men, 44,027 cases (or 30.4% of all male

deaths due to cancer) were recorded for the whole period. This cancer site was the fifth cause of mortality for women with age-standardised rates of 5 deaths per 100,000 women: 4,532 cases (or 5.5% of all female deaths) in that 22 year period. Figure 2.3 and Figure 2.4 show the burden due to each cancer site according to number of deaths for men and women, respectively.

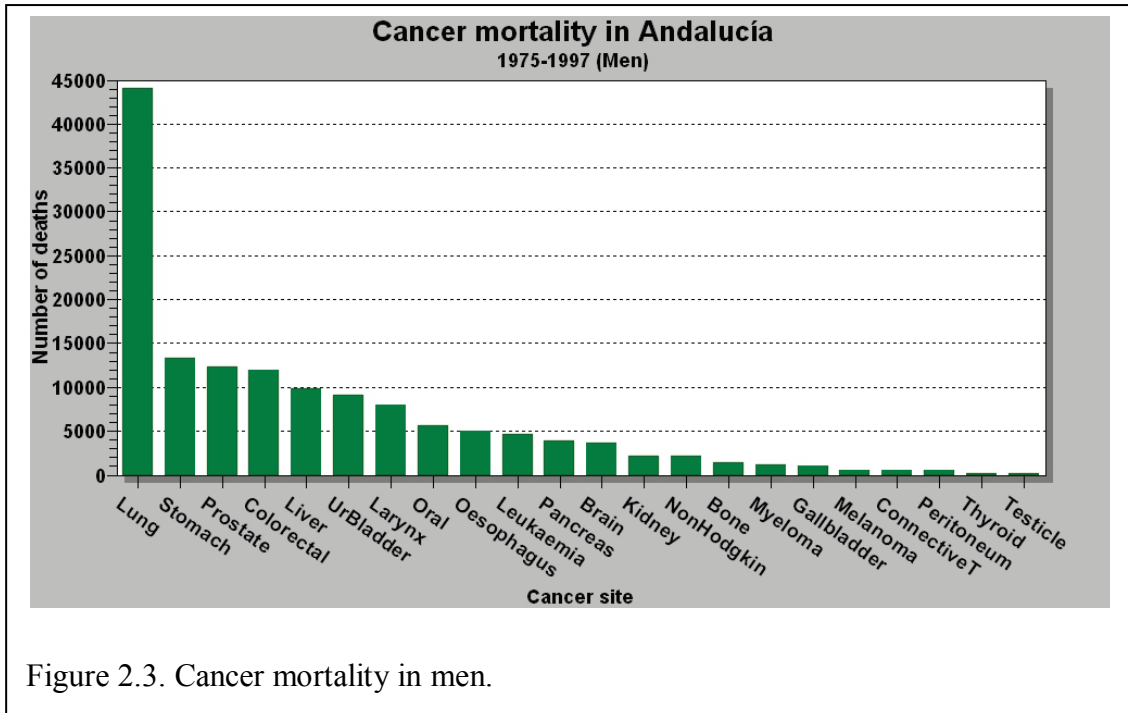


Figure 2.3. Cancer mortality in men.

A small-area analysis at the municipal level (8,000 Spanish towns) was published by López-Abente et al. [16] for a period (1989-1998) overlapping that of the report by the Andalusian Health Office (1975-1997) [23]. Poisson log-linear hierarchical regression models were used to account for spatial autocorrelation, which is an important source of overdispersion in models dealing with counting data. Specifically, the BYM model was used. Updated information on lung cancer was provided by the authors who highlighted that this tumour still had, in 2004, a very poor prognosis (only a five-year 12% age-adjusted survival rate) and was the most frequent malignancy in men (28% of mortality due to neoplasms); in women lung cancer caused 5% of all deaths due to cancer. According to the authors, age-adjusted rates in men reached maximum levels in 1995 and then declined. Conversely, age-adjusted rates in women started to rise at the end of the 1980s. The authors observed specific cohort effects in women: those born before 1917 experienced a progressive increment in risk; mortality decreased

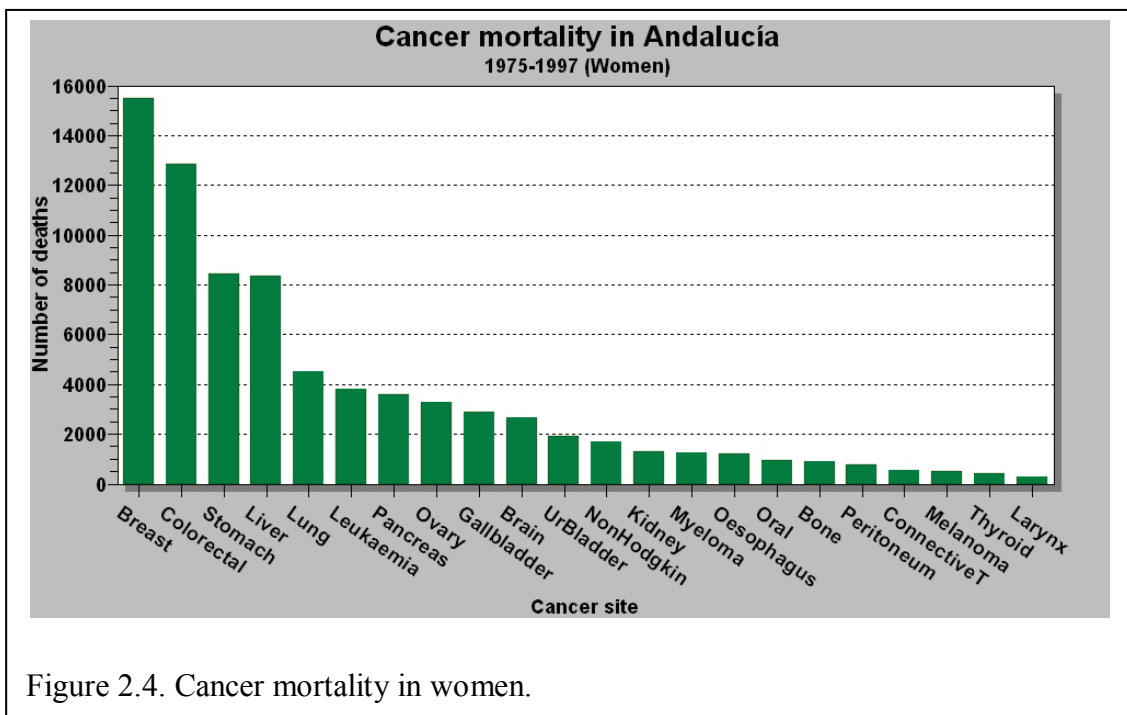


Figure 2.4. Cancer mortality in women.

then in women born before 1940 and risk rose again for birth cohorts born after 1940, in parallel with tobacco smoking consumption amongst women. This led the authors to hypothesise that a lung cancer epidemic in women could be expected.

The characteristic geographical pattern was again found in this small-area analysis: mortality due to lung cancer was higher in towns in south-western Spain (provinces of Cádiz, Huelva, Málaga, and Sevilla). However, this pattern previously observed had

been extended during this study period (1989-1998) to the adjacent autonomous community of Extremadura, to the northwest of Andalucía. As the geographical unit of analysis (towns) was smaller than the one used in previous studies (provinces) the authors could describe in more detail how towns on the coast line had the highest rates in known high-risk provinces. This finding was attributed to higher urbanisation of those municipalities. The authors considered of special interest mapping of lung cancer mortality in women, given that mortality in this period was mainly represented by birth-cohorts older than the generation born after 1940, when Spanish women massively acquired the habit of tobacco smoking. Therefore, risk factors (e.g. environmental exposures) other than tobacco smoking could be responsible for any geographical pattern in women's mortality. Thus, the high mortality rates also observed in north-west Spain (autonomous region of Galicia) were considered to be potentially associated with radon-gas exposure; these conclusions were supported by high levels of radon-gas detected in this area. On the other hand, high rates in Barcelona (north-east Spain) were presumed to be due to industrial pollution. Nevertheless, no hypothesis (other than urbanisation) was offered for the high rates observed in towns of south-western Andalucía.

Additionally, the authors claimed that distinct risk factors could be responsible for differences between men and women. This hypothesis was based on distinct histological types usually found between sexes: squamous-cell carcinoma and SCLC, which are strongly related to tobacco smoking, are more frequent in men. In contrast, adenocarcinoma is more commonly diagnosed in women. Another cancer site, larynx, was also found to have a geographical pattern of mortality similar to that of lung cancer. Larynx cancer has been causally associated with tobacco smoking (and alcohol intake). In 2004, Spain was the European country with the highest incidence and mortality due to larynx cancer, in men. Conversely, in women, incidence and mortality rates due to larynx cancer was amongst the lowest in Europe. In Andalucía, the provinces of Huelva, Sevilla, and Cádiz showed the highest mortality rates, similar to rates of mortality due to lung cancer. However, unlike lung cancer, larynx cancer showed a high age-adjusted survival rate (60% five-year survivorship).

2.4.1 Aetiology and epidemiology of lung cancer

One of the earliest investigations into the association between tobacco smoking and carcinoma of the lung was a case-control study published by Doll and Hill [87], that

compared more than 2,000 hospitalised patients; cases had been diagnosed of cancer of the lung, stomach and large bowel, while a second group of patients with diagnoses other than cancer were used as controls. A much larger proportion of smokers were found amongst lung cancer patients than control. Also, a dose-response relationship between tobacco smoking and lung cancer was found, although no differences were found, for the effect of smoking, between those that inhaled and did not inhale the smoke, a finding that the authors could not explain. At that time, arsenic was the only known substance present in tobacco manufactures thought to have a possible (but not yet proved) carcinogenic effect. In this study [87], no association was found between tobacco smoking and incidence of cancer other than lung cancer or non-cancer diseases (including other respiratory conditions and cardiovascular diseases).

The authors were very cautious about drawing any conclusions concerning a potential causal association between smoking and lung cancer, given the weak biological plausibility of such a relationship at that time. Nevertheless, this case control study was carefully designed and analysed: subjects were comparable as they were all recruited from the same setting (hospitalised patients). Lack of any associations between tobacco smoking and diseases other than lung cancer, as well as with the smoking pattern (smoke inhalation) would be afterwards contradicted by the analysis of a large cohort-study also published by Doll [105, 106]. This disagreement in the results between both studies could have been due to the small number of cases analysed in the case-control study, as compared with the cohort study (2,475 vs. 34,439). An ample group of people were studied that suffered from different diseases, including cancer sites other than lung, which was useful to counteract any differences attributable to recall bias. The finding of a dose-response relationship (drawn by means of a detailed and structured smoking history) supported the tenet of a causal relationship between tobacco smoking and lung cancer.

Tobacco smoking has been causally associated not only with cancer of the lung but also with cancer that affects other close organs such as the mouth, pharynx, larynx and oesophagus, as well as distant ones such as bladder and kidney. Contrary to the state of knowledge at the time when Doll and Hill accomplished their case-control study in 1950 [87], nowadays it is known that tobacco smoking entails exposure to thousands of substances, 100 of which, at least, are known to have possible carcinogenic effect [107]. According to a review by Shields [108], one of the most important carcinogenic

substances present in tobacco smoke are tobacco-specific nitrosamines (TSNs) as the concentration of this substance in tobacco manufacturing has increased. In contrast to TSNs, nicotine (which is responsible for addiction to tobacco smoking) has decreased with time. This has, in turn, led smokers to consume more cigarettes and to inhale smoke more deeply so that they are able to maintain nicotine concentration in their blood and thus avoid abstinence syndrome [108].

The mechanism by which TSNs contribute to develop lung cancer (as well as cancer of other sites) is well understood [107, 108]. TSNs are formed during the process of tobacco manufacturing and are known to induce deoxyribonucleic acid (DNA) damage by forming different types of chemical adducts. As DNA contained within cell nuclei is responsible for the genetic information involved in cell replication, alteration of this process leads to uncontrolled reproduction of organ cells, which initiates carcinogenesis. The ultimate mechanism by which carcinogenic substances present in tobacco smoke exert their effect seems to be mediated by interfering with DNA repair through gene mutations. The level of exposure to these carcinogenic substances present in tobacco smoke seems to be determined by the individual smoking habit of each tobacco user: firstly, the lifespan of the habit and number of cigarettes smoked per day; secondly, the type of cigarettes consumed as composition varies between brands and thirdly, the way cigarettes are consumed (e.g. the depth of inhalation and frequency). Individual susceptibility is also thought to play an important role in determining cancer risk [108]. Thus, increased susceptibility to mutagenic effects has been found in lung cancer patients that were smokers.

Differences in cancer risk are also known to exist between sexes. Men tend to suffer from SCLC, while adenocarcinoma is more frequently diagnosed in women; moreover, women have twice as high a risk as men. Some researchers have hypothesised that these differences between sexes could be related to exposure to different environmental carcinogens: tobacco smoke for men and radon-gas for women [16]. Alternatively, Shields proposed that these differences could be due to different smoking patterns [108]. Hence, women would be exposed to greater concentrations of TSNs as they acquired the tobacco habit more recently, i.e., when cigarettes already had higher concentrations of this carcinogenic substance. There is also evidence of higher levels of DNA adducts mediated by other chemical compounds, such as Polycyclic Aromatic Hydrocarbons (PAH), in women, which

supports the hypothesis that women are more susceptible to the adverse effects of tobacco smoking.

Alberg et al. published a comprehensive review on the aetiology of lung cancer. In this paper, the authors claimed that both epidemiological and biological evidence have undisputedly established the causal relationship between tobacco smoking and lung cancer [109]. Moreover, tobacco smoking is considered to be responsible for more than 90% of all lung cancer cases. This association between tobacco smoking and lung cancer had been found in many case-control studies [87, 110] in the UK and the USA (amongst other countries) in the 1950s and was later on confirmed by large studies such as the British doctors' cohort study by Doll et al. [87, 111] that followed a cohort of more than 34,000 British male doctors for a 50-year period (1951-2001). Data on participants' habits were periodically assessed. This study provided new insight into tobacco smoking and mortality due to cancer of different sites. Tobacco smoking was associated not only with lung cancer but with many other cancer sites, such as oral and nasal cavities, sinuses, larynx, oesophagus, liver, stomach, pancreas, kidney, bladder, uterus, and with myeloid leukaemia [111]. Although only one in ten smokers suffers from lung cancer, 50% of the smokers die prematurely from a tobacco-related disease. This study showed that a smoker's life expectancy is reduced by 20 years as compared to a non-smoker. Nevertheless, quitting smoking at any age partially reduces this difference between smokers and non smokers. Results from the study by Doll et al. [87, 106] were closely in agreement with a review by the International Agency for Research on Cancer (IARC) concerning the carcinogenic effect of tobacco smoke [112]. This study found a positive association between tobacco smoking and cancer of 28 different sites; for these types of cancer, a dose-response relationship with tobacco smoking was also found.

It has been shown that smokers have a 20-fold increase in risk for lung cancer compared to non-smokers [109]. Furthermore, rates of tobacco smoking predict those of lung cancer 20 years later. Amongst the main determinants, duration of the smoking habit is now considered to be the most relevant predictor of lung cancer development, over and above the number of cigarettes smoked. Although quitting smoking is always beneficial, risk in ex-smokers remains higher than in never-smokers for more than 40 years after the habit has been abandoned [109]. Research in molecular epidemiology [107, 113] has found that individual susceptibility is associated with gene-environment

interaction that may determine heterogeneity of outcomes after exposure to similar levels of tobacco smoke.

Thus, gene-environment interaction can modulate factors such as metabolism of carcinogenic substances and production of DNA adducts [107, 108], which is thought to also underlie race and sex differences for susceptibility to tobacco smoke, as well as patterns of smoking behaviour (mediated by dopamine receptors in the brain). These patterns can explain why changes introduced in cigarette manufacturing in the 1950s (such as low tar and low nicotine, as well as filtered cigarettes) that were thought in the past to entail a lower risk for lung cancer, caused exactly the opposite effect. Doll et al. [106] compared risk of mortality within the cohort of British physicians between the two 20-year periods and showed a higher risk of mortality for the second half of the follow-up period. This has been explained by changes in the smoking pattern due to lower content of nicotine and higher content of TSNs present in cigarettes manufactured since 1950.

Some epidemiological reviews [107] have included cohort studies which have shown that tobacco smoke is associated with lung cancer, in non-smokers who are passively exposed to tobacco smoke. Thus, it has been reported that non-smokers who were married to smokers had a 20% increase in lung cancer risk [109]. Although a dose-response relationship between tobacco smoking and lung cancer has been shown to exist, it is interesting to note that a threshold level seems not to exist; that is to say, some risk still remains even at levels of exposure much lower than those experienced by active smokers. It is considered by some authors [107-109] that tobacco smoke can lead to different histological types of cancer: the more common ones are squamous-cell carcinoma, adenocarcinoma, and SCLC, while others [16, 114] have hypothesised that these differences can be the result of distinct environmental exposures (such as radon-gas).

Many environmental factors other than tobacco smoke have also been associated with lung cancer. Thus, occupational factors such as arsenic, chromium, nickel and asbestos (the last one interacting synergistically, in a multiplicative way, with tobacco smoke) cause lung cancer [109]. Ionizing radiation is also known to be a risk factor to develop lung cancer. This is the case for High Linear Energy Transmission (LET) radiation, such as radiation from radon-gas exposure, which produces more organ damage than low-LET radiation (e.g. x-rays) [109]. Radon-gas is known to emit alpha particles that

cause permanent damage of tissues in organs. As for tobacco smoke, a non-threshold dose-response relationship is thought to exist between exposure to radon-gas and lung cancer [115]. Radon is now considered to be second to tobacco smoke in the number of lung cancer cases attributable to exposure to environmental factors [116]. Radon-gas has been considered to be responsible for 10% of all lung cancer cases in the US [117]. It is considered that tobacco smoke can act synergistically with other factors to initiate or promote lung cancer. For instance, it is thought that tobacco smoke and radon-gas exposure have a supra-additive (but not multiplicative) effect for lung cancer risk [114].

Indoor air pollution due to both second-hand tobacco smoke and radon-gas exposure are considered to be the most important environmental risk factors for lung cancer. Conversely, outdoor, air pollution is thought to be accountable for a small fraction (compared with tobacco smoking) of lung cancer cases (around 1% to 2%) [114]. This could partially explain the association consistently found between the degree of urbanisation and lung cancer mortality. Nevertheless, other factors such as smoking patterns and occupation could contribute to these differences. In a small-area analysis about the effect of urbanisation on lung cancer Pearce et al. [118], after adjusting for smoking rates at the area-level, found that tobacco smoking explained most of the risk associated with urbanisation, although some residual variation remained unexplained. This excess of risk associated with urbanisation was thought to be due to factors such as air pollution, occupation, or selective migration of people at higher risk for lung cancer.

Although the study by Pearce et al. [118] was devised as an ecological design, it was analysed at the small-area level, which is thought to lessen the potential bias due to the ecological fallacy [1]. Interestingly, information about the smoking pattern was available by output areas (which comprise around 50 households). The observed number of cases was modelled using multivariate Poisson regression analysis, while adjusting for age-group, sex, tobacco smoking behaviour at area level, and population density. Although potential overdispersion due to spatial autocorrelation was not accounted for, a scan statistic was used for clustering detection.

Bray et al published an age-period-cohort analysis in 15 European countries for the period 1967-1999 which showed that lung cancer was the leading cause of mortality due to cancer; this cancer site accounted for 90% of cancer cases in men and 60% in

women [119]. Differences in mortality rates amongst countries were attributed to heterogeneity in the prevalence and pattern of tobacco smoking. To differentiate between effects due to smoking patterns and carcinogenic exposures which occurred many years in the past (attributable to changes in tobacco manufacturing) young cohorts were studied. During this study period (1967-1999) death rates in Spanish men aged 35-65 years started to stabilise. In contrast, there was evidence of a rise of epidemic proportions (3% annual increase) for death rates in Spanish women. Data pointed at women born around 1950 as those accounting for this cohort effect, because of the increase in the prevalence of smoking among women, which is consistent with previous knowledge about trends in the prevalence of smoking amongst Spanish women [16].

Another study by Levi et al. [120] further studied lung cancer mortality in young women. Mortality due to lung cancer in females aged 20-44 years was analysed for the period 1970-2004 in six European countries. In Spain, mortality rates decreased between 1979 and 1985 and then steadily increased (from 0.8 deaths /100,000 people in 1985-1989 to 5.0/100,000 in 2000-2004). Between these two periods, the prevalence of smoking in young women rose from less than 40% to around 50%. If public health interventions do not counteract the prevalence of smoking in Spain, the current situation is expected to lead to a lung cancer epidemic in women, within the next 20 to 30 years. Mortality rates could reach 20/100,000, according to these authors. Although this is an ecological study, tobacco smoking is known to be responsible for most cases of lung cancer [107]. This is why the conclusions of the study by Levi et al. [120], concerning a rising in mortality due to lung cancer amongst young Spanish women, are in accordance with data on the trends of the smoking prevalence in women.

2.4.2 Aetiology and epidemiology of Chronic Obstructive Pulmonary Disease (COPD)

It is interesting to note that cancer is not the only health hazard causally associated with tobacco smoke [113, 121]. COPD is a health condition that causes permanent damage of the airflow and eventually leads to disability and death. COPD is known to be mainly due to tobacco smoking. Respiratory diseases (from which COPD is the major component) were the third most important cause of mortality in both men and women residing in Andalucía during the period 1975-1997 [23] (see Figure 2.1 and

Figure 2.2). What is more intriguing is the fact that some evidence suggests that COPD could be responsible for lung cancer as well, that is to say, after accounting for the effect of tobacco smoking [100, 122]. However, given the strong association between tobacco smoking and COPD, it seems analytically difficult to separate both effects as COPD might be an indicator of a heavier exposure to carcinogens from tobacco smoke.

In a review by Viegi et al. [100], COPD was considered to be the third most common cause of morbidity and mortality in Europe. This was the also the case for Andalucía during the period 1975-1997. COPD is an inflammatory disease which leads to progressive, non-reversible, airflow limitation. The two main COPD components are chronic bronchitis and emphysema. Chronic inflammation of the bronchi produces characteristic symptoms such as frequent cough and expectoration that helps in diagnosing COPD episodes on clinical grounds. The second component, emphysema, is related to the non-reversible nature of COPD course, as it describes histological changes comprising destructive enlargement of walls in the smallest, more distant, air spaces (alveoli). Emphysema eventually leads to Chronic Respiratory Failure (CRF), as exchange of oxygen (needed for normal cell function) and carbon dioxide (or CO₂, a toxic metabolite which is exhaled) takes place within the blood vessels irrigating the alveoli walls. CRF, in turn, is characterised by low levels of oxygen (hypoxaemia) and high levels of CO₂ (hypercapnea) in the blood. All these changes are responsible for progressive deterioration of performance status. Patients suffer from shortness of breath after variable efforts when they are at the initial stage of the disease or even at rest, when alveoli destruction is at the end-stage. Moreover, COPD is frequently associated with other diseases (co-morbidity) such as other respiratory diseases (pneumonia, asthma and pulmonary embolism [100, 123]), cardiovascular conditions (ischaemic heart disease and heart failure [124]), malignancies (lung cancer [125, 126]), endocrine diseases (diabetes [123]) and psychiatric disorders (depression and anxiety [127]), amongst many others.

Therefore, COPD has a very strong negative impact on health-related quality of life (HRQoL) measures. COPD has been causally associated with tobacco smoking, which has been identified as the major risk factor for COPD incidence and mortality. Furthermore, Doll et al. showed a dose-response relationship between tobacco smoking and mortality due to COPD, from the analysis of their 50-year follow-up

cohort study on male British doctors [105]. Age at which the smoking habit starts, the number of cigarettes smoked and current smoking status are all good predictors of mortality due to COPD. There is also a dose-response relationship between tobacco smoking and severity of COPD symptoms. Although some other risk factors for COPD exist (such as air pollution, occupational exposures, and genetic factors) smoking cessation is the single most important preventive measure. Quitting tobacco smoking is also beneficial for COPD sufferers as it helps in diminishing the rate of deterioration of lung function. Viegi et al. [100] had also reviewed other cohort studies where some differences in risk were found between only-pipe smokers and only-cigar smokers. The former had been reported to have an increased risk for mortality due to COPD; the latter were shown to have an increased risk for COPD incidence. Environmental tobacco smoking (ETS), both at work and home, has also been associated with COPD. Hence, second-hand tobacco smoking is responsible for numerous deaths due to COPD and lung cancer in females. Particulate matter (PM), nitrogen dioxide (NO₂) and carbon monoxide (CO) and biological allergens are other potential indoor pollutants that can cause respiratory disease. Some urban-related factors, such as traffic load and outdoor NO₂, have also been associated with the prevalence of COPD symptoms. It is important to note that COPD is no longer considered to exclusively affect a small proportion of elderly male smokers. Contrary to previous knowledge, COPD is now known to affect a large proportion of smokers (22% in a prevalence study of Spanish smokers aged 40-76 years [128]); it may already be present in those as young as 20-45 years and the differences between sexes are decreasing. Prevalence of COPD is frequently underestimated given the poor correlation between lung function status and presence of symptoms (cough, expectoration and dyspnoea). This is partly due to the fact that patients change their habits to prevent dyspnoea. Therefore, symptoms may not be present until the end-stage of COPD. Nevertheless, COPD can be diagnosed using spirometry tests even at early stages of the disease [100, 128].

In another review, Mannino et al. [122], highlighted the relevance of COPD due to morbidity, mortality and health costs attributed to this disease and also that this public health problem is only expected to increase due to the ageing population across the world. According to this review, in 2001 COPD was recognised to be the fifth leading cause of mortality in high-income countries and the sixth in low-income ones. COPD

also accounts for a high number of cases of disability. Different COPD phenotypes are thought to exist depending on which disease component predominates - cough and expectoration, airways reactivity, emphysema- or genetic factors. It was stressed that diagnosis should be based on (post-bronchodilator) spirometry tests as it is known that clinical diagnosis may under-estimate COPD prevalence and spirometry (without bronchodilation) may over-estimate presence of COPD. Furthermore, lung-function spirometry tests are good predictors of mortality, especially when used in conjunction with measurement of Body Mass Index (BMI), as well as dyspnoea and exercise level [129]. Although tobacco smoking was admitted to be the major risk factor to develop (and die from) COPD, other factors were also recognised to be responsible for a small proportion of COPD cases. Thus, alpha-1 antitrypsin deficiency is thought to account for 1% to 3% of all COPD cases, although the risk of developing this disease is enhanced by tobacco smoke [130].

This paper by Mannino et al. [122] also reviewed exposure factors such as outdoor and indoor air pollution. Around 19% of COPD cases in the USA have been considered to be caused by occupational exposures (fumes, dust, and chemical vapours). Non-smoking Chinese women in rural areas may suffer a threefold increased rate in COPD compared to non-smoking women in urban areas, as a result of their indoor exposure to fumes (e.g. from coal and wood). Notwithstanding these other risk factors, it is important to note that tobacco smoking is thought to account for 73% of mortality due to COPD; also, that contrary to previous knowledge it has been shown that a high proportion of smokers (up to 50%) develop COPD. Interestingly, in contrast to the relationship found between environmental tobacco smoking (ETS) and lung cancer, second-hand tobacco smoking has been found to increase the risk for respiratory symptoms, but not for COPD. Outdoor air pollution has been estimated to be of much less importance than tobacco smoke and occupational exposures in the development of COPD (only 1% to 2% of all cases). This review also found that differential prevalence between sexes seems to be diminishing as there has been a massive increase in women's smoking.

Low socio-economic status (SES) has also been found to be associated with the incidence of (and complications from) COPD [100, 121]. SES is considered to be a surrogate measure for exposure to various risk factors (such as tobacco smoking and other pollutants, as well as infections). As COPD patients tend to suffer from many

other co-morbid diseases, mortality due to COPD is known to be frequently attributed to other causes (e.g. cardiovascular diseases). Although tobacco smoking is the major risk factor for COPD, a significant proportion of smokers do not develop the disease, which highlights the influence of other risk factors [131]. The increasing number of women and adolescents who smoke tobacco is contributing to the increment in the incidence of COPD. Much of the variation in the prevalence of COPD may be caused by differences in the way the disease is diagnosed, as various organizations have published different disease definitions. Longitudinal studies have shown that reversion of airway obstruction by treatment can improve survival rates of COPD patients [126].

The 10-year survival rate of COPD patients has been reported to be only 50%, which highlights the importance of this disease as a cause of mortality given that, on average, people are first diagnosed when they are 40-50 years old [121]. COPD progresses from a lack of appropriate development of lung function during infancy through a progressive impairment in adulthood for several decades. Mortality has been shown to be associated with some clinical components of the disease, namely mucus hypersecretion (that leads to expectoration) and breathlessness. Mucus hypersecretion, in turn, is associated with impairment of lung function as is reflected by a decrease in Forced Expiratory Volume in 1 second (FEV1) and hospitalisation due to lower respiratory infections. HRQoL is also known to be greatly affected by the disease. Prevalence of COPD is difficult to estimate as clinicians usually see only severe cases but miss mildly ill patients who are the main bulk of the disease. Mortality due to COPD is also thought to be under-estimated due to co-morbidity and misclassification, especially if only the underlying cause of death is used to classify cases. Common causes of death in these patients are pulmonary infections and embolism, as well as complications involving the heart ('cor pulmonale') [132].

Evidence from longitudinal studies suggests that women are more susceptible to COPD than men. It is thought that bronchial hyperreactivity in response to environmental exposures may lead to a higher degree of decline in FEV1 for either smoker or ex-smoker women as compared with men. This review [121] also considered tobacco smoking as the major risk factor for COPD development. Both cross-sectional [133] and longitudinal studies [134] have shown an association between tobacco smoking and decreased FEV1. A dose-response relationship has also been shown to exist between both. Low socio-economic status (SES) is also associated

with lower FEV1. Different components of SES, such as poor schooling, poor housing and low income, have all been shown to be independent predictors of impaired lung function. These socio-economic variables are considered to be surrogate measures for exposures either in utero, or early in life (e.g. smoking, respiratory infections, nutritional, occupational or housing factors).

A brief review by Devereux [135] recognised the association between COPD and all kinds of tobacco smoking. Although cigarettes are the most important risk for COPD, pipe and cigar smoking have also been associated with COPD development. The main components of COPD are known to be airflow obstruction, chronic bronchitis and emphysema. Asthma is usually considered to be a separate entity, although it can occur in association with COPD. Up to 40-50% of COPD cases may remain undiagnosed given that spirometry tests are not always undertaken. COPD used to be more common in men and is known to be associated with low socio-economic status. The author considered that COPD was expected to become the third leading cause of mortality in Europe by 2020. Case-control studies [133, 135] have found that second-hand tobacco smoking is associated with COPD development. Smoking during pregnancy is also known to impair the ventilatory function during infancy, childhood and adulthood. Hence, antenatal exposure is thought to be of greater impact on health than postnatal exposure.

2.4.3 Aetiology and epidemiology of larynx cancer

A pooled analysis of case-control studies undertaken in Europe and America was devised to estimate the multiplicative interaction parameter and population attributable-risk (PAR) due to the biological interaction between tobacco smoking and alcohol drinking in the development of head and neck cancers [136]. Of all head and neck cancer sites, 72% were attributed to tobacco smoke or alcohol; tobacco smoke alone was accountable for 33% of cases, while 4% of cases were attributed to alcohol alone, and 35% of cases to the combined use of tobacco and alcohol. The estimated joint effect of both tobacco and alcohol use, on the incidence of all head and neck cancer sites (including larynx cancer, although not statistically significant), was greater than multiplicative. A statistically significant more than additive interaction (between tobacco smoke and alcohol) was found for larynx-cancer risk [136]. Estimates were adjusted for educational level and sex. The PAR (due to both tobacco smoke and alcohol) for laryngeal cancer was 89% (95% CI: 82-92). Both risk factors

combined are responsible for a greater proportion of cases in men than in women and in the older age groups, while in women, tobacco smoke alone is responsible for a greater number of cases than the combination of both exposure factors.

Although the relationship between tobacco smoking and lung cancer was established in the 1950s, the associations of tobacco smoke with other cancer sites was found around thirty years later. In a meta-analysis of studies dealing with tobacco smoking and cancer of different sites, Gandini et al [137] found that the pooled relative risk (RR) estimate (current vs. former smokers) for larynx cancer (RR =6.98; 95% CI = 3.14 - 15.52) was the highest one after lung cancer (RR = 8.96; 95% CI = 6.73 - 12.11). Other findings were that RR estimates varied by study design, gender, and adjustment for confounding factors. Thus, RR estimates were higher for case-control studies than cohort studies. High incidence rates of larynx cancer have been found in men from southern and central Europe, people from South America and black people living in the USA [138]. The predominant histological type is squamous-cell carcinoma (more than 90%). The risk for larynx cancer is 10 to 15 times greater for smokers than for non smokers and this neoplasm predominantly affect the glottis area (that is, the voice box). Most cases of larynx cancer in rich countries are attributed to tobacco smoking, alcohol drinking, or the combined effect of both toxic agents. As for the association between tobacco smoking and lung cancer, a dose-response relationship also exists between tobacco smoke and laryngeal cancer: therefore, the risk increases with duration of the habit and amount of tobacco smoked. The same way, the risk progressively decreases and approaches non-smokers risk after 15 years of smoking cessation. Dark tobacco users seem to undergo a higher risk for larynx cancer than Virginia tobacco smokers. It seems that filters may provide some protection. Forms of tobacco use other than cigarettes (including smokeless tobacco) also increase the risk for laryngeal cancer.

Smoking is known to account for up to 15% of all cancer cases. The proportion of attributable-cases is higher in men and in rich countries. Stopping smoking has been recognised as the most important preventive measure even for long term smokers [113]. Mortality is lower amongst smokers of low tar cigarettes; however, it is known that smokers of low-nicotine, low-tar cigarettes, increase depth of inhalation to maintain blood levels of nicotine. This, in turn, increases their exposure to carcinogenic substances present in tobacco smoke. The mainstream smoke produced

by cigarette combustion, that is, the smoke inhaled by the smoker, is known to contain thousands of chemicals. Many of the by-products present in tobacco smoke are known to have carcinogenic effects and 80% of these particles deposit in the trachea and bronchi. Conversely, sidestream smoke reaches the ambient air directly from a smouldering cigarette; this smoke contains more tobacco substances as it has not been filtered. Although sidestream smoke is diluted in the ambient air, it is important to note that no safe limit exists for exposure to carcinogenic substances. Particles from the sidestream smoke deposit in the smaller lung airways. Carcinogenesis starts when the balance between cellular mitosis (replication) and apoptosis (death) is lost. This happens as a consequence of mutations in either oncogenes (genes that promote cell growth) or suppressor genes (that determine apoptosis).

For tobacco smoke to be detoxified carcinogenic substances must be transformed by phase I enzymes and then eliminated by phase II enzymes. However, carcinogenic substances can be activated by phase I enzymes, which produce DNA-adducts. This, in turn, allows cells to grow uncontrollably [109]. As cells have their own repair mechanisms, decades of exposure to tobacco smoke are needed to eventually develop cancer. Nowadays it is estimated that more than a billion people in the world smoke, mainly in east Europe and central Asia [113]. Tobacco smoking has become a habit of the poor and globally of men. However, the situation is changing in developed countries where wealthier people quit smoking more frequently.

Interestingly, a protective effect seems to exist for some diseases, namely endometrial cancer and female breast cancer, as well as prostate cancer; this seems to be due to the anti-oestrogenic effect of tobacco smoke on the former two instances, and the anti-testosterone effect on the latter [113]. Other exposure factors such as diet and genetic traits can act as effect modifiers of tobacco smoke. Thus, high fruit and vegetables intake is thought to give some protection against lung cancer as high levels of some vitamins (E, C, retinol, alpha-tocopherol and beta-carotene) were found to be negatively associated with presence of Polycyclic Aromatic Hydrocarbon (PAH) DNA adducts, therefore protecting smokers from cancer. Alcohol is also known to be an effect modifier as it would facilitate penetration of carcinogenic substances from tobacco smoke within human tissues. Cancer is known to be more frequent amongst the elderly, which has been associated with longer duration of exposure to smoking and impaired DNA-repair processes. The same inverse relationship exists between

inherited absence of the enzyme glutathione S-transferase mu gene (GSTM1) and presence of PAH DNA-adducts, which in this case entails higher risk for larynx cancer as cells would not be able to excrete metabolites of carcinogenic substances. Evidence also suggests that the same mechanisms are implicated in cancer development due to second-hand tobacco smoke where haemoglobin adducts have been identified [139].

Therefore, tobacco smoking has been known for a long time to be a major risk factor for disease incidence, disability, and mortality. Thousands of chemical components produced during tobacco combustion exert such a potent effect, that second-hand tobacco smoke, as an indoor pollutant, has also been long recognised to be a main public health problem. More recently, potential health-hazards due to third-hand smoke (THS) have been under investigation [140]. THS has been characterised by the so called three Rs, as tobacco pollutants: *remain* on surfaces and dust for a long time (at least months); they can be *re-emitted* into the ambient air, and *react* with other chemicals in the environment to further produce new contaminants. For instance, one of the most well known tobacco by-products, nicotine, has been found to persist for a long time in the dust of homes and cars of smokers. Nicotine contained onto surfaces can later react with other indoor pollutants, such as nitrous acid from gas hobs, to produce tobacco specific nitrosamines (TSNAs), which are potent carcinogenic substances; nicotine is also capable of reacting with ozone to produce very small particles that can reach different body organs. Although it is still to be determined if exposure to THS would entail a significant health risk, this query is thought to be answerable as millions of children and non-smoking adults around the world are exposed to second-hand tobacco smoke and presumably to THS.

2.5 Socio-economic status and mortality due to cancer

The term *social class* comes from the industrial revolution in the nineteenth century. Social class is a construct devised to infer the material state of people [141]. The relevance of this construct for health allied disciplines is due to the proven strong relationships of social class, and derived measures of socio-economic status (SES), with patterns of disease and mortality. So, health conditions, survival rates, and life expectancy are all worse in poorer, developing countries. The same relationship is well established within rich, developed and highly industrialised countries. In this case, a pattern of health differences between more and less affluent people has also been found. There is nowadays a wide consensus on the great influence that social

structures exert on the health status of the populations. Therefore health inequalities are, to a large extent, considered to be rooted in social inequalities [24, 142]. These inequalities are increasing not just between countries, but also among social classes within the same country. The mechanisms by which SES might influence the health status of populations are considered to be related to distinct patterns of environmental or occupational exposures across the whole SES scale [32, 104, 143-145]. People of lower SES might be exposed to higher levels of ambient pollutants due to either a preference for pollution-related sources to be placed in less affluent areas, or migration of disadvantaged people to unhealthy places [103].

Moreover, a complex influence of socio-economic factors on populations' behaviour is thought to exert a great impact on health. Thus, it is nowadays notorious how people of lower SES (either those living in poorer countries when compared to people living in wealthy regions, or less affluent people within rich countries) are more vulnerable to tobacco smoking advertising. Furthermore, regarding smoking cessation, the reverse is also shown: people of higher SES benefit the most from health promotion interventions aimed at stopping the habit. The latest Spanish atlas of mortality [16], which analysed municipalities for the period 1989-1998, revealed the relevance of all SES variables considered (income, illiteracy and unemployment). A north-south pattern was shown that pointed out to Andalucía, as one of the poorest Spanish regions. Furthermore, a high variation was hypothesised to exist within cities. The strong influence of SES on health can help to explain why most studies have shown both incidence and mortality due to different cancer sites (especially lung cancer) to be higher in people of lower SES.

The mechanisms by which some socio-economic factors influence health status are quite complex. Unemployment [24] has been found to be a risk factor for cancer incidence (mainly lung cancer) after taking into account tobacco smoking, alcohol intake, and SES. It is therefore worthy of note that known risk factors cannot completely explain the strong relationship between SES and health. Finally, it is important to point out that SES have been widely recognised to exert a high impact on the health status both at an individual and aggregated area-levels [25, 37, 40, 146-149]. Therein its pivotal relevance while considering public health research given the high impact that changes at the population level can achieve [150]. Different approaches have been used to measure SES as a broader concept than social class:

historically it was restricted to traits of individual wealth, prestige and power [151]. SES at the individual level has been measured by means of one or more characteristics frequently arising from information over income, education and/or occupation (using a single variable, or a compound index). These are thought to be proxy measurements of features such as health related behaviours, social status, and access to resources [152].

It is important to bear in mind that there is no one measurement strategy that is completely satisfactory and often the chosen methodology is based on data availability. Therefore, unemployment has been used as a proxy measure for income and material resources, and is thought to be useful to predict health disparities, as well as accessibility to health-care services in small-areas [153]. Education is considered to measure both material and social deprivation. Occupation has been used to a great degree, especially in the U.K., since the beginning of the last century. The British Registrar General classified occupation according to the level of education or skill and it has been shown to be able to predict health inequalities. Some limitations of this measure have been pointed out [147], as difficulties to assess SES for women or lacking of research to investigate the mechanisms underlying health inequalities. After being adapted according to the Spanish National Classification of Occupations (NCO) as of 1979, this measure by the British Registrar General has also been widely used in Spain. Later, the Spanish Epidemiologic Society devised a different classification using the 1994 version of NCO.

However, individual-level SES is not always available; e.g. large-scale Health Surveys do not usually provide estimates of SES for small geographical areas, such as census tracts. To address this gap, different area-level deprivation measures have been proposed. Two of them, widely used in the U.K. and with some modifications also abroad, are the Carstairs-Morris and Townsend indexes. Both of them have been proven to be useful to predict mortality and health-related behaviours, such as smoking [102, 154]. The rationale for adapting both the Carstairs-Morris and Townsend indexes, for use in countries other than the U.K., is a matter of practicability as well as a conceptual issue [155]. Information at the small-area level is often lacking on census databases, precluding its direct application in the past. Also, direct use of those indexes assumes that the individual variables are of explanatory value in the socio-economic context where the index is going to be implemented.

It has to be pointed out that compound indexes, as well as single measures, have some drawbacks [152]. They tend to mask differences due to the possibility that two different composite measurements eventually give the same score. Some recently devised indexes have been calculated using Factorial Analysis of Main Components. These indexes allow objective weighting, while some former approaches are based on compound measures which attribute the same importance to all variables. Moreover, studies comparing both individual and area-based socio-economic characteristics have shown that compound indexes are good predictors of different health events. One of these studies, implemented in Spain [15, 28], analysed mortality by census tracts in the capital cities of provinces in the autonomous regions of Andalucía and Cataluña. Socio-economic factors at the area-level (percentages of manual labourers, unemployment and illiteracy) were shown to be better predictors of differences in mortality across geographical areas. Mortality was modelled by means of Hierarchical Bayesian Regression, and main results showed a positive relationship between male mortality and a deprivation index, in all the capital cities of Andalucía. In contrast, results for females were suggestive of a lack of association between mortality and deprivation at the area-level. Furthermore, a similar pattern of male mortality in association with deprived areas was shown to occur in Cataluña, a region in which per capita income was at that time around 54% higher than that in Andalucía. These findings substantiate this deprivation index, as being sensible enough to behave consistently in quite different scenarios, given that cumulated evidence from different studies suggest that deprivation is a continuum along the social scale [152].

A growing number of studies based on the joint analysis of individual and area-level SES [40, 102, 146, 152, 156] suggests that deprivation indexes at aggregate level are relevant surrogate measures for missing estimations of individual SES. They are also thought to capture aspects of the related social context of ‘neighbourhoods’ in which people live [152]. Thus, availability and accessibility to health services, the kind of infrastructures, as well as attitudes and behaviours, can greatly influence health status. Various studies [7, 25, 27, 29, 154, 157, 158] highlighted the interest of ecological analyses as a means to better describing the health status of populations, and to also address relevant public health concerns. It is thought that the area-level variables might be a proxy measurement of individual-level characteristics, while lacking estimations at the area-level (neighbourhoods) would prevent a better understanding of

causes and mechanisms of health inequalities [152]. Neighbourhood has been considered to express lifetime exposure to *contextual variables*, that is to say, socio-economic characteristics at the area-level which are associated with health outcomes; different studies have consistently found slightly higher risks for mortality in deprived neighbourhoods, while *compositional variables* (individual-level socio-economic characteristics) show a stronger relationship with health events than contextual variables.

A health survey undertaken in Barcelona in 1992 [40] was used to test the association between SES and several health outcomes: perceived health status, smoking habit, and presence of chronic diseases. Area-level as well as individual-level SES variables were used as a means to check external validity for the ecological variables. To this end, percentages of unemployed, illiterate, and occupationally unskilled people were used for the former as extracted from the 1991 Spanish census; individual-level information included education (as the highest level achieved) and social class (as adapted from the British Registrar General classification). The authors found that worst health outcomes were associated with lower educational level, as well as lower social class. This association was shown for measures of both area-level and individual-level SES. Interestingly, smoking among women showed a negative association with lower, individual-level (but not area-level), SES.

The association between tobacco smoking and lung cancer after adjusting for SES was investigated within the European Prospective Investigation into Diet and Cancer (EPIC) [32]. SES was defined by the highest level of education achieved; sex and region within the 10 participant countries were also accounted for. The analysis of a sub-cohort of nearly 400,000 people and around 2,000 incident cases of lung cancer studied the amount of variation left after fitting a model that adjusted for smoking behaviour. Participants were followed for a mean period of eight years. Lower SES was known to be associated with higher risk of both lung cancer incidence and mortality. Within the EPIC project, results for northern Europe were consistent with previous studies. However, after adjusting for tobacco smoking differences between SES strata were no longer statistically significant for southern European regions (including Spain). Smoking was found to explain 50% of the variation between SES strata. The association between incidence and mortality due to lung cancer and lower SES was stronger for small cell carcinoma. This association was also statistically

significant for squamous-cell carcinoma. After adjusting for tobacco smoking, differences for adenocarcinoma were no longer statistically significant. Adjusting for fruit and vegetables consumption did not make any difference. These results suggest that factors other than tobacco smoking may explain differences in risk for disease incidence and mortality due to lung cancer (e.g. use of health-care resources or willingness to adopt healthier life-style patterns).

The association between social class and mortality was assessed through an ecological study that retrieved demographic information from the 1996 Spanish census [149]. Mortality concerning the autonomous region of Madrid was obtained from registries for the two-year period 1996-1997. In this study, a gradient in mortality was shown to exist depending on social class based on occupation according to the Spanish national classification of occupations. Mortality risk was found to be highest in groups VI and VII (manual workers) and lowest in groups I and II (managers and professionals). The highest gradient in mortality explained by occupation occurred for respiratory diseases and the lowest gradient was seen for cardiovascular diseases. The authors attributed this differential to the stronger association between tobacco smoking with the respiratory diseases and the less important relationship with the cardiovascular diseases. It was shown that men in the lower-class occupational groups (VI and VII) had achieved lower educational levels than men in higher-class occupational groups (I and II), which explained most variation in mortality between occupational categories. Employment status (either employee or employer) only explained a small amount of variation between occupational categories. The mechanisms by which higher education poses a lower risk of mortality is thought to be associated with better control over daily life stressful situation which, in turn, would influence lifestyle choices. Higher education is also known to be associated with higher incomes which determine living standards. Higher rates of tobacco smoking, physical inactivity, and alcohol drinking had been shown for Spanish people in lower educational groups at that time. Also, Spanish people in higher educational groups had higher incomes, which was determined by academic qualifications, rather than work experience.

2.6 Radon-gas exposure

Even though tobacco smoking is considered to be the most important risk factor for lung cancer, indoor radon-gas pollution is widely acknowledged for exerting a synergistic effect along with smoking [114, 159]. Also, the heterogeneous

geographical distribution of lung cancer (especially notorious among both sexes) would support the importance of environmental factors interacting with tobacco smoking. Radon-gas (Rn^{222}) is a decay product derived from radium (Ra^{226}) which, in turn, is derived from uranium (Ur^{238}) [116]. Radon-gas can be found underground where uranium ores are present. It is remarkable that radon, in contrast to its precursors, has a very short half-life of around 3.8 days [116, 160]. It quickly spreads from the ground into the air, where it can attach to dust particles, clothing and other materials alike, allowing humans exposed to the polluted environment to inhale the gas. The short half life of radon and radon daughters (by-products) is so short that the human respiratory system cannot remove the pollutants from the body before they have had a harmful effect. Radon daughters have short half-lives of less than 30 minutes. Furthermore, radon cannot be perceived by human senses, because it is odourless, colourless and tasteless. Moreover, acute exposure to radon does not cause any symptoms that allow its presence to be suspected. Consequently, only direct measurement allows detection. Radon (and its daughters) is primarily a problem of enclosed spaces, where it can accumulate if the space is not ventilated.

Lung cancer has been the only adverse health effect clearly associated with indoor radon exposure [115, 116]. Knowledge about radon health effects came up from epidemiological studies on uranium miners [115]. More recently, at least one meta-analysis [161], and two pooled-analyses of case-control studies implemented in Europe and the U.S. have been able to support the association, as well as the dose-response relationship, between residential exposure to radon-gas and lung cancer [162, 163]. Most cancers associated with radon-gas exposure are located in the bronchi, which are the anatomic sites where radon particles accumulate. Moreover, all histological types of cancer are deemed able to arise in association with radon exposure. Radon-gas exposure is nowadays considered as one of the most important ambient-related causes of death. Its relevance concerning lung cancer is thought to follow immediately after that of tobacco smoking. Mortality from lung cancer attributed to radon-gas exposure is considered to be even higher than that due to passive smoking [115]. It is estimated that 15000 cases of lung cancer a year (14% of all cases) in the U.S. and 2000 cases a year (6% of all cases) in the U.K., are due to radon exposure [115, 116]. Also, it is estimated that from 900 radon-attributed cases a year diagnosed in Sweden, two thirds could be preventable [164]. In addition, it is

believed that there is a synergy between tobacco smoking and radon exposure that underlies different patterns of lung cancer incidence between smokers and non-smokers exposed to radon [115, 116], as set out under heading 2.6.1.

Radon-gas became a public health concern in 1984 [160]: an electrical engineer working at the Limerick nuclear plant of Pennsylvania (U.S.A.), who was not supposed to be in contact with any radioactive materials, caused the contamination alarm to go off. As this happened both at exiting and entering work, the engineer's house was later identified as the source of radon decay products attached to his clothing. The U.S.A. Environmental Protection Agency had fixed safety limits for radon at 4 pCi/L (or 148 Bq/m³). Remedial actions were recommended when those limits were surpassed. In contrast, concentrations of radon daughters at this engineer's house exceeded safety limits in as much as 500 times. This was almost 70 times higher than the occupational exposure tolerated for miners in most countries [159]. It was then found that radon could seep into buildings, throughout floor cracks, or dirt floors and even throughout certain building materials (e.g. concrete). Still worse, some building materials can be a source of indoor radon pollution (e.g. granite, brick [165], and shale [116]). Radon can also enter buildings accompanying water supply (mainly groundwater), and diffuse over the surrounding environment.

Once radon-gas diffuses into houses, it tends to accumulate in the lowest levels of the building (such as basements) and is able to spread to other levels, depending on several variables such as ventilation rate, or temperature; seasonal and even daily variations are known to influence indoor radon concentration [116, 166]. Therefore, many distinct factors are responsible for radon pollution inside buildings, such as lithology underneath the houses and building materials [61, 165, 167-172], atmospheric environment, ventilation habits of the occupants, and origin of the water supply [58]. In summary, tobacco smoking and radon-gas exposure are currently the primary aetiological risk factors for lung cancer. Since primary prevention measures are available for both of them, the most important public health interventions to be considered are tobacco smoking cessation, and reduction of environmental radon exposure (whether occupational [173] or residential). Different kinds of measures can be implemented to mitigate indoor radon pollution. Most of them are directed to prevent the soil-gas entry into the buildings, rather than to evacuate the indoor gas.

Nevertheless, exhausting the gas is also considered to be a useful measure [116, 174, 175].

As already mentioned, due to the chemical characteristics inherent to radon-gas, it can only be detected by direct measurement. Therefore, to implement appropriate interventions that mitigate indoor radon pollution, a quantitative estimate of actual concentration of gas inside buildings is needed. Given that available radon tests and mitigation remedies are resource consuming, several health policy strategies have been devised to quantify indoor radon pollution. They range from universal scrutiny (one or two step confirmatory measures) to targeted measurement on high-risk areas. To help provide an informed decision-making process some cost-effectiveness analyses have been undertaken [176], where the latter option (measurements on previously identified high-risk areas) was shown to be the most cost-effective one. Many studies in the U.S.A. and Europe have been carried out to produce risk maps at the national, regional, or local level [165, 167, 168, 172, 177, 178]. These maps have been based on direct or indirect measurements of indoor radon-gas concentration. Different kinds of radiation detectors were used throughout short-term (some days), or long-term (up to several months) follow-up periods. Random sampling measurement of radon-gas concentration inside buildings has been used while bearing in mind features such as seasonal and/or daily fluctuation, type of building or geologic characteristics of the soil. The aim is to take sampling measurements that are as much representative of the area under study, as possible. Such studies have shown to be useful in Spain with a view to highlighting large areas worthy of closer investigation. A series of such investigations implemented in Spain, have been published between 1991 and 2004 [58, 61, 165, 179-181].

As in other countries [182], a national survey regarding indoor radon-gas pollution was implemented. The Spanish survey [165] was carried out during winter time (where maximum radon concentrations are reported to be found) in 1988 and replicate measures were taken the following year. This survey identified, at a national scale, geographical areas of high indoor radon concentrations (e.g., the autonomous region of Galicia, to the North West of the country) which are also known for having soils of granitic composition. In this study the median levels of radon-gas were between 17.6 and 117.6 Bq/m³ (the latter one in Galicia). The median value for the country as a whole (41.1 Bq/m³) was reported to be similar to values measured in other countries

[159]. According to this study, 13% of investigated houses in Spain, had radon concentrations above recommended EPA limits for remedial actions to be implemented. This proportion was as high as 39%, in some specific areas of the country [180]. Limitations inherent in the methods for radon-gas measurement (such as cost [61, 167]) have forced random sampling as a design feature of research while choosing areas to be measured. Also, replicate measurements (so that more precise estimations are obtained) have suffered from constraints related to cost.

Due to the great number of different factors able to modify effective radon exposure (such as temperature, ventilation habits, building materials and water supply) other approaches have been developed. They are essentially aimed to using easily accessible surrogate measures for potential radon exposure. In some cases methods have been devised as a complement to allow a better characterisation of areas where few measurements were previously taken [61, 165]. Several studies have tried to assess the extent to which surficial geology is a good predictor for potential radon-exposure, when the gold standard of radiation measurement methods is impractical or too expensive [61, 167-169, 172, 183-185]. One of these studies, implemented in Spain [61], compared mapping of natural gamma radiation from soils (obtained by radiometric measurements) with geological maps of the country. A good correlation was found between gamma radiation and geology. Then a radon mapping was predicted from gamma radiation and compared to direct radon measurements, obtained from a former national survey. A good correlation was also found between observed and expected values for radon concentration [165].

Notwithstanding this close similarity between the distributions of spatial gamma-radiation, geology, and measured as well as predicted values, indoor radon concentration was only warranted by visual inspection of choropleth maps; no further analysis was presented. Furthermore, one would expect (at least to a degree) some correlation to arise as an artefact due to design issues, given that they had to estimate some missing radiometric measurements from geological characteristics. Finally, although a repeated measurement design was used (30 measurements on each location) throughout the whole country, many places (such as urban areas) remained unmeasured. For the whole region of Andalucía (87,547 Km², or 18% of Spanish surface [186]), measurements were only taken in 8 distinct places. In reference to the above methodological issues, some researchers [182, 187] have pointed out that the

sampling distribution of radon concentration measurements is typically a log normal one (as it was also shown by the Spanish report [165]). The usual parameter of interest to be estimated is the percentage of homes which geometric mean of radon concentration is on, or above, the limits set by the EPA. To this aim, 30 replicate measurements would be enough for the standard error of estimates being less than 20%, given the variability found in these studies [167, 168].

Therefore, the number of measurements at each sample point was probably sufficient to estimate the frequency distribution of radon levels at each place. However, the total number of points sampled in Andalucía was too small to provide an effective map of radon risk at the small-area level. When considering representativeness of sample measurements (which is more than only a statistical issue) it is important to bear in mind that radon concentration can greatly vary by smaller areas than the ones usually analysed. This could be partly explained by the presence, at some restricted areas, of permeable deposits that allow radon-gas to diffuse.

It is also worthy of comment that the preceding study [168] reported a very poor response rate: 3,215 out of 9,080 (or 35%) mailed home owners applied to joining the survey. Subsequently, 1,645 out of 3,215 (or 51% of them) produced effective measurements. That is to say, only 18% of the potential study population participated. This could have been a serious flaw provided that a bias (such as a self selection) had occurred. Nevertheless, although the authors did not report any kind of analysis to address this potential drawback, it seems plausible that missing values had happened randomly.

It is also worth noting that, in this study, the geometric mean of radon concentration for each town and city was estimated as a compound measure made from a variable number of existent radon measurements (up to 30 readings) or radon measurements plus correlations of measurements to the surficial geology. More recently, published research on radon-risk mapping [183, 185] has taken advantage of geo-statistic techniques to support the idea that the spatial distribution of radon concentration (or radon potential, as a derived variable) has a main component, the trend, which can be modelled using surficial geology as a categorical variable. In fact, different classifications made from geologic and lithologic characteristics of soils, as a surrogate measurement for radon potential. The variability shown by data and explained by the fitted model depends (within a limited range from around 5% to 11%)

upon how detailed the geologic/lithologic information is. Nevertheless, even a coarse classification in a few geologic categories is shown to be useful to model the geometric mean of radon potential. Of course, a residual component was still remained and most probably was not related to geology/lithology, but to other variables controlling radon concentration.

Concerning the scale at which geology should be used as a surrogate measure for radon concentration, the previous study pointed out that the most relevant issue has to do with the aim of the research. A high resolution (scale 1:50,000) might be necessary if a local description is going to be considered. Moreover, it is of most importance to bear in mind that traditional geology, which is mainly based on rocks' age, might not be the best classification method to be used as a surrogate, categorical, variable for radon concentration, or radon potential, in some instances. Lithology, which takes into account rock composition, was shown in this study to be useful while modelling radon potential trend. Other structural variables as texture (which may be a good proxy for soil permeability) and geo-chemistry were considered to be worthy of investigation in the future.

2.6.1 Joint effect of radon-gas exposure and tobacco smoking

As mentioned in section 2.5, different patterns of lung-cancer mortality between smokers and non-smokers, who are both exposed to radon pollution, could be explained by a synergistic effect of tobacco smoking and radon [114]. Statistical interaction shown on large scale cohort studies, suggests a multiplicative or a mixture between additive and multiplicative risk models [114, 159, 188]. It indicates effect modification of radon exposure on lung cancer incidence while a concomitant exposure to smoking occurs. So, it is considered that among people suffering from lung cancer due to radon exposure, most of them (95 % of men and 90% of women) had ever smoked. Conversely, other cohort [117] and case control studies [189] did not find any statistical interaction that suggests the effect of radon-gas exposure be modified by tobacco smoke.

Given the existing interdependence between radon and tobacco effects on lung cancer, it is of great importance to take into account the distribution of tobacco smoking while analysing radon exposure, either at an individual or area-level. Different attempts have been made to estimate smoking prevalence in small area studies. Since there is a good

correlation between perceived health status and health indicators, such as mortality [156], it would be very helpful to investigate the problem at the large scale taking advantage of Health Surveys.

Moreover, one might claim the superiority of individual-level information coming from cross-sectional studies like Health Surveys, which are not prone to bias due to ecological fallacy, which is the main drawback of aggregate studies. Nevertheless, even though information provided by large-scale Health Surveys, at national or regional level, would be very useful at the small-area level, they are not usually designed with such a purpose in mind. Therefore, estimates for smaller areas (by using sub-samples) would produce very imprecise results. To overcome this drawback, different approaches have been devised by taking into account both individual-level characteristics and a measurement of the geographical context (socio-economic features and environmental factors, with which people interact). The reasoning underlying analysis, jointly at the aggregate and individual level (the so called multilevel or contextual analysis [152, 156, 158]) is that a better insight about the complex relationships of exposure and disease would be reached. In this respect, small-area ecological studies can be of great value.

To assess the smoking habit at the small-area level, some researchers made use of information already available from large-scale Health Surveys. Others, made predictions from surrogate sources, such as SES at the aggregate level (deprivation indices [154, 157]), or local availability of tobacco (convenience stores [157]). As an example, one of the preceding studies [154] showed a highly significant association between individual smoking behaviour and socio-economic deprivation at the area-level using the Carstairs-Morris index, after adjustment for age and sex. Introduction of individual socio-economic group, still allowed the Carstairs-Morris index to remain in the model as a significant variable, collinearity between both individual and aggregate socio-economic variables was considered to be nonexistent. According to the hypothesis pointed out above, which stresses the relevance of multilevel analysis, these results showed a higher prevalence of smoking for both individuals in lowest socio-economic strata as well as those living in most deprived areas. That is to say, smoking behaviour variability could be better explained when SES was measured not only for individuals, but also for neighbourhoods in which those individuals lived.

Another multilevel study [102], used the Norfolk cohort of the European Prospective Investigation into Cancer (EPIC) study to also assess the predictive value of area-level SES (using the Townsend index) in association with the smoking prevalence. It was found that both individual and area-level SES independently predicted smoking behaviour. A more recent study [157], also concluded that the area-level components could exert an important effect, independently of individual SES. In this case a higher concentration of convenience stores, where tobacco was easily accessible, was positively associated with smoking prevalence as ascertained by individual-level information. The concentration of convenience stores was reported to operate differently in people of high compared to low SES, the former group being protected to a degree. Nevertheless, people of high SES, living in deprived areas, or where a greater concentration of convenient stores occurred, were more likely to be smokers. The relationship between tobacco accessibility at the area-level and smoking behaviour was shown not to be altered when different measures of accessibility, other than convenience store density, were considered.

2.6.2 Literature review summary

Several ecological studies have described a characteristic pattern of higher mortality in western Andalucía, for different overlapping periods between 1981 and 2006, in both men and women [7, 10, 11, 13, 16, 96]. This pattern has been reported to exist for all-cause mortality, as well as for some specific causes such as lung cancer [9, 11]. In Andalucía, lung cancer was the leading cause of mortality due to cancer in men, and the fifth cause in women, from 1975 to 1997 [23]. Different hypotheses have been suggested that would explain this excess of mortality in western Andalucía, from lifestyle-related exposures to environmental pollutants [101], while there is consensus in the need for measuring area-level deprivation, as a surrogate measure (and a potential confounder) for exposure to different risk factors [1, 7, 24, 28-31, 34, 103]. One such factor, radon-gas exposure, has been recognised to be the second most important cause of lung-cancer mortality, after tobacco smoking [109, 115-117, 189]. This is the reason why many countries have implemented programmes to mapping the spatial distribution of potential radon-gas exposure [61, 165, 167, 182, 187].

However, measurements of indoor radon-gas concentration have some drawbacks due to costs, and problems of interpretation in terms of their correlation with actual human exposure [190, 191]. Difficulties in taking actual measurements of indoor radon-gas

concentration has led to obtaining national maps of rather low resolution, when compared to the information needed for studies at the small-area level [165]. To tackle these difficulties, different alternatives have been implemented to deriving potential radon-gas exposure; most of them take advantage of the correlation between content of radon-gas in the soil and surficial lithology and geology [58, 61, 168, 169, 171, 172, 185, 192, 193]. Nevertheless, even though a digitised, high-resolution, lithology map is available for Andalucía [60], there is sparse published research in Spain that has made use of lithological information to deriving radon maps at the small-area level [61].

Surrogate measurements for potential radon-gas exposure have been usually derived from modelling of actual samples of concentration measurements [61, 168, 169, 171, 192, 194]. However, in the case of the Andalusian radon map, measurements had been taken in just eight sample points [165] across the whole region; this seems to be a situation where modelling of latent (unobserved) variables is appropriate. Although SEM has been used with applications in the spatial epidemiology of health events [195-197], no references were found concerning the estimation of potential exposure to radon-gas, by means of SEM.

Chapter 3. Data collection and handling

3.1 Overview

The geographical and temporal study scope will be presented along with a description of data format and sources. Digitised boundaries were available at the municipality level (see 3.2); population estimates, mortality data (see 3.3), and socio-economic data (see 3.4) were obtainable with the same geographical resolution. Therefore, both the SMRs and the socio-economic deprivation score were computed for all the municipalities in Andalucía. Lithological information (see 3.2) was obtained for the whole Andalusian region; data for each individual municipality was subsequently extracted, by means of GIS software, to be used in the analysis stage (see 5.2.1).

3.2 Administrative Boundaries and lithological data

The municipality is the smallest geographical area at which mortality information was available. Therefore, further geographical subdivisions (*collective and singular population-entities, nuclei and scattered populations*) were not used in this study. On a yearly basis, the National Statistics Institute publishes an updated catalogue on place names, where an eleven-digit code is used to identify geographical areas. Those codes were assigned for the first time during the 1981 census was accomplished and have remained in use. Terminated codes are not reused (unless the corresponding place names are introduced again), and new places are assigned additional codes. Only the first five digits were of interest for the analysis stage: the first two digits correspond with the province, while the following three represent the municipality.

Due to administrative changes from 1975 to 2001, several municipalities had to be aggregated and/or separated. Hence, to provide population inter-census estimates which are geographically homogeneous through the period 1981-2002, those changes had to be considered. The Andalusian Statistics Institute provides population data for individual municipalities whenever possible. Otherwise (individual information not being available for every single year) data belong to aggregations of two to four joined municipalities. Thus, 21 municipality codes were the result of aggregations corresponding with 47 formerly individual municipalities. Therefore, while the original database comprised 770 municipalities they became only 759. To merge both datasets, the latter was aggregated by the author of this research thesis, using my own

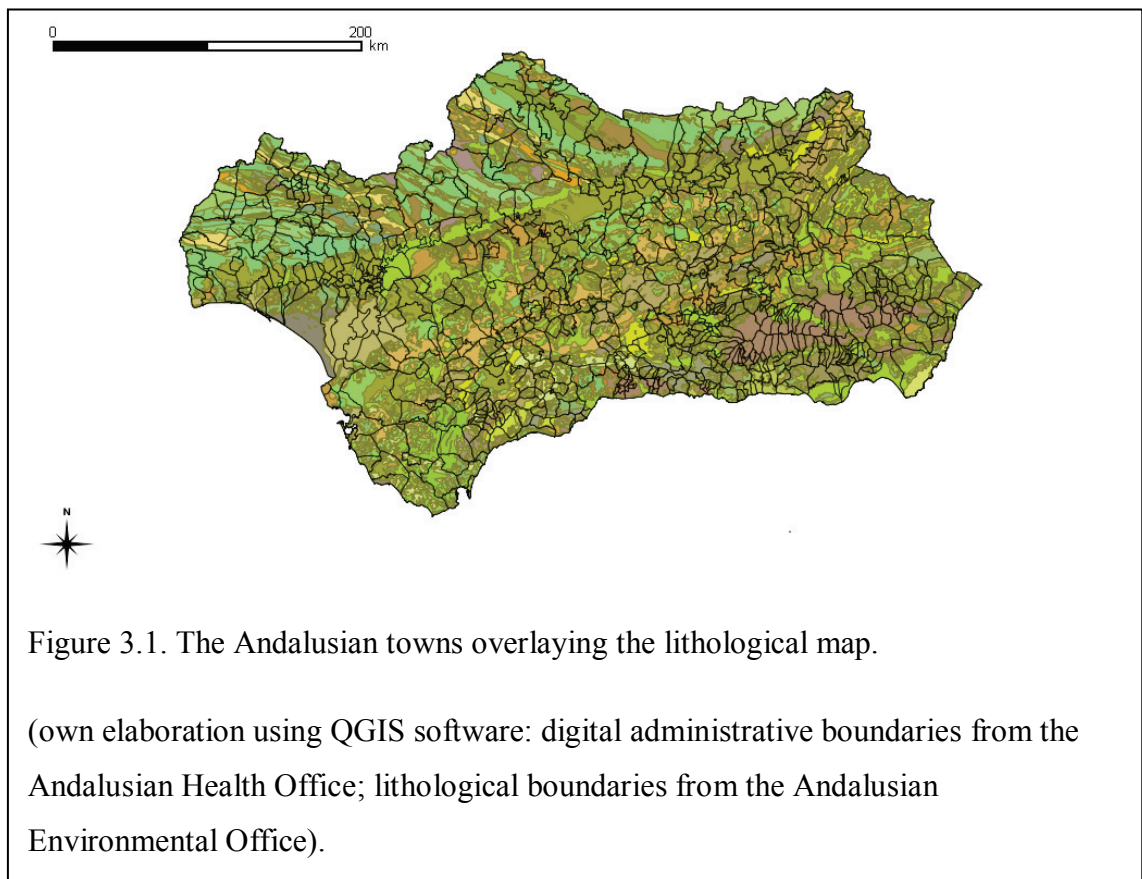
Epi Info scripts. The same changes needed to be reflected onto the digital boundaries to match all data and maps.

The digital map of Andalucía was available, from the Andalusian Health Office, as *shapefile* format. Shapefiles have been devised by the Environmental Systems Research Institute, Inc (ESRI) for use in Geographical Information Systems (GIS) representation [198]. They can store vector-data (points, lines and polygons) as well as its related feature attributes (ID codes, names, area, or population). A shapefile is actually a set of files which is comprised of three main datasets: a geometry file (.shp), after which the term shapefile is named, that stores information for object representation (administrative borders, roads, rivers, streets, buildings); an index file (.shx) which speeds access to data; and a dBASE format file (.dbf) that contains the information on the feature attributes to be represented on the map. In this case, SMRs and RRs, were plotted by using colour shades (choropleth maps). Shapefiles are not only used by proprietary products like ESRI ArcGIS, they are also handled by free and open-source software like GRASS, Epi Map, GeoBUGS, GeoDa, QGIS and R [50]. GeoBUGS, a WinBUGS module (see section 4.2.2), is especially relevant as it made possible instant mapping of results after data analysis [199].

The Andalusian municipal map was exported to GeoBUGS, after its boundaries were modified according to municipality aggregation status. The original shapefile map was first read into ArcGIS to modify its boundary limits, according to the data aggregation already discussed. To rearrange the boundaries, those sets of municipalities to be combined were first given a common code, within the attribute table. The boundaries were then combined using the *Dissolve ArcGIS tool*. As a result, a new shapefile was obtained that only had 759 polygons, instead of the 770 original areas. The modified map was afterwards read from R software using the *readShapePoly* function built within the *maptools* library [200]. To make the map eventually readable by GeoBUGS, it was exported into *S-Plus* format using the *sp2WB* function. Although ArcGIS is more flexible for GIS representation, GeoBUGS (an add-on to WinBUGS) offers some convenient features: the possibility of immediate mapping, after the modelling stage, was considered an essential vantage point.

The lithological map of Andalucía (Figure 3.1) was available online from the Andalusian Environmental Office, in shapefile format [60]. The file is publicly

available through the Andalusian Environmental Information Network (Red de Información Ambiental de Andalucía, REDIAM) which has integrated, environmental-related information produced by different regional institutions and made available various downloadable products. The lithological map had been jointly edited with the Regional Office for Transport and Infrastructure. The map was designed with a scale of 1:400,000, based on the national Mining Geological Map at the same scale. It was further improved with information from the Spanish Institute of Geology and Mining: the National Geological Map (Mapa Geológico Nacional, MAGNA) with scale of 1:50,000. Unlike other geological maps, the ground was classed according to the physical and chemical composition of the rocks, irrespective of its chronological evolution or age. This is relevant given the intimate link between potential radon exposure and bedrock composition [61], as presence of radon in the



soil depends on the content of uranium in the underlying rocks (section 2.6).

The attribute table accompanying the lithological map consisted of 41 different rock classes which belonged to four main groups: volcanic (3 classes), plutonic (4 classes),

metamorphic (15 classes) and sedimentary (19 classes) [60]. In Spain, radium is present mainly in some types of rocks such as granite (that belongs in the plutonic group), clay (which is a sedimentary rock), and shale (metamorphic) [58, 61]. However, other rocks, such as sandstone (sedimentary) and carbonate rocks (metamorphic) can also be a radium (and hence, radon) source. Therefore, classification of rocks in the four main lithological groups (volcanic, plutonic, metamorphic, and sedimentary) were considered appropriate to deriving a surrogate measure for potential radon-gas exposure. With the aim of estimating the surface that each lithological group occupied within each municipality, the digitised version of the lithological map of Andalucía was imported into ArcGIS. All different lithological ID codes were re-coded to fit into the four main lithological groups and their respective areas (in square kilometres) were computed using ArcGIS software.

3.3 Mortality data

Data from the Andalusian Mortality Registry were directly provided by the regional Health Office (*Consejería de Salud*). The Health Office is the governmental body in charge of public-health policy development. It is also responsible for supervision of health-care management and supply [201]. Several other public institutions are also involved in supplying death-related information to help accomplish all the necessary registering activities, which leads eventually to electronic mortality records. One of the collaborating institutions is the Andalusian Statistics Institute (*Instituto de Estadística de Andalucía*), which is responsible for the coordination of statistical activities implemented by attached bodies. The Institute is also in charge of creating, maintaining and managing regional statistical-databases using available information from various administrative sources [202]. So, death-related information sources are comprised of death certificates and death statistical forms (*Boletín Estadístico de Defunción*). As required by law, the physician certifying the death provides all the information included in the former, while they only complete the latter on those sections related to the causes of death. The rest of this form contains information about the identity of the deceased, which is provided by relatives or acquaintances. The municipal Civil Registry where the death takes place, supply additional administrative data. On a monthly basis, Civil Registries from all 770 municipalities send collected certificates and statistical forms to each of the eight corresponding provincial branches of the Statistics Institute [203].

The Andalusian Statistics Institute then implements quality-control activities. It produces electronic records while checking for comprehensiveness and consistency of information. At a further stage, it sends those electronic files to the Natural Population Movement Unit (*Unidad de Movimiento Natural de la Población*). This unit, comprising staff from both the Health Office and the Statistics Institute, is responsible for coding all causes of death. The set of criteria used for this task is the International Classification of Diseases (ICD), as established by the World Health Organization (WHO) [67]. Information on deaths has been collected electronically from the year 1975 onwards. For that purpose, the ICD-8th revision has been in use to record deaths that occurred from 1975 to 1979; the ICD-9th revision was used from 1980 until 1998, while the ICD-10th revision was introduced in 1999. Quality-control activities are systematically implemented for both the socio-demographic and death-cause variables: data retrieval is accomplished wherever there is some missing information on the death statistical forms; coding revision and checking of consistency, between the underlying cause of death and socio-demographic variables are also implemented [203].

The resulting socio-demographic information is eventually passed onto the Andalusian Mortality Registry, within the Health Office. Available data include: date (day, month and year) and place of birth (municipality and province); sex, marital status (single, married, widow, or separated/divorced); occupation, according to twelve main groups of the National Classification of Occupations (*Clasificación Nacional de Ocupaciones*); place of residence (province and municipality (see section 3.2) and place and date of death registration, which usually (but not always) coincides with each other. For statistical purposes, place of usual residence (instead of place of death) is recorded, so that international standards are fulfilled. Even though mortality data are available for analysis since 1975, year-by-year population data (by age-group, sex and municipality) are only obtainable since 1981 [204]. Given that population data are required to estimate the expected number of cases and therefore the SMRs, mortality data previous to 1981 were discarded for the modelling stage of the work.

Information on deaths, as provided by the Andalusian Health Office, needed data handling before analysis. Data were provided as a *Microsoft Access* file, where anonymised information had been aggregated according to the number of deaths by municipality, year, sex, and cause. The original *wide-code* format (19 distinct age-

group variables, from '0-1' to '85 and older') was converted into a *long-code* format (one single age-group variable with 18 values, from '0-4' year olds to '85 and older'). By doing so, comparability with age-groups used by available population data (see section 3.4 below) was made possible. This produced a more than twofold increase in the number of records, although it gave a ready-to-analyse file. Epi Info software versions 3.5.1 (launched in 2008) to 3.5.3 [205] were used to handle data import and conversion given its relational-database capabilities and Microsoft Access compatibility and the previous experience of the author. Since then, a new version of Epi Info has been released [206]. Many different scripts were also written (using Epi Info and R), or adapted (using WinBUGS and R), to support quality of data-acquisition and analysis. In this way, any disagreement between original and derived files was double-checked by reviewing and amending, where needed, the corresponding script. Further data-handling was required, due to changes in administrative boundaries throughout the study period. The Andalusian Statistics Institute provides online information about aggregation and segregation of municipalities [204]. In accordance with that information, some codes had to be recoded so that they fitted the boundaries later used for the mapping process (see section 3.2). Recoding affected 11 out of 770 (or 1%) geographical codes.

After that, cases and populations were aggregated by municipality for each year, death-cause, age-group, and sex. To reach this stage, I wrote (specifically for this purpose) several Epi Info scripts. They allowed addition of variables that labeled codes and, therefore, made analysis output easier to interpret and less prone to error. That was the case for variables such as death-cause and sex. Another crucial step, to make sure that population data were accurate, was to produce zero-count records (for the variable *number of cases*) where no deaths had occurred. These zero-count records, represented as missing values in the original 19 age-variables, were unavoidably lost while adding the number of cases by age. Taking advantage of Epi Info relational-database capabilities, the case-file was linked to an aggregate population file. This dataset only shared some variables with the former (municipality, age-group and sex) while the case-file also contained data on death-cause and year. To prevent manually repeating the same task, and reducing the risk of error, I wrote new specific scripts to be run within Epi Info. Missing values were replaced with due codes: death-cause,

year of reference or zero-counts. As a consequence, computability of both the *expected number of cases* and SMRs figures (see 4.2.1 below) were assured.

All data preparation eventually produced a first file ready for initial descriptive-analyses of mortality. Only 759 different municipal codes were left, after the recoding process. Given that Epi Info allows for files to be exported to (and imported from) different formats, this capability was used throughout the process. It was not only useful for data-handling, but also helped in the transition to data modelling (especially where exporting data to R software). Mortality data were directly read into *Epi Info* from *Microsoft Access* files, while population data (see 3.4 below) were imported from *Microsoft Excel* files.

3.4 Population and socio-economic data

The Andalusian Statistics Institute (see section 3.1 above) has published online population-data at the municipal level [204]. Three different data sources are available: decennial censuses, yearly Municipal Register of Inhabitants (*Padrón Municipal de Habitantes*) and year-by-year inter-census population estimates. Censuses involve large-scale operations at the national level and are paramount for civil services to plan, manage, implement and follow-up public policies [207]. Both the national and regional governments have authority on statistics affairs at their respective scales. Therefore, a collaborative agreement exists between the Andalusian Statistics Institute and its national counterpart, the Spanish National Statistics Institute (*Instituto Nacional de Estadística, INE*), to coordinate efforts for censuses production [207]. There are three different types of censuses that record data about resident population, dwellings, and buildings and premises, respectively. To collect information on both population and dwellings, four different questionnaires are used which have been devised to be self-administered by the interviewees themselves. Nevertheless, concerned people can be also assisted by civil servants if required.

One of these questionnaires (*hoja padronal*) includes data on individual identification variables collected from municipal registries. It is intended for the interviewee to review it and amend it where needed. These variables include place of residence (province and municipality), date of birth, sex, place of birth (in case of foreigners, just country of origin) and nationality. A second questionnaire is the *home* one, which collects information on marital status, achieved level of studies and type of studies.

Occupational status classified people as either in the labour force (employed or unemployed) or economically inactive.

Another source of population data is The Municipal Register of Inhabitants, which constitutes the official administrative record that proves place of residence [208]. These data bases are recorded and maintained by every city council across the country and collect information from all population centres. Although intended for administrative purposes, as determining financial quotas and legislative representation, they are also useful for statistical applications. Thus, Municipal Registers (like censuses) supply information about population counts and its demographical structure, including age and sex [209]. Both the Andalusian and the National Statistics Institute provide online access to the Municipal Register of Inhabitants. The National Statistics Institute server hosts much of the information as *PC-axis* files. This free-software format has been developed by *Statistics Sweden* and is used by many statistical offices around the world. It is a convenient tool for data tabulation, which also allows for files to be exported using different formats [210, 211]. In contrast, the regional website provides on-screen spreadsheet views that can only be copied and pasted, which would make data retrieval cumbersome [212]. Therefore, PC-Axis software (2007 version) was also downloaded from the National Statistics Institute to read and export data from the Municipal Register of Inhabitants. Inter-census population estimates (by municipality, sex and five-year age-groups), were available for the period 1981-2001. A single PC-Axis file was available through the Andalusian Statistics Institute website. It comprised population data by municipality age-group and year, which included both the study period (1986-1995) and the period used to provide prior probabilities to implement a sensitivity analysis, concerning the clustering and heterogeneity components (1981-1985). This file was exported to dBASE format and then read from Epi Info to combine all 18 age-variables into a single one, using a purpose-written script.

Socio-economic information was drawn from the census. Data from the 1991 census is available online both through the Andalusian and the National Statistics Institute websites [212, 213]. Therefore, population census data needed to compute area-level socio-economic deprivation were downloaded from the National Statistics Institute website as PC-axis files. Three different files were obtained on the number of people, by municipality, who were illiterate, unemployed and doing manual jobs. As those

files consisted of information concerning all Spanish municipalities, they were exported to exploit Epi Info relational-database capabilities. This made it possible to select only Andalusian municipalities, more efficiently than through a highlight-and-select process available within PC-Axis. A previous step though, was to export these files to Microsoft Excel format. The aim was to exclude some values of no use and make some calculations prior to computing the deprivation scores.

The original PC-Axis file related to literacy level had three fields: municipality, sex and literacy level. The files on employment level and job description had the first two fields (municipality and sex) in common. The *municipality* field had 8,127 unique numerical codes followed by their literal names, as one single character-string within the same field; *sex* had values for both sexes and the total number of people; the *literacy* level was classified according to thirteen different classes (from illiterate to doctorate, plus several subtotals and a grand-total value). Since only three of these values on literacy level were needed, the rest were not exported to Microsoft Excel. Then, only the total-population count, and the number of people who were illiterate (not able to read or write) or had no studies degree were exported to Excel format. Sex counts were not exported, as the area-level deprivation index did not intend to address sex differences in populations. *Illiteracy* has been previously defined as the number of people (10 years or older) who were illiterate or had no studies [28, 155]; it was computed by the author (using Microsoft Excel) as the percentage out of the total (10 years or older) population.

The employment status had been classified in the original PC-Axis file using eleven different categories. Both the economically-active (16 to 64 year olds) and inactive (all others) populations had been included by the National Statistics Institute. The former group had been divided in three different classes: employed, unemployed looking for their first job, unemployed who had worked before. The latter had been classified in four groups: retired, students, doing housework, and others. Additional subtotals and grand-total counts completed the original variable about employment level. The *unemployment* component has been previously defined as the number of unemployed people within the economically-active population [28, 155]. It was computed as the percentage out of the total economically-active population. The *Manual workers* group is defined as people belonging to any of the following five (out of twenty) different

classes: those specialised in building construction, mines and metallurgic industries, any other industries, machinery and facilities, and non-skilled workers [155].

Once all deprivation components (percentages of illiteracy, unemployment, and manual workers) were computed, a Microsoft Excel file was created that also included the municipality codes. That file was then imported into Epi Info to select only those records which municipality code belongs to Andalucía (see section 3.2). After that, the file was exported to R software (as a dBASE file) to implement a Principal Component Analysis (PCA) and subsequently produce an area-level (by municipality) deprivation score. This final deprivation score (computed for the 759 municipalities) had a median value of 0.01 and standard deviation 1.18. The minimum and maximum values were -3.46 and 3.38, respectively. The interquartile range was 1.58. As a measure of material deprivation, the higher the score, the more deprived an area is.

Chapter 4. Methods

4.1 Overview

This section will describe the health outcomes that were analysed (mortality due to lung cancer, larynx cancer and COPD) and how the magnitudes of their effects were estimated and subsequently modelled and mapped. Details will be given on how mortality estimates were computed for both men and women. Firstly, the use of internal, indirect, standardisation to compute the SMRs for all three mortality causes will be presented. Secondly, the modelling process will be described in detail.

Two different models were used to explain geographical heterogeneity in the mortality distribution. Firstly, a Structural Equation Model (SEM) [195, 196] was fitted to confirm that rock composition (as a surrogate measure for potential content of radon-gas in the soil) explained spatial heterogeneity in a lithology score. This lithology score, in turn, was produced from a Conditional Autoregressive (CAR) model as it was hypothesised to be spatially auto-correlated. That is to say, lithology of neighbouring areas was expected to be more similar to each other than to geographically-distant areas. Secondly, a BYM model was used that split the residual (not explained by the model) variance into two different components: spatially auto-correlated heterogeneity (CH, or clustering) and uncorrelated heterogeneity (UH, or random heterogeneity). In both cases (the SEM and BYM models) adjustment for socio-economic status (SES) at the area-level was implemented using a deprivation score. This deprivation score was computed by means of Principal Component Analysis (PCA) that made use of the percentage of illiterate and unemployed people, as well as the percentage of manual workers, by municipality.

Lastly, mapping of SMRs, and RRs obtained from the BYM model will be presented for lung-cancer mortality, separately for both men and women. Individual RR maps will be shown for each of the model components so that they are visually appraised. Thus, maps of RR due to lithology, deprivation and the residual variance (both clustering and heterogeneity) will be presented. Also, exceedance probabilities maps (of an RR being greater, or less, than 1) were produced to convey the likelihood that there is an excess, or lack, of risk of mortality for lung cancer, at some specific areas.

4.2 Health outcomes estimates

4.2.1 *Estimates of the expected number of cases*

Any mortality (or morbidity) frequency measure used to compare different populations must consider structural differences that may exist among them. Then, age and sex, as well as social class are considered to be common potential confounders to be adjusted for. This consideration is based on: firstly, these covariates may be simultaneously related to both the outcome and the exposure of interest; secondly, these relationships may be independent of each other; thirdly, the populations may differ in the distribution of the covariates. When these circumstances are present, a confounding effect may bias the statistical association between the exposure of interest and the outcome. As a result, any association (e.g. as measured by means of the relative risk) may be either overestimated or underestimated. When an exposure-outcome relationship is confounded, a true statistical association may not be detected; and the reverse, a finding of a spurious statistical association, may also happen. To address a potential confounding effect in the analysis stage of observational studies, different solutions can be implemented. Three different techniques have been used in this thesis: standardisation, stratification, and multivariable regression analysis. Standardisation was used to take account of differences in the age structure of the populations under comparison. Stratification was applied so that data for males and females were analysed separately. Multivariable regression analysis adjusted for area-level deprivation while estimating the effect of lithology, on mortality.

To accomplishing age-standardisation, the *indirect, internal*, method was used; it started with rates coming from age-groups of an internal population (the whole Andalusian population) which were then multiplied by the within-strata study-population sizes corresponding to each geographical area [214, 215]. In this way, the expected numbers of cases were estimated and, then, summed across strata (age groups). Then, the ratio of observed to expected numbers was computed to derive a frequency measure. This ratio is the SMR. In this scenario (a small number of cases arising from a relatively large population), the observed number of cases is considered to be Poisson distributed. Under this assumption (which must be checked) the SMR is the Maximum Likelihood Estimate (MLE) of the RR [43, 63, 73].

Another important step in the SMR computation process is to choose the population providing the rates [43]. *Internal standardisation* was used where the rates came from the addition of every single study population, as a whole. An iterative computational method devised by Mantel and Stark and subsequently simplified by Breslow and Day has been used in the past for rate standardisation [70, 71]. These methods are based on the assumption of a multiplicative model for the distribution of the observed number of cases. Consequently similar results can be achieved by fitting a Poisson regression model on the log scale [43, 47, 90]. Nevertheless, modelling of the SMRs by basic Poisson regression has some limitations. One of the restrictions of the Poisson model is that the variance and the mean are assumed to be equal. This assumption is, in practice, difficult to maintain and overdispersion (that is, the variance being larger than the mean) may occur. Overdispersion can arise due to one or more of the following: spatial autocorrelation, an excess of zero-event values (such as in a rare-disease situation), or just random heterogeneity [44, 90, 216, 217]. Where a Poisson model does not fit the data, it underestimates the standard error of the point estimates for the explanatory variables.

As an alternative a Negative-Binomial model, which allows for overdispersion, might be fitted, instead. The Negative-Binomial distribution would give the same point estimates, but larger standard errors, and hence, wider confidence intervals. Another difficulty that both the Poisson and Negative-Binomial models can encounter is when fitting data where an excess of zero-values (sparseness) is present; this may be the case where rare diseases are analysed. In these instances, a Zero Inflated Poisson (ZIP), or Zero Inflated Negative Binomial (ZINB) model can be useful alternatives. However, neither ZIP models, nor ZINB models, take spatial auto-correlation into consideration. Nevertheless, both ZIP and ZINB models can be further extended to accommodate complex hierarchical structures that account for both, spatial auto-correlation (clustering), and unstructured (heterogeneity) effects.

Therefore, to account for the potential confounding due to differences in the age-structure of the populations being analysed, age-adjusted SMRs estimates were calculated for both men and women in every Andalusian municipality. Estimates were calculated for a total of 759 municipalities, for the periods 1981-1985 and 1986-1995. *Internal, indirect standardization* [51, 62, p. 312-5] was used that obtained the rates from the whole study population. Subsequently, the rates and the corresponding study

populations were used to estimate the expected number of cases. These figures were applied, in turn, to model the SMRs via Bayesian regression analysis (see 4.2.2). The SMRs were computed for all three distinct mortality causes: lung cancer, larynx cancer, and COPD.

To obtain age-and-sex adjusted rates, the *glm* (*generalised linear models*) function (within R *stats-library* [218]) was used to fit separate Poisson regression models to the data concerning mortality due to lung cancer, larynx cancer and COPD, respectively. The outcome of interest was the observed number of cases and the variable *population* was specified as an *offset*. The starting point was a saturated model, where the predictor variables ‘age-group’, ‘sex’ and the interaction ‘age-group by sex’ were included. The Akaike Information Criterion (AIC), or *penalised log-likelihood*, guided model fitting [77, p.353-4]. The AIC is a derivation of a *likelihood ratio test* [215, p. 309-10] which in addition takes into consideration (penalises) complexity of the model, according to the number of parameters included. The automated *stepAIC* function was used: it drops one parameter at a time and prints the value of AIC for each model. The model with the minimum-significant AIC was chosen. The saturated model (*age-group + sex + [age-group*sex]*), remained as the minimum adequate model.

The *subscript* utility, available within the R software, was used to write a script that recorded the estimated rates of age-groups for each sex. This utility allows for access and manipulation of any elements stored within R objects (vectors, matrices, arrays, data frames and lists) [219]. The output produced after fitting a Poisson regression model (by means of the *glm* function) produces a list object or, more precisely, a list of lists. One of its elements contains the regression coefficients estimated by the model. These coefficients can be extracted as a group, using the ‘*coef*’ function available in the R *stat-library* [218]. Alternatively, the regression coefficients can be individually referred to by means of the subscripting utility, which allows for the manipulation of its values. So, the regression coefficients resulting from Poisson regression analysis were accessed and the estimated rates were computed in the original, multiplicative, scale: that is, as the *antilog* of the corresponding linear combination of parameters (age-group, sex and the interaction between them, plus the intercept). The resulting variable, the estimated rates, was then merged with the file containing the observed number of cases by municipality. To accomplish this task,

both files were linked by common fields (age group and sex) by means of the same script. Additional information contained in the final file included yearly population size, as obtained during data collection (see 3.4).

The estimated rates previously obtained allowed the computation of the expected number of cases and, consequently, of the SMRs. Firstly, the rates were multiplied by the population size to calculate the expected number of cases. Figures were obtained for age group, sex and yearly strata within every municipality. The data were aggregated by municipality where each one had a total number of observed and expected cases, per year. All this computation was accomplished using Epi Info software, where the *summarise* function (within the *Analyse Data* module) allowed for data aggregation. The next step, computing the SMRs, required further modelling implementation.

Although SMR calculation (as the ratio of observed over the expected number of cases) is apparently straightforward, two different issues were to be addressed: computational difficulties and spatial auto-correlation. When SMRs are calculated at the small area level, instability of the ratios (due to small expected number of cases) is likely to be encountered, leading to imprecise estimates. This can happen in the presence of either rare health events, and/or very small study populations. The second issue, spatial auto-correlation, concerns the lack of independence of observations. Both difficulties were addressed by modelling the SMRs using WinBUGS software, assuming that the observed number of cases followed a Poisson distribution. The previously estimated expected number of cases, instead of the populations was used as an offset [220]. Age-group and sex (as well as the interaction between both variables) were adjusted for as in the previous model and for the same periods of time (1981-1985 and 1986-1995). To allow for spatial auto-correlation, the BYM model was used; it partitions the residual variance into two different components: correlated heterogeneity (CH, or clustering) and uncorrelated heterogeneity (UH, or random heterogeneity) [63, p. 123-7, 221, p. 84-92, 119]. The clustering component arises from a Conditional Autoregressive (CAR) model; in the BYM model, the log disease-rate of a particular area is a function of both, explanatory variables, and potential confounders. The local average of disease rate in neighbouring areas partially pools (or smoothes) the original rates towards a local mean-value [222]. For the present analysis a *queen-style* adjacency weight-matrix was defined using the 'nb2WB' R-

software function, implemented within the R ‘spdep’ library [223]. This neighbouring definition (which borrows its name from chess moves) considers polygons to be neighbours if they share either a single boundary or vertex (section 4.2.2). The second component of the residual variance in the above-mentioned BYM model is the spatially-uncorrelated (or random) heterogeneity. This component was modelled as a normal distribution.

4.2.2 Modelling of Standardised Mortality Ratios

Observations arising from the same or close geographical areas tend to be similar to each other, while observations at locations which are far apart from each other tend to be dissimilar. These kinds of processes give rise to observations that are said to be clustered (or pseudo-replicated); that is to say, they are not independent from each other. In this situation, usual statistical estimates would produce too-narrow Credible Intervals (CIs), so that the effect of the explanatory variable of interest would be imprecisely estimated. As a further downside, this analytical method would prevent from gaining knowledge about any residual variability that is spatially correlated.

Consequently, a specific statistical approach is needed to address spatial autocorrelation. One simple alternative could be to summarise information for each individual area (*no-pooling* analysis). The drawback of such an approach is the potential instability of the SMRs [63 p. 4-5]. Extreme values would be estimated for areas with small population size and, hence, low number of expected cases. These extreme estimates would have over-estimated standard errors. To overcome this difficulty, individual-area estimates can be weighted (*partial-pooling analysis, shrinking, or smoothing*) according to their relative variance, as compared to an average variance. Estimates based on smaller denominators would express a value close to the average; conversely, estimates based on larger denominators would show a magnitude closer to the individual (un-weighted) area-value. In this way, emphasis is laid on the most reliable estimates. To weight the estimated SMRs, different approaches can be made to decide about the kind of smoother to use; this, in turn, is closely related to the computation of the adjacency matrix, which is a crucial element when Conditional Autoregressive (CAR) distributions are used to implement hierarchical models [224].

The adjacency matrix is actually comprised of three different matrices that contain related pieces of information. Two of them contain the polygon identification and the number of its adjacencies (neighbouring polygons) which provide the neighbour definition adopted by the researcher. A third one gives the weights assigned to each polygon, which will contribute to the smoothing of outcome estimates. Even though GeoBUGS (version 1.2) can easily generate the adjacency matrix, a potential flaw exists: this software does not check that any particular area is not specified as its own neighbour. For this reason, R (instead of WinBUGS) was chosen to compute the adjacency matrix. The *spdep* (spatial dependence) library [223] has different functions to create neighbours lists from polygon data frames. So, the *poly2nb* function was used to create an R neighbour list from the imported municipal shapefile. Then, the *nb2WB* function exported that information into WinBUGS, 3-dimensional array, format. Differently to WinBUGS, R allowed for checking that no area was declared as a neighbour of itself. The function *nb2mat* produced a binary weights matrix, where neighbour relationships were coded as 1 and lack of vicinity as 0. It was then straightforward to use the *diag* function to check values from the matrix main diagonal: all of them were 0, as the leading diagonal represented municipality self-matches.

Different generic terms are in use to refer to models devised to allow for clustered observations: Multilevel, mixed models, cross-sectional time series, random effects, as well as hierarchical-models, which is the term used henceforth in this thesis. Among the vast array of hierarchical-models applicable to this study, many of them assume that the observed number of cases follows a Poisson distribution. In these models, the mean value (for each area and stratum) is the product of the estimated rate times the expected number of cases. Nevertheless, this assumption has to be checked given that, in a very rare-disease situation, it might not be valid. In these cases, sparseness of data may lead to an excess of zero values, which would make it inappropriate to model the data as if they followed a Poisson distribution. To overcome this difficulty a Zero Inflated Poisson (ZIP) model can be fitted (section 4.2.1).

Two main strands of computational techniques can be followed to fit spatial models: frequentist and Bayesian analytical approaches. The former has been the standard statistical approach to data analysis for a long time. Nevertheless, Bayesian statistics have gained widespread use in the last few years. This is mainly due to the availability

of fast hardware, modern computational techniques, and software. Current hardware helps taking advantage of Bayesian strengths while managing computational demands; computing techniques based on simulation, like Markov Chain Monte Carlo methods (MCMC), assist in modelling complexities. Practical feasibility of Bayesian analysis has influenced its widespread use as the benefits now outweigh previous difficulties. One of the advantages of using a Bayesian approach is related to the overall performance of Bayesian estimates. From the frequentist point of view, the best estimator (the Maximum Likelihood Estimate [MLE]) is the minimum-variance, unbiased estimator. Performance is then measured by the Mean Squared Error (MSE), which is a linear combination of both, variance, and bias. Even when the frequentist criterion is applied to assess Bayesian estimates, these usually outperform the frequentist ones. This happens as the former can be much more precise than the latter. This causes the MSE to be lower for Bayesian estimates in many instances, especially with small sample sizes.

Some other advantages of Bayesian estimation are related to the integration of information, as well as interpretability. Frequentist inferences are based on the MLE; this is the most likely value that the sample statistic would represent, assuming an underlying probability model. This statistic would estimate the unknown, but fixed, parameter with certain error (which determines the confidence interval width). All of it provided the, unrealistic, scenario that the experiment under consideration was repeated an indefinite number of times. Therefore, both the point estimate and the confidence interval are not referred to the sample actually obtained; it is a theoretical range of values that would be obtained in the long-run. In contrast, the Bayesian approach brings together two different sources of information to produce inferences: information coming from the actual data under the assumed probability model (the *likelihood*), and previous beliefs (the *prior* probability). These two give the inference (the *posterior* probability). Its foundation is based on the Bayes' rule that relates to conditional probabilities. Using Bayes' rule, it is possible to estimate the probability of any conditional event, if the probability of the related one is known. This foundation makes the inferential process divert greatly from frequentist methods.

Consequently, a direct probability statement can be made about the parameters of interest, as they are considered to be random variables. And the same direct interpretation applies to estimates of error (credible intervals). A further advantage of

Bayesian analysis is that inference is not limited to point estimates (and error measurement); the posterior probability gives the whole probability distribution of the estimated parameter. It is also important to note that even when numerical results obtained by both methods are similar, interpretative differences still remain. Similar results may be obtained by both methods as they all use information provided by the likelihood, in the inferential process. In the Bayesian approach, though, the likelihood is weighted by the prior probability; therefore, a low weight (*vague prior*) would not modify the likelihood to a great extent.

Notwithstanding this circumstantial agreement in the results, some more advantages can still favour the use of Bayesian methods, as these incorporate prior beliefs into the modelling stage and can take advantage of simulation (random number generation). Use of the prior probabilities allows for inclusion of uncertainty about the parameters, which are now considered to be random variables. This is useful as new knowledge is an ever cumulative experience. It is also feasible given that researchers are usually aware of some kind of previous information. As data quality is always essential, choice of prior information is a key element, as it influences (together with the likelihood) the posterior estimates. This is the reason why a sensitivity analysis is frequently advocated to decide on the best prior to use.

Simulation is another asset that Bayesian analysis can use. Inferences based on simulation rely on random number generation, instead of point estimates and standard errors, to summarise results. As a result, an exhaustive description of inferences is obtained in the form of a probability density function. Simulation is considered to be the most reliable method to address inferential uncertainty and is well suited for very small sample size situations. In these cases, frequentist methods rely on the Central Limit Theorem to assume that the normal distribution assumption is valid. Simulation, instead, allows for an increment of sample size nearly at will and hence, helps to reduce uncertainty. It also accommodates complicated models, which makes it convenient to fit hierarchical structures, irrespective of the assumed probability model. Notwithstanding the advantages that simulation entails, Bayesian analysis can also be tackled from a different perspective.

Bayesian models can be broadly categorised as Empirical Based (EB) or Full Bayes (FB) methods. The former approximate the posterior distribution and estimate

hyperprior values from the data; conversely, the latter draw samples from the exact posterior distribution and estimate hyperpriors from different data sources. FB methods use a range of algorithms within the common family known as Markov Chain Monte-Carlo (MCMC) methods. By using MCMC, FB methods overcome some difficulties that EB methods may encounter. EB methods are based on numerical integration to calculate the posterior distribution, which may be difficult where a high number of parameters are to model. In these situations, only an approximation to the posterior may be achieved. As an alternative to calculating the posterior distribution, FB methods draw a random sample from the posterior. An immediate advantage of this method is that the sample size can be increased to reach the desired precision. Also, given that FB computation is not a major issue nowadays, a vast array of models with varying complexity can be fitted.

Several hierarchical models have been proposed for the spatiotemporal analysis of epidemiological data. The BYM model is a FB method that allows for spatial autocorrelation [62, p. 321-32, 63, p.123-7, 92, 225, 226]. A hierarchical model is assumed, in which a random effect variance-component is set as a mixture of correlated (spatially structured) and uncorrelated heterogeneity. The spatially-structured variance is then given a prior distribution under the Conditional Autoregressive (CAR) assumption which shrinks SMRs according to a local mean depending on neighbouring estimates [62, p. 282-7]. The *car.normal* distribution function (available in WinBUGS) was used to model the prior probability for the spatially-structured component of the variance [63, p. 70-1, 123-7]. Fitting this model required information about the adjacency matrix which defines neighbouring of spatial polygons (see 3.2). This information was supplied and exported as data, from R into WinBUGS. A binary weighting list was also required by the model, which assigns the value 1 in case a polygon is a neighbour of some specified area, and 0 otherwise. This is the simplest way to build an adjacency matrix and the accepted standard when no other assumptions are being considered; that is, just the mere existence of neighbouring areas, with no additional knowledge or hypotheses concerning geographical links.

4.3 Software description and analysis implementation

To be able to model the SMRs by means of the BYM model, different pieces of software were used: R [218] and WinBUGS [227] were especially relevant. Both R and WinBUGS are free software, readily available on the internet. R is very well suited for data analysis, statistical modelling and graphical representation, as well as data manipulation (see 4.2.2). One of its main advantages is the availability of many different packages that can be installed to tailor specific needs. The spatial epidemiology field is not an exception and different packages have been developed to assist in different steps: from data import through data manipulation, analysis and export [50]. Especially relevant is the ability of R to import/export data with different formats. This helped in data manipulation and analysis, as files could be transferred from and to different specialist software, like Epi Info, WinBUGS and GeoBUGS.

WinBUGS is also free software, devised for complex data analysis using a Bayesian approach through MCMC methods (specifically the Gibbs sampling algorithm). The BUGS project has become open-source [228] and future developments will be only made for this version. Nevertheless WinBUGS v1.4.3, which is a stable version, will remain available. GeoBUGS is an add-on module to WinBUGS (and OpenBUGS) that allows for spatial representation of data. It is particularly convenient for immediate mapping of data after they are modelled using WinBUGS. GeoBUGS can also assist in creating the adjacency matrix needed to fit Conditional Autoregressive (CAR) models. Nevertheless, it does not check that each polygon is not included as its own neighbour; for this reason R was used instead, at this step (see 3.2). Different R packages were used to accomplish these tasks: ‘maptools’ [229] and ‘spdep’ [223] were useful to address boundary data (see 3.2) and the spatial information related to the adjacency matrix.

Convergence is at heart of MCMC methods. All simulated chains are expected to reach a common equilibrium state, beyond which they would keep giving the same estimation. This estimation (the posterior distribution) would be an accurate representation of the target distribution, irrespective of the initial starting point for each chain. The BGR statistic is a convergence diagnostic tool that can be used when more than one Markov chain is run. It is calculated as the ratio of the variability of pooled chains over the average variability of all chains. At an early stage, the BGR

statistic (\hat{R}) tends to be greater than 1. As simulated chains reach a state of equilibrium, the statistic becomes closer to 1. Gelman suggests a value of $\hat{R} \leq 1.1$ to consider that convergence has been approached, or at least $\hat{R} \leq 1.5$ for some parameters, if the process is slow. This latter value is the one Spiegelhalter suggests be used. It may be also interesting to analyse convergence using WinBUGS to map results in GeoBUGS, immediately after that.

WinBUGS can apply a number of diagnostic-tools. So, autocorrelation histograms help in deciding about the *thinning* interval, the *burn-in* period, and the total number of *iterations* to run. Given that the initial estimates of any MCMC chain tend to be highly auto-correlated, it is standard procedure to discard part of it; this is the *burn-in* period, which can be incremented to try sampling from the posterior distribution at its equilibrium state. The autocorrelation graph also provides details about the lag beyond which autocorrelation becomes negligible. This information is used to reduce the number of iterations kept, which saves computer memory. This is quite relevant as WinBUGS, like R, stores all output analysis in the computer random-access memory (RAM). Consequently, too much output-data can cause the software to crash by exhausting all available memory.

There are at least two circumstances where computer-memory exhaustion may be encountered: first, if too many parameters are monitored at the same time; secondly, if too many iterations are run. The former may arise where several estimates for many different areas (such as the 759 different municipalities, in this study) are monitored. The latter may happen where precision of estimates needs enhancing, by running long chains. To address the first issue, parameter monitoring should proceed gradually. To counteract the second one, a thinning interval can be used; in this way, only one in several iterations is actually kept (e.g. 1 in 10, if thinning is set to 10). After the software has finished running a first set of foreseen iterations, convergence has to be checked.

When the MCMC process consists of more than one chain, WinBUGS allows for graphing of BGR statistic against the number of iterations. The graph represents values of BGR in three different lines: The green one shows the variability (as 80% width intervals) of posterior estimates of pooled chains. The blue one corresponds with the average within-chain variability. Finally, the red one is the ratio of between-

chain to within-chain variability (\hat{R}). As all the chains approach the equilibrium state, they become similar to each other. Therefore, the BGR statistic is close to 1 and both, the lines representing variance between chains, and within chains, tend to stabilise. Other graphs are also available to check convergence. So, trace plots represent sampled estimates against the iteration number. Where chains are approaching convergence, they tend to mix with each other adopting the *'fat hairy caterpillar'* shape. It is important to allow that the chains start from different points and afterwards assess convergence towards a common distribution.

To run different chains, initial values have to be provided for every stochastic node (random parameter). In the model that was fitted, initial values were set for elements that composed the residual variance, that is, clustering and heterogeneity. Different possibilities exist to decide on the initial values for each chain. Thus, WinBUGS can generate initial values. However, it has been reported that this method may cause the software to crash. Therefore, random values were generated in R, and passed as data into WinBUGS. An important decision concerning initial values has to do with the underlying distribution from which the values are generated. This is especially relevant where estimates concern parameters of prior distributions (hyperparameters).

Consequently, it is worth considering a sensitivity analysis where alternative initial values, arising from different distributions, are used each time. Some researchers especially advocate not using the inverse-gamma vague prior to estimate variance parameters. The rationale behind this recommendation is that this distribution, which is 'L' shape, strongly constrains the posterior. As a result, the posterior distribution becomes very sensitive to the chosen parameters. When vague priors are used, some researchers suggest generating values from normal distributions for all stochastic nodes, with the exception of variance parameters, which are constrained to be positive, in which case the uniform distribution would be used, instead of the inverse-gamma one. Yet another possibility is to take advantage of previous knowledge from actual data; this information can be used, therefore, as the prior probability. This seems most appropriate, as FBM are intended to integrate past knowledge into current data.

According to this, the BYM model was fitted to mortality data from 1981-1985 to generate prior information, about hyperparameters; this hyperprior values were used, afterwards, to fit data from the period 1986-1995.

4.4 Ecological analysis

4.4.1 *Socio-economic Status*

Socio-economic Status (SES) is a highly relevant covariate to take into consideration both in individual-level studies and ecological research (see 2.4). It has been extensively reported as a confounder in many epidemiological associations between different exposures, and health-related events. Furthermore, SES has been also considered a relevant explanatory contextual variable by itself. It was accounted for through an area-level deprivation index. This index was based on percentages (by municipality) of: unemployed and illiterate people, as well as manual workers. Principal Component Analysis (PCA) was used to derive this area-level deprivation score.

Subsequently, unmeasured variables with potential spatial dependencies (also known as contextual effects) were taken into consideration. To adjust for these unmeasured, spatially auto-correlated effects, general clustering of mortality rates was taken into consideration. To this end, a BYM model was fitted to lung cancer mortality data in both men and women. This way, the residual (not explained by the model) variance was split into two different components: clustering (or spatially correlated variability) and heterogeneity (or non-spatially correlated variability). The BYM model took also account of both area-level deprivation score from PCA analysis, and the lithological risk score derived from the SEM.

4.4.2 *Potential radon-gas exposure*

Spatial heterogeneity in rock composition (lithology) was hypothesised to be associated with geographic disparities in mortality rates due to lung cancer. This hypothesis was based upon two grounds: firstly, the correlation between lithology and content of radon-gas in the soil, according to previous studies; secondly, the reported effect of radon-gas exposure, which is considered to be a main risk factor in lung cancer development. The spatial dependence of mortality on lithology was also evaluated for two additional outcomes: chronic obstructive pulmonary disease (COPD) and larynx cancer. The reason for extending the analysis to these additional outcomes was based on previous knowledge showing that while tobacco smoking was a major risk factor for all the three conditions, radon-gas exposure has only been associated with lung cancer incidence.

Structural Equation Modelling (SEM) was used to assess the value of lithology in explaining geographical differences in mortality rates. The structural part of the SEM took account of a lithological risk score derived from a spatial Conditional Autoregressive (CAR) distribution. The measurement part of the SEM assessed the explanatory value of lithology on the lithological risk score. The SEM was fitted to mortality data due to each one of these three distinct causes: lung cancer, COPD and larynx cancer.

4.5 Disease Mapping

GeoBUGS software v 1.2 (an add-on to WinBUGS) was used to map raw and smoothed SMRs, the latter ones being labelled as RR to differentiate between them (sections 4.2.1 and 4.2.2). Also, statistically significant RRs were mapped as the probability of an RR being greater than 1. Given the small range of posterior RR estimates beyond 1, under the BYM model, no other threshold references were considered. Both spatially-structured and uncorrelated heterogeneity were mapped, where a relevant pattern was important to highlight. For this purpose, regional digital-boundaries in shapefile format were imported into R; afterwards, the file was exported into *S plus* format to be read from GeoBUGS (see section 3.2). Once the map was read into GeoBUGS, mapping was accomplished following the modelling stage implemented using WinBUGS. After modelling of the SMRs was completed, some other issues had still to be considered; among these, which estimate components were relevant to be mapped and how to represent them.

It is useful to produce maps that convey different sorts of information: thus, raw (SMRs) and smoothed (RR) maps, as well as individual RR regression components. By comparing raw and smoothed maps, the degree of shrinking (rendered during the modelling stage) can be conveyed graphically. This is relevant to be aware of over-smoothing that would hide the underlying risk variation [230]. Mapping of individual regression components, on the other hand, can show interesting graphical information generated through the modelling stage [63]. This is equivalent to partitioning the RR into estimates of risk that originate from different sources. This is accomplished by taking the antilog of the corresponding regression coefficients, which can be programmed using WinBUGS code. In this way, the geographical heterogeneity due to

these different sources is highlighted. So, variability in the RR explained by a variable (such as SES, or lithology) can be mapped.

Especially interesting is mapping of the residual RR. This helps to have a feeling of the overall goodness-of-fit of the model, which has to be also formally tested (see 4.2.2). This component contains the estimate of the variability not captured by the explanatory variables (and covariates) allowed for in the model. Under the BYM model, the residual RR is calculated as the antilog of the intercept plus both, the clustering and uncorrelated components (see 4.2.2). The last two components can be also calculated and mapped independently from each other. Mapping of these components in isolation allows for a graphical representation of where the residual RR is mostly laid. So, although different diseases can naturally arise in clusters, spatially-structured variability may also be due to unspecified area-level explanatory variables; among these, environmental risks or contextual (area level) effects may be potential explanatory variables for this residual RR. The uncorrelated heterogeneity, on the contrary, contains random-noise variability.

Another set of maps that can help understanding the modelling performance is exceedance probability maps, which represent the probability of area-level RRs being greater than some specified value. To represent this kind of map, some decisions have to be made: first, about the *threshold reference* for the RR to be detected; so, an RR greater than 1, where the number of observed cases is greater than expected (see section 4.2.1), may be decided. Secondly, about which *cut-off*–*posterior-probability* should be considered unusually high to deserve attention (e.g. 0.80, but not necessarily this value). In this way, exceedance-probabilities maps can help highlight individual high-risk (*hot-spot clustering*) areas. Thus, some researchers have analysed different decision rules concerning both, the RR threshold, and cutoff probabilities, by simulation from various Bayesian models [230]. The posterior distribution of RR in different scenarios, as compared with true values generated by simulation, was used as a guideline for decision making.

One reported simulated scenario corresponded with a situation similar to this research thesis: first, the total number of observed cases equated the total number of expected cases (that is, internal standardisation was simulated); second, simulation was addressed to render a realistic mixture of observed and expected cases (reflecting a

scenario comprised of populated and rural areas). Trying different cut-off-probabilities is important as the BYM model has shown to be conservative; to put it another way: it tends to miss small RRs, due to over-smoothing. As in most simulated scenarios an RR greater than 1.5 is rarely encountered, it seems reasonable to keep an RR threshold of 1, while adjusting the cut-off probabilities; this allows for the method to be set at different sensitivity and specificity values, according to the aims of the mapping process.

Chapter 5. Results

5.1 Overview

Outputs from two separate models will be presented. Firstly, results from a Structural Equation Model (SEM). This model will be separated, in turn, into the measurement (section 5.2.1) and the structural (section 5.2.2) parts of the model. Secondly, results from a BYM model will be presented (sections 5.3 and 5.3.4). Immediately after the model results, maps of SMRs, before and after modelling (Relative Risk maps), will be shown (sections 5.3.3 and 5.3.4).

The posterior parameter distributions corresponding to all sets of analyses will be described in tabular form by means of its percentile values (2.5%, 50%, and 97.5%) as well as both the posterior mean and the posterior standard deviation. The Monte Carlo (MC) error will be presented also so that precision of estimates can be appraised; the aim was to achieve a MC error with magnitude less than 5% of the posterior standard deviation of each estimate. Additionally, the whole posterior distributions of parameter estimates will be presented as probability-density graphs. To provide a visual perception of the effect of modelling on the SMRs mapping of SMRs, by municipalities, before and after modelling (RR maps) will be presented. Maps of RR for lung-cancer mortality will be presented for men and women separately. To help appraise the relative importance of each explanatory variable, RR maps will be decomposed into the components due to each explanatory variable: lithology, deprivation, and the two components of the Variance Partition Coefficient (clustering and heterogeneity). Exceedance probability maps of an RR being greater (and less) than 1 will also be presented; these maps are intended to provide a geographical perception of how meaningful the posterior RR estimates are for each municipality.

5.2 Structural Equation Modelling

5.2.1 Measurement model

Table 5.1 shows the results from the measurement part of the Structural Equation Model (SEM). All three of the loading factors (represented by rock composition) were positively associated with the lithological risk score. The posterior mean values and 95% credible intervals (CI) for metamorphic, plutonic and volcanic rocks were 1.16 [1.07-1.17], 1.37 [1.30-1.44] and 0.46 [0.41-0.51], respectively. In other words, all of these three types of rocks were positively associated with the lithology score. The most relevant soil-feature was the existence of plutonic rocks, followed by metamorphic and volcanic ones.

Rock-type node	mean	sd	MC error	2.5%	median	97.5%	start	sample
Metamorphic	1.16	0.02389	0.001307	1.071	1.116	1.165	4001	5100
Plutonic	1.365	0.03677	0.001793	1.292	1.366	1.437	4001	5100
Volcanic	0.4586	0.02475	5.249E-4	0.4115	0.4584	0.5083	4001	5100

Table 5.1. Measurement model. Lithology-indicator loadings: posterior estimates.

Given that the lithological characteristics of all Andalusian municipalities were summarised in only four main classes (sedimentary, metamorphic, plutonic and volcanic rocks) many zero values were generated for all places where any of these rocks were nonexistent. The ratio variance/mean was much higher than 1 for the frequency distribution of all four lithological classes: 255.08 for sedimentary rocks, 111.61 for metamorphic, 144.55 for plutonic, and 84.17 for volcanic rocks. Therefore, a ZIP model was fitted for this measurement part of the SEM. The number of square kilometres taken by each rock within any municipality was considered to follow a multinomial distribution; therefore, an equivalent method was used which consisted of fitting a Poisson regression model against a baseline (sedimentary rocks in this case)

for non-zero values. Zero values were modelled as a random effects binomial distribution, which accounted for the extra-variability due to presence of zero counts.

Figure 5.1 shows that all three posterior probability-densities were on a positive axis and did not include the zero value. Therefore, zero is not a believable value for the regression coefficients concerning the rocks composition variables that explain the lithological risk score.

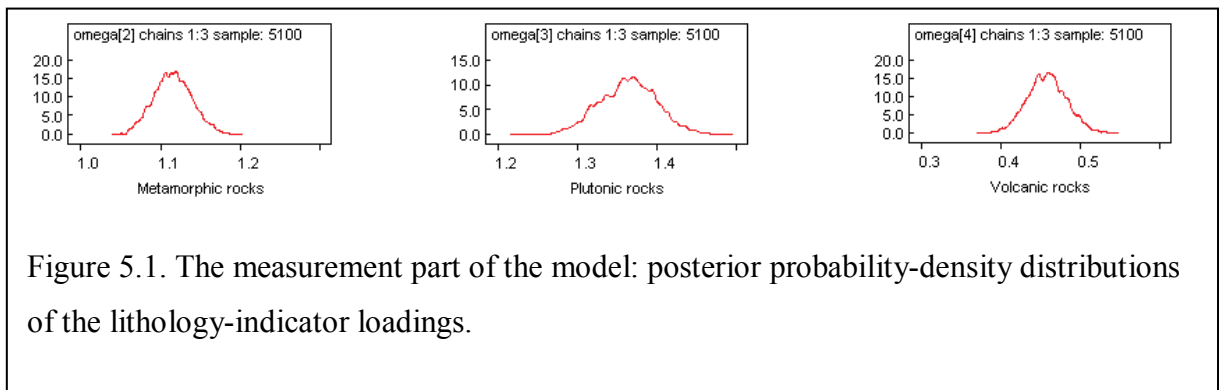


Figure 5.1. The measurement part of the model: posterior probability-density distributions of the lithology-indicator loadings.

Figure 5.2 shows how convergence was reached for the loading factors estimates in the measurement part of the SEM, after using a thinning interval of 40. History plots show how the three independent chains, for each one of the different factor loadings, had eventually mixed adequately (Figure 5.3, with red, blue, and green-coloured chains). The Monte Carlo error was no greater than 5% of the posterior standard deviation, for all three factor-loading estimates (Table 5.2). That is to say, precision was achieved to the aimed standard.

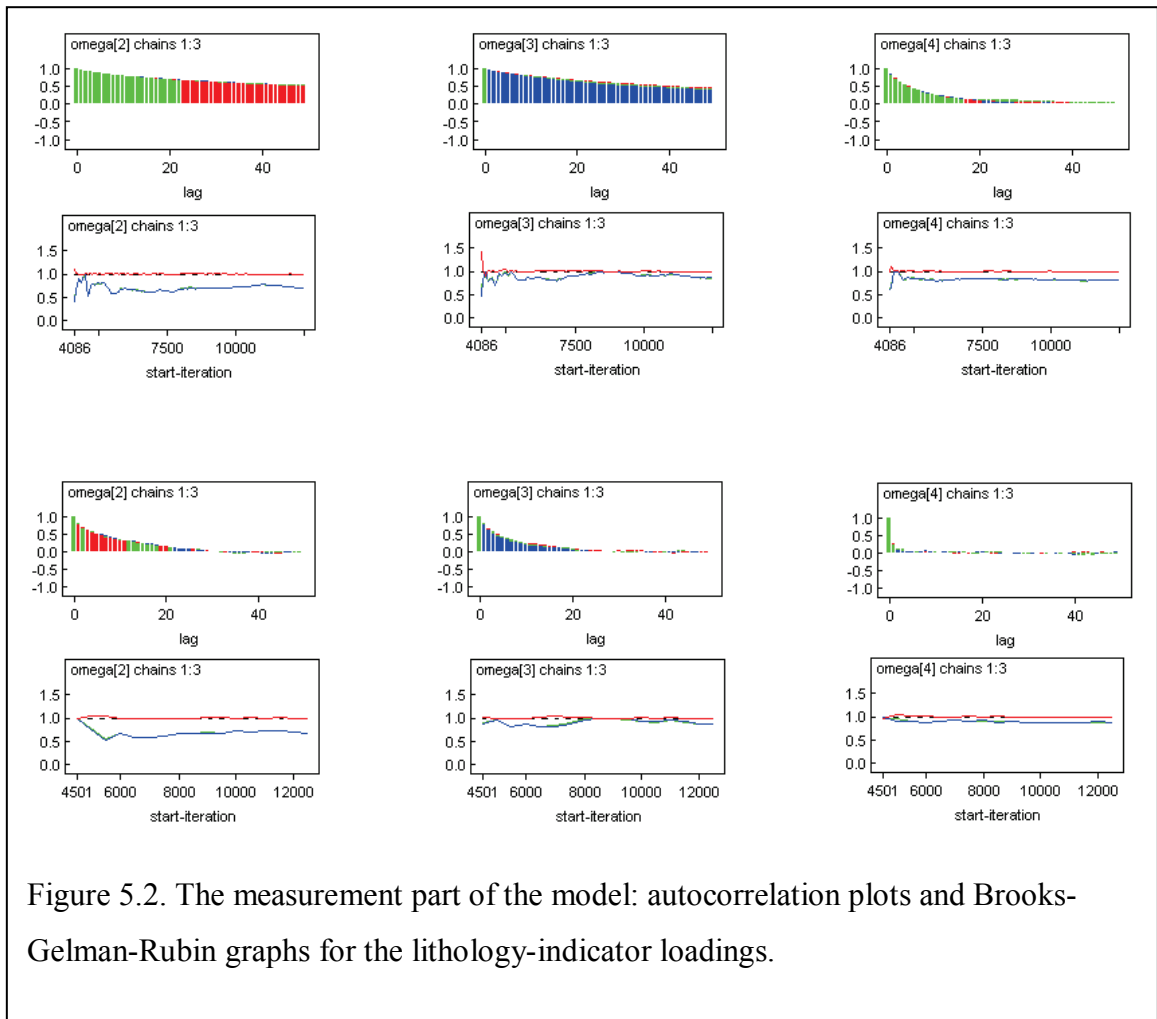


Figure 5.2. The measurement part of the model: autocorrelation plots and Brooks-Gelman-Rubin graphs for the lithology-indicator loadings.

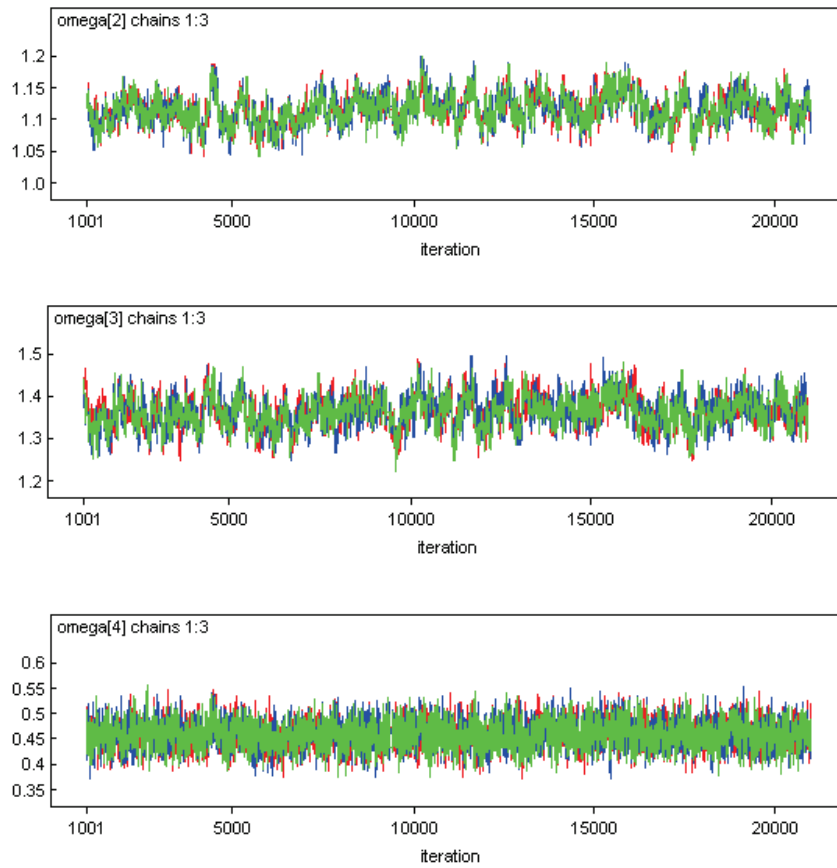


Figure 5.3. The measurement model. Lithology-indicator loadings: history plots.

5.2.2 Structural model

Table 5.2 shows the results from the structural part of the SEM model. The posterior mean values for the regression coefficients concerning the first two mortality causes, COPD and larynx cancer, were -0.01 and -0.015, respectively. These results suggest a negative association between the lithology score and mortality due to either COPD or larynx cancer. However, inspection of their respective 95% credible intervals (95% CIs) shows that they include zero as a likely value. Thus, the 95% CIs ranged from -0.040 to 0.019 and from -0.044 to 0.015, for COPD and larynx cancer respectively. The posterior mean value for the regression coefficient from lung-cancer mortality data was positive (0.023). In addition, the 95% CI for the regression coefficient did not include zero; it ranged from 0.011 to 0.035.

Lithology-score node	mean	sd	MC error	2.5%	median	97.5%	start	sample
COPD	-0.01018	0.01493	1.977E-4	-0.03991	-0.01014	0.01939	11001	30000
Larynx cancer	-0.01513	0.01486	1.964E-4	-0.04442	-0.01523	0.01453	11001	30000
Lung cancer	0.02252	0.006198	8.384E-5	0.0107	0.02242	0.03483	11001	30000

Table 5.2. Structural Model: lithology-score regression coefficients estimates for Chronic Obstructive Pulmonary Disease (COPD), larynx cancer, and lung-cancer mortality, in men.

As a visual aid to interpretation, the whole posterior probability density for the lithology score (for all three mortality causes) can be assessed in Figure 5.4. The upper and bottom rows show the densities on the logarithmic and the ratio scale (RR), respectively. It can be seen that the first two densities included the null value (zero on the log scale and one on the original, ratio scale) as a likely estimate. Conversely, the whole posterior density concerning lung cancer did not include the null value. The middle row in Figure 5.3 shows this fact more clearly. It depicts both the areas of the respective curves at (or below) the null value (*marked as '0'*) and above the null value

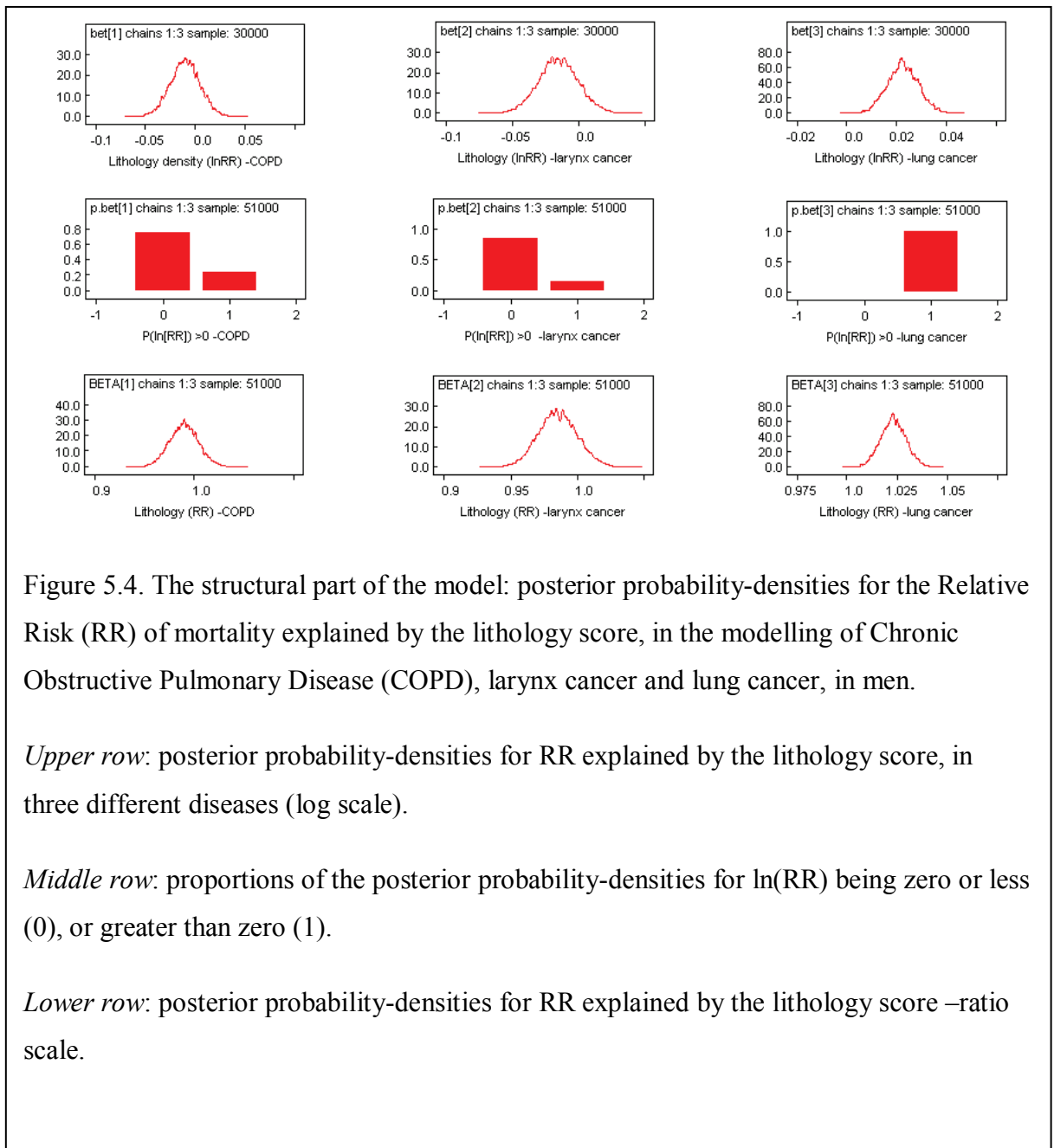


Figure 5.4. The structural part of the model: posterior probability-densities for the Relative Risk (RR) of mortality explained by the lithology score, in the modelling of Chronic Obstructive Pulmonary Disease (COPD), larynx cancer and lung cancer, in men.

Upper row: posterior probability-densities for RR explained by the lithology score, in three different diseases (log scale).

Middle row: proportions of the posterior probability-densities for ln(RR) being zero or less (0), or greater than zero (1).

Lower row: posterior probability-densities for RR explained by the lithology score –ratio scale.

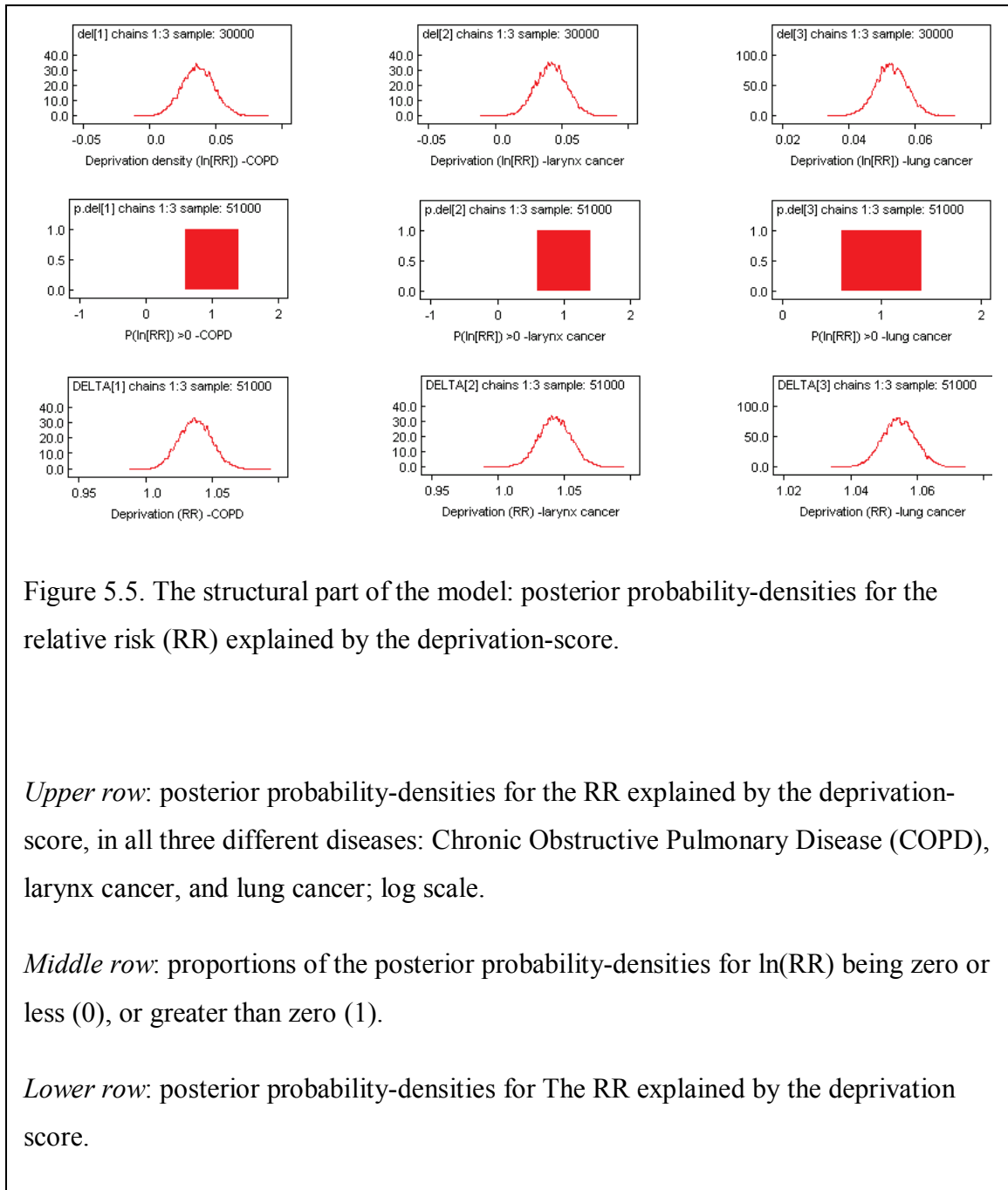
(marked as '1'). It can be seen that the whole posterior regression-coefficient density was above zero, or one on the ratio scale, only for lung-cancer. For the other two mortality causes, the densities included the null value; moreover, the areas above the null value were relatively small (24% and 16% for COPD and larynx-cancer, respectively). Therefore, the distribution of lung-cancer deaths (but not COPD or larynx-cancer deaths) was positively associated with the lithological risk score.

Table 5.4 presents posterior estimates for the regression coefficients accounting for area-level deprivation. In contrast to the lithology score, the mean posterior values for deprivation in all three diseases are positive; 0.037, 0.042 and 0.053 for COPD, larynx cancer and lung cancer, respectively. Their 95% CIs range from 0.013 to 0.061, from 0.020 to 0.065 and from 0.044 to 0.062, for COPD, larynx cancer and lung cancer, respectively. Therefore, there is evidence of a positive association between the SES scoring (deprivation) and all three of the mortality causes.

Deprivation-score node	mean	sd	MC error	2.5%	median	97.5%	start	sample
COPD	0.03681	0.01216	2.576E-4	0.01315	0.03672	0.06097	11001	30000
Larynx cancer	0.04221	0.01164	2.18E-4	0.01975	0.04224	0.06523	11001	30000
Lung cancer	0.05301	0.00475	1.037E-4	0.0437	0.05295	0.06242	11001	30000

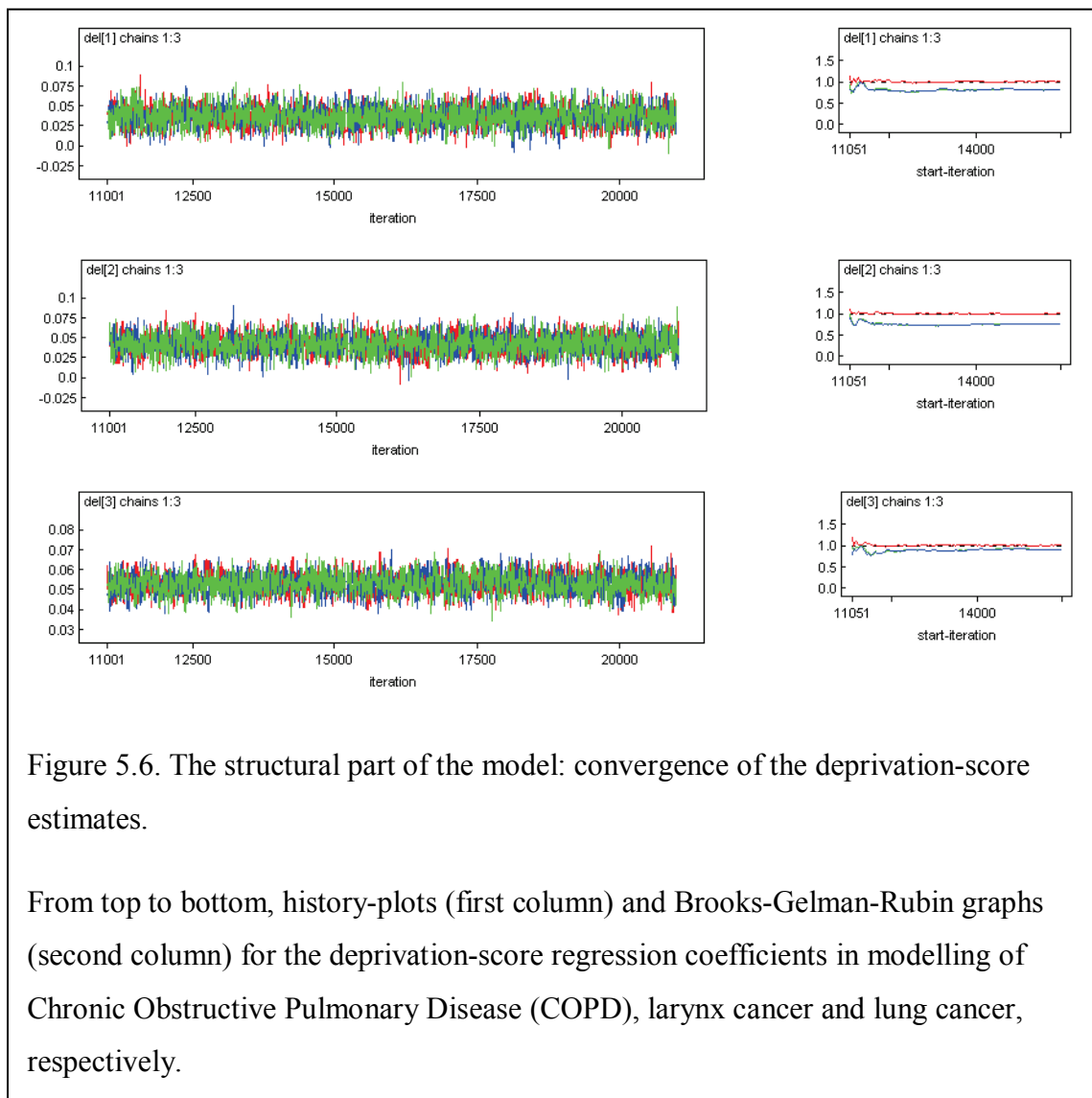
Table 5.3 The structural part of the model: estimates for the deprivation-score regression coefficients. Chronic Obstructive Pulmonary Disease (COPD), larynx cancer, and lung-cancer mortality, in men.

The same interpretation can be drawn from the shape of their whole posterior densities shown in Figure 5.5. The upper and bottom rows show the probability densities on the log and ratio (Relative Risk -RR) scales, respectively. It can be seen that none of the densities for all three diseases (COPD, larynx and lung cancer) included the null value.



This is also depicted by the graphs in the middle row (Figure 5.4) where the whole area under the density curve is *marked as 1* (as they were greater than the null value) for all three diseases.

Lastly, Figure 5.6 provides additional assessment of convergence for deprivation estimates. History plots show adequate mixing of the three independent chains in all the three cases (COPD, larynx and lung cancer). The BGR diagnostic graph also shows that the BGR ratio statistic (in the colour red) had stabilised close to the value of one. All these diagnostic criteria helped in demonstrating that the posterior estimates had been drawn from the target distribution.



5.2.3 Summary of the Structural Equation Model

Presence of metamorphic, plutonic and volcanic rocks, are all features that correlate well with a lithology score that presumes spatial similarity (autocorrelation) of nearby geographical areas. Furthermore, this lithology score is positively associated with the spatial distribution of deaths due to lung cancer in men, and the association remains after controlling for deprivation in the model. The deprivation score turns out to also be positively associated with the spatial distribution of male deaths due to lung cancer. Similarly, there exists a positive association between deprivation and the spatial distribution of deaths due to both COPD and larynx cancer. However, there is no evidence of an association between lithology and the number of deaths due to either COPD, or larynx cancer.

5.3 Lung-cancer mortality modelling

5.3.1 Besag-York-Mollié model: males

A BYM model was fitted to lung-cancer mortality data in men. The lithology score derived from the SEM (see 5.2), as well as area-level deprivation were included in all models. Five different models were simultaneously fitted: An intercept-only model (model 'y1'); intercept plus the lithology score (model 'y2'); intercept, plus lithology and deprivation scores (model 'y3'); a further model that included a clustering component (model 'y4'), and the last one which also included a random-heterogeneity component (model 'y5'), which is the full BYM model. The relative merit of all these models was assessed for both, the goodness of fit of observed data as well as their predictive ability. To assess the relative goodness of fit of the observed data, the Deviance Information Criterion (DIC) was used to determine the optimal model. The model with the smallest DIC value was chosen as the best fitting model amongst those compared. This model (Table 5.4) turned out to be the full BYM model with the lithology and deprivation scores included (model 'y5'). In this case, the DIC was 4,050, much lower than the second best one (model 'y4') which gave a DIC value of 4,552.

	Dbar	Dhat	pD	DIC	Model
y1	5265.610	5265.240	0.373	5265.980	I
y2	5247.930	5247.120	0.812	5248.740	I + L
y3	5120.540	5118.970	1.568	5122.100	I + L + D
y4	4294.880	4037.320	257.563	4552.440	I + L + D + CH
y5	3767.430	3484.760	282.667	4050.090	I + L + D + CH + UH
total	23696.400	23153.400	542.984	24239.400	
<p>Dbar = posterior mean of the Deviance (average deviance)</p> <p>Dhat = Deviance of the posterior mean</p> <p>pD = Effective number of parameters (Dbar - Dhat)</p> <p>DIC = Deviance information Criterion (Dhat + 2pD = Dbar + pD). <i>Lower values of DIC are preferred.</i></p> <p>I = Intercept only</p> <p>L = Lithology score</p> <p>D = Deprivation score</p> <p>CH = Correlated –spatially structured- Heterogeneity</p> <p>UH = Uncorrelated Heterogeneity</p>					

Table 5.4 Besag-York-Mollié model: relative goodness of fit of observed data, for all different models. Lung-cancer in men.

To assess the relative predictive ability of the different models two different loss functions were used that measured the difference between the observed and the predicted values (also known as Posterior Predictive Loss). The loss functions used were the Mean Square Predictive Error (MSPE), which is shown in Table 5.5, and the Mean Absolute Predictive Error (MAPE), in Table 5.6. As for the DIC, the model with the smallest value (either for the MSPE or the MAPE) is preferred. The model with the lowest MSPE value was the full BYM model (model 'y5', MSPE = 65), while the second best one (model 'y4') had a much larger value (MSPE = 782). Models were ranked the same way when the MAPE was taken into consideration. The full BYM model ('y5') had a posterior mean MAPE value of 4.6, while the second best model ('y4', which was the one without the random-heterogeneity component) had a value of 7.2. Therefore, the full BYM gave the best fit for both the observed values and the predicted ability. The Posterior Predictive Loss (PPL) can also be used as a mean to assess convergence. Table 5.5 and Table 5.6 show that the Monte Carlo error (MC error) for both the MSPE and MAPE estimates (and all the models compared) was around 1% of their posterior standard-deviation estimates, which demonstrates that convergence had been achieved; this is required for the estimates to arise from the target distribution.

MSPE	mean	sd	MC error	2.5%	median	97.5%	start	sample	Model
y1	403.1	50.22	0.3613	310.9	400.5	507.8	1001	21990	I
y2	419.1	52.1	0.362	324.9	416.5	527.9	1001	21990	I + L
y3	224.0	27.82	0.1895	175.8	222.0	284.7	1001	21990	I + L + D
y4	782.3	170.0	2.265	483.2	770.6	1149.0	1001	21990	I + L + D + CH
y5	65.05	14.06	0.09957	45.05	62.53	99.29	1001	21990	I + L + D + CH + UH
MSPE = Mean Squared Predictive Error. <i>Lower values of MSPE are preferred.</i>									
I = Intercept only									
L = Lithology score									
D = Deprivation score									
CH = Correlated Heterogeneity									
UH = Uncorrelated Heterogeneity									

Table 5.5 Besag-York-Mollié model. Relative goodness of predictive ability (MSPE) for all different models. Lung cancer in men.

MAPE	mean	sd	MC error	2.5%	median	97.5%	start	sample	Model
y1	7.722	0.1767	0.001221	7.378	7.723	8.07	1001	21990	I
y2	7.68	0.1779	0.001232	7.331	7.679	8.032	1001	21990	I + L
y3	7.174	0.18	0.001173	6.825	7.175	7.526	1001	21990	I + L + D
y4	7.167	0.3873	0.005444	6.427	7.159	7.941	1001	21990	I + L + D + CH
y5	4.545	0.1834	0.001524	4.199	4.54	4.914	1001	21990	I + L + D + CH + UH

MAPE = Mean Absolute Predictive Error. *Lower values of MAPE are preferred.*

I = Intercept only
L = Lithology score
D = Deprivation score
CH = Correlated Heterogeneity
UH = Uncorrelated Heterogeneity

Table 5.6 Besag-York-Mollié model. Relative goodness of predictive ability (MAPE) for all different models. Lung cancer in men.

Once the model had converged, posterior estimates were obtained for the regression coefficients for both the lithology and deprivation scores. The posterior mean-estimates on the log scale were 0.023 and 0.04 for the lithology and deprivation scores, respectively. Their respective 95% CIs ranged from 0.015 to 0.031 and 0.033 to 0.046 (Table 5.7). An interaction term between the lithology score and area-level deprivation (as surrogate measures for potential radon-gas exposure and tobacco smoking, respectively) did not improve the goodness of fit of the model; the mean posterior estimate for the interaction term was -0.001 with 95% CI [-0.002, 0.002].

Node	mean	sd	MC error	2.5%	median	97.5%	start	sample
Intercept	0.01229	0.004091	3.664E-5	0.004321	0.01227	0.02027	8331	38010
Lithology	0.02292	0.00389	3.166E-5	0.0153	0.02291	0.03051	8331	38010
Deprivation	0.03953	0.003565	4.049E-5	0.03257	0.03955	0.04647	8331	38010

Table 5.7 Besag-York-Mollié model. Regression-coefficients estimates (log scale). Lung-cancer in men.

Therefore, there is a positive association between the lithology score and mortality due to lung cancer in men. There is also a positive association between the deprivation score and lung cancer mortality in men. The same interpretation can be seen on the ratio (RR) scale. The computed posterior mean-values were 1.02 and 1.04 for the lithology and deprivation scores, respectively. Their respective posterior 95% CIs varied from 1.015 to 1.031 for the former and 1.033 to 1.048 for the latter (Table 5.8).

Node	mean	sd	MC error	2.5%	median	97.5%	start	sample
Lithology	1.023	0.00398	3.24E-5	1.015	1.023	1.031	8331	38010
Deprivation	1.04	0.003709	4.212E-5	1.033	1.04	1.048	8331	38010

Table 5.8 Besag-York-Mollié model: regression-coefficients estimates (ratio scale). Lung-cancer in men.

This means that the mortality risk due to lung cancer increases 2% on average, for every unit of increment in the lithology score (from 1.5% to 3.1%, according to its 95% CI). The effect for the deprivation score was twice as much as for the lithology score; a 4% average increment in risk for every unit that the deprivation score increases (it ranged from 3.3% to 4.8%). It can be seen from both Table 5.7 and Table 5.8 that all these estimates were obtained with a MC error of around 1%, of their respective posterior standard-deviation estimates.

The Relative Risk of lung-cancer mortality in men, averaged over all 759 municipalities was 1.04 with an interquartile range of 0.24 (Table 5.9); the average Monte Carlo error was less than 5% of the average standard deviation, which shows that convergence, amongst all three chains that were run, was achieved. The range of the RR varied between 0.49 and 2.42 while the range of the SMR was between 0 and 3.25 which shows the smoothing effect of modelling; this effect is also seen in the difference of the mean values averaged across all municipalities (Table 5.9): the average RR was pooled towards one, which is the RR value of no effect. However, after modelling, the RR interquartile range increased over the SMR interquartile range, which improved differentiation between high and low-risk areas.

	mean	sd	MC error	2.5%	97.5%	IQR
SMR	0.88	0.46	5.11e-9	0.876	0.884	0.003
RR	1.05	0.18	0.003	0.72	1.45	0.24

Table 5.9 Average values of the SMR and RR, for lung-cancer mortality in men.

SMR = Standardised Mortality Ratio

RR = Relative Risk

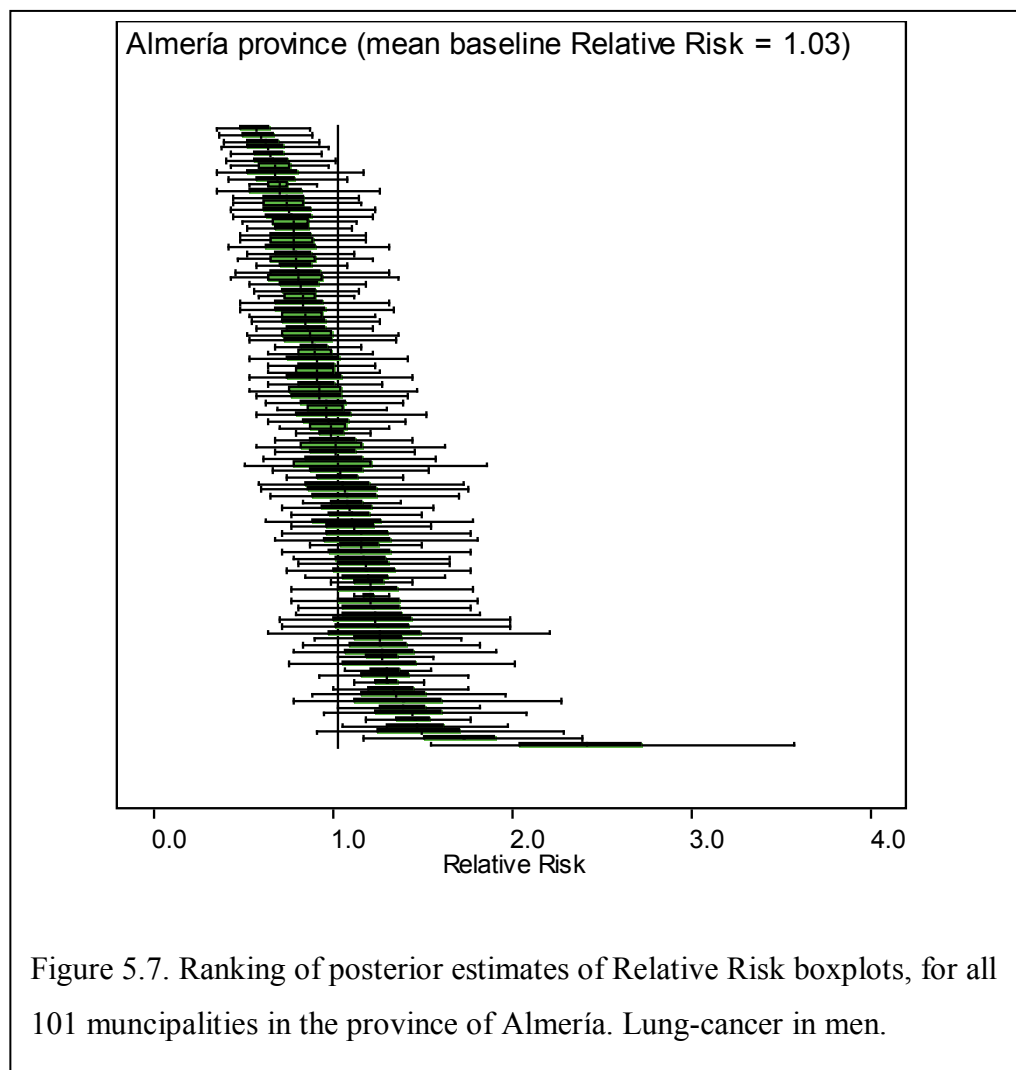
sd = Standard deviation

MC error = Monte Carlo error

2.5% = 2.5 percentile

97.5% = 97.5 percentile

Figure 5.7 to Figure 5.14 show the distribution of posterior RR estimates across all 759 municipalities analysed, while being grouped by provinces. Box plots limits represent the posterior quartiles; the middle bars within the boxes are the posterior mean values, and the whisker lines reach the 2.5% and 97.5% posterior percentiles. The reference line represents the posterior mean which was averaged over all municipalities (within each province). It can be seen that the mean posterior RR were highest in the provinces of Cádiz (mean RR 1.35; Figure 5.8), Sevilla (mean RR 1.34; Figure 5.14) and Huelva (mean RR 1.15; Figure 5.11) while they were lowest in the provinces of Jaén (mean RR 0.80; Figure 5.12) and Granada (mean RR 0.89; Figure 5.10). However, there was ample heterogeneity within provinces and the RR estimates which represent lower and higher risk than the average value, for any particular province, can be clearly identified from their individual box plots, as their green areas represent 95% CI.



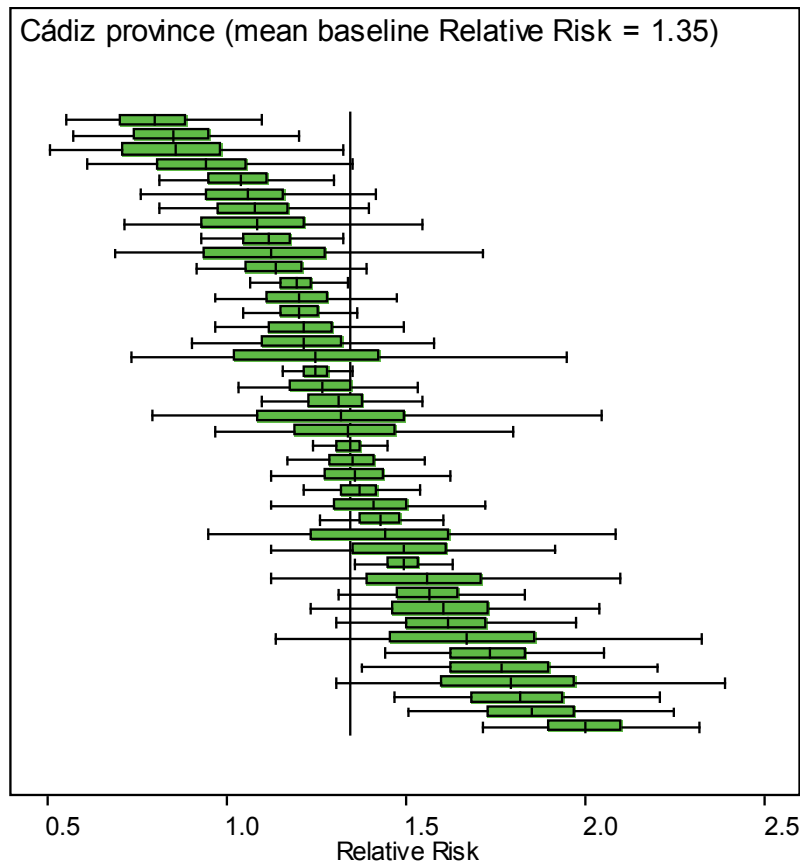


Figure 5.8. Ranking of posterior estimates of Relative Risk boxplots, for all 42 municipalities in the province of Cádiz. Lung-cancer in men.

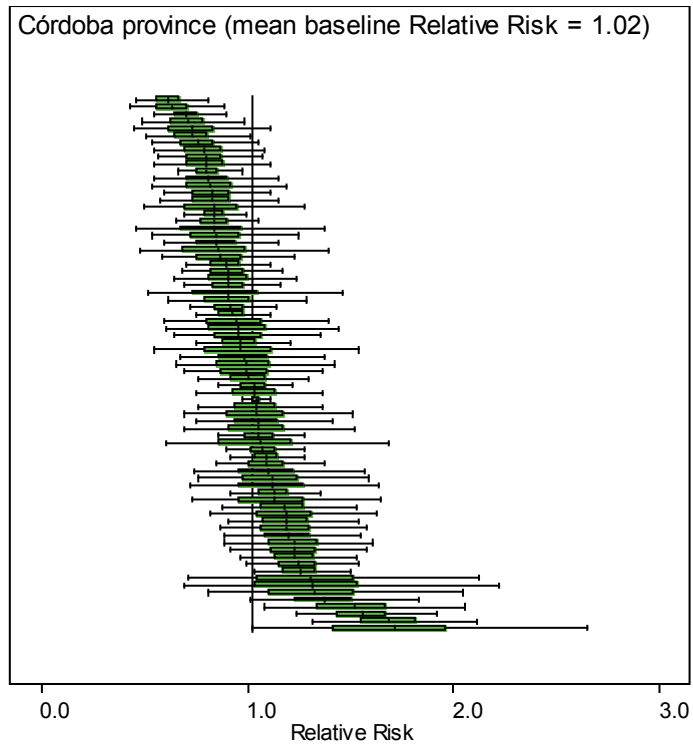


Figure 5.9. Ranking of posterior estimates of Relative Risk boxplots, for all 75 municipalities in the province of Córdoba. Lung-cancer in men.

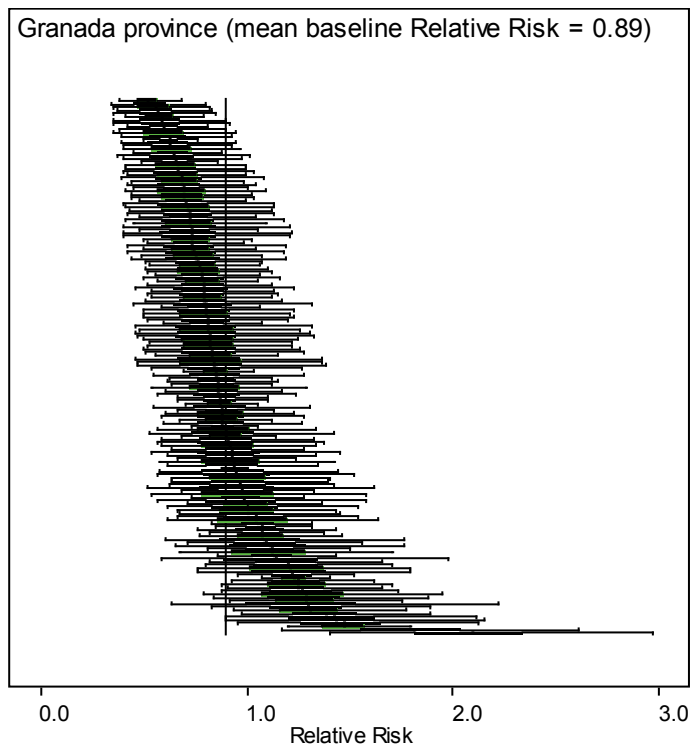
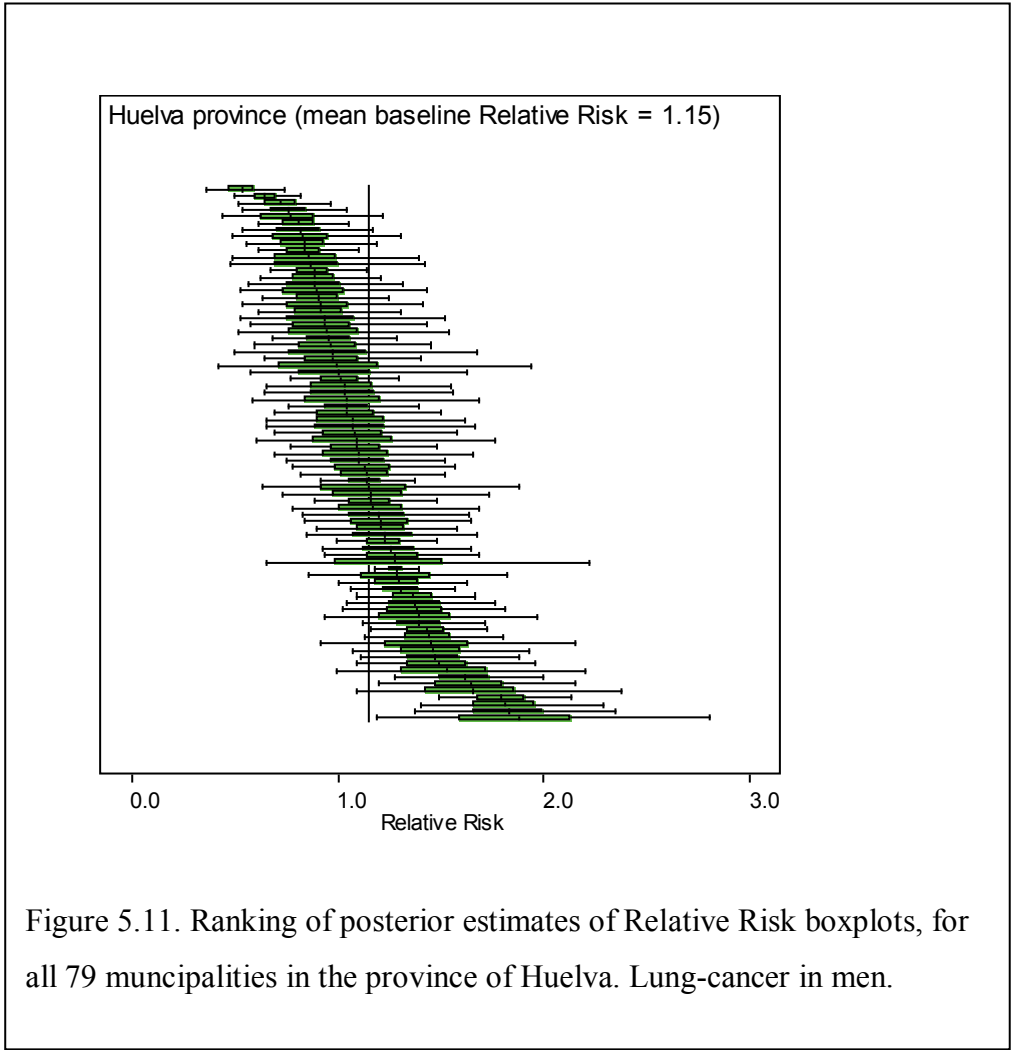


Figure 5.10. Ranking of posterior estimates of Relative Risk boxplots, for all 166 municipalities in the province of Granada. Lung-cancer in men.



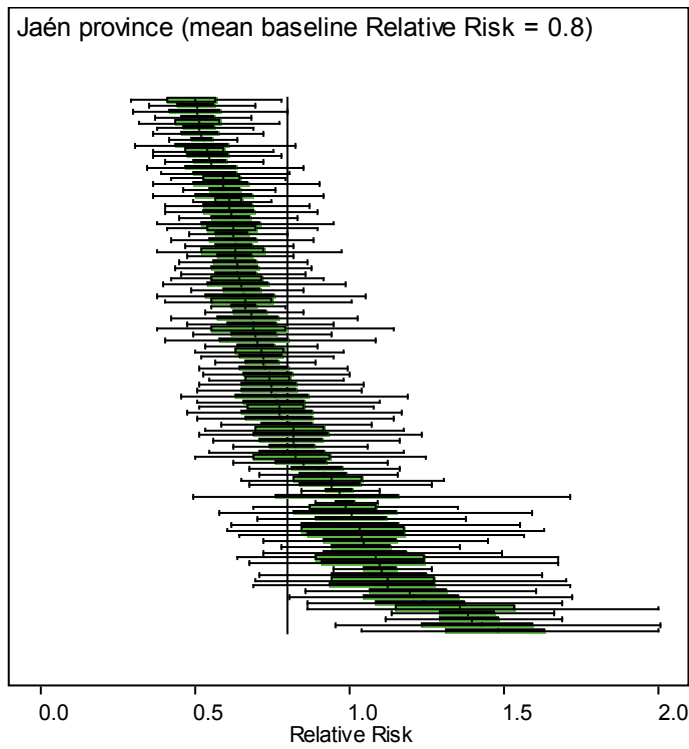


Figure 5.12. Ranking of posterior estimates of Relative Risk boxplots, for all 96 municipalities in the province of Jaén. Lung-cancer in men.

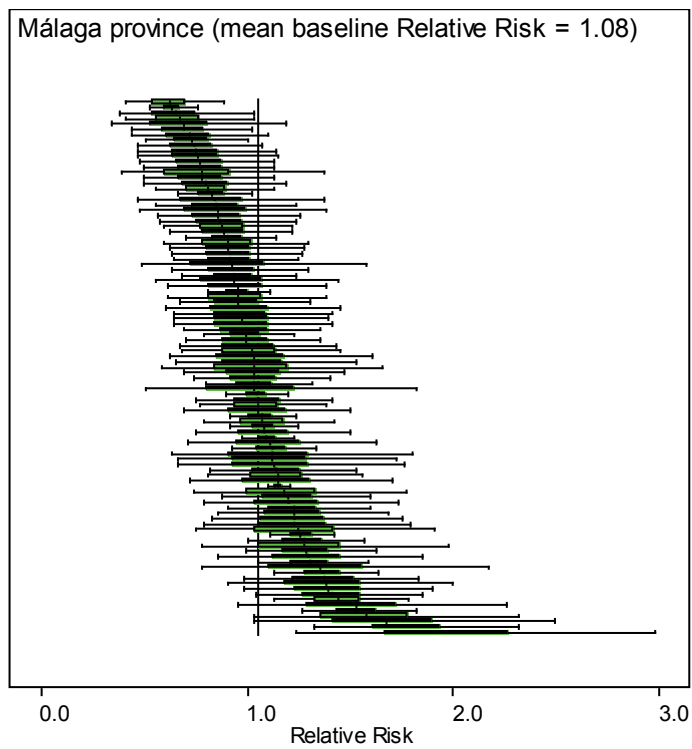


Figure 5.13. Ranking of posterior estimates of Relative Risk boxplots, for all 99 municipalities in the province of Málaga. Lung-cancer in men.

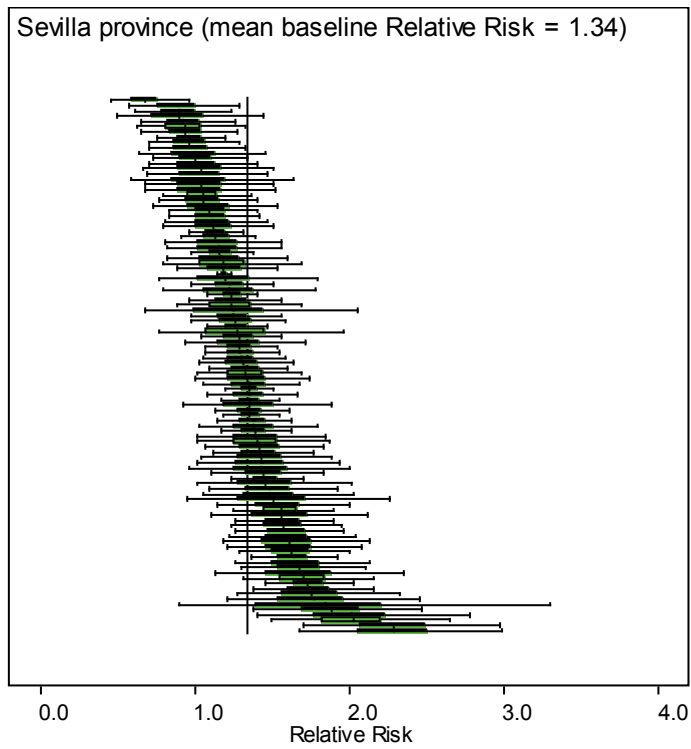


Figure 5.14. Ranking of posterior estimates of Relative Risk boxplots, for all 102 municipalities in the province of Sevilla. Lung-cancer in men.

The frequency distribution of the observed number of lung-cancer cases in men was overdispersed (ratio variance/mean = 518.3; Bohning’s statistic 53.81, p value < 0.001). Therefore, further analysis was implemented for checking if overdispersion was only due to unstructured heterogeneity (e.g., because of excess of zero counts: 4.4% of all records in the male lung-cancer dataset) or spatial autocorrelation was also present. A Moran’s I Monte Carlo test was run as well within R software, for testing the spatial dependency of the SMRs distribution; the adjacency matrix was used as weights for this test (Moran’s I statistic = 0.25 after 1,000 simulations, p value = 0.001). Given that spatial autocorrelation was present, a hierarchical BYM model was fitted afterwards, where separate estimates for the residual variance components were computed: namely, spatially-correlated (clustering) and uncorrelated (random) heterogeneity. This allowed for the Variance Partition Coefficient (VPC) to be calculated. The posterior mean estimate of the VPC was 0.95 and its posterior 95% CI ranged from 0.93 to 0.97 (Table 5.10).

Node	mean	sd	MC error	2.5%	median	97.5%	start	sample
VPC	0.9541	0.009781	2.011E-4	0.9326	0.9552	0.9708	41001	2742

Table 5.10. Besag-York-Mollié model: Variance Partition Coefficient (VPC) estimates. Lung-cancer in men.

Consequently, most (95%) of the residual variance (not explained by the model) was due to spatial autocorrelation of the estimates amongst nearby municipalities, and just a small amount (5%) was due to random variability within geographical areas. Therefore, most of the variability not explained by the model was due to (unmeasured) factors that vary across geographical areas.

5.3.2 Besag-York-Mollié model: females

The same BYM model previously used (see 5.3.1) was applied to model mortality due to lung-cancer in women. Five different models were also adjusted and simultaneously compared. From the simplest to the most complex one, those models were: an intercept-only model (‘y1’); model ‘y2’, which added the lithology score to the

previous one; model ‘y3’ increased complexity by further accounting for area-level SES (deprivation); model ‘y4’ included a clustering component (correlated heterogeneity [CH]) to all the previous covariates; finally, model ‘y5’ adjusted for all those variables plus uncorrelated heterogeneity (UH). As with the model previously used to fit data concerning lung-cancer mortality in men, the Deviance Information Criterion (DIC) was used as a measure of relative goodness of fit of observed data. Table 5.11 shows DIC values for all the five models fitted to the data. As in section 5.3.1, the whole BYM model (‘y5’) was the preferred one as it had the smallest DIC value (1,815); the second best model (‘y4’) was the one excluding the UH term (DIC value of 1,817). According to their DIC values, the relative goodness of fit of observed data, for these two models, was not clearly different; nevertheless, they were far better

	Dbar	Dhat	pD	DIC	Model
y1	1988.170	1987.820	0.346	1988.510	I
y2	1987.890	1987.160	0.730	1988.620	I + L
y3	1961.890	1960.460	1.425	1963.310	I + L + D
y4	1694.050	1571.460	122.590	1816.640	I + L + D + CH
y5	1692.260	1569.160	123.099	1815.360	I + L + D + CH + UH
total	9324.250	9076.060	248.190	9572.440	
Dbar = posterior mean of the Deviance (average deviance) Dhat = Deviance of the posterior mean pD = Effective number of parameters (Dbar - Dhat) DIC = Deviance information Criterion ($Dhat + 2pD = Dbar + pD$). <i>Lower values of DIC are preferred.</i> I = Intercept only L = Lithology score D = Deprivation score CH = Correlated Heterogeneity UH = Uncorrelated Heterogeneity					

Table 5.11. Besag-York-Mollié model: Relative goodness of fit of observed data, for all different models. Lung cancer in women.

than models ‘y1’, ‘y2’ (DIC values of 1,989 for both models) and ‘y3’ (DIC of 1,963).

Goodness of fit of predicted values was also assessed by means of loss type functions:

Table 5.12 shows estimates of the Mean Square Predictive Error (MSPE) for each model. The lowest (preferred) values happened for models ‘y4’ and ‘y5’ (mean estimated value of around 6, for both models); while the estimates for model ‘y3’ (MSPE = 7) and models ‘y1’ and ‘y2’ (MSPE = 10) were higher.

MAPE	mean	sd	MC error	2.5%	median	97.5%	start	sample	Model
y1	1.361	0.04935	2.787E-4	1.265	1.361	1.458	1001	30000	I
y2	1.359	0.04883	3.03E-4	1.264	1.358	1.456	1001	30000	I + L
y3	6.924	1.34	0.007901	4.864	6.735	10.04	1001	30000	I + L + D
	1.311	0.0493	2.764E-4	1.216	1.31	1.408	1001	30000	I + L + D
y4	1.154	0.05856	4.505E-4	1.045	1.152	1.275	1001	30000	I + L + D + CH
y5	5.573	1.788	0.01544	3.335	5.154	10.14	1001	30000	I + L + D + CH + UH
	1.146	0.0562	3.81E-4	1.041	1.144	1.262	1001	30000	I + L + D + CH + UH

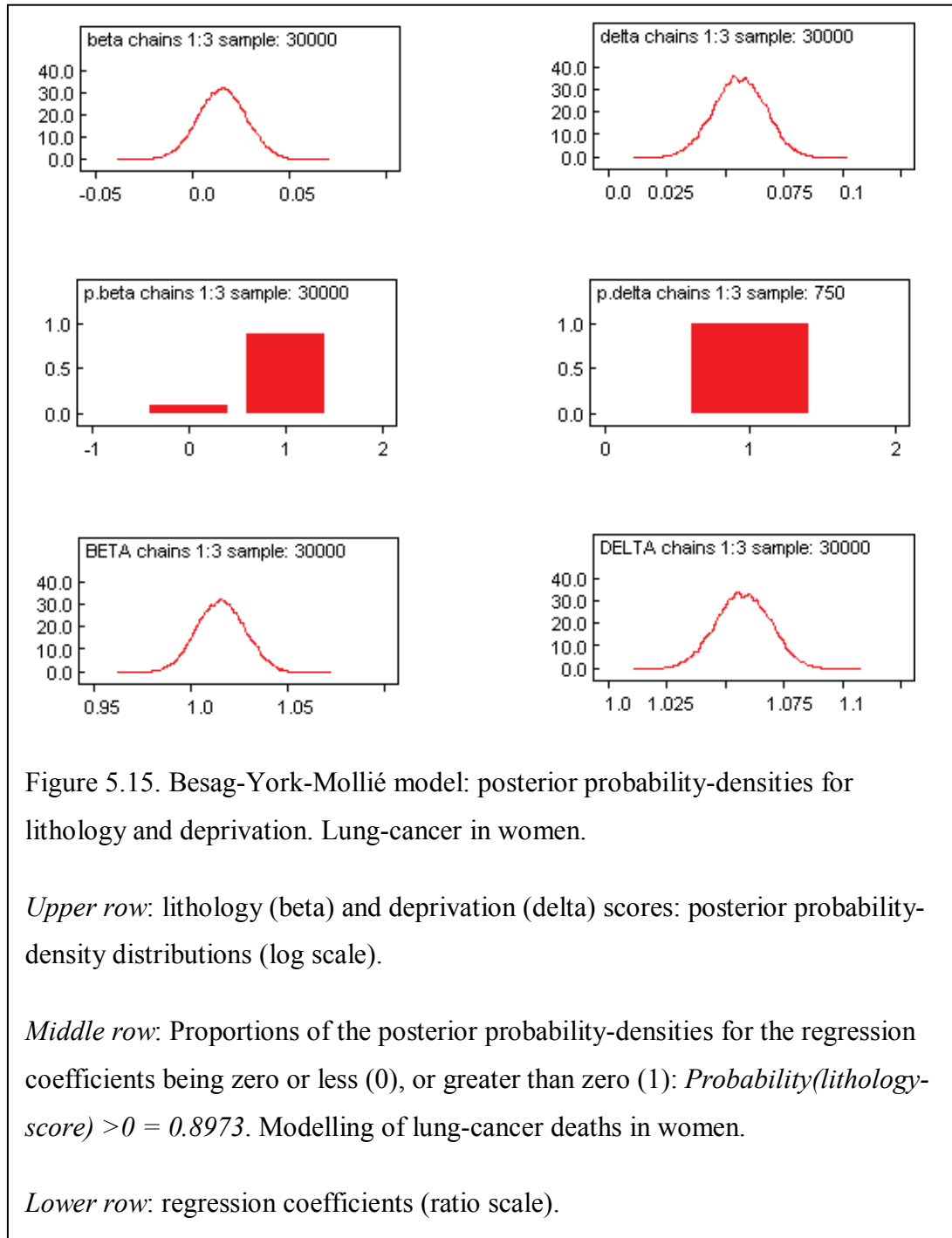
MAPE = Mean Absolute Predictive Error. Lower values of MAPE are preferred.
 I = Intercept only
 L = Lithology score
 D = Deprivation score
 CH = Correlated Heterogeneity
 UH = Uncorrelated Heterogeneity.

Table 5.12. Besag-York-Mollié model: relative goodness of predictive ability (MSPE) for all the different models. Lung cancer in women.
 Table 5.13. Besag-York-Mollié model: Relative goodness of predictive ability (MAPE) for the different models. Lung cancer in women.

Table 5.13 shows posterior estimates for a second form of loss function (Mean Absolute Predictive Error [MAPE]). Again, the lowest mean values were obtained for

model 'y5' and 'y4' (MAPE = 1.1 and 1.2, respectively). The estimated MAPE was 1.4 for both models 'y1' and 'y2', and 1.3 for model 'y3'. All these results (DIC, MSPE and MAPE) showed that the BYM model was the best one (amongst those compared) to fit lung-cancer mortality data in women. However, there was not much difference between the model adjusting for both correlated (CH) and uncorrelated (UH) heterogeneity and the one including only a CH term (plus lithology and deprivation as covariates).

A visual guide for the relevance and magnitude of both the lithology and deprivation scores is given in Figure 5.16. The first and last rows in this graph show the posterior probability-densities for both variables, on a linear and ratio (RR) scales, respectively. In contrast to the results obtained from fitting the BYM model to the male dataset, the posterior probability density for the lithology score includes the null value (zero, or one, on the linear and ratio scales, respectively).



This result suggests that lithology is not associated with the geographical distribution of lung-cancer mortality in women. However, it is worth noting that most of the density (90%) is above the non-effect value (Figure 5.16, middle row). For the deprivation score, the estimated posterior probability-density curve was completely above zero (or one on the RR scale). All these results can also be checked in Table 5.14, where some posterior point-estimates regarding both lithology and deprivation are given. On the ratio scale, the posterior mean estimates for the RRs are 1.016 and 1.057 for lithology and deprivation respectively. This suggests that the risk of mortality due to lung cancer (in women) increases 1.6% for each unit of increment in the lithology score; also, that the risk of mortality raises 5.7% for each unit of increment in the deprivation score. Table 5.14 also shows 95% Credible Intervals (CIs). The 95% CI for lithology (on the RR scale) ranged from 0.991 to 1.041, while the 95% CI for deprivation ranged from 1.035 to 1.081.

These results (as the probability-density curves in Figure 5.16) show that there is evidence of a positive association between deprivation and lung-cancer mortality in women. Concerning lithology, the results also suggest a positive association with lung-cancer mortality in women; nevertheless, lack of such an association cannot be completely excluded in women (see section 5.3.1 for results in males). The same conclusions are obtained from the examination of the posterior point estimates on a

node	mean	sd	MC error	2.5%	median	97.5%	start	sample
Lithology	0.01562	0.01238	1.2E-4	-0.00866	0.01563	0.03978	1001	30000
Deprivation	0.05582	0.01111	1.345E-4	0.03401	0.05584	0.07744	1001	30000
exp(Lithology)	1.016	0.01257	1.218E-4	0.9914	1.016	1.041	1001	30000
exp(Deprivation)	1.057	0.01175	1.422E-4	1.035	1.057	1.081	1001	30000

Table 5.14. Besag-York-Mollié model: regression coefficients estimates on the log scale (two upper rows) and ratio scale (two lower rows). Lung-cancer in women.

linear scale, where zero is the null (non-effect) value (Table 5.14, two upper rows).

As for the model in males (see pg. 97), an interaction term between area-level deprivation and lithology did not improve the goodness of fit of the model for the female distribution of lung-cancer mortality; in this case the posterior mean value for the interaction term was 0.04 with 95% CI [-0.004, 0.007].

Table 5.15 shows the posterior point-estimates for the Variance Partition Coefficient (VPC). The mean posterior estimate of the VPC was 0.999 (or 99.9%). This means that virtually all the residual (not explained by the model) variability is due to the Correlated Heterogeneity (CH) component (or clustering). This is the reason why models with, or without, the Uncorrelated Heterogeneity (UH) component were considered to be equivalent in terms of goodness of fit. These results suggest again (see 5.3.1) that there exist some socio-economic or environmental factors (not measured in this study) related to lung-cancer mortality, which have effect across neighbouring areas (contextual effects).

node	mean	sd	MC error	2.5%	median	97.5%	start	sample
VPC	0.9986	0.001564	1.592E-4	0.9943	0.9991	0.9998	1001	750
	VPC =Variance Partition Coefficient. $VPC = CH / CH + UH$; if close to 1 indicates relevance of a hierarchical model.							
	CH = Spatially Correlated Heterogeneity							
	UH = Uncorrelated Heterogeneity.							

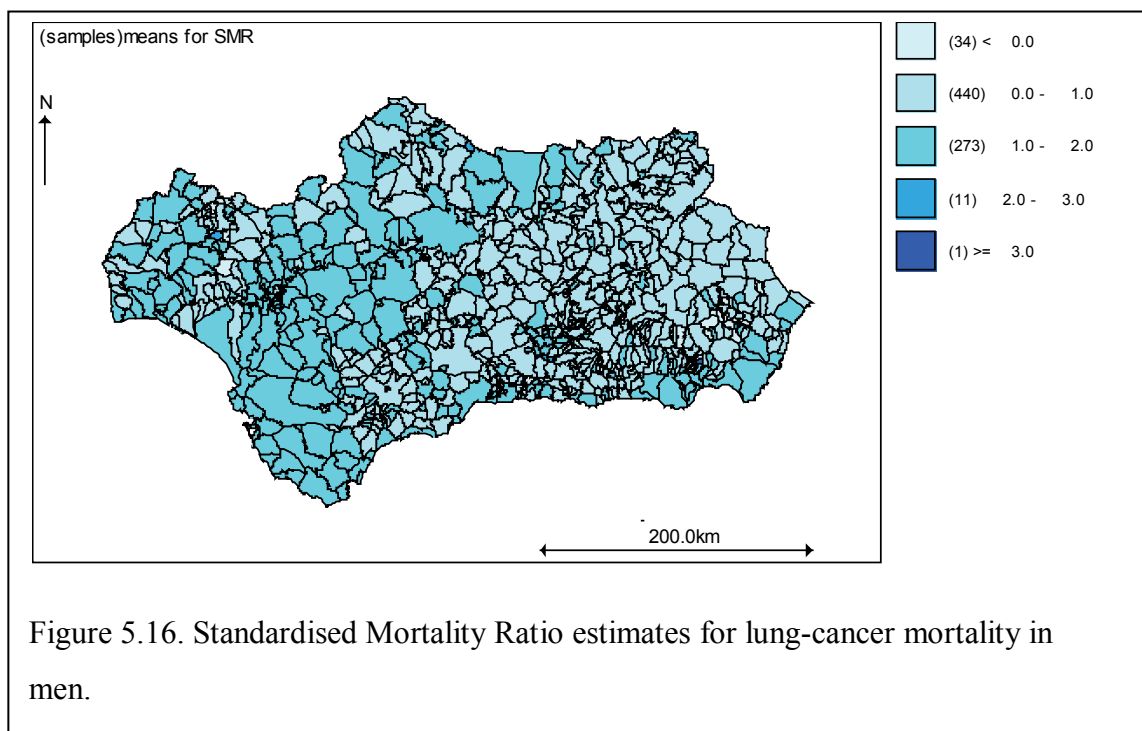
Table 5.15. Variance Partition Coefficient: posterior estimates. Lung-cancer in women.

As for the male dataset (see pg. 107) the frequency distribution of the observed number of female lung-cancer deaths was overdispersed (ratio variance/mean = 61.47; Bohning's statistic = 4.31, p value < 0.001). Although the number of zero values was much higher for females (46% of all records) than for males (only 4.4%), the clustering component of the residual variance was again much higher than the heterogeneity component (VPC = 99.9%, Table 5.15); therefore, a hierarchical BYM

model was again justified, as spatial autocorrelation, rather than random heterogeneity, seemed to be responsible for virtually all overdispersion.

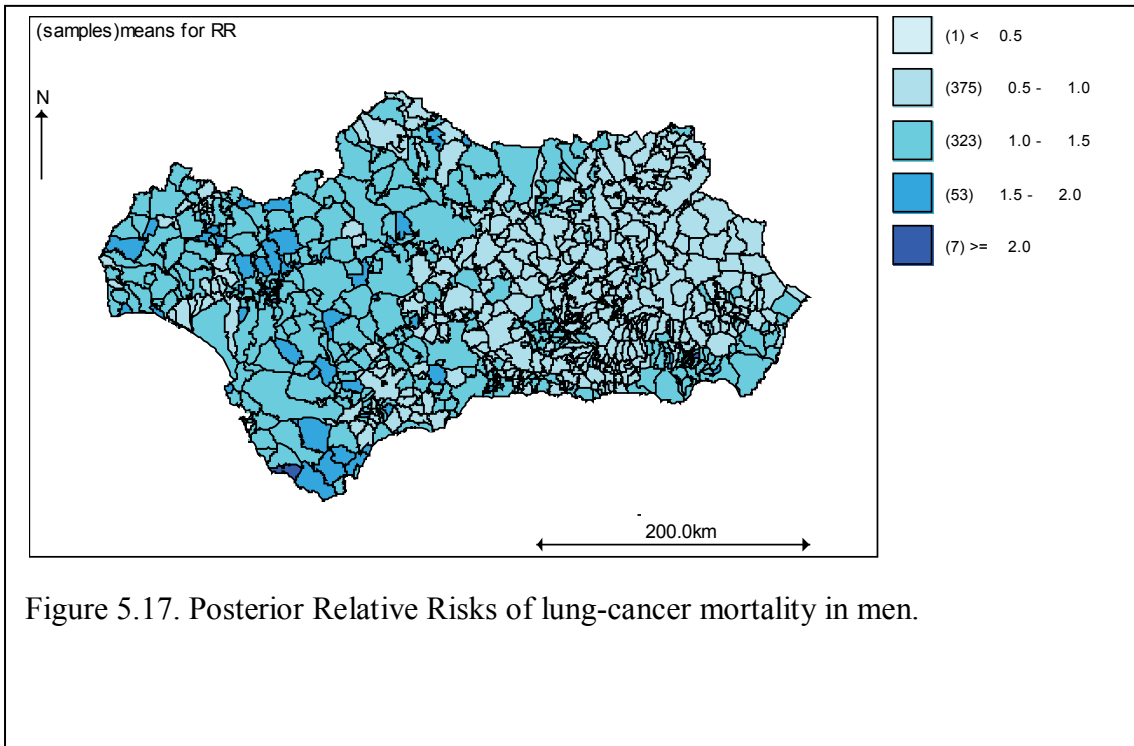
5.3.3 Mapping of lung-cancer mortality modelling: males

Figure 5.17 shows the Standardised Mortality Ratios (SMRs) due to lung-cancer mortality in men. It represents the observed (that is, before modelling) SMRs values, where there is a high concentration of municipalities with values greater than one to the west of the region, as reported by previous studies.



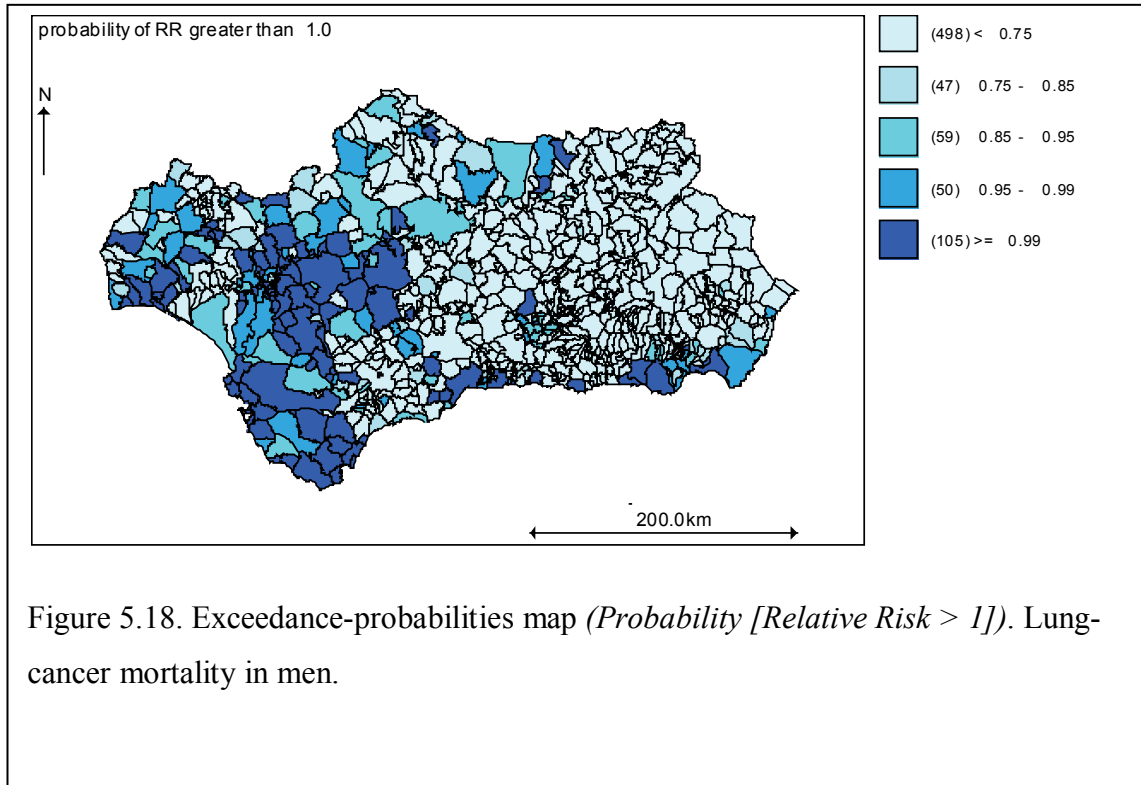
To distinguish between observed SMRs values and posterior (modelled) estimates, the latter had been labelled as Relative Risks (RR). To visually appraise the relative magnitude of each model component (see 5.3), mapping of RR of lung-cancer mortality in men was implemented by taking into consideration all the modelling components and, separately, each one of them. Figure 5.18 maps the posterior lung-cancer RR estimates in men, for each one of the 759 municipalities in the whole region. These estimates were obtained from the full BYM model that accounted for both lithology and deprivation scores. The model also included a variance component that comprised spatial autocorrelation and random heterogeneity.

Figure 5.18 gives the number of municipalities (within parenthesis) for each RR cut-off point. It can be seen that amongst municipalities with a high-risk of mortality, 323 (84%) had an estimated RR up to 50% higher than expected. 53 municipalities (14%) had an RR of lung-cancer mortality which was up to 100% above expectation. Finally, only 7 municipalities (2%) had an increased RR beyond 100% of expected.

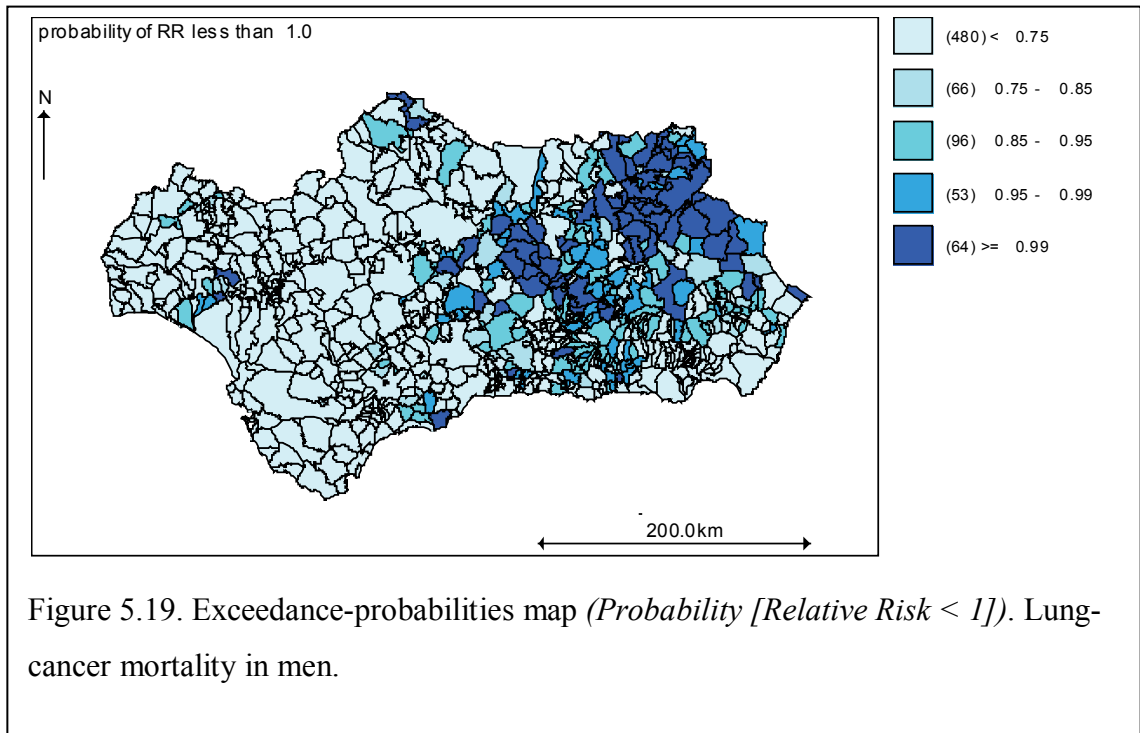


To aid interpretation of these estimates, Figure 5.19 presents an exceedance-probabilities map. Given that the whole posterior RR density was available for every municipality, it was possible to compute the area under the curve lies above some specific value. In this case, the map was devised to classify the municipalities according to the probability that its estimated RRs were greater than 1, which is the null RR. The more area under the RR curve would lie above the value of 1, the more the hypothesis of an RR greater than expected would be supported. This map (Figure 5.19) shows that there were 47 municipalities for which the probability of an RR greater than 1 ranged between 0.75 and 0.85; another 59 areas had a probability of an excessive risk between 0.85 and 0.95; in another 50 areas that probability varied between 0.95 and 0.99. Lastly, for 105 further areas the probability of an excessive risk was virtually 1; in other words, for each of these 105 municipalities, all of the area belonging to their respective posterior RR probability-density curves was situated

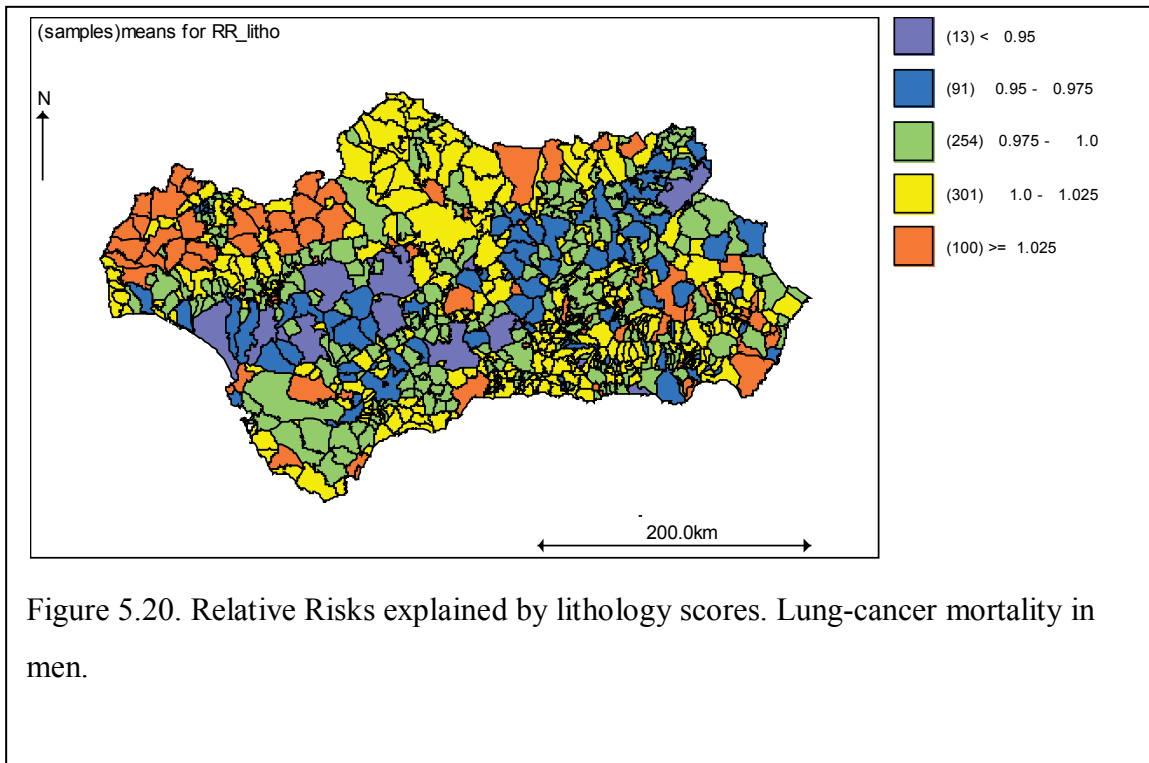
above the value of 1. This smoothed exceedance-probabilities map clearly shows how municipalities with higher risk concentrated to the west of the region, as reported in previous studies [10, 13].



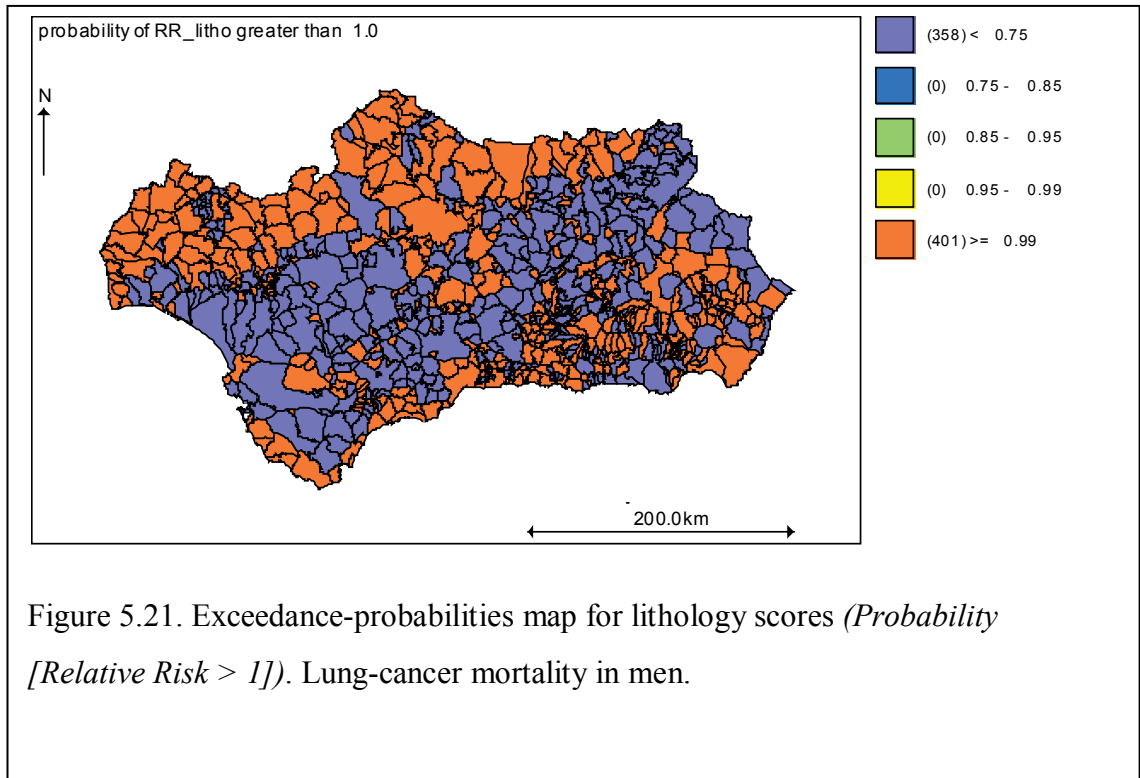
Later in this section (pg. 124), it will be explained that clustering is the model component responsible for this spatial pattern. A mirror image of the previous map is given by Figure 5.20, which gives, for each municipality, the probability of their RR being less than expected. It shows that the areas with the highest probability of their posterior RRs being less than 1 are concentrated to the east of Andalucía.



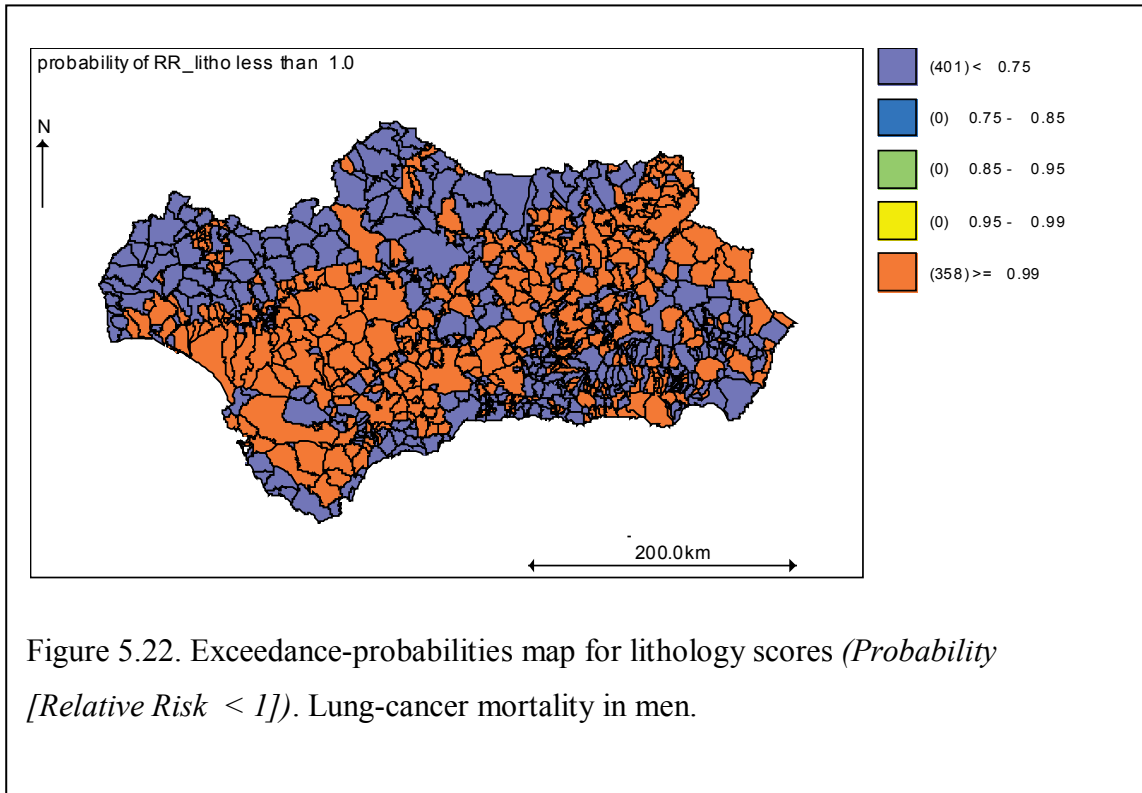
To further analyse the fitted model, mapping was presented separately for each model component. Figure 5.21 represents the RR explained only by lithology scores, where 401 municipalities out of a total of 759 (or 53%) were classified as areas with an RR (due to lithology) greater than expected. Of these high risk areas, 301 (75%) had an RR up to 2.5% higher than expected; 100 municipalities (25%) had an RR greater than 2.5% above expectation.



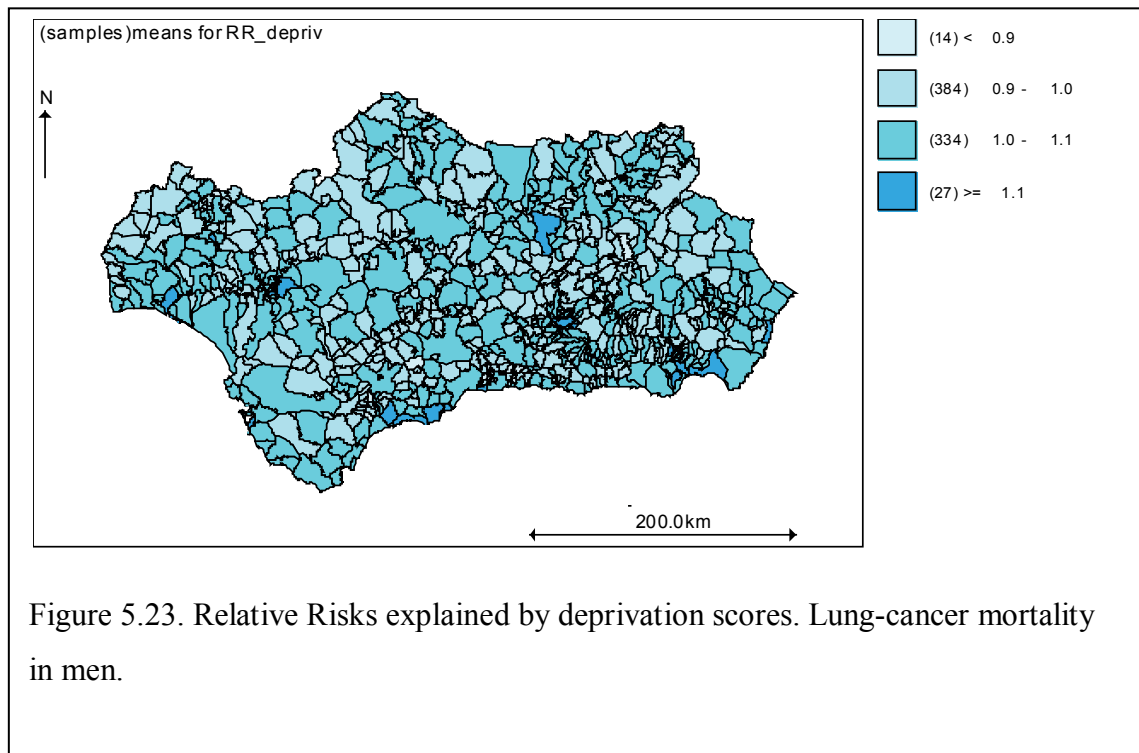
The corresponding exceedance-probabilities map (Figure 5.22) shows that 401 municipalities (or 53%) had RR estimates for which virtually all their probability-density curves were above the value of 1. These geographical areas were mainly situated on two separated strips across the north and south of the region.



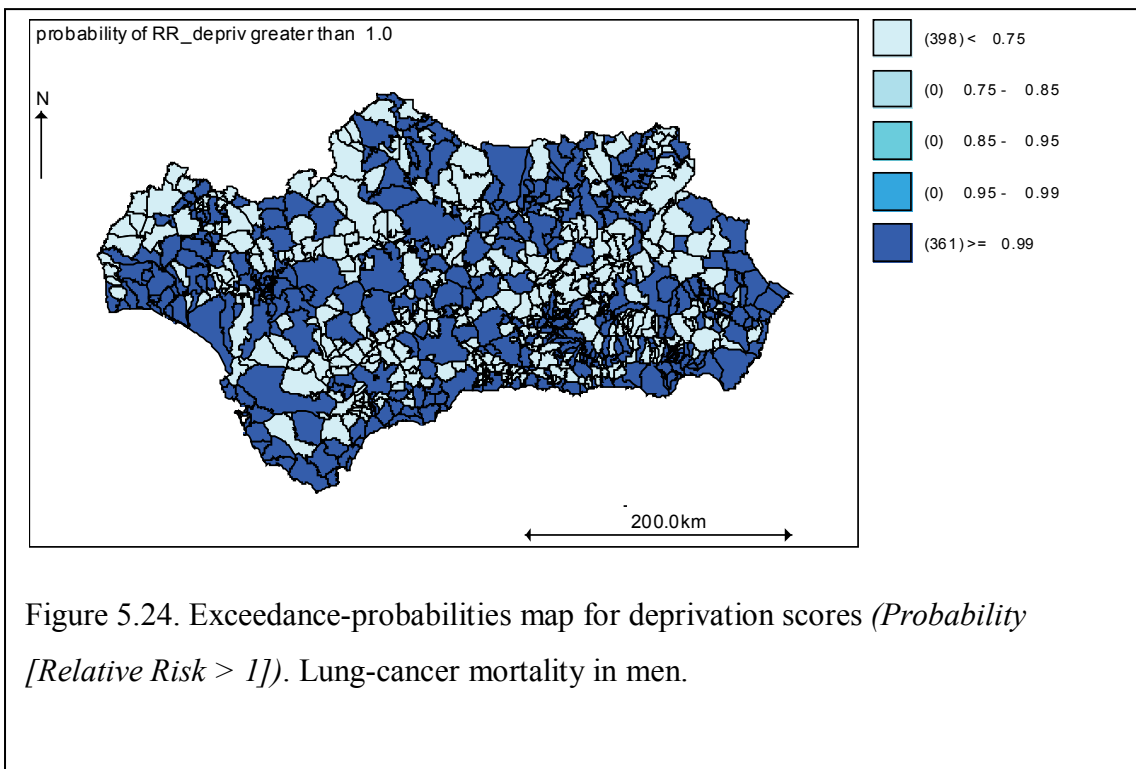
The complementary map (Figure 5.23) shows the areas (a middle band across the whole region) where the probabilities of an RR, due to lithology, being less than 1 were higher.



A second RR component individually analysed was SES at area level, which was represented by the deprivation score. Figure 5.24 displays 361 geographical areas out of a total number of 759 (or 48%) that showed an RR –due to deprivation- greater than 1. Within all these high-deprivation areas, 334 municipalities (93%) had an excess of risk up to 10% greater than expected. Only 27 areas (or 7%) had a risk increased above 10% of expectation.



Exceedance-probabilities maps for the RR due to deprivation are shown in Figure 5.25 (for an RR greater than 1) and Figure 5.26 (for an RR less than 1). There were 361 municipalities (48%) for which the probability of an RR being greater than expected was virtually 1 (or 100%). Unlike the risk associated with the lithology component, the one due to deprivation does not seem to concentrate on any particular area. The clustering component was actually not captured by either of the two explanatory variables (lithology or deprivation) included in the model.



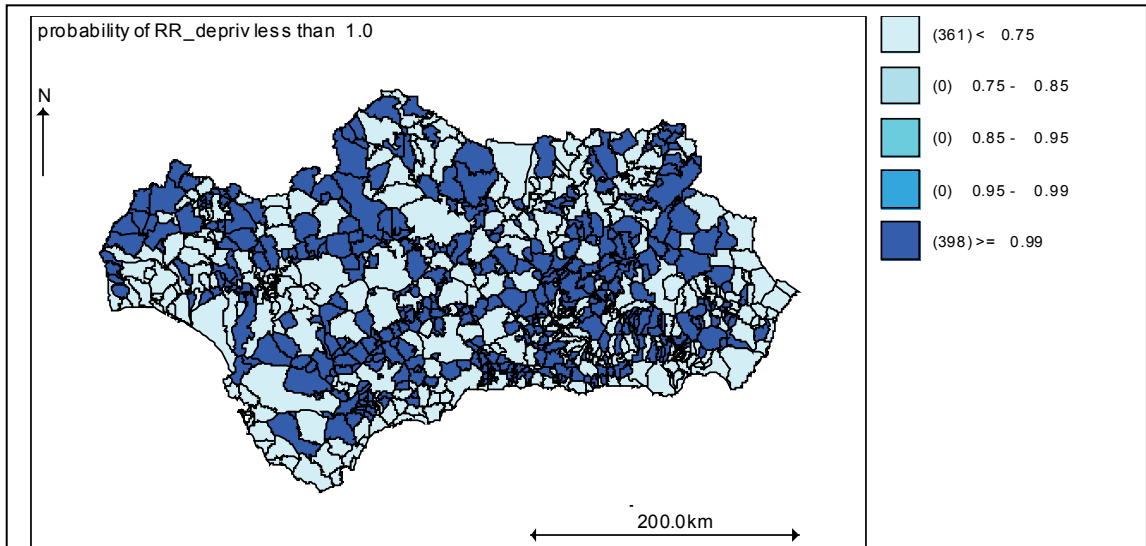


Figure 5.25. Exceedance-probabilities map for deprivation scores (*Probability [Relative Risk < 1]*). Lung-cancer mortality in men.

The residual RR and its two components (clustering and heterogeneity) was the third (and last) RR component analysed. Figure 5.27 shows the map of posterior RR estimates due to the residual variability. In this map, 317 geographical areas of high-risk of mortality (or 83%) had a risk which increased up to 50% beyond expected (RR from 1 to 1.5). 58 areas (15%) had an increment in risk between 50% and up to 100% (RR between 1.5 and 2). 6 areas (2%) showed a risk increment greater than 100% (RR greater than 2). The map exhibiting the residual RR is very similar to the one showed in Figure 5.18, which took into consideration all the explanatory variables plus the residual-variance components. This shows that the factor responsible for this characteristic spatial pattern of mortality was not captured by any of the two explanatory variables included in the model.

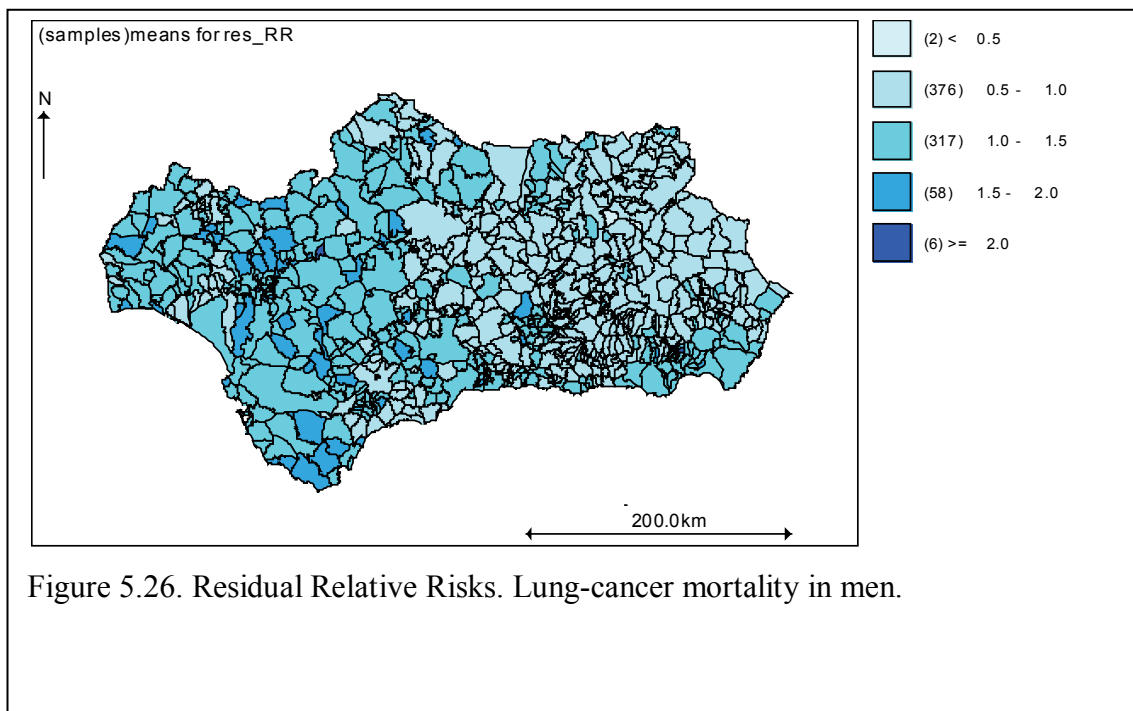
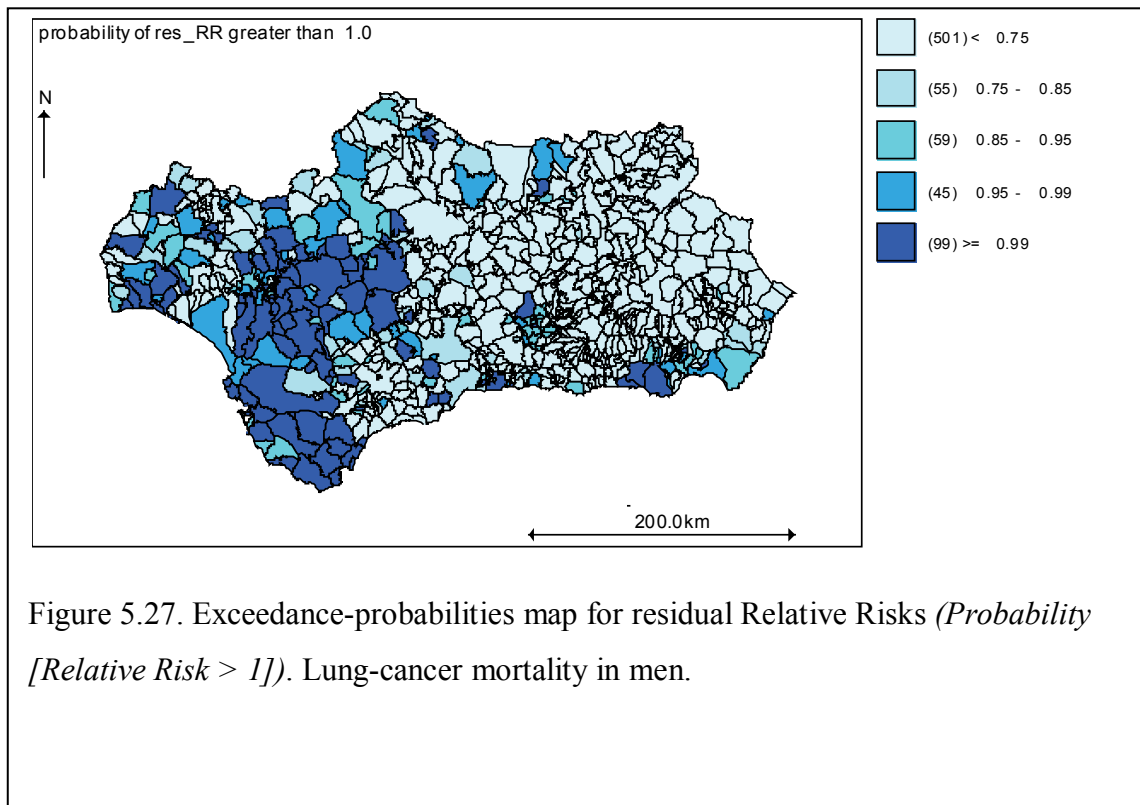
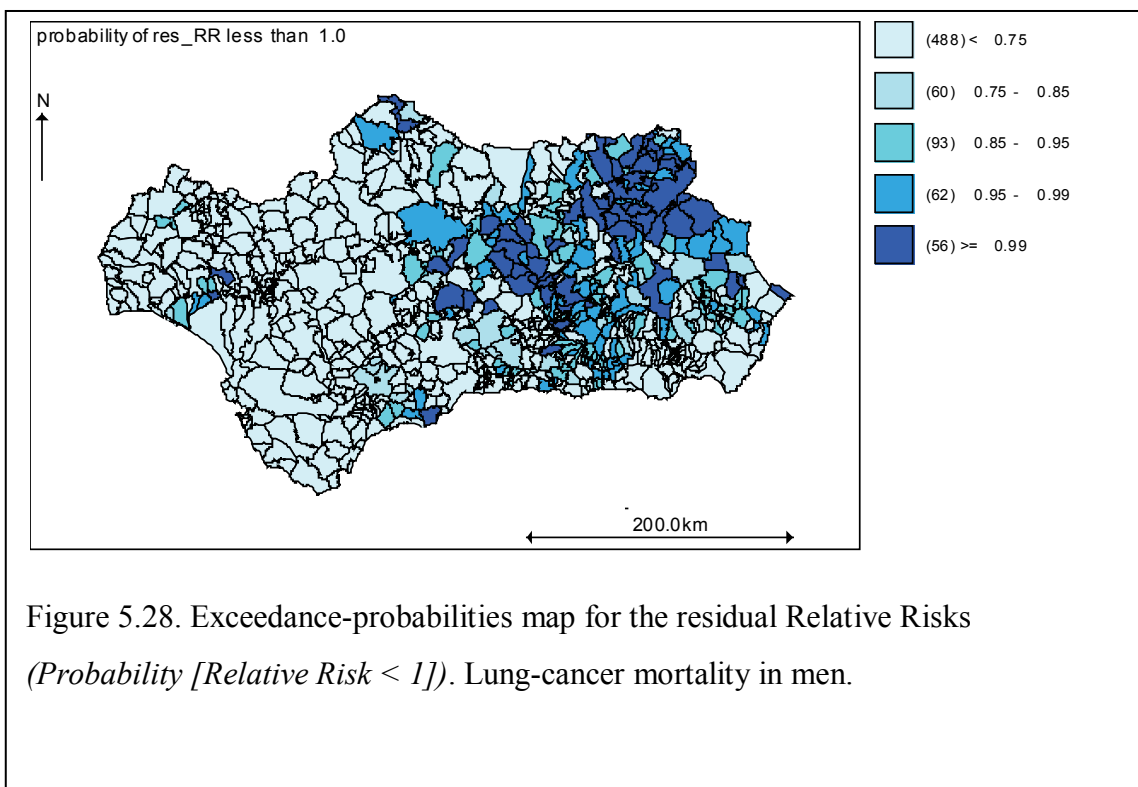


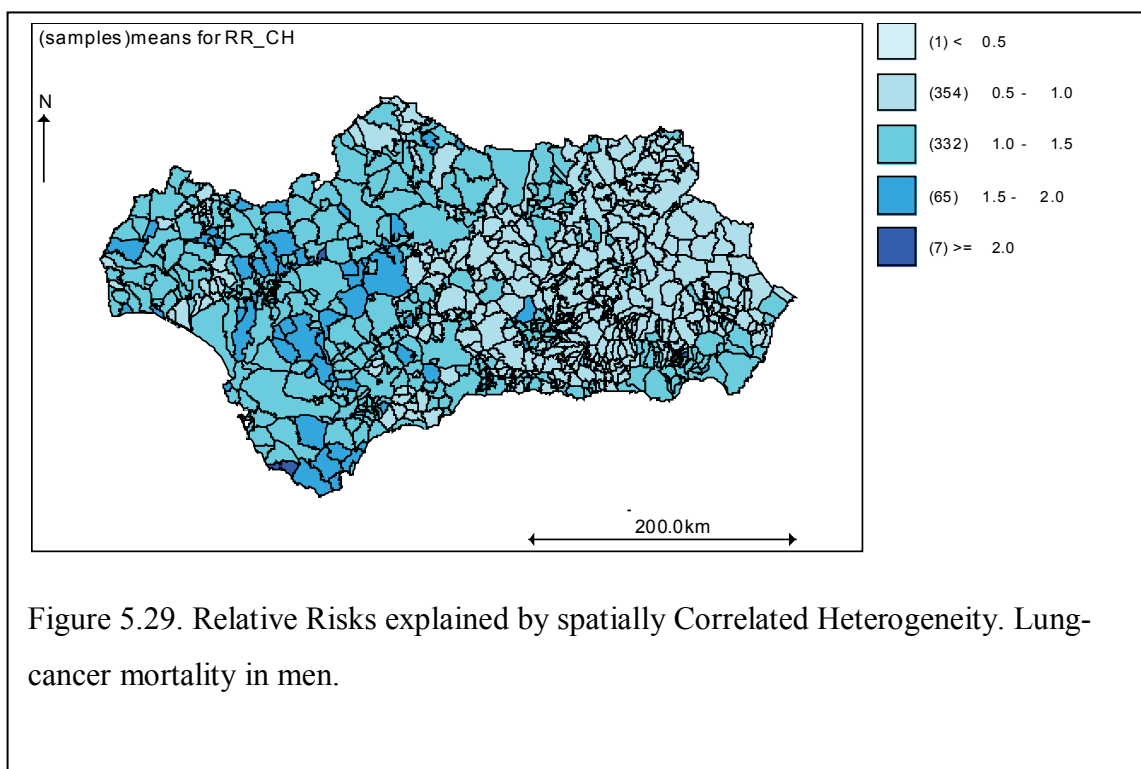
Figure 5.28 gives additional information as an exceedance-probabilities map for the residual RR. It shows that there were 99 municipalities (13%) for which their whole probability-density curves were above the value of 1. That is to say, all the posterior values indicate a greater than expected residual RR. 45 additional municipalities (6%) also had an extremely high probability (between 0.95 and 0.99) of having residual RRs greater than 1. Moreover, these areas were mainly concentrated to the west of Andalucía.



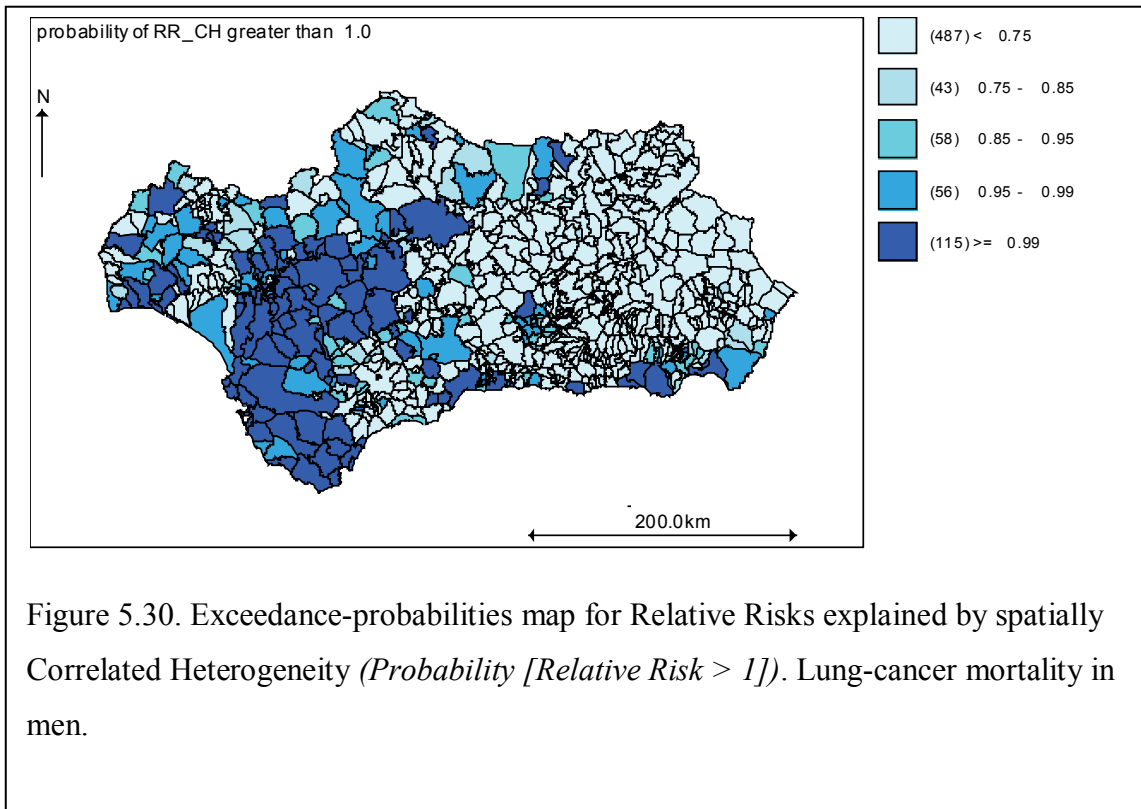
An opposite pattern is shown in Figure 5.29, which presents an exceedance-probabilities map of the residual RR being less than 1. It can be seen that 56 geographical areas (7%) had virtually all their residual-RR curves below the null value, while for 62 additional municipalities (8%), between 95% and 99% of the area of their probability-density curves were below the value of 1. In contrast to the previous map (Figure 5.28) these low-probability risk areas are mainly concentrated to the east of Andalucía.



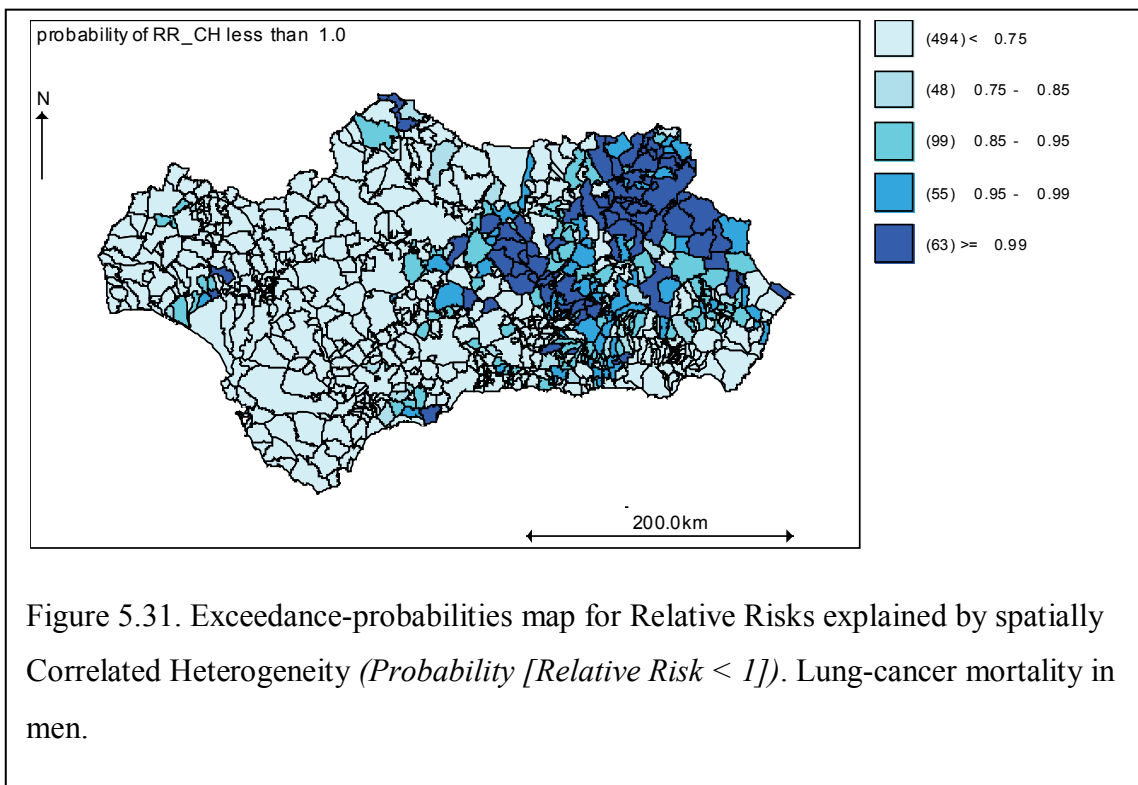
The BYM model allows for the residual RR to be partitioned into two different components: the spatially-correlated (or clustering) and the uncorrelated (heterogeneity). Figure 5.30 shows the first of these residual components, also known as clustering. There were 404 areas (53%) that had posterior estimates indicating a high risk due to clustering (or spatially Correlated Heterogeneity [CH]). Of all these areas, 332 (82%) had an increased in risk up to 50% above the null value (RR greater than 1 and up to 1.5). 65 of these high risk municipalities (16%) showed an increment of between 50% and 100% beyond expected (RR from 1.5 to 2). Another 7 geographical areas exhibited an increment in risk, due to clustering, greater than 100% (RR greater than 2). The clustering-component map showed concentration of high-risk municipalities to the west of Andalucía. This means there must be some factors (unmeasured in this study) that have a strong, spatially-correlated, effect that makes risk to vary smoothly across geographical areas.



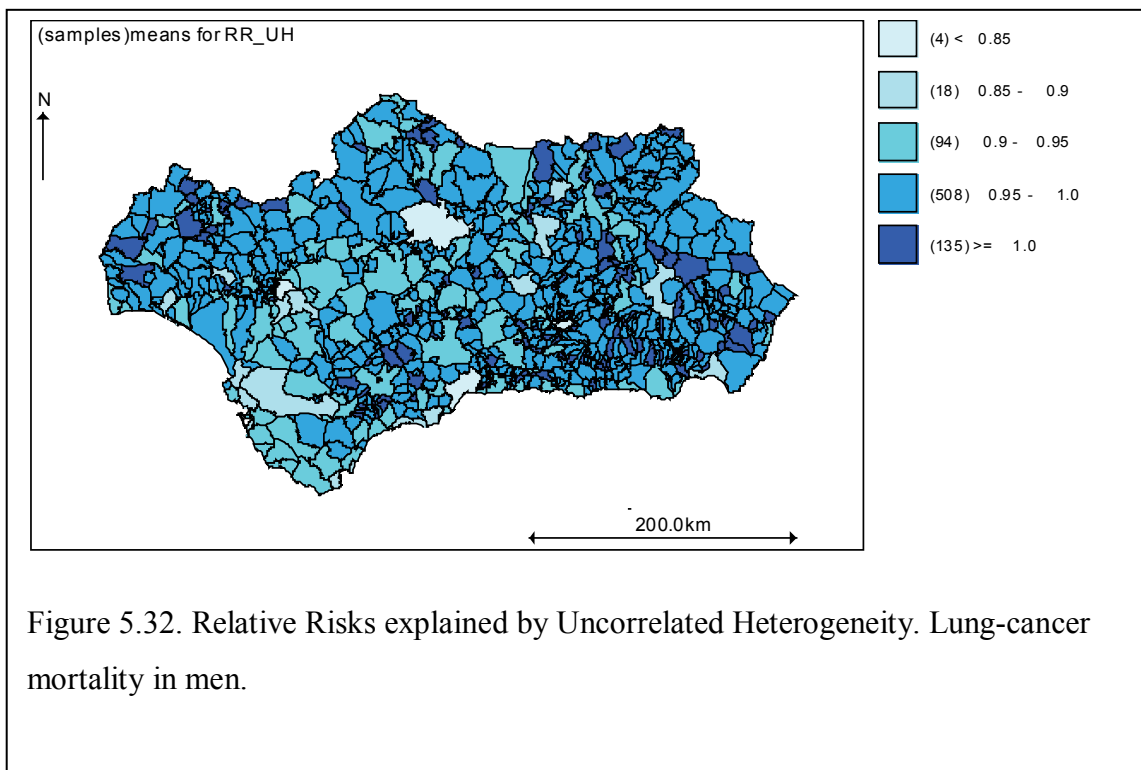
To further assess the high and low-risk posterior estimates, Figure 5.31 and Figure 5.32 show the exceedance-probability maps. The former gives the probabilities of an RR being greater than 1, while the latter shows the probabilities of an RR being less than 1. It can be seen (Figure 5.31) that there were 115 municipalities (15%) for which virtually all the area (at least 99%) under their respective RR curves were above the value of 1 being, therefore, representative of high-risk values. Another 56 (7%) municipalities had high probability (0.95 to 0.99, or 95% to 99%) of being representative of high-risk zones. Again, the probabilities of finding high-risk municipalities are greater to the west of Andalucía, as shown previously by the RR map due to the clustering component.

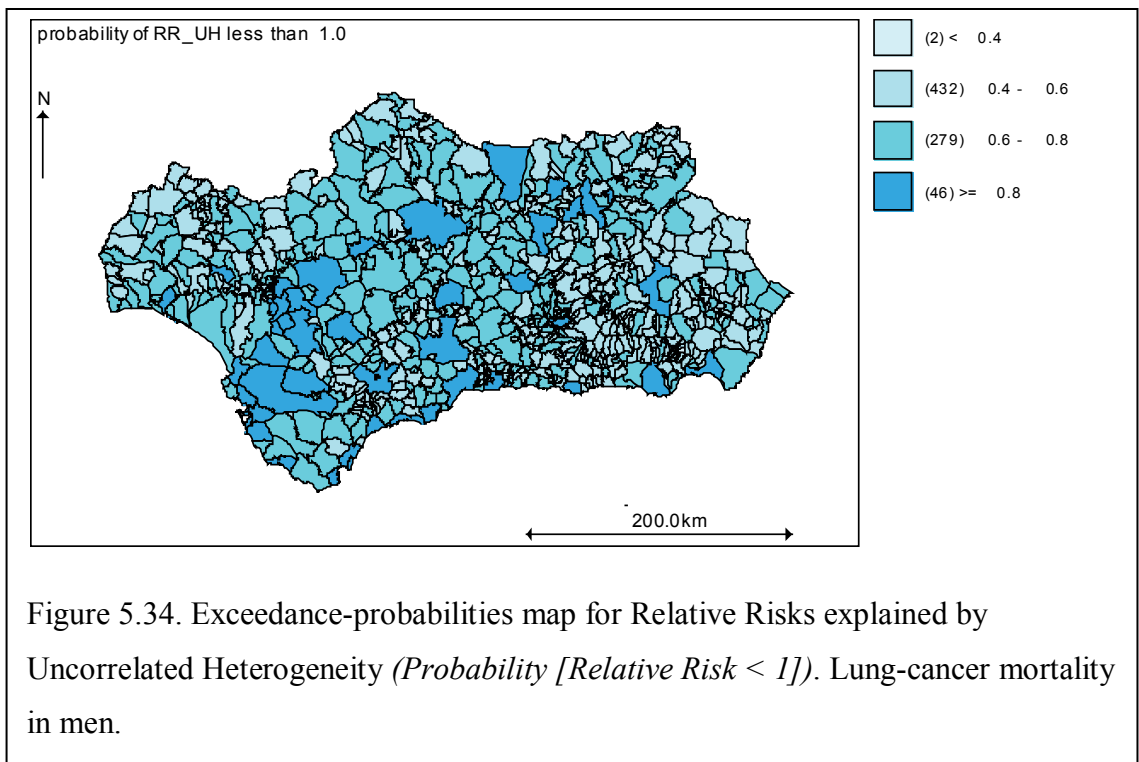
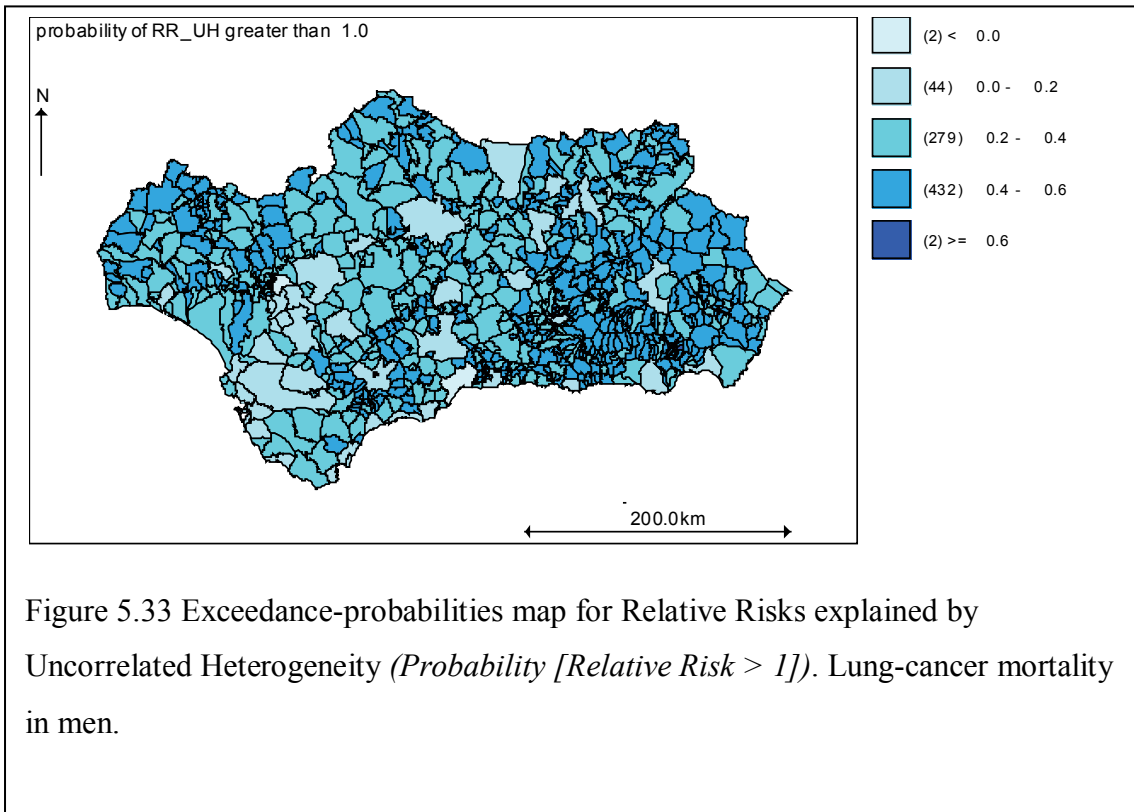


The opposite can be seen in Figure 5.32 where the probability of finding a low RR (due to clustering) municipality was at least 0.99 (or 99%) for 63 of them out of 759 (or 8% of all the municipalities). While that probability varied from 0.95 to 0.99 (or 95% to 99%) for another 56 (7%) municipalities. Most of these high-probability low-risk areas were concentrated to the east of Andalucía. These two complementary maps show that the unmeasured factor (or factors) responsible for this spatial pattern seems to operate to the west of the region.



The second residual RR component, Uncorrelated Heterogeneity (UH) was mapped in Figure 5.33, Figure 5.34, and Figure 5.35. Mapping of the RR due UH (or random within-area variability) did not show a clear pattern, contrary to the one due to clustering; that is to say, random noise is not responsible for this spatial pattern of higher mortality to the west of the region. The maps show that 135 out of 759 areas (18%) had an uncorrelated-RR of at least 1, and they were all scattered throughout the region. Furthermore, only 2 municipalities showed a probability of being high-risk areas, of 60% or greater (Figure 5.34) and 46 municipalities (6% of all geographical areas) had a probability of at least 80% of being low-risk zones (Figure 5.35).





5.3.4 Mapping of lung-cancer mortality modelling: females

Similarly to the mapping implemented in section 5.3.3, the SMRs, before and after modelling (in this case labelled as RRs), were mapped. Figure 5.36 presents the SMRs, while Figure 5.37 shows the posterior RRs. It can be seen that while the SMRs ranged from 0 to 8, the RRs were smoothed, the estimated values ranging only from 0 to 1.5, which is a characteristic inherent to multilevel models (such as the BYM model). This smoothing effect was lower when fitting the males' dataset (Figure 5.17 and Figure 5.18) as the RR estimates were based on a greater number of cases. This, in turn, produced more reliable estimates which were not pulled down towards the average value.

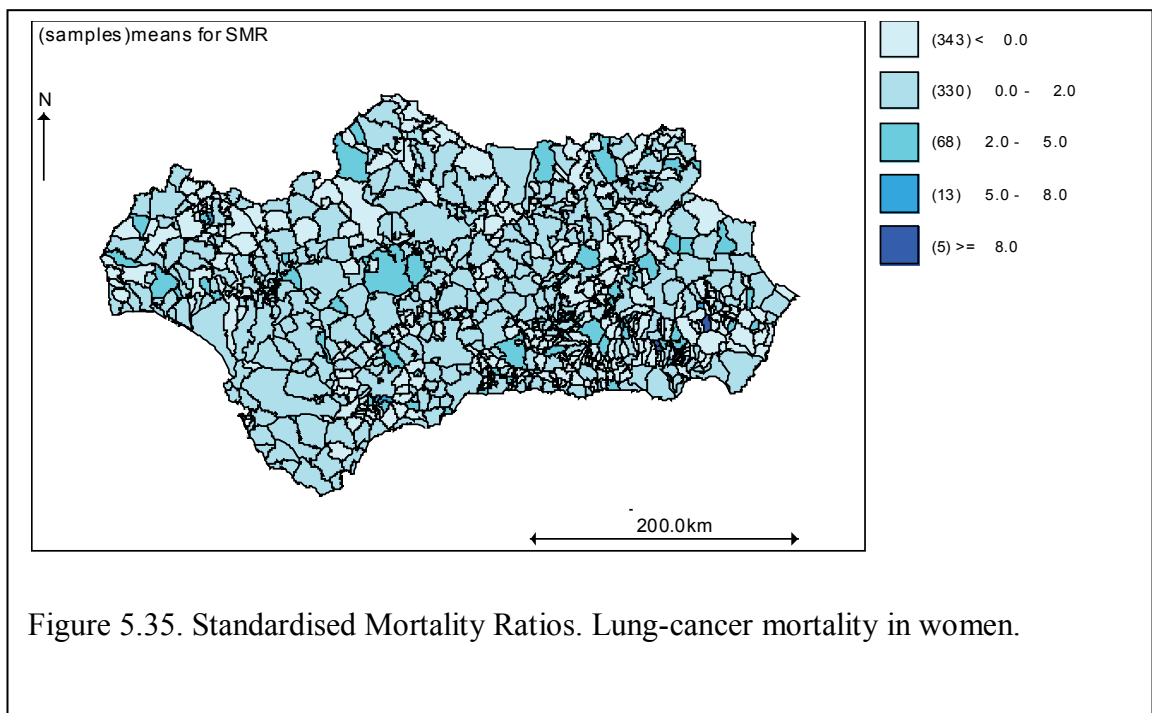
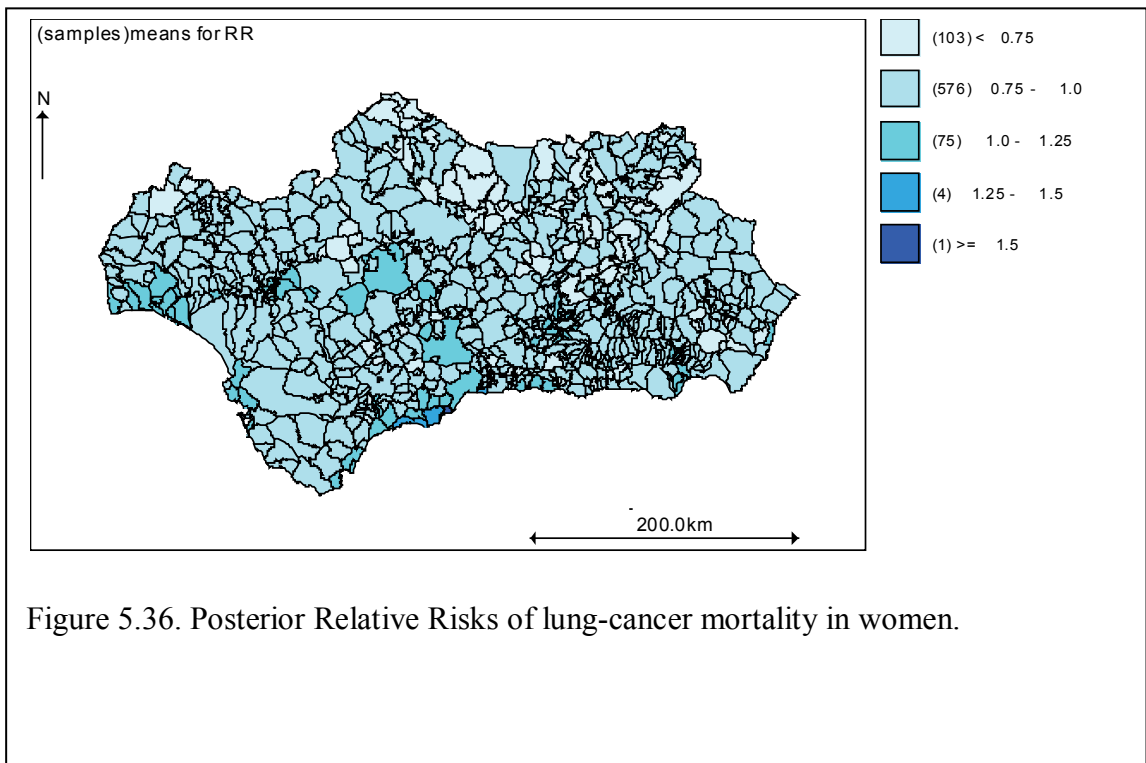


Figure 5.37 shows that only 80 municipalities out of 759 (or 10%) had a posterior RR greater than 1. Most of these areas of high-risk mortality (75, or 95%) had up to a 25% increment in risk. In contrast, 383 municipalities (or 50%) were classified as high risk areas when the same BYM model was used to fit the males' dataset (see 5.3.3 and Figure 5.18). There is also a noticeable difference, between women and men, in the magnitude of the risk: 323 of all high-risk areas (or 84%) showed up to a 50% increment in risk. These results suggest a differential effect between men and women of the explanatory variables included in the model. The spatial distribution of lung-cancer mortality is also different for women; there is not a clear pattern of high-risk areas concentrated to the west of the region (in contrast, see 5.3.3 for males' results).



The exceedance-probabilities map of an RR being greater than 1 helps identify those municipalities likely to be high-risk areas. Figure 5.38 shows that the probability of an RR being greater than 1 was lower than 0.75, for most of the areas (748 out of 759, or 99% of all municipalities). This means that, for these municipalities, less than 75% of the area under their estimated probability-density curves was above the RR-value of 1. Therefore low-risk values (lower than 1) are also likely (probability of 0.25).

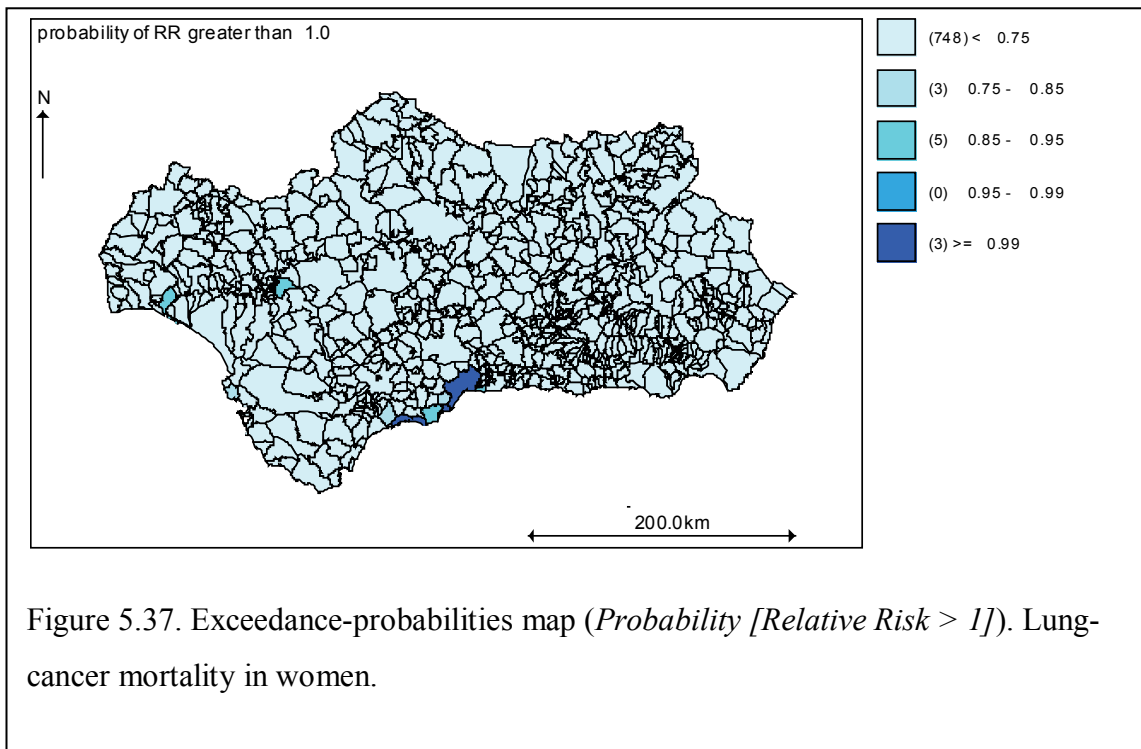
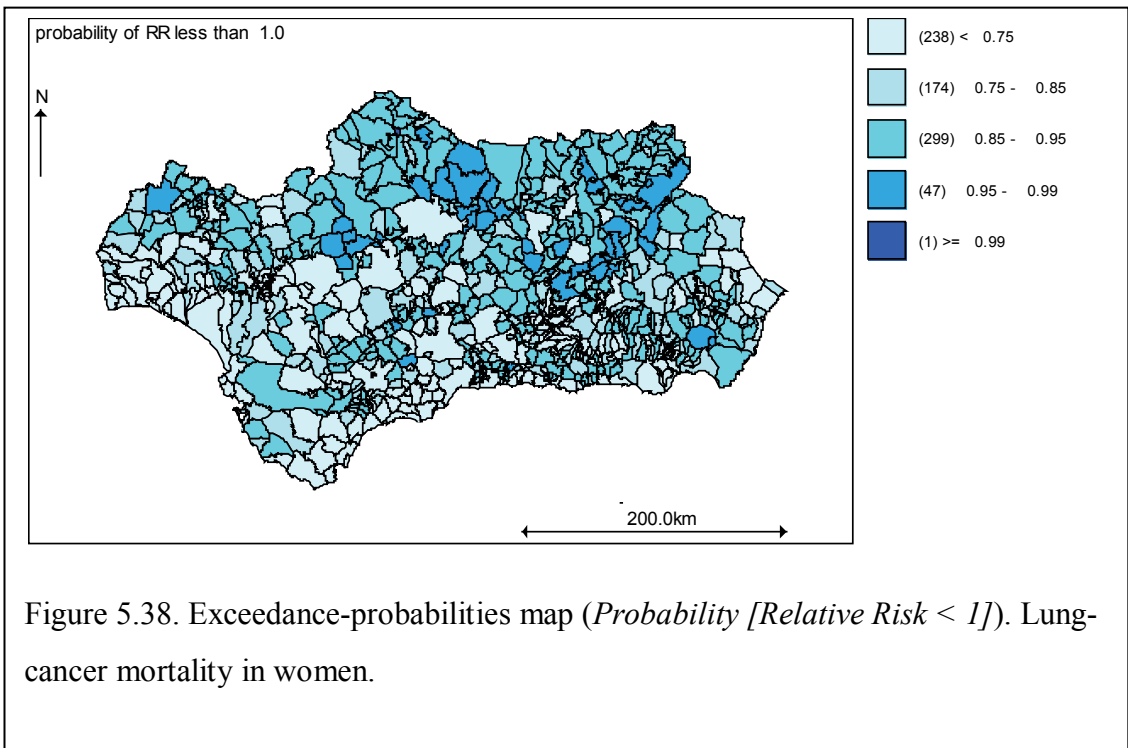


Figure 5.39 shows the exceedance-probabilities map of an RR being lower than 1. This is a mirror image of Figure 5.38, which highlights probability of low-risk areas. Thus, there are 299 areas (or 39%) for which the probability of being low-risk areas ranged between 0.85 and 0.95. 47 areas (or 6%) were classified as low-risk areas with probability between 0.95 and 0.99. Only 1 area had an estimated probability which was, at least, 0.99.



Mapping of the clustering component for the women model (Figure 5.40) shows some similarities with the model in men (Figure 5.30), as there seems to be a higher risk of mortality, due to the clustering component, in the west (but also in the south) of Andalucía.

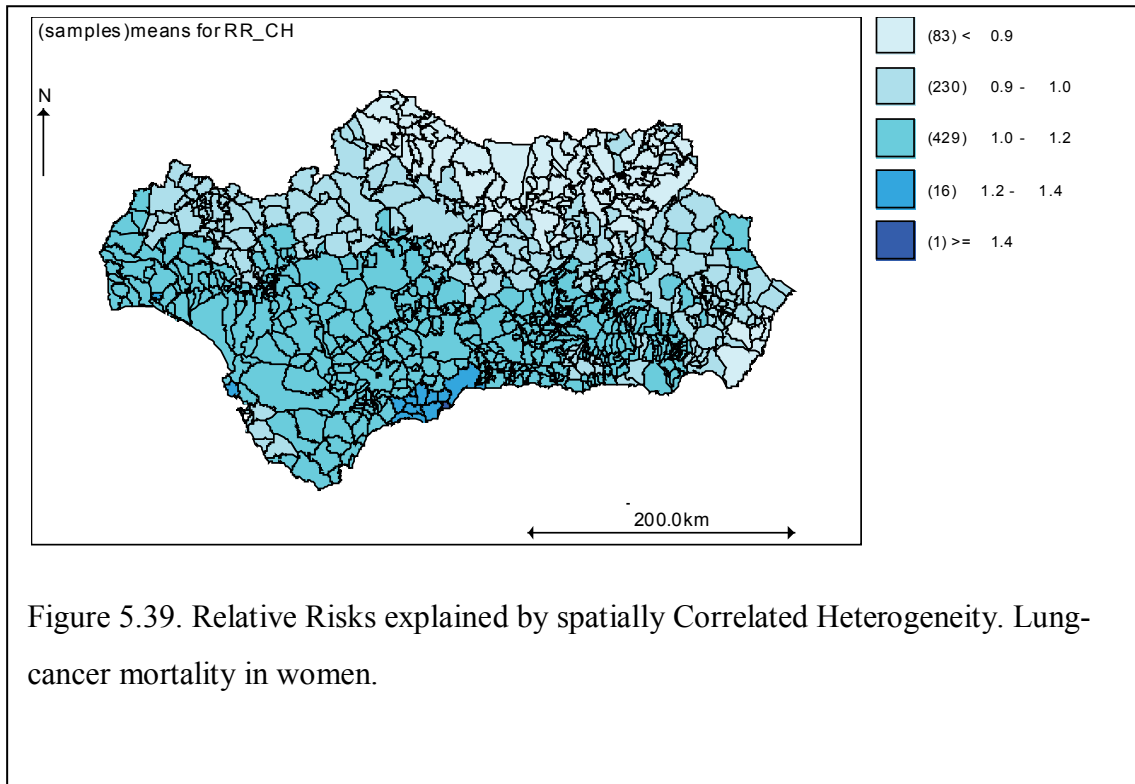


Figure 5.39. Relative Risks explained by spatially Correlated Heterogeneity. Lung-cancer mortality in women.

5.4 Summary of lung-cancer mortality modelling

When compared to the model in section 5.2 (with just lithology and deprivation as explanatory variables) model in section 5.3.1 was preferred based on different functions. In this new model, there is also evidence of a positive association between the lithology score and mortality due to lung cancer in men. Likewise, there exists a positive association between deprivation and lung cancer mortality in men.

Additionally, the geographical variability in lung cancer mortality in men not captured by either lithology or deprivation was also estimated. These estimates show that most of the unexplained variance seems to be due to some factor (or factors), unmeasured in this study, with a strong effect over neighbouring areas to the west of Andalucía.

Nevertheless, lithology is still shown to be an explanatory variable for lung-cancer mortality in men.

Chapter 6. Discussion

6.1 Findings

The spatial distribution of lung-cancer deaths in Andalucía was found to be associated with a lithology score, especially devised for this study as a surrogate measure for potential radon-gas exposure. Furthermore, this association remained after adjusting for area-level deprivation so that the potential confounding effect of tobacco smoking was taken into account. These findings are in agreement with current scientific knowledge: firstly, different epidemiological studies have consistently found an association between lung cancer and radon-gas exposure [115, 189, 231], which is known to be the second most important cause (after tobacco smoking [106]) of lung cancer; secondly, presence of radon in the soil is known to depend on the bedrock composition (e.g. there is high content of radon in granite [58, 61]), which explains the high correlation that exists between radon content in the soil and lithology [61, 169, 170, 183, 190, 232, 233].

A positive (although weak) association was found, in this study, between the spatial distribution of male lung-cancer deaths, across the Andalusian municipalities, and the lithology score. This association was, on average, also positive for female lung-cancer deaths; however, lack of such an association could not be excluded for women: the posterior distribution for the estimate of the regression coefficient was scattered around zero (see Figure 5.16). Some authors have hypothesised that the predominance of distinct histological types in men (SCC) and women (adenocarcinoma) might be explained by the exposure to different environmental factors: tobacco smoking and radon-gas in men and women, respectively [16]. This hypothesis has been thought to be supported by findings of a higher mortality rate due to lung cancer, in some cohorts of women residing in northwest Spain. That is to say, those who were born before the 1940s (mostly non-smoking women) and resided in a predominantly granitic region [5, 16, 61, 165, 179, 180]. Nevertheless, there is epidemiological evidence of gender susceptibility to tobacco smoke exposure [108]. This differential susceptibility has been associated with higher levels of DNA adducts formation in women, which in turn, is thought to be due to higher levels of female TSNs exposure. The number of adenocarcinoma diagnoses increased in parallel with the female smoking prevalence that, in Spain, started to reach epidemic proportions since the 1970s [234].

Additionally, it has been reported that major changes occurred in the tobacco composition (such as manufacturing of filtered, as well as low-nicotine, cigarettes) at that time. Hence, some researchers have attributed the responsibility for the histological differences between male and female lung cancer, to these biological, epidemiological, and manufacturing characteristics [107, 108].

Tobacco smoking is also thought to modify the effect of radon-gas exposure [114, 115]. From the statistical point of view, this interaction has been reported to have a multiplicative (or nearly multiplicative) effect. This way, exposure to radon-gas would entail a higher risk of lung-cancer development amongst smokers compared to non-smokers. The way tobacco smoking modify the effect of radon-gas exposure is not completely understood [116, 117]. However, several (non-exclusive) hypotheses exist: radon-gas can penetrate the smaller airways by attaching to dust particles in the ambient air; ventilation and deposition patterns differ between smokers and non-smokers; the carcinogenic effect exerted by each exposure can eventually occur at different, or similar, stages. Therefore, tobacco smoking and radon-gas can be responsible for lung-cancer mortality by exerting their effect either independently from each other, or synergistically. Consequently, it is important to take into account both the potential confounding and interaction effects of tobacco smoking while studying the association between lung-cancer mortality and lithology. Even though direct information on tobacco smoking was not available, area-level deprivation was used as a surrogate measure for tobacco smoking; this decision was based on reported evidence about the association between smoking prevalence and area-level deprivation [152, 156, 157]. It is important to note that in some instances [154], deprivation was found to predict the smoking habit even after adjusting for individual-level SES.

In Spain, lower individual-level SES (as measured by educational level, or occupational class) has been reported to be associated with higher rates of tobacco smoking, as well as poorer self-perceived health status and higher prevalence of chronic diseases [40]. Interestingly, measures of area-level deprivation were, overall, reported to be in agreement with individual-level SES measures. The only exception was for the association between female SES and the tobacco smoking habit. In this case, lower individual-level SES was associated with lower prevalence of tobacco smoking, while area-level deprivation was not associated with the smoking prevalence. It is worth mentioning that the same area-level deprivation index and

census (the one from the year 1991) have been used in the present study. This disagreement between individual-level SES and area-level deprivation measures suggests that the latter may not be valid for adjusting on tobacco smoking, in this female cohort. A study at the European level on a cohort recruited in the 1990s [32] has confirmed the reverse association between female individual-level SES in Spain at that time, and the smoking prevalence; however, no comparisons were made with area-level deprivation in this instance.

Area-level deprivation is relevant in this context, not only because of its proven association with measures of individual-level SES (with some exceptions [40]) which, in turn, have been shown to be proxy measures for the prevalence of tobacco smoking, as well as other health-related exposures. In addition, area-level deprivation has been reported to be associated with radon-gas exposure [103]; interestingly, although environmental pollution tends to be higher in most deprived areas, the association between area-level deprivation and radon-gas exposure is the opposite way round: least deprived areas are exposed the most to radon-gas (Figure 6.1). This inverse association between deprivation and radon-gas has been explained by Briggs et al. [103] by the fact that urban areas (which concentrate highly deprived zones) are usually settled in lowland areas, where radon-gas concentration is lowest. In contrast, high-altitude rural areas are both more exposed to radon-gas, and less deprived. Therefore, area-level deprivation, as a surrogate measure for the prevalence of tobacco smoking, can be used to check for the potential modifying effect (statistical *interaction*) of smoking, on the association between lung cancer and radon-gas exposure. Furthermore, adjusting for area-level deprivation (if interaction was not present) is also important to controlling for the potential *confounding* effect of deprivation on this same relationship between radon-gas exposure and lung-cancer mortality. Notwithstanding the proven association between area-level deprivation and both lung-cancer mortality and radon-gas exposure, it may be the case that the deprivation index which was used, did not attain to reach a strong association with either lung-cancer or radon-gas because of the individual components (percentage of illiterate, unemployed, and unskilled workers) that comprises this index of deprivation. Other possibilities exist and all have been reported to have a variable degree of association depending on the outcome under consideration and the age groups that are analysed [30].

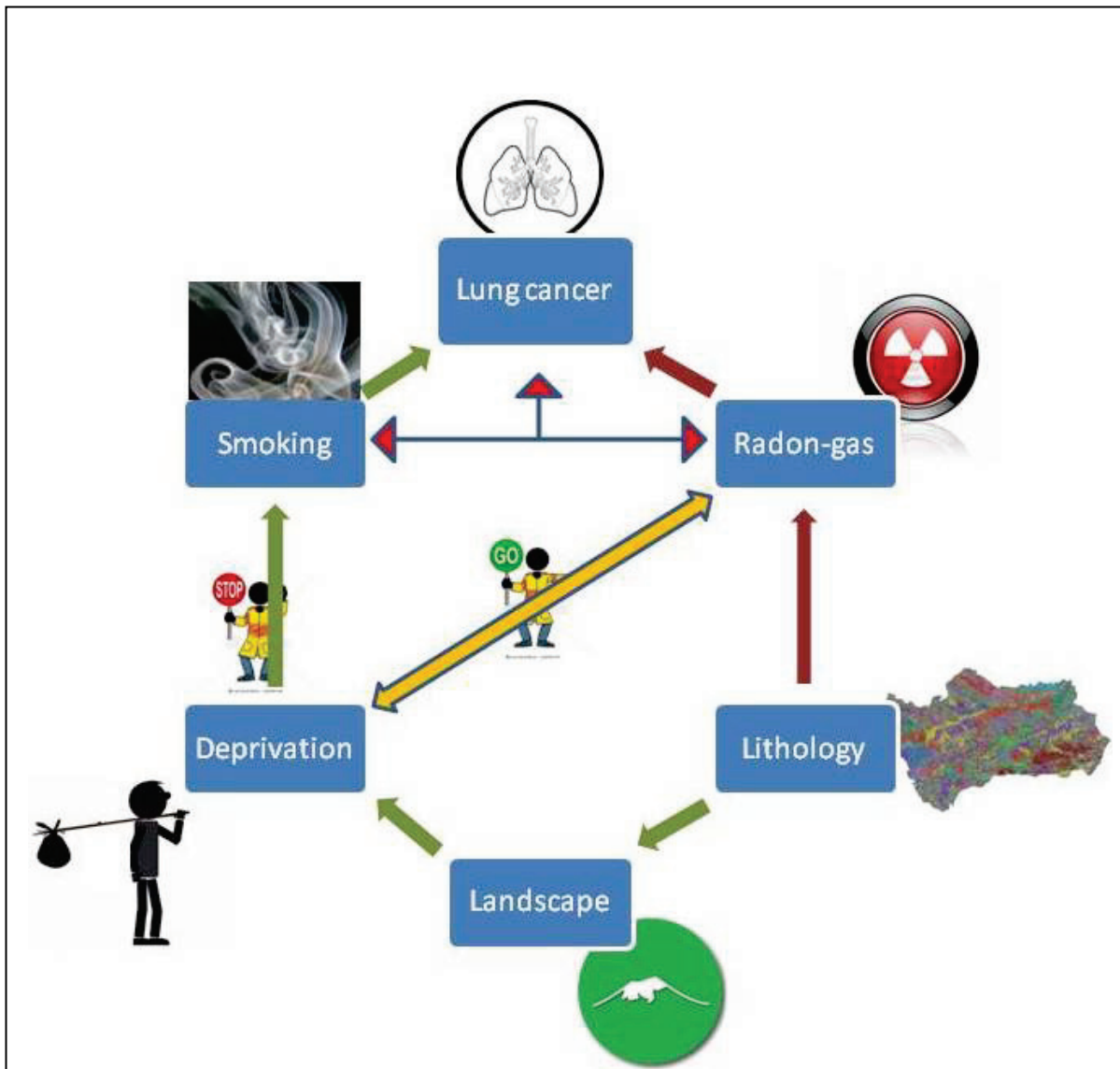


Figure 6.1. Pathways in the association of deprivation with lung cancer and radon-gas.

 = inverse association
  = direct association

 = confounding
  = interaction

(Both causal and non-causal associations are indicated by arrows)

An alternative explanation for the absence of a clear association between lithology and lung-cancer mortality in women can be based on two grounds: firstly, the modifying effect of tobacco smoking on radon-gas exposure, as it has been reported that most deaths due to radon-gas occur amongst smokers [115]; secondly, the prevalence of smoking amongst women during the study period (1986-1995). Given that most female deaths due to lung cancer took place in women aged 60 years and older, they may mostly represent deaths of non-smoking women (the Spanish women born before 1940 did not have joined the tobacco-smoking habit yet). Consequently, a much smaller risk (mean RR in women = 1.016 vs. mean RR in men = 1.023) may have become undetectable due to the lack of statistical power (see 5.3.1 and Table 5.8, and 5.3.2 and Table 5.14): the same number of units of analysis (759 municipalities) were used to detect a smaller RR [235]. Interaction (modelled as a multiplicative term between area-level deprivation and the lithology scores) was not statistically significant for either men or women. This can be explained by the fact that the area-level deprivation is a proxy measure not only for tobacco smoking (at least in men) but also for other various exposures; many of them may not modify the effect of radon-gas exposure.

There is some research evidence that substantiates a small attributable risk due to domestic radon-gas exposure in non-smoking women (1-4%), after 25 or more years of exposure [236]. This was shown for a population of non-smoking women residing in areas where the median radon-gas concentration was 4 pCi/L (or 150 Bq/m³): this coincides with the threshold limit for which the US Environmental Protection Agency (EPA) establishes the need to implement remedial actions. In contrast, some studies have reported that the mean potential indoor radon-gas concentration in Andalucía is around 25 Bq/m³. Nevertheless, it has also been reported that there exists some risk even at lower levels than the limit set by the EPA. For instance, Darby et al. have reported averaged estimates (from case-control studies) of RR = 1.06, for exposures to doses around 100 Bq/m³ (95% confidence interval: 1.01-1.10) compared to non-exposure. Also at concentrations of 20 Bq/m³ reported to be the average value in the UK (lower than the mean estimated values in Andalucía), it was estimated to exist a cumulative risk of lung-cancer death of 30% for smokers. This risk was only 0.8% for non-smokers. The proportion of cases attributed to radon-gas exposure, alone, was calculated to be 1% [115], which is in agreement with estimates reported by other

researches [189]. In the present study, the estimated magnitude of the average male RR due to lithology (when comparing the highest vs. the lowest quintile of the lithology score) was 1.07 (95% CI: 1.04-1.09).

Although extensively investigated, only lung-cancer has been associated with radon-gas exposure, but no association has been established between other cancer sites and radon [237, 238]. The findings in the present study are consistent with this. Tobacco smoking is known to be the major risk factor for both COPD [100, 121, 131] and larynx cancer [113, 239, 240]. In contrast, radon-gas exposure has not been related to either of them [117, 238] (see 2.4.2 and 2.4.3 for COPD and larynx cancer, respectively). Interestingly, the spatial distribution of male deaths due to either COPD, or larynx cancer was not associated with the lithology score devised for this study (see 5.2.2). In contrast, all three diseases (lung cancer, COPD, and larynx cancer) were positively associated with the area-level deprivation score; this is consistent with current scientific knowledge concerning the association between lower SES and higher rates of mortality due to all these diseases (see 2.4 and 2.5). These results point towards a specific, plausible association between the spatial distribution of male lung-cancer deaths in Andalucía, and the lithology score (as a surrogate measure for potential radon-gas exposure).

However, some important factors remained unmeasured, as the residual variance revealed. The individual estimation of the clustering and heterogeneity components allowed the computation of the VPC (see Table 5.10 and Table 5.15). The VPC was 95% and 100% for the male and female models, respectively. This means that virtually all the variance not explained by the models was due to the general clustering. This component, which is spatially auto-correlated, is usually interpreted in terms of unmeasured area-level factors that vary smoothly across the geographical areas; that is to say, any particular area shares some (modelled) level of risk with its neighbouring areas and differentiates from distant places.

Figure 5.30 and Figure 5.40 present the maps with the RRs due to the clustering component for women and men, respectively. It can be observed that there is a pattern of higher RRs of lung-cancer mortality (for both men and women) to the southwest of Andalucía. This pattern of spatial variation in risk was not due to either lithology (or not completely) or SES, but to some other unmeasured factor. Environmental factors

are frequently hypothesised to be responsible for this residual, spatially correlated, variability.

Area-level deprivation is not only important as a surrogate measure for tobacco smoking, but also because poorer health status has been consistently associated with lower SES [142]. Furthermore, lung cancer incidence and mortality rates are higher amongst people of lower SES even after adjusting for tobacco-smoking [32]. This is due to the fact that SES can act as a proxy measure for many other lifestyle, as well as environmental and work exposures (such as diet, physical activity, alcohol intake and exposure to toxic substances). In this study, the spatial distribution of deaths due to all three diseases (lung cancer, COPD, and larynx cancer) in both men and women has been found to be positively associated with lower area-level deprivation. For lung cancer, the mean estimated value of the RR due to area-level deprivation was 2% higher than the RR due to lithology (1.04 vs. 1.02, Table 5.8); this is in agreement with previous research that showed that the association between tobacco smoking and SES was stronger for men than women [241].

6.2 Strengths and limitations

Small-area analysis is characterised by the small number of events under scrutiny within the units of analysis. It is this characteristic that allows modelling of sparse data by means of the Poisson distribution [235]. However, this theoretical probability distribution is based on the strong assumption that the variance/mean ratio equals one. If this premise does not hold due to the variance being greater than the mean, overdispersion is said to exist. Three main overdispersion sources are unstructured (or random) heterogeneity, spatially-correlated (or clustering) heterogeneity, and excess of zeros in the data (due to the fact that this kind of analysis deals with rare events) [90]. Another strong premise when modelling the RRs is the proportionality assumption [14, 99, 220, 235], which requires that the RRs in each stratum of the confounding variable (e.g. age) be proportional to the corresponding strata in all the geographical areas under study.

6.2.1 Bayesian analysis and modelling

Hierarchical Bayesian methods are well suited for the spatial analysis of epidemiological data, as they allow the researcher to address these statistical issues (see 6.2) [80]. Furthermore, Bayesian analysis offers some advantages over its

frequentist counterpart [79], such as incorporating prior knowledge into the analysis, producing estimates with lower MSE than the frequentist ones, and allowing for a direct interpretability of CIs, while a single postulate is used in any scenario: the Bayes' rule (see 4.2.2). Some of the modelling possibilities include the Poisson-gamma, the log-normal and the BYM model; a further modification of the latter one, by Waller, takes time into consideration. The Poisson-Gamma model is, from a mathematical point of view, the simplest one. It models the observed number of cases as Poisson distributed and considers the RR as a Gamma-distributed random effect [63], which results in a Negative-Binomial posterior distribution [76, 242]. Although mathematically convenient, as it addresses overdispersion (see 4.2.1), two main points remain unresolved: covariate adjustment and spatiotemporal autocorrelation (or clustering). Conversely, the log-normal model offers some advantages by modelling the Poisson parameter on a log scale; this, allows for a linear combination of different covariates to be included. A random component for the RR is included, which is Gaussian distributed. This model can also accommodate a range of hierarchical structures to analyse the spatiotemporal components of health-related events. One of these hierarchical structures is implemented by means of the BYM which was used in this study. This model splits the random component into CH and UH. The CH component is, in turn, modelled by means of a CAR distribution (see 4.2), which requires a definition of what neighbouring areas are to be considered, by means of the adjacency matrix.

The way 'neighbouring' is defined (through the adjacency matrix) has been reported to greatly affect the regression estimates. As a consequence, some researchers have advocated a sensitivity analysis to take account of this issue [224]. These same researchers showed the differences to be expected under distinct neighbourhood structures. In all these settings, the comparative performance was assessed by means of various common criteria. They took into consideration the degree of smoothness attained as well as the magnitude of the clustering effect introduced; also, the effect on the Deviance Information Criterion (DIC, see 4.2.2) which is used for model selection. To quantify the agreement between observed and predicted values, the Kappa index was used, a low-value being due to a high smoothing effect (see 4.2.2). Interestingly, these researchers resorted to the Receiver Operating Characteristics (ROC) curve to find the most appropriate predictive cutoff points; the aim was to

decide which one gives the best compromise between sensitivity and specificity; with the same aim, other researchers have advocated fixed cut-off points based on simulation studies (see 4.4).

The ROC curve analysis offers some advantages over the fixed cut-off point proposal: firstly, it allows for the setting of cut-off points to be tailored to the actual data under scrutiny; secondly, any predicted value across the whole variable range can be assessed by means of the ROC curve. This is also advantageous, as different decision rules (favouring either sensitivity or specificity) may be preferable under diverse circumstances. The ROC curve is built by graphing the true positive ratio (sensitivity) against the false negative ratio (1-specificity) [224, 225]; they are usually represented on the y and x axis, respectively. To find these values, researchers studying modelling performance under different neighbourhood definitions, cross tabulated observed and predicted values [224]. Afterwards, they calculated the true positive and false negative ratios within tertiles of the variable range. When the ROC curve is used to assess modelling performance, the cut-off points defining the highest area under the curve are preferred; this happens when the highest true-positive ratio and lowest false-negative ratio co-occur. In this case, it was reported to happen under a predictive probability of 0.33; much different from the 0.7 cut-off point advised from simulation studies (see 4.4) [230]. The researchers concluded that neighbourhood structures based on adjacencies (as in this study) produce the highest smoothing effect on the RR estimates. Hence, they produce the least agreement between observed and predicted values ($\kappa = 0.05$). Conversely, distance-based models produce lower smoothing and, therefore, higher agreement with observed values ($\kappa = 0.07$). On the other hand, adjacency-based neighbourhoods introduce the least amount of clustering, when compared with distance-based models. They also determined that DIC reached the highest values for adjacency matrices; this would make other structures (like distance-based models) to be preferred, under this criterion.

Therefore, different possibilities (other than contiguity neighbours) exist, which can be implemented. So, distance-based neighbours could also be devised; in this approach, different lag distances (from their centroids) might be defined, as the number of neighbours would increase with distance [224]. Also, adjacency matrices of order higher than 1 (lists of neighbours of neighbours) can be considered; this was shown to improve sensitivity from 77% to 78% and specificity from 41% to 43%,

when the first-order Queen-style model was compared with its second-order counterpart. Distance-based models (or adjacency-based structures of order higher than 1) may be important where some processes (like migration flows) are nested into the weighting matrix; in this case, binary values would turn to different weights (e.g. average of inflow/outflow migration rates). If such a tenet seems plausible, different neighbouring definitions and weighting schemes should be tested in a sensitivity analysis [224]. This is relevant when a CAR model is implemented, where differences in neighbouring definitions and weighting schemes can be highly influential. This is because they determine the smoothing rate, which is at the core of Bayesian hierarchical modelling-techniques. Smoothing is designed to lessen random noise due to the statistical instability inherent in the SMRs calculation. However, how much smoothing is desirable constitutes a compromise between variance and bias.

As already discussed, the FB BYM model (that was used in this study) implements smoothing by means of locally-varying weights; conversely, most EB methods use global smoothers. There are some other important similarities (and differences) between EB and FB methods. There is an EB version by Marshall, which uses local smoothers, as the BYM model; the method devised by Marshall produces the least shrinking effect when compared to other EB counterparts. Another similarity between EB and FB methods is that some EB techniques fit the data through a log-normal model; these EB models are considered to be the most statistically stable amongst its class [62]. Despite all the affinities between these two kinds of Bayesian models, none of the EB methods take into consideration inferential uncertainty (hyperprior-estimates coming from the data itself). Hence, their RR estimates show less variability than those produced by FB methods. This downside can also be considered advantageous, due to the higher simplicity and quicker computation of EB methods.

In the present study, prior knowledge was incorporated into the analysis by fitting the BYM model to male lung-cancer mortality data concerning the period 1981-1985. A vague gamma hyperprior with parameters 0.5, 0.0005 was used to estimate both components of the residual variance (CH and UH). The posterior estimates of these two components were then used in the study of male lung-cancer mortality for the period 1986-1995. In this second stage, a sensitivity analysis was done to assess the effect of different hyperpriors on the RR estimates. The use of vague hyperpriors was

compared with the informed ones obtained in the previous step: there were not any meaningful differences in the range of the RR estimates.

Further methods have more recently been proposed. These alternatives have arisen from geostatistics, in view of the limitations of EB methods and complexity of FB techniques; among the latter, the high shrinking effect of the BYM and subjectivity to choose the adjacency matrix have encouraged new options. Some of these models recently proposed rely on methods used to interpolate unknown values based on known sample points (Kriging) [62, 77, 243-246]. Thus, Area-to-Area Poisson Kriging has been claimed to outperform both EB and FB methods [246]. This superiority has been grounded on modelling properties and practical results, as modelling through Poisson Kriging can still produce a full posterior distribution, like FB models (under a Gaussian assumption, this time). Results based on simulation studies have also shown better discrimination between high-risk and low-risk RRs, for Poisson Kriging. However, this depends on the sensitivity and specificity and which threshold values are set by choosing different cutoff points.

An additional benefit of the Poisson Kriging method is that the characteristics and effects of different adjacency matrices can be thoroughly described, which allows an informed selection to be made. Also, smaller errors concerning both inferential and predictive uncertainty have been reported, when compared to Bayesian methods [246]. Notwithstanding these findings, it is worthy of note that Area-to-Area Poisson Kriging (as EB methods) does not address parameter uncertainty; this, in turn, provides with an artifactual reassurance about the estimates precision, as all the information comes from the data itself. All the arguments considered throughout this chapter contributed turning to FB methods (specifically the BYM model) for the analysis stage.

A trade-off between sensitivity and specificity is always at issue where *diagnostic* tools are used. This is also the case when the mapping process is meant to detect areas of unusual high/low risk. As both characteristics counteract each other, the researcher always has to decide to favour either sensitivity or specificity. In spatial analysis, sensitivity refers to the ability of the mapping process (and the underlying model) to detect true raised-risk areas. This is equivalent to the conditional probability of some areas being classified as high-risk ones, given that its true risks are raised. Vice versa, specificity names the capacity to detect true lowered-risk areas. Likewise, it is the

conditional probability of some areas being classified as low-risk ones, given that its true risks are lowered. Most importantly, the researcher is interested about a different set of conditional probabilities: the so called positive and negative *predictive values*.

Therefore, once the modelling stage has classified some areas as high-risk ones, the probability of their true risks being raised is sought; this would be given by the positive predictive value (PPV). The negative predictive value (NPV), would address the opposite question: once the model has classified some areas as low-risk ones, the probability of their true risks being lowered is of interest. These are the sort of conditional probabilities that the modelling process addresses, through the estimates obtained from the posterior distribution. Both sensitivity and specificity are mainly inherent to the model itself, while the predictive capacity can vary under different circumstances. So, the BYM model is known to produce over smoothing on both the background and raised-risk areas, in general terms. This causes the model to have high specificity and lower sensitivity, which may prevent from identifying small risks; such a situation may be encountered where environmental risks are implicated in small-area analysis [230], which is the case in this study.

Concerning predictive ability, the modelling performance may be affected by different circumstances, such as the distribution of high-risk areas (either isolated or in clusters) as well as the magnitude of the risk to be identified. Furthermore, for the same magnitude of the RR, the number of cases expected may affect the predictive performance (PPV and NPV); nevertheless, this affects the smoothed RRs in a much lesser extent than the raw RRs. Therefore, the smoothed RRs are highly shrunk to the value of 1 (under most conditions) for background (not raised-risk) areas. In contrast, the raw RRs remain over-dispersed. It is also important to consider that all the above characteristics (sensitivity/specificity and predictive values) are interrelated. This interrelationship can be summarised as follows: high sensitivity leads to a high NPV through a decrease in the number of false-negative results. Whereas high specificity results in a high PPV by lessening the number of false-positive results [225]. Similarly, whenever sensitivity is set to a high value (by assuming a higher probability of false positive results) specificity drops. And the reverse is also true; if high specificity is sought (by assuming a higher probability of false-negative results) sensitivity decreases.

To adjust sensitivity and specificity, some research based on simulation has addressed the above issues to produce practical decision rules [230]. These decision rules are meant to allow choosing the best compromise between sensitivity and specificity (RR detection threshold) for a desired predictive value (or posterior probability *cutoff* point). To select the most appropriate values, several *loss* functions were used where false positive and false negative results were weighted using different rules [230]. The aim was to find the smallest value for any particular loss function; all of it, within a reasonable range of probabilities of detecting certain RR magnitude. An RR *threshold* of 1 and a probability value of 0.80 were advocated when the CAR distribution (see 4.2.2) is applied. This was shown to be a decision rule with high specificity (around 97%), but lower sensitivity (around 71%). Keeping an RR threshold of 1 and changing to a cutoff point of 0.7, sensitivity raised to 82%, while specificity dropped just to 94% (under the assumption of a true RR of 1.65).

Another decision to be made, involves a common topic to any kind of map: how many categories should be represented and which break points should be used. To address this issue concerning class intervals, it is important to realise that different methods can convey quite different information [62]. One method which is extensively used consists of using *quantiles* (e.g. tertiles, quartiles or quintiles); the corresponding break points can be used to partition the range of the cumulative distribution function of the variable to represent. This method would distribute the number of observations evenly in each class, across the whole range of the variable. Nevertheless, it is far from being perfect; values of magnitude that are far apart from each other may be classified in the same interval. This may happen as the only criterion used by the quantiles method is the number of observations per class, rather than their magnitude. Although the quantiles method may be useful to map uniform distributions, these are not usually encountered in spatial analysis; more frequently, the risk surface is spatially heterogeneous. Nevertheless, it may be acceptable where highly shrunk risks are mapped, which is usually the case when the BYM model is used.

An alternative method is the *equally spaced intervals (or absolute cut-points)*. This technique (as well as the quantiles one) is supplied by GeoBUGS; in this case, the range of the distribution is partitioned into class intervals of the same width; again, this is appropriate to map variables that are uniformly distributed. In contrast, other methods are meant to minimise the within class variance and maximise the between

class variance; it helps to label similar observations within the same class. Amongst these, the Fisher-Jenks method uses this sort of '*natural breaks*'; this technique is especially useful to map multimodal distributions. Another common method, addresses variables that are Gaussian-like distributed; in this case, classes can be devised to take into consideration dispersion from the mean value, in terms of standard-deviation units.

Chapter 7. Conclusions

7.1 Summary

Results from the measurement part of a confirmatory SEM showed a positive association between a spatially-correlated score variable and lithology (rock composition) as a surrogate measure for potential radon-gas exposure (see 5.2.1); this association was, as expected (see pg. 58), highest for plutonic and metamorphic rocks (Table 5.1). The structural part of the SEM showed a positive association between the lithology score, derived from the measurement part of the SEM, and the spatial distribution of male lung-cancer deaths in Andalucía, for the period 1986-1995 (Table 5.2 and Figure 5.4). Moreover, this association remained after adjusting for area-level deprivation, so that the potential confounding effect of deprivation [103], on the association between lithology (as a surrogate measure for potential radon-gas exposure) and the spatial distribution of lung-cancer mortality, was controlled for (Table 5.7 and Table 5.8).

Lithology was also associated with the spatial distribution of female lung-cancer deaths, although lack of such an association could not be completely excluded (Figure 5.16 and Table 5.14). A multiplicative interaction term between area-level deprivation and lithology (as surrogate measures for tobacco smoking and potential radon-gas exposure, respectively) was shown not to improve the goodness of fit of either the male (see pg. 97) or the female model (see pg. 113). In contrast with the association found between lithology and lung-cancer mortality in men, no association was found between the lithology score and the spatial distribution of mortality due to either larynx cancer or COPD (Table 5.2 and Figure 5.4). After adjusting for deprivation, most of the residual (not captured by the model) variance, as measured by the VPC, was due to spatial autocorrelation rather than random (non-spatial) heterogeneity (Table 5.10 and Table 5.15). In contrast with lithology, deprivation was positively associated with the spatial distribution of mortality due to all three diseases (lung cancer, COPD and larynx cancer) in men (Figure 5.5, Table 5.7 and Table 5.8).

According to the DIC, the best model (in both men and women) was the one which included not only lithology and deprivation, but also a clustering component (which accounted for spatial autocorrelation), as well as a random-heterogeneity component (Table 5.4 and Table 5.11). The full (all variables) model was also the one with least

predictive error, as shown by the results of the computed MSPE and MAPE (Table 5.5, Table 5.6, Table 5.12 and Table 5.13). The model accounting for spatial autocorrelation attained a high smoothing effect on the SMR, while improving the distinction between high and low-risk areas (Table 5.9). This, in turn, eased the identification of high-risk municipalities. Even though the provinces of Cádiz (Figure 5.8) and Huelva (Figure 5.11) show the highest mean posterior RR (1.35 and 1.34, respectively) there is ample heterogeneity amongst municipalities (Figure 5.7-Figure 5.14). At the other extreme, the provinces of Jaén (Figure 5.12) and Granada (Figure 5.10) show the lowest mean posterior RR (0.80 and 0.89, respectively).

Therefore, the well-known pattern [9, 10, 13, 16] of higher lung-cancer mortality in western Andalucía, for the period 1986-1995 was confirmed (Figure 5.17-Figure 5.19). Mapping of the residual variance in men showed that the spatial variation in risk was not completely explained by the model (Figure 5.27 and Figure 5.28).

Furthermore, the residual variance was mainly due to the clustering component (Figure 5.30 and Figure 5.31), which is the sort of influences that have been linked to the so called contextual variables [98, 152, 156, 230]; in contrast, the random-heterogeneity component did not show any visual patterning (Figure 5.33 and Figure 5.34). Notwithstanding these results, lithology can partially explain the spatial distribution of lung-cancer mortality in Andalucía (Figure 5.21-Figure 5.23), especially in men. Differences were found between men and women, in the effect of the clustering component on the spatial distribution of lung-cancer mortality. A clear pattern of higher risk in western Andalucía was seen in men (Figure 5.30 and Figure 5.31), while in women there was also higher risk to the south (Figure 5.40).

7.2 Contribution

This is the first time that the spatial distribution of potential radon-gas exposure from the Andalusian soils has been comprehensively analysed without the aid of direct radon measurements. Previous research had mainly relied on the availability of radon-gas measurements for the design of risk maps by large areas [58, 61, 165, 179, 180]. Surrogate measures for radon-gas concentration had been only used when missing values for actual measurements had to be confronted [61]. Although there has been extensive research on the correlation between both geology and surface lithology, and potential radon-gas exposure [168, 169, 171, 192] modelling of radon-gas

concentration as a latent (unobservable) variable (see 4.4.2 and 5.2.1) had not been previously accomplished. The SEM approach to modelling had been already applied to research on health related outcomes [195-197], but not to the analysis of the association between lithology and lung-cancer mortality at the small-area level (see 5.2.2).

The present study has explored a novel lithology score which can partially explain the spatial distribution of lung-cancer deaths in Andalucía. Lithology, as a surrogate measure for potential radon-gas exposure, overcomes some difficulties inherent in the actual measurement of radon-gas concentration. One such difficulties is the cost of measurements that limits the number of sampled places [165]; also, lack of measurements reliability due to spatial and seasonal variation in radon levels [116, 166, 173], as well as differing patterns of behaviour styles of the people dwelling in the buildings [58]. In contrast a wealth of lithological information, of a high resolution level, is available at no cost for the Andalusian soils [60]. FB methods are well suited for the analysis of small RR due to environmental pollutants [1, 103], such as the one posed by radon-gas exposure [115]; this is especially the case in Andalucía, where the mean levels of radon-gas concentration are low [61]. The model developed in this study has the potential for future improvement, so that it helps to guide public health policy concerning potential radon-gas exposure in Andalucía; one key advantage is the possibility to individually identify high-risk areas (Figure 5.7 and Figure 5.14). In addition, this model can identify areas according to the risk which is solely due to potential radon-gas exposure (Table 5.7, Table 5.8, Figure 5.21 and Figure 5.22), which can be useful to prioritising municipalities where direct radon measurements should be implemented, so that remediation actions be taken where needed [176].

7.3 Future research

The lithology score devised in this study (section 5.2) can be further elaborated in different directions. Given that there is availability of comprehensive information on the lithology of the Andalusian soils (see pg. 56 and Figure 3.1)[60], the SEM can be used to explore different measurement approaches to accounting for the latent variable (potential radon-gas exposure). Thus, extension of geological faults or different lithological classes can be used [58, 61] for a better ascertainment of the latent variable; simultaneously alternatives to the CAR model that was used to derive the

lithology score (section 5.2.1) can be checked by exploring model sensitivity to different definitions of the adjacency matrix other than contiguity (see pg. 69); this way, proximity, concentration, or intensity, concerning the latent variable (presence of radon-gas), could be better captured [103].

Given that the area-level deprivation has been shown to be inversely associated with radon-gas exposure [103], as well as (in a variable way) with lung-cancer mortality, it seems appropriate to investigate the potential confounding effect of other choices of deprivation indices (see pg. 4). Therefore, instead of using the so called index I (illiteracy, unemployment, unskilled work), index II (illiteracy, unemployment, house overcrowding) could be adjusted for [30]. As the chances are that neither index I or II be associated with smoking in the women's cohort that was analysed (section 6.1) [40], a different surrogate measure for tobacco smoking should be used to test for the potential interaction effect between lithology and smoking (Figure 6.1). An interesting variable to use as a surrogate measure for tobacco smoking is COPD incidence, given that this condition is mainly caused by tobacco smoke (section 2.4.2). Because of the very poor survivorship of lung cancer patients (see pg. 5), there may not be a great difference between modelling either lung-cancer incidence or mortality. In contrast, COPD is characterised by a much better prognosis (section 2.4.2) that can make it difficult distinguish between aetiological and prognostic factors, which, in turn would produce biased results. In addition, using information concerning histological types could also help to checking the hypothesis that different histological types (SCLC in men and mainly adenocarcinoma in women) are due to distinct aetiological causes, namely tobacco-smoking in men and radon-gas exposure in women [16]. Last but not least, smaller geographical areas can be used to lessen the potential bias due to the ecological fallacy. To this aim, digital boundaries at the census tract level are readily available [27, 28].

Chapter 8. References

1. Elliott, P. and Wartenberg, D., *Spatial epidemiology: current approaches and future challenges*. Environ Health Perspect, 2004. **112**(9): p. 998-1006.
2. Lopez-Abente Ortega, G., Gervas Camacho, J.J., and Errazola Saizar, M., *Analysis of geographic differences in mortality in Spain*. Med Clin (Barc), 1985. **84**(7): p. 264-7.
3. Vioque, J. and Bolumar, F., *Trends in mortality from lung cancer in Spain, 1951-80*. J Epidemiol Community Health, 1987. **41**(1): p. 74-8.
4. Errezola, M., Lopez-Abente, G., and Escolar, A., *Geographical patterns of cancer mortality in Spain*. Recent Results Cancer Res, 1989. **114**: p. 154-62.
5. López-Abente, G., Pollán, M., and Jiménez, M., *Female Mortality Trends in Spain Due to Tumors Associated with Tobacco Smoking*. Cancer Causes & Control, 1993. **4**(6): p. 539-45.
6. Barrado Lanzarote, M.J., Medrano Albero, M.J., and Almazan Isla, J., *Mortality from ischemic cardiopathy in Spain: the trends and geographic distribution*. Rev Esp Cardiol, 1995. **48**(2): p. 106-14.
7. Benach, J. and Yasui, Y., *Geographical patterns of excess mortality in Spain explained by two indices of deprivation*. J Epidemiol Community Health, 1999. **53**(7): p. 423-31.
8. Olalla, M.T., et al., *Time trends, cohort effect and spatial distribution of cerebrovascular disease mortality in Spain*. Eur J Epidemiol, 1999. **15**(4): p. 331-9.
9. Lopez-Abente Ortega, G., et al., *Atlas of cancer mortality and other causes of death in Spain 1978-1992*. 2001, Ministerio de Sanidad y Consumo. Instituto de Salud Carlos III: Madrid.
10. Benach, J., *Geografía de la salud: el suroeste español bajo el microscopio*. Revista de Calidad Asistencial, 2002. **17**(6): p. 317-18.
11. Benach, J., et al., *Examining geographic patterns of mortality: the atlas of mortality in small areas in Spain (1987-1995)*. Eur J Public Health, 2003. **13**(2): p. 115-23.
12. Boix Martinez, R., Aragoes Sanz, N., and Medrano Albero, M.J., *Trends in mortality from ischemic heart disease in 50 Spanish provinces*. Rev Esp Cardiol, 2003. **56**(9): p. 850-6.

13. Benach, J., et al., *The geography of the highest mortality areas in Spain: a striking cluster in the southwestern region of the country*. *Occup Environ Med*, 2004. **61**(3): p. 280-1.
14. Ferrandiz, J., et al., *Spatial analysis of the relationship between mortality from cardiovascular and cerebrovascular disease and drinking water hardness*. *Environ Health Perspect*, 2004. **112**(9): p. 1037-44.
15. Ocana-Riola, R., et al., *Research protocol for the mortality atlas of the provincial capitals of Andalusia and Catalonia (AMCAC Project)*. *Rev Esp Salud Publica*, 2005. **79**(6): p. 613-20.
16. Lopez-Abente Ortega, G., et al., *Municipal Atlas of Cancer Mortality in Spain, 1989-1998*, Carlos III Health Institute, Editor. 2006.
17. Spanish National Statistics Institute. *Estimate of the Municipal Register at 1 January 2009. Provisional data*. [Web] 2009 [cited 30/03/2012]; Available from: http://www.ine.es/en/prensa/np551_en.pdf.
18. Consejería de Medio Ambiente. *Datos Basicos de Medio Ambiente en Andalusia*. [Web] 2008 [cited 30/03/2012]; Available from: http://www.juntadeandalucia.es/medioambiente/site/web/menuitem.a5664a214f73c3df81d8899661525ea0/?vgnnextoid=4b2a6b2464f4e110VgnVCM1000001325e50aRCRD&vgnnextchannel=f40a776da8e5e110VgnVCM1000001325e50aRCRD&lr=lang_es.
19. Quantum GIS development team. *Quantum GIS Geographic Information System. Open Source Geospatial Foundation Project*. [Web] [cited 30/03/2012]; Available from: <http://qgis.org/>.
20. Patterson, T. and Vaughn Kelso, N. *Natural Earth*. [Web] [cited 30/03/2012]; Available from: <http://www.naturalearthdata.com/>.
21. Instituto Nacional de Estadística (INE). *INEbase. List of place names. Methodology*. [Web] [cited 05/04/2012]; Available from: <http://www.ine.es/nomen2/Metodologia.do?L=1>.
22. Instituto de Estadística de Andalucía (IEA). *Catalogue of Entities and Population Centres. Andalusia*. [Web] [cited 05/04/2012]; Available from: <http://www.juntadeandalucia.es/institutodeestadistica/nomenclator/index-en.htm>.

23. Consejeria de Salud. *Estadísticas vitales: Evolución de la mortalidad en Andalucía de 1975 a 1997* [Web] 1999 [cited 30/03/2012]; Available from: <http://www2.uca.es/hospital/EV7597/index.htm>.
24. Kogevinas, M., et al., *Social Inequalities and Cancer*, in *IARC Scientific Publication No. 138*, N.P. M. Kogevinas, M. Susser and P. Boffetta, Editor. 1997, International Agency for Research on Cancer, Lyon,.
25. Dominguez-Berjon, M.F. and Borrell, C., *Mortalidad y privación socioeconómica en las secciones censales y los distritos de Barcelona*. Gac Sanit, 2005. **19**(5): p. 363-9.
26. Ruiz-Ramos, M., et al., *Evolución de las desigualdades sociales en la mortalidad general de la ciudad de Sevilla (1994-2002)*. Gac Sanit, 2006. **20**(4): p. 303-10.
27. Ocana-Riola, R., et al., *Mortality Atlas of the provincial capitals of Andalusia, 1999-2002.*, ed. R. ocana Riola. 2007, Granada: Escuela Andaluza de Salud Publica. Consejeria de Salud. Junta de Andalusia.
28. Ocana-Riola, R., et al., *Area deprivation and mortality in the provincial capital cities of Andalusia and Catalonia (Spain)*. J Epidemiol Community Health, 2008. **62**(2): p. 147-52.
29. Benach, J., et al., *The public health burden of material deprivation: excess mortality in leading causes of death in Spain*. Preventive Medicine, 2003. **36**(3): p. 300-8.
30. Benach, J., et al., *Material deprivation and leading causes of death by gender: evidence from a nationwide small area study*. J Epidemiol Community Health, 2001. **55**(4): p. 239-45.
31. Tomatis, L., *Poverty and cancer*, in *Social Inequalities and Cancer*, M. Kogevinas, et al., Editors. 1997, International Agency for Research on Cancer (IARC): Lyon.
32. Menvielle, G., et al., *The Role of Smoking and Diet in Explaining Educational Inequalities in Lung Cancer Incidence*. J. Natl. Cancer Inst., 2009. **101**(5): p. 321-30.
33. International Epidemiological Association (IEA), *The development of modern Epidemiology: Personal reports of those who were there* 1st ed, ed. W. Walter, J. Olsen, and C.d.V. Florey. 2007, Oxford: Oxford University Press. 456 pp.

34. Elliott, P., *Investigation of disease risks in small areas*. Occup Environ Med, 1995. **52**(12): p. 785-9.
35. Salmond, C. and Crampton, P., *Heterogeneity of deprivation within very small areas*. Journal of Epidemiology and Community Health, 2002. **56**(9): p. 669-70.
36. McNally, R.J. and Eden, T.O., *An infectious aetiology for childhood acute leukaemia: a review of the evidence*. Br J Haematol, 2004. **127**(3): p. 243-63.
37. Borrell, C. and Pasarín, M.I., *Desigualdades en salud y territorio urbano*. Gac Sanit, 2004. **18**(1): p. 1-4.
38. Ahs, A.M. and Westerling, R., *Mortality in relation to employment status during different levels of unemployment*. Scand J Public Health, 2006. **34**(2): p. 159-67.
39. Banks, J., et al., *Disease and disadvantage in the United States and in England*. JAMA, 2006. **295**(17): p. 2037-45.
40. Dominguez-Berjon, F., et al., *The usefulness of area-based socioeconomic measures to monitor social inequalities in health in Southern Europe*. Eur J Public Health, 2006. **16**(1): p. 54-61.
41. Poole, C., et al., *Socioeconomic status and childhood leukaemia: a review*. Int. J. Epidemiol., 2006. **35**(2): p. 370-84.
42. Manda, S., Feltbower, R., and Gilthorpe, M., *Investigating spatio-temporal similarities in the epidemiology of childhood leukaemia and diabetes*. Eur J Epidemiol, 2009. **24**(12): p. 743-52.
43. MacNab, Y.C. and Dean, C.B., *Spatio-temporal modelling of rates for the construction of disease maps*. Stat Med, 2002. **21**(3): p. 347-58.
44. Agarwal, D.K., Gelfand, A.E., and Citron-Pousty, S., *Zero-inflated models with application to spatial count data*. Environmental and Ecological Statistics, 2002. **9**(4): p. 341-55.
45. Silva Ayçaguer, L., *Análisis espacial de la mortalidad en áreas geográficas pequeñas. El enfoque bayesiano*. Rev Cubana Salud Pública, 2003. **29**(4): p. 314-22.
46. Kaminska, I.A., Oldak, A., and Turski, W.A., *Geographical Information System (GIS) as a tool for monitoring and analysing pesticide pollution and its impact on public health*. Ann Agric Environ Med, 2004. **11**(2): p. 181-4.

47. Nakaya, T., et al., *Geographically weighted Poisson regression for disease association mapping*. *Statistics in Medicine*, 2005. **24**(17): p. 2695-717.
48. Ugarte, M.D., Ibáñez, B., and Militino, A.F., *Detection of spatial variation in risk when using CAR models for smoothing relative risks*. *Stoch Environ Res Risk Assess*, 2005. **19**(1): p. 33-40.
49. Kraak, M.J., *Why maps matter in GIScience*. *Cartographic Journal*, 2006. **43**(1): p. 82-9.
50. Bivand, R., *Implementing Spatial Data Analysis Software Tools in R*. *Geographical Analysis*, 2006. **38**(1): p. 23-40.
51. Martínez-Martínez, J.M., *Statistical Applications in Geographical Health Studies*. 2006, Universitat Politècnica de Catalunya: Barcelona.
52. Greenland, S., *Bayesian perspectives for epidemiological research: I. Foundations and basic methods*. *Int. J. Epidemiol.*, 2006. **35**(3): p. 765-75.
53. Reibel, M., *Geographic Information Systems and Spatial Data Processing in Demography: a Review*. *Popul Res Policy Rev*, 2007. **26**(5): p. 601-18.
54. Greenland, S., *Bayesian perspectives for epidemiological research. II. Regression analysis*. *Int. J. Epidemiol.*, 2007. **36**(1): p. 195-202.
55. Elliott, P., et al., *The Small Area Health Statistics Unit: a national facility for investigating health around point sources of environmental pollution in the United Kingdom*. *J Epidemiol Community Health*, 1992. **46**(4): p. 345-9.
56. Singh, G.K. and Hiatt, R.A., *Trends and disparities in socioeconomic and behavioural characteristics, life expectancy, and cause-specific mortality of native-born and foreign-born populations in the United States, 1979-2003*. *Int. J. Epidemiol.*, 2006. **35**(4): p. 903-19.
57. Laflamme, D.M. and Vanderslice, J.A., *Using the Behavioral Risk Factor Surveillance System (BRFSS) for exposure tracking: experiences from Washington State*. *Environ Health Perspect*, 2004. **112**(14): p. 1428-33.
58. Lopez, R., et al., *Natural radiation doses to the population in a granitic region in Spain*. *Radiat Prot Dosimetry*, 2004. **111**(1): p. 83-8.
59. García-Pérez, J., et al., *Description of industrial pollution in Spain*. *BMC Public Health*, 2007. **7**(1): p. 1-13.
60. Consejería de Medio Ambiente. *Mapa litológico de Andalucía [Andalusian lithological map]*. [Web] 2005 [cited 29/04/2012]; Lithological map of Andalucía, based on the Spanish National Geologic Map -MAGNA-, and the

Geologic and Miner Map of Andalusia. Scale 1:400,000]. Available from:

http://www.juntadeandalucia.es/medioambiente/site/rediam/menuitem.04dc44281e5d53cf8ca78ca731525ea0/?vgnextoid=3097d2aa40504210VgnVCM100001325e50aRCRD&vgnnextchannel=7b3ba7215670f210VgnVCM1000001325e50aRCRD&vgnnextfmt=rediam&lr=lang_es.

61. Quindos Poncela, L.S., et al., *Natural gamma radiation map (MARNA) and indoor radon levels in Spain*. Environ Int, 2004. **29**(8): p. 1091-6.
62. Bivand, R.S., Pebesma, E.J., and Gomez-Rubio, V., *Applied Spatial Data Analysis with R*. Use R!, ed. R. Gentleman, G. Parmigiani, and K. Hornik. 2008, New York: Springer.
63. Lawson, A.B., Browne, W.J., and Vidal-Rodeiro, C.L., *Disease Mapping with WinBUGS and MLwiN*, in *Statistics in Practice*, S. Senn and V. Barnett, Editors. 2003, John Wiley & Sons: Chichester.
64. Dolk, H., et al., *A standardisation approach to the control of socioeconomic confounding in small area studies of environment and health*. J Epidemiol Community Health, 1995. **49 Suppl 2**: p. S9-14.
65. Bithell, J.F., et al., *Controlling for socioeconomic confounding using regression methods*. J Epidemiol Community Health, 1995. **49**(Suppl_2): p. S15-19.
66. Kogevinas, M. and Porta, M., *Socioeconomic differences in cancer survival: a review of the evidence*, in *Social Inequalities and Cancer*, M. kogevinas, et al., Editors. 1997, International Agency for Research on Cancer (IARC). p. 177-206.
67. World Health Organization. *International Statistical Classification of Diseases and Related Health Problems. 10th Revision. Version for 2007*. [Web] [cited 05/04/2012]; Available from: <http://www.who.int/classifications/icd/en/>.
68. Benavides, F.G., Bolumar, F., and Peris, R., *Quality of Death Certificates in Valencia, Spain*. American Journal of Public Health, 1989. **79**(10): p. 1352-4.
69. Perez-Gomez, B., et al., *Accuracy of cancer death certificates in Spain: a summary of available information*. Gac Sanit, 2006. **20 Suppl 3**: p. 42-51.
70. Mantel, N. and Stark, C.R., *Computation of Indirect-Adjusted Rates in the Presence of Confounding*. Biometrics, 1968. **24**(4): p. 997-1005.

71. Breslow, N. and Day, N., *Indirect Standardization and Multiplicative Models for Rates, With Reference to the Age Adjustment of Cancer Incidence and Relative Frequency Data*. J Chronic Dis, 1975. **28**: p. 289-303.
72. Osborn, J., *A Multiplicative Model for the Analysis of Vital Statistics Rates*. Applied Statistics, 1975. **24**(1): p. 75-84.
73. Clayton, D. and Kaldor, J., *Empirical Bayes Estimates of Age-Standardized Relative Risks for Use in Disease Mapping*. Biometrics, 1987. **43**(3): p. 671-681.
74. Armstrong, B.G., *Comparing standardized mortality ratios*. AEP, 1995. **5**(1): p. 60-4.
75. Lee, W.-C., *A Partial SMR Approach to Smoothing Age-specific Rates*. AEP, 2003. **13**(2): p. 89-99.
76. Bolstad, W.M., *Introduction to Bayesian Statistics*. 2nd ed. 2007: Wiley.
77. Crawley, J.M., *The R Book*. 2007, Chichester: Wiley.
78. Gelman, A. and Hill, J., *Data Analysis Using Regression and Multilevel/Hierarchical Models*. 2007, Cambridge: Cambridge University Press.
79. Dunson, D.B., *Commentary: practical advantages of Bayesian analysis of epidemiologic data*. Am J Epidemiol, 2001. **153**(12): p. 1222-6.
80. Graham, P., *Intelligent smoothing using hierarchical bayesian models*. Epidemiology, 2008. **19**(3): p. 493-5.
81. Ioannidis, J.P.A., *Why Most Published Research Findings Are False*. PLoS Med, 2005. **2**(8): p. 696-701.
82. Greenland, S., *Principles of multilevel modelling*. Int. J. Epidemiol., 2000. **29**(1): p. 158-67.
83. Feltbower, R.G., et al., *Detecting small-area similarities in the epidemiology of childhood acute lymphoblastic leukemia and diabetes mellitus, type 1: a Bayesian approach*. Am J Epidemiol, 2005. **161**(12): p. 1168-80.
84. National Center for Biotechnology Information. U.S. National Library of Medicine. *PubMed*. [Web] [cited 27/06/2012]; Available from: <http://www.ncbi.nlm.nih.gov/pubmed>.
85. Consejería de Salud. *Estadísticas vitales: Distribución espacial y tendencia de la mortalidad por cáncer y otras causas. Andalucía, 1975-1997*. 1998

[cited 05/04/2012]; Available from:

<http://www2.uca.es/hospital/AtlasAnda/indice.htm>.

86. Consejeria de Salud. *Estadísticas Vitales 1992-2003. Datos Andalucía y Provincias* Statistics [PDF files] 2003 [cited Sep 15 2009]; Available from: <http://www.juntadeandalucia.es/institutodeestadistica/ema/index.htm>.
87. Doll, R. and Hill, A.B., *Smoking and carcinoma of the lung; preliminary report*. BMJ, 1950. **2**(4682): p. 739-48.
88. Clayton, D.G., Bernardinelli, L., and Montomoli, C., *Spatial correlation in ecological analysis*. Int J Epidemiol, 1993. **22**(6): p. 1193-202.
89. Thonsom Reuters. *EndNote*. [Web] [cited 27/06/2012]; Available from: <http://www.endnote.com/>.
90. Ugarte, M.D., Ibanez, B., and Militino, A.F., *Modelling risks in disease mapping*. Stat Methods Med Res, 2006. **15**(1): p. 21-35.
91. Ramis Prieto, R., et al., *Modelling of municipal mortality due to haematological neoplasias in Spain*. J Epidemiol Community Health, 2007. **61**(2): p. 165-71.
92. Lawson, A.B., et al., *Disease mapping models: an empirical evaluation*. Statist Med, 2000. **19**(17-18): p. 2217-41.
93. Ghosh, S.K., Mukhopadhyay, P., and Lu, J.-C. (2006) *Bayesian analysis of zero-inflated regression models*. Journal of Statistical Planning and Inference **136**, 1360-1375.
94. Lawson, A.B. and Clark, A. (2002) *Spatial mixture relative risk models applied to disease mapping*. Statistics in Medicine **21**, 359-370.
95. Aragonés, N., et al., *Oesophageal cancer mortality in Spain: a spatial analysis*. BMC Cancer, 2007. **7**: p. 1-13.
96. Ocana-Riola, R. and Maria Mayoral-Cortes, J., *Spatio-temporal trends of mortality in small areas of Southern Spain*. BMC Public Health, 2010. **10**.
97. Lopez-Abente Ortega, G., Aragonés, N., and Pollan, M., *Solid-tumor mortality in the vicinity of uranium cycle facilities and nuclear power plants in Spain*. Environ Health Perspect, 2001. **109**(7): p. 721-9.
98. Lopez-Abente Ortega, G., et al., *Geographical pattern of brain cancer incidence in the Navarre and Basque Country regions of Spain*. Occup Environ Med, 2003. **60**(7): p. 504-8.

99. Ferrándiz, J., et al., *Statistical relationship between hardness of drinking water and cerebrovascular mortality in Valencia: a comparison of spatiotemporal models*. *Environmetrics*, 2003. **14**(5): p. 491-510.
100. Viegi, G., et al., *Definition, epidemiology and natural history of COPD*. *Eur Respir J*, 2007. **30**(5): p. 993-1013.
101. Escolar-Pujolar, A. *Atlas de mortalidad por cancer en la provincia de Cádiz (1975-1979)*. XIII congreso de la Sociedad Española de Salud Pública y Administración Sanitaria [Conference] 2009 [cited 05/04/2012]; Available from: <http://www.sespas.es/congresosevilla2009/ponencias.html>.
102. Shohaimi, S., et al., *Residential area deprivation predicts smoking habit independently of individual educational level and occupational social class. A cross sectional study in the Norfolk cohort of the European Investigation into Cancer (EPIC-Norfolk)*. *J Epidemiol Community Health*, 2003. **57**(4): p. 270-6.
103. Briggs, D., Abellan, J.J., and Fecht, D., *Environmental inequity in England: small area associations between socio-economic status and environmental pollution*. *Soc Sci Med*, 2008. **67**(10): p. 1612-29.
104. Woodward, A. and Boffetta, P., *Environmental exposure, social class, and cancer risk*, in *Social Inequalities and Cancer*, M. kogevinas, et al., Editors. 1997, International Agency for Research on cancer (IARC). p. 361-7.
105. Doll, R., et al., *Mortality in relation to smoking: 50 years' observations on male British doctors*. *BMJ*, 2004. **328**(7455): p. 1519.
106. Doll, R., et al., *Mortality from cancer in relation to smoking: 50 years observations on British doctors*. *Br J Cancer*, 2005. **92**(3): p. 426-9.
107. Shields, P.G., *Molecular epidemiology of smoking and lung cancer*. *Oncogene*, 2002. **21**(45): p. 6870-6.
108. Shields, P.G., *Epidemiology of tobacco carcinogenesis*. *Curr Oncol Rep*, 2000. **2**(3): p. 257-62.
109. Alberg, A.J. and Samet, J.M., *Epidemiology of lung cancer*. *Chest*, 2003. **123**(0732-183X (Print)): p. 21S-49S.
110. Sasco, A.J., Secretan, M.B., and Straif, K., *Tobacco smoking and cancer: a brief review of recent epidemiological evidence*. *Lung Cancer*, 2004. **45 Suppl 2**: p. S3-9.

111. Boyle, P., *Tobacco smoking and the British doctors' cohort*. Br J Cancer, 2005. **92**(3): p. 419-20.
112. IARC, I.A.f.R.o.C., *Tobacco Smoking and Tobacco Smoke in IARC Monographs on the Evaluation of Carcinogenic Risks to Humans and their Supplements: A complete list*. 2002.
113. Kuper, H., Adami, H.O., and Boffetta, P., *Tobacco use, cancer causation and public health impact*. J Intern Med, 2002. **251**(6): p. 455-66.
114. Alavanja, M.C.R., et al., *Estimating the attributable risk of residential radon among nonsmoking women: initial results and methodologic challenges*. Environ Int, 1996. **22**(1001): p. 1005-13.
115. Darby, S., Hill, D., and Doll, R., *Radon: A likely carcinogen at all exposures*. Ann Oncol, 2001. **12**(10): p. 1341-51.
116. ATSDR. *Radon Toxicity. Case Studies in Environmental Medicine (CSEM) 2000* [cited 29/062012]; Available from:
<http://www.atsdr.cdc.gov/csem/radon/docs/radon.pdf>.
117. Committee on Health Risks of Exposure to Radon (BEIR VI). *Health Effects of Exposure to Radon: BEIR VI*. 1999 [cited 29/06/2012]; Available from:
<http://books.nap.edu/openbook.php?isbn=0309056454>.
118. Pearce, J. and Boyle, P., *Is the urban excess in lung cancer in Scotland explained by patterns of smoking?* Soc Sci Med, 2005. **60**(12): p. 2833-43.
119. Bray, F., Tyczynski, J.E., and Parkin, D.M., *Going up or coming down? The changing phases of the lung cancer epidemic from 1967 to 1999 in the 15 European Union countries*. Eur J Cancer, 2004. **40**(1): p. 96-125.
120. Levi, F., et al., *Trends in lung cancer among young European women: the rising epidemic in France and Spain*. Int J Cancer, 2007. **121**(2): p. 462-5.
121. Anto, J.M., et al., *Epidemiology of chronic obstructive pulmonary disease*. Eur Respir J, 2001. **17**(5): p. 982-94.
122. Mannino, D.M. and Buist, A.S., *Global burden of COPD: risk factors, prevalence, and future trends*. The Lancet, 2007. **370**(9589): p. 765-73.
123. Gudmundsson, G., et al., *Mortality in COPD patients discharged from hospital: the role of treatment and co-morbidity*. Respir Res, 2006. **7**: p. 109.
124. Huiart, L., Ernst, P., and Suissa, S., *Cardiovascular morbidity and mortality in COPD*. Chest, 2005. **128**(4): p. 2640-6.

125. Fuhrman, C., et al., *Deaths from chronic obstructive pulmonary disease in France, 1979-2002: a multiple cause analysis*. Thorax, 2006. **61**(11): p. 930-4.
126. Piccioni, P., et al., *Predictors of survival in a group of patients with chronic airflow obstruction*. J Clin Epidemiol, 1998. **51**(7): p. 547-55.
127. Wagena, E.J., et al., *Psychological distress and depressed mood in employees with asthma, chronic bronchitis or emphysema: a population-based observational study on prevalence and the relationship with smoking cigarettes*. Eur J Epidemiol, 2004. **19**(2): p. 147-53.
128. Clotet, J., et al., *[Spirometry is a good method for detecting and monitoring chronic obstructive pulmonary disease in high-risk smokers in primary health care]*. Arch Bronconeumol, 2004. **40**(4): p. 155-9.
129. Celli, B.R., et al., *The body-mass index, airflow obstruction, dyspnea, and exercise capacity index in chronic obstructive pulmonary disease*. N Engl J Med, 2004. **350**(10): p. 1005-12.
130. Salvi Ss Fau - Barnes, P.J. and Barnes, P.J., *Chronic obstructive pulmonary disease in non-smokers*. The Lancet, 2009. **374**(1474-547X (Electronic)): p. 733-43.
131. Mannino, D.M., *COPD: Epidemiology, Prevalence, Morbidity and Mortality, and Disease Heterogeneity*. Chest, 2002. **121**(5 suppl): p. S121-6.
132. Holguin, F., et al., *Comorbidity and mortality in COPD-related hospitalizations in the United States, 1979 to 2001*. Chest, 2005. **128**(4): p. 2005-11.
133. Kerstjens, H.A., et al., *Decline of FEV1 by age and smoking status: facts, figures, and fallacies*. Thorax, 1997. **52**(9): p. 820-7.
134. Rijcken, B. and Britton, J., *Epidemiology of Chronic Obstructive Pulmonary Disease*. Eur Respir Mon, 1998. **7**: p. 41-3.
135. Devereux, G., *ABC of chronic obstructive pulmonary disease. Definition, epidemiology, and risk factors*. BMJ, 2006. **332**(7550): p. 1142-4.
136. Hashibe, M., et al., *Interaction between tobacco and alcohol use and the risk of head and neck cancer: pooled analysis in the International Head and Neck Cancer Epidemiology Consortium*. Cancer Epidemiol Biomarkers Prev, 2009. **18**(2): p. 541-50.

137. Altieri, A., et al., *Alcohol consumption and risk of laryngeal cancer*. Oral Oncol, 2005. **41**(10): p. 956-65.
138. De Stefani, E., et al., *Supraglottic and glottic carcinomas: Epidemiologically distinct entities?* Int J Cancer, 2004. **112**(6): p. 1065-71.
139. Benowitz, N.L., *Biomarkers of environmental tobacco smoke exposure*. Environ Health Perspect, 1999. **107 Suppl 2**: p. 349-55.
140. Burton, A., *Does the smoke ever really clear? Thirdhand smoke exposure raises new concerns*. Environ Health Perspect, 2011. **119**(2): p. A70-4.
141. Susser, I., *Social theory and social class*, in *Social Inequalities and Cancer*, M. Kogevinas, I. Susser, and P. Boffetta, Editors. 1997, International Agency for Research on Cancer (IARC). p. 41-50.
142. Mackenbach, J.P., et al., *Socioeconomic inequalities in health in 22 European countries*. N Engl J Med, 2008. **358**(23): p. 2468-81.
143. Kahn, H.S., et al., *Pathways between area-level income inequality and increased mortality in U.S. men*. Ann N Y Acad Sci, 1999. **896**: p. 332-4.
144. Regidor, E., et al., *Trends in cigarette smoking in Spain by social class*. Prev Med, 2001. **33**(4): p. 241-8.
145. Coma, A., Marti, M., and Fernandez, E., *[Education and occupational social class: their relationship as indicators of socio-economic position to study social inequalities in health using health interview surveys]*. Aten Primaria, 2003. **32**(4): p. 208-15.
146. Dominguez-Berjon, M.F., Borrell, C., and Pastor, V., *Indicadores socioeconómicos de área pequeña en el estudio de las desigualdades en salud*. Gac Sanit, 2003. **18**(2): p. 92-100.
147. Benach, J. and Amable, M., *Las clases sociales y la pobreza*. Gac Sanit, 2004. **18**(Supl 1): p. 16-23.
148. Sundquist, K., Malmström, M., and Johansson, S.E., *Neighbourhood deprivation and incidence of coronary heart disease: A multilevel study of 2.6 million women and men in Sweden*. Journal of Epidemiology and Community Health, 2004. **58**(1): p. 71-7.
149. Regidor, E., et al., *Occupational social class and mortality in a population of men economically active: the contribution of education and employment situation*. Eur J Epidemiol, 2005. **20**(6): p. 501-8.

150. Pearce, N., *Why study socioeconomic factors and cancer?*, in *Social Inequalities and Cancer*, M. Kogevinas, et al., Editors. 1997, International Agency for Research on Cancer (IARC). p. 17-23.
151. Berkman, L.F. and Macintyre, S., *The measurement of social class in health studies: old measures and new formulations*, in *Social Inequalities and Cancer*, M. Kogevinas, et al., Editors. 1997, International Agency for Research on Cancer (IARC). p. 51-64.
152. Pickett, K.E. and Pearl, M., *Multilevel analyses of neighbourhood socioeconomic context and health outcomes: a critical review*. *J Epidemiol Community Health*, 2001. **55**(2): p. 111-22.
153. Dominguez-Berjon, M.F., et al., *Medidas de privación material en los estudios de áreas geográficas pequeñas*. *Gac Sanit*, 2001. **15**(Supl. 4): p. 23-33.
154. Kleinschmidt, I., Hills, M., and Elliott, P., *Smoking behaviour can be predicted by neighbourhood deprivation measures*. *Journal of Epidemiology and Community Health*, 1995. **49**(SUPPL. 2): p. S72-7.
155. Sanchez-Cantalejo, C., Ocana Riola, R., and Fernandez, A., *Deprivation index for small areas in Spain*. *Soc Indic Res*, 2007. **89**(2): p. 259-73.
156. Malmstrom, M., Sundquist, J., and Johansson, S.E., *Neighborhood environment and self-reported health status: a multilevel analysis*. *Am J Public Health*, 1999. **89**(8): p. 1181-6.
157. Chuang, Y.-C., et al., *Effects of neighbourhood socioeconomic status and convenience store concentration on individual level smoking*. *J Epidemiol Community Health*, 2005. **59**(7): p. 568-73.
158. Twigg, L. and Moon, G., *Predicting small area health-related behaviour: a comparison of multilevel synthetic estimation and local survey data*. *Social Science & Medicine*, 2002. **54**(6): p. 931-7.
159. Axelson, O., *Cancer risks from exposure to radon in homes*. *Environ Health Perspect*, 1995. **103 Suppl 2**: p. 37-43.
160. Nicholls, G., *The Ebb and Flow of Radon*. *Am J Public Health*, 1999. **89**(7): p. 993-5.
161. Pavia, M., et al., *Meta-analysis of residential exposure to radon gas and lung cancer*. *Bull World Health Organ*, 2003. **81**(10): p. 732-8.

162. Darby, S., et al., *Radon in homes and risk of lung cancer: collaborative analysis of individual data from 13 European case-control studies*. *BMJ*, 2004: p. 1-6.
163. Krewski, D., et al., *A Combined Analysis of North American Case-Control Studies of Residential Radon and Lung Cancer*. *Journal of Toxicology and Environmental Health, Part A*, 2006. **69**(7): p. 533 - 97.
164. Akerblom, G., *Methodology for assessment of exposure to environmental factors in application to epidemiological studies: assessment of exposure to natural ionizing radiation*. *Sci Total Environ*, 1995. **168**(2): p. 155-68.
165. Quindos, L.S., Fernandez, P.L., and Soto, J., *National survey on indoor radon in Spain*. *Environ Int*, 1991. **17**(5): p. 449-53.
166. Li, X., et al., *A study of daily and seasonal variations of radon concentrations in underground buildings*. *J Environ Radioact*, 2006. **87**(1): p. 101-6.
167. Kitto, M.E., Kunz, C.O., and Green, J.G., *Development and distribution of radon risk maps in New York State*. *Journal of Radioanalytical and Nuclear Chemistry*, 2001. **249**(1): p. 153-7.
168. Kitto, M.E., *Assessing radon concentrations in areas with few measurements*. *Environ Monit Assess*, 2003. **83**(2): p. 163-75.
169. Sundal, A.V., et al., *The influence of geological factors on indoor radon concentrations in Norway*. *Sci Total Environ*, 2004. **328**(1-3): p. 41-53.
170. Gillmore, G.K., Phillips, P.S., and Denman, A.R., *The effects of geology and the impact of seasonal correction factors on indoor radon levels: a case study approach*. *J Environ Radioact*, 2005. **84**(3): p. 469-79.
171. Miles, J.C. and Appleton, J.D., *Mapping variation in radon potential both between and within geological units*. *J Radiol Prot*, 2005. **25**(3): p. 257-76.
172. Andersen, C.E., et al., *Prediction of ²²²Rn in Danish dwellings using geology and house construction information from central databases*. *Radiat Prot Dosimetry*, 2007. **123**(1): p. 83-94.
173. Denman, A.R., Lewis, G.T., and Brennen, S.E., *A study of radon levels in NHS premises in affected areas around the UK*. *J Environ Radioact*, 2002. **63**(3): p. 221-30.
174. Scivyer, C.R., *Radon protection for new buildings: a practical solution from the UK*. *Sci Total Environ*, 2001. **272**(1-3): p. 91-6.

175. Howarth, C.B., *The reliability of radon reduction techniques*. Sci Total Environ, 2001. **272**(1-3): p. 349-52.
176. Ford, E.S., et al., *Radon and lung cancer: a cost-effectiveness analysis*. Am J Public Health, 1999. **89**(3): p. 351-7.
177. Bochicchio, F., et al., *The Italian Survey as the Basis of the National Radon Policy*. Radiat Prot Dosimetry, 1994. **56**(1-4): p. 1-4.
178. Nikolopoulos, D., et al., *Radon survey in Greece--risk assesment*. Journal of Environmental Radioactivity, 2002. **63**(2): p. 173-86.
179. Quindos, L.S., et al., *Radon and Lung Cancer in Spain*. Radiat Prot Dosimetry, 1991. **36**(2-4): p. 331-3.
180. Quindos, L.S., Fernandez, P.L., and Soto, J., *Study of areas of spain with high indoor radon*. Radiation Measurements, 1995. **24**(2): p. 207-10.
181. Sainz, C., et al., *High Background Radiation Areas: the Case of Villar De La Yegua Village (Spain)*. Radiat Prot Dosimetry, 2007. **125**(1-4): p. 565-7.
182. Dubois, G. *An overview of Radon Surveys in Europe*. [Web] 2005 [cited 29/04/2012]; Available from: http://europa.academia.edu/GregoireDubois/Papers/429267/An_overview_of_radon_surveys_in_Europe.
183. Dubois, G., Bossew, P., and Friedmann, H., *A geostatistical autopsy of the Austrian indoor radon survey (1992-2002)*. Sci Total Environ, 2007. **377**(2-3): p. 378-95.
184. Bossew, P. and Lettner, H., *Investigations on indoor radon in Austria, Part 1: Seasonality of indoor radon concentration*. J Environ Radioact, 2007. **98**(3): p. 329-45.
185. Bossew, P., Dubois, G., and Tollefsen, T., *Investigations on indoor Radon in Austria, part 2: Geological classes as categorical external drift for spatial modelling of the Radon potential*. J Environ Radioact, 2007. **99**(1): p. 81-97.
186. Institute of Statistics of Andalucia. *Basic information of Andalucia*. Territory and Environment [Web] 2005 [cited 05/04/2012]; Available from: <http://www.juntadeandalucia.es/medioambiente/site/aplica/medioambiente/site/web/menuitem.a5664a214f73c3df81d8899661525ea0/?vgnnextoid=135873bdd06f9010VgnVCM1000000624e50aRCRD&vgnthroid=f798223622e54010VgnVCM1000001625e50aRCRD>.

187. Verdi, L., Caldognetto, E., and Trotti, F., *Radon mapping in south Tyrol: comparison between two different procedures*. Radiat Prot Dosimetry, 2004. **111**(4): p. 439-43.
188. Alavanja, M.C., et al., *Residential radon exposure and risk of lung cancer in Missouri*. Am J Public Health, 1999. **89**(7): p. 1042-8.
189. Darby, S., et al., *Radon in homes and risk of lung cancer: collaborative analysis of individual data from 13 European case-control studies*. BMJ, 2005. **330**(7485): p. 223-8.
190. Smith, B.J. and Field, R.W., *Effect of housing factors and surficial uranium on the spatial prediction of residential radon in Iowa*. Environmetrics, 2007. **18**(5): p. 481-97.
191. Vaupotic, J. and Kobal, I., *Correlation between short-term and long-term radon measurements*. Isotopes Environ Health Stud, 2002. **38**(1): p. 39-46.
192. Zhu, H.C., Charlet, J.M., and Poffijn, A. (2001) *Radon risk mapping in southern Belgium: an application of geostatistical and GIS techniques*. Sci Total Environ **272**, 203-10.
193. Friis, L., et al., *Validation of a geologically based radon risk map: are the indoor radon concentrations higher in high-risk areas?* Health Phys, 1999. **77**(5): p. 541-4.
194. Skeppstrom, K. and Olofsson, B., *A prediction method for radon in groundwater using GIS and multivariate statistics*. Sci Total Environ, 2006. **367**(2-3): p. 666-80.
195. Congdon, P., *A spatial structural equation model for health outcomes*. Journal of Statistical Planning and Inference, 2008. **138**(7): p. 2090-105.
196. Congdon, P., et al., *A spatial structural equation modelling framework for health count responses*. Statist. Med., 2007. **26**: p. 5267-84.
197. Liu, X., Wall, M.M., and Hodges, J.S., *Generalized spatial structural equation models*. Biostat, 2005. **6**(4): p. 539-557.
198. Environmental Systems Research Institute, I.E. *ESRI Shapefile Technical Description*. [Web] 1998 [cited 05/04/2012]; Available from: <http://www.esri.com/library/whitepapers/pdfs/shapefile.pdf>.
199. The BUGS Project. *Geobugs*. 2010 [cited 2010]; Available from: <http://www.mrc-bsu.cam.ac.uk/bugs/winbugs/geobugs.shtml>.

200. Lewin-Koh, N.J., et al. *Tools for reading and handling spatial objects*. [Web] [cited 03/08/2012]; Available from: <http://CRAN.R-project.org/package=mapproj>.
201. Consejería de Salud. *Portal de Salud*. [Web] [cited 05/04/2012]; Available from: <http://www.juntadeandalucia.es/salud/sites/csalud/portal/index.jsp>.
202. Instituto de Estadística de Andalucía (IEA). *Instituto de Estadística y Cartografía de Andalucía*. [Web] [cited 05/04/2012]; Available from: <http://www.juntadeandalucia.es/institutodeestadisticaycartografia/ieagen/sea/esquema/instituto.htm>.
203. Instituto de Estadística de Andalucía (IEA). *Estadísticas de Mortalidad de Andalucía. Defunciones en Andalucía*. [Web] [cited 05/04/2012]; Available from: <http://www.juntadeandalucia.es/institutodeestadisticaycartografia/ema/index.htm>.
204. Instituto de Estadística de Andalucía (IEA). *Estimaciones intercensales de población para el periodo 1981-2002*. [Web] [cited 05/04/2012]; Available from: <http://www.juntadeandalucia.es/institutodeestadisticaycartografia/eiep/index.htm>.
205. Centers for Disease Control and Prevention (CDC). *Epi Info 3.5.3*. [Web] [cited 05/04/2012]; Available from: <http://wwwn.cdc.gov/epiinfo/html/prevVersion.htm>.
206. Centers for Disease Control and Prevention (CDC). *Epi Info 7*. [Web] [cited 05/04/2012]; Available from: <http://wwwn.cdc.gov/epiinfo/7/index.htm>.
207. Instituto de Estadística de Andalucía (IEA). *Censos de 2001*. [Web] [cited 05/04/2012]; Available from: <http://www.juntadeandalucia.es/institutodeestadisticaycartografia/censo2001/index.htm>.
208. Instituto Nacional de Estadística (INE). *What kinds of population figures does INE publish?* [Web] [cited 05/04/2012]; Available from: http://www.ine.es/en/inebmenu/mnu_cifraspob_en.htm.
209. Instituto de Estadística de Andalucía (IEA). *Municipal Register of Inhabitants*. [Web] [cited 05/04/2012]; Available from:

- <http://www.juntadeandalucia.es/institutodeestadisticaycartografia/padron/index.htm>.
210. Instituto Nacional de Estadística (INE). *PC-Axis, the electronic publications format*. [Web] [cited 05/04/2012]; Available from: <http://www.ine.es/ss/Satellite?L=0&c=Page&cid=1254735116596&p=1254735116596&pagename=ProductosYServicios%2FPYSLayOut#a1259925031852>.
 211. Statistics Sweden. *PC-Axis*. [Web] [cited 05/04/2012]; Available from: http://www.scb.se/Pages/StandardNoLeftMeny___314045.aspx.
 212. Instituto de Estadística de Andalucía (IEA). *Sistema de información multiterritorial de Andalucía (SIMA)*. [Web] [cited 05/04/2012]; Available from: <http://www.juntadeandalucia.es/institutodeestadisticaycartografia/sima/index2.htm>.
 213. Instituto Nacional de Estadística (INE). *Population figures and demographic censuses*. [Web] [cited 05/04/2012]; Available from: http://www.ine.es/en/inebmenu/mnu_cifraspob_en.htm.
 214. Fleiss, J.L., *Statistical Methods for Rates and Proportions*. 2nd ed. Wiley Series in Probability and Mathematical Statistics. 1981: John Wiley & Sons.
 215. Kirkwood, B.R. and Sterne, J.A.C., *Essential Medical Statistics*. 2nd ed. Science. 2004: Blackwell Publishing.
 216. Pickle, L.W., *Exploring spatio-temporal patterns of mortality using mixed effects models*. *Statistics in Medicine*, 2000. **19**(17-18): p. 2251-63.
 217. Biggeri, A., et al., *Non-parametric maximum likelihood estimators for disease mapping*. *Statistics in Medicine*, 2000. **19**(17-18): p. 2539-54.
 218. R Development Core Team. *R: A language and environment for statistical computing*. [Web] [cited 05/04/2012]; Available from: <http://www.R-project.org/>.
 219. Spector, P., *Data Manipulation with R*. Use R!, ed. R. Gentleman, K. Hornik, and G. Parmigiani. 2008, New York: Springer.
 220. Pascutto, C., et al., *Statistical issues in the analysis of disease mapping data*. *Statistics in Medicine*, 2000. **19**(17-18): p. 2493-519.
 221. Lawson, A., *Bayesian Disease Mapping. Hierarchical Modelling in Spatial Epidemiology* *Interdisciplinary Statistics*. 2009, Boca Raton: Chapman & Hall/CRC.

222. Ryan, L. *GIS and Spatial Statistics*. Gene-Environment Interactions: Role in the Modulation of Pulmonary and Autoimmune Disease Risks. The Biomedical & Life Sciences Collection [Web] 2007 [cited 05/04/2012]; Available from: http://www.hstalks.com/main/browse_talk_view.php?t=78&s=78&s_id=24&c
223. Bivand, R. *spdep: Spatial dependence: weighting schemes, statistics and models*. [Web] [cited 05/04/2012]; Available from: <http://CRAN.R-project.org/package=spdep>.
224. Earnest, A., et al., *Evaluating the effect of neighbourhood weight matrices on smoothing properties of Conditional Autoregressive (CAR) models*. Int J Health Geogr, 2007. **6**(1): p. 54-65.
225. Wray, N.R., et al., *A comparison of some simple methods to identify geographical areas with excess incidence of a rare disease such as childhood leukaemia*. Statist Med, 1999. **18**(12): p. 1501-16.
226. Held, L., et al., *Towards joint disease mapping*. Stat Methods Med Res, 2005. **14**(1): p. 61-82.
227. Spiegelhalter, D., et al. *WinBUGS*. [Web] [cited 05/04/2012]; Available from: <http://www.mrc-bsu.cam.ac.uk/bugs/welcome.shtml>.
228. Lunn, D.J., et al. *OpenBUGS*. [Web] [cited 05/04/2012]; Available from: <http://openbugs.info/w/FrontPage>.
229. Nicholas, J., Lewin-Koh., and Bivand, R. *maptools: Tools for reading and handling spatial objects. R package version 0.8-10*. [Web] [cited 05/04/2012]; Available from: <http://CRAN.R-project.org/package=maptools>.
230. Richardson, S., et al., *Interpreting posterior relative risk estimates in disease-mapping studies*. Environ Health Perspect, 2004. **112**(9): p. 1016-25.
231. Field, R.W., et al., *An Overview of the North American Residential Radon and Lung Cancer Case-Control Studies*. J Toxicol Environ Health A, 2006. **69**(7): p. 599 - 631.
232. Miles, J., *Use of a model data set to test methods for mapping radon potential*. Radiat Prot Dosimetry, 2002. **98**(2): p. 211-8.
233. Ielsch, G., et al., *Study of a predictive methodology for quantification and mapping of the radon-222 exhalation rate*. J Environ Radioact, 2002. **63**(1): p. 15-33.

234. Fernandez, E., et al., *Prevalencia del consumo de tabaco en Espana entre 1945 y 1995. Reconstruccion a partir de las Encuestas Nacionales de Salud*. Med Clin (Barc), 2003. **120**(1): p. 14-6.
235. Ocana-Riola, R., *Common errors in disease mapping*. Geospat Health, 2010. **4**(2): p. 139-154.
236. Alavanja, M.C.R., et al., *Attributable risk of lung cancer in lifetime nonsmokers and long-term ex-smokers (Missouri, United States)*. Cancer Causes Control, 1995. **6**(3): p. 209-16.
237. Darby, S.C., et al., *Radon and Cancers Other Than Lung Cancer in Underground Miners: a Collaborative Analysis of 11 Studies*. J. Natl Cancer Inst., 1995. **87**(5): p. 378-84.
238. Kreuzer, M., et al., *Radon and risk of extrapulmonary cancers: results of the German uranium miners' cohort study, 1960-2003*. Br J Cancer, 2008. **99**(11): p. 1946-53.
239. Kuper, H., Boffetta, P., and Adami, H.O., *Tobacco use and cancer causation: association by tumour type*. J Intern Med, 2002. **252**(3): p. 206-24.
240. Gandini, S., et al., *Tobacco smoking and cancer: a meta-analysis*. Int J Cancer, 2008. **122**(1): p. 155-64.
241. Stellman, S.D. and Resnicow, K., *Tobacco smoking, cancer and social class*. IARC Sci Publ, 1997(138): p. 229-50.
242. Ntzoufras, I., *Bayesian Modeling Using WinBUGS*. Computational Statistics, ed. P. Giudici, G.H. Givens, and B.K. Mallick. 2009, New Jersey: Wiley.
243. Goovaerts, P., *Geostatistical analysis of disease data: visualization and propagation of spatial uncertainty in cancer mortality risk using Poisson kriging and p-field simulation*. Int J Health Geogr, 2006. **5**:52.
244. Goovaerts, P., *Geostatistical analysis of disease data: accounting for spatial support and population density in the isopleth mapping of cancer mortality risk using area-to-point Poisson kriging*. Int J Health Geogr, 2006. **5**:52.
245. Goovaerts, P., *Geostatistical analysis of disease data: estimation of cancer mortality risk from empirical frequencies using Poisson kriging*. Int J Health Geogr, 2005. **4**:31.
246. Goovaerts, P. and Gebreab, S., *How does Poisson kriging compare to the popular BYM model for mapping disease risks?* Int J Health Geogr, 2008. **7**:6.